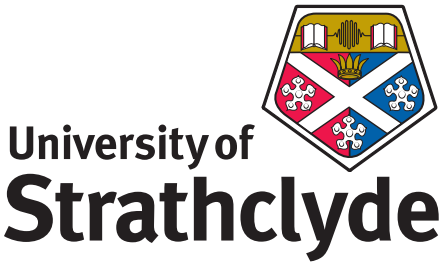

Mathematical modelling of the transmission of Salmonella between pigs

Andrew Hill
Department of Mathematics and Statistics
University of Strathclyde
Glasgow, UK
October 2007

This thesis is submitted to the University of Strathclyde for the degree of Doctor of Philosophy in the Faculty of Science.

For my family, especially Oswin - hopefully by the time you're old enough to decide on whether to do postgraduate study, I have forgotten all the stress, pain and time it took, so that I can happily encourage you to do it!

The copyright of this thesis belongs to the author under the terms of the United Kingdom Copyright Acts as qualified by University of Strathclyde Regulation 3.50. Due acknowledgement must always be made of the use of any material in, or derived from, this thesis.

Acknowledgements

I would like to warmly thank my supervisors, Dr. Louise Kelly and Dr. Steven Webb, for their expertise, knowledge, support, advice and most of all, patience. My decision to do a PhD was made to widen my mathematical skill and knowledge, and it has certainly done that. Doing a PhD has been interesting and frustrating in equal measure, but the former has been guaranteed by the enthusiasm of Louise and Steve.

I would also like to thank the Animal Health and Veterinary Laboratories Agency for funding this PhD, and providing support where necessary. I would especially like to acknowledge Dr. Emma Snary and Dr. Robin Simons, for dealing with stupid questions that I just couldn't wait to take to Glasgow. In addition, funding for much of the project work at AHVLA that contributed to the thesis came from Defra, the Food Standards Agency and the European Food Safety Authority, and many persons in each of the organisations also deserve my thanks. There are a whole host of other persons and organisation which have provided information on pigs, Salmonella, maths, veterinary practices and all manner of random facts that I needed to find out. I owe a huge deal to all of these people, without whom I would barely know a weaner from a finisher.

I would like to thank my parents for always encouraging me to further my education and subsequently my career; I would not have done this had it not been for the years of support before going to university and realising just what education can do. Finally, my warmest thanks should probably go to Crystle and Oswin, who have been incredibly patient and understanding while I wrote up my thesis over what seems like several dozen years!

Abstract

Salmonella spp. are the second most common cause of foodborne illness in the United Kingdom (UK) and the European Union (EU). Pigs are relatively more likely to be infected with *Salmonella spp.* compared to other species of livestock. A recent EFSA survey isolated Salmonella from 21.2% of lymph node samples. Given the high prevalence of Salmonella infection in pigs, with a serotype of human health significance, pig meat is thought to be the third most important contributor to Salmonella infection in humans, behind poultry meat and eggs (EFSA, 2006). This has prompted the EU to set targets for reduction of *Salmonella spp.* in slaughter-age pigs and breeding pigs, which are due to come into force in the next 1-2 years.

For reductions in the prevalence of Salmonella infection in live pigs, intervention at the farm level (be it at the sow or pig level) will be required. Current evidence for the effect of farm level interventions such as the use of organic acids in feed/water or vaccination is scarce, as experimental or observational studies are expensive and so studies thus far have been small. Hence, the relevance of these limited and small studies is limited when interpreting the results for the development of a National Control Plan for Salmonella in pigs, therefore mathematical modelling studies are useful to assess the effectiveness of on-farm interventions in reducing the burden of human salmonellosis.

This thesis presents a number of determinsitic and stochastic models on the subject of Salmonella introduction/transmission between pigs, progressing from a simple determinstic SIR model of grower-finisher production to a detailed stochastic model incoproating all stages of production and considering the source of infection. The dynamics of infection in the deterministic models was similar. With current parameter estimation, infection was self-sustaining in pen populations across the models, whether there were 1 or 300 pens. Stability analysis of each of the models suggested that the homogeneous infected steady state would be the result of at least one infected pig entering the herd. Travelling wave analysis of the multi-pen models suggested that the speed of transmission between pens, via faecal-oral transmission, was relatively slow, such that infection would probably be limited to a few pens by the time pigs were sent to slaughter. Very different dynamics were observed for the stochastic models, where stochastic fade-out was the most

common result from infection entering a herd.

The models developed in this thesis allow an insight into the complex dynamics of transmission and intervention on pig farms, which is currently not possible through observational study due to the large number of variables that must be controlled. The final model incorporates several advancements in the field of Salmonella in pig transmission modelling that have not been considered before (e.g. the explicit inclusion of the magnitude of (intermittent and variable) shedding, farm management systems and sources of infection). These advances highlight new and interesting dynamics, suggesting that the sow is by far the most important source of infection of pigs. In particular, the level of Salmonella shedding of individual pigs/sows appears to be crucial to the dynamics of infection, but this has not been captured before. This seems a fairly intuitive conclusion, given that Salmonella is mainly transmitted via the faecal-oral route and is dose-dependent. However, it is not normally captured in models because of the complexity of doing so, and the lack of data to parameterise such a model. In the case of Salmonella in pigs, when dealing with various sources, complex management systems and highly variable shedding rates, then the inclusion of shedding dynamics at a more detailed level appears warranted, as the dynamics change markedly according to whether it is included or not.

In conclusion, this thesis has established a set of models for the investigation of the introduction, transmission and intervention of Salmonella in pigs. The final model suggests that the sow is a major source of infection, and hence intervention should first and foremost be introduced to the breeding herd. However, decreasing the resistance of the weaner/finisher pig to infection, and conducting All-In-All-Out production, would lessen the transmission of infection between pigs during later stages of production. The final model has already been used to inform the development of the UK National Control Plan (to investigate the accuracy of several sampling schemes and as an input for Cost-Benefit Analysis), and research will continue to improve the assumptions and parameter estimation of the model.

Contents

Chapter 1

Introduction

1.1 Salmonella in pigs

Salmonella spp. are the second most common cause of foodborne illness in the United Kingdom (UK) and the European Union (EU). The total number of reported cases in the EU was 131,468 in 2008 (EFSA, 2010b). Over 10,000 of these were reported by the UK Health Protection Agency (HPA) (EFSA, 2010b). Given an under-reporting factor of at least 1 in 3 (Wheeler et al., 1999) the total number of cases in the UK are likely to be over 30,000 per year. In 2010, the most common serotype, *Salmonella* Enteritidis, accounted for 4,361 (39%) of total reported cases in the UK, and is predominantly associated with poultry and egg consumption.

The second most commonly isolated human serotype is *Salmonella* Typhimurium, where 1,923 (17% of total) cases were reported in 2008 (HPA, 2009). This serotype has a much broader host range, and can be found in poultry and all major mammalian livestock species (pigs, cattle, sheep). It is especially common in pigs; in a recent survey by the European Food Safety Authority (EFSA) over 70% of

Salmonella isolates taken from slaughter pig lymph node samples in the UK were serotyped as *S.* Typhimurium (EFSA, 2008b). Pigs are relatively more likely to be infected with *Salmonella spp.* compared to other species of livestock. The same EFSA survey isolated Salmonella from 21.2% of lymph node samples, whereas a similar EFSA survey for the second most commonly infected species, broiler chickens, isolated Salmonella from just over 8% of broiler flocks in the UK (EFSA, 2010a).

Given the high prevalence of Salmonella infection in pigs, with a serotype of human health significance, pig meat is thought to be the third most important contributor to Salmonella infection in humans, behind poultry meat and eggs (EFSA, 2006). As part of European Commission (EC) Regulation 854/2004 a commitment was made to reduce the level of zoonotic pathogens in food. This has prompted the EU to set targets for reduction of *Salmonella spp.* in live animals for many livestock species, including layer chickens, turkeys, broiler chickens and pigs. Four National Control Programmes (NCPs) have already been put in place for specific types of poultry (including laying chickens and broilers) for a number of years (Defra, 2010). Due to vaccination and other measures, the UK has currently achieved all of its targets.

As poultry-related Salmonella infection is reduced, then the relative importance of *S.* Typhimurium, and pig-meat borne salmonellois, increases. As a result the EU have set in process a chain of research to establish the human cost-benefit and evidence base for setting targets for each Member State to reduce Salmonella in slaughter and breeding pigs. Two surveys, one in slaughter pigs and one on breeding holdings, have been carried out by EFSA (EFSA, 2008b, 2009a) to set the baseline against which the targets will be measured against. Each Member State (MS) will be required to develop their National Control Plan to achieve the

given targets within a specified timeframe (yet to be agreed). Two NCPs, one for breeding pigs and one for slaughter pigs, are to be required from each MS.

For reductions in the prevalence of Salmonella infection in live pigs, intervention at the farm level (be it at the sow or pig level) will be required. Current evidence for the effect of farm level interventions such as the use of organic acids in feed/water or vaccination is scarce, as experimental or observational studies are expensive and so studies thus far have been small. Hence, the relevance of these small studies is limited when interpreting the results for the development of a NCP, and risk assessment/mathematical modelling studies are thus required to assess the effectiveness of on-farm and abattoir interventions in reducing the burden of human salmonellosis.

1.2 Pig production

The management of fattening pigs is extremely variable, with many systems in place to rear pigs to slaughter weight. However, for the purposes of this thesis we need only consider differences in management systems that affect Salmonella introduction and/or transmission. First, the vast majority of pigs slaughtered in the EU, especially in the large pork-producing countries (e.g. Denmark, Germany and France) will be produced on large intensive farms. These farms will produce perhaps 80-90% of of all pigs destined for slaughter in the EU. In the UK, this weighting towards commercial pig production is even more pronounced; we estimate that the vast majority of pigs for slaughter, over 95%, will originate from large, commercial farms (Hill, prep).

Within typical commercial production in the UK there are two largely distinct

categories of farm: breeding and fattening. At the top of the production pyramid are the breeding herds, including the nucleus and multiplier herds (see Figure 1.1). The nucleus herd is highly specialised, and focused solely on improving the genetic characteristics of the pig population. Sows within the nucleus herd are chosen for desirable genetic characteristics, and are bred with similarly valuable boars (through natural or artificial insemination). There may be only a few nucleus herds within each individual company, and so in order to provide enough pigs for the production cycle, the offspring of the nucleus sows are then sent to one of 10-20 multiplier herds, where the desired traits (related to meat quality, production rate etc...) are scaled up in terms of the number of pigs by breeding these sows. Any inferior quality stock from nucleus and multiplier herds may be sold for slaughter, but the pigs from these herds are not primarily produced for meat.

The offspring from the multiplier herds may be sold as gilts or weaners, and are then sent to the production herds for either further breeding purposes (replacement gilts producing pigs for slaughter on a farrow-to-finish farm), or are reared from weaning to slaughter on specialised contract finishing farms. It is these farrow-to-finish and contract finishing farms that will be considered in this thesis, as it is the pigs from these farms that make up the majority of pigs slaughtered in the UK and the EU. In the UK, pig production is roughly split half and half (in numbers of pigs slaughtered), between farrow-to-finish (production) and multi-site farms (sow herds selling pigs to specialist contract finishing herds). For the rest of the thesis, we define 'sows', unless otherwise specified, as those on farrow-to-finish farms producing pigs for slaughter, and 'pigs' as the offspring of those sows that are solely intended for meat production.

Within production herds the time it takes to rear pigs to slaughter weight, and the phases of rearing which each pig goes through, is fairly standard (see Figure

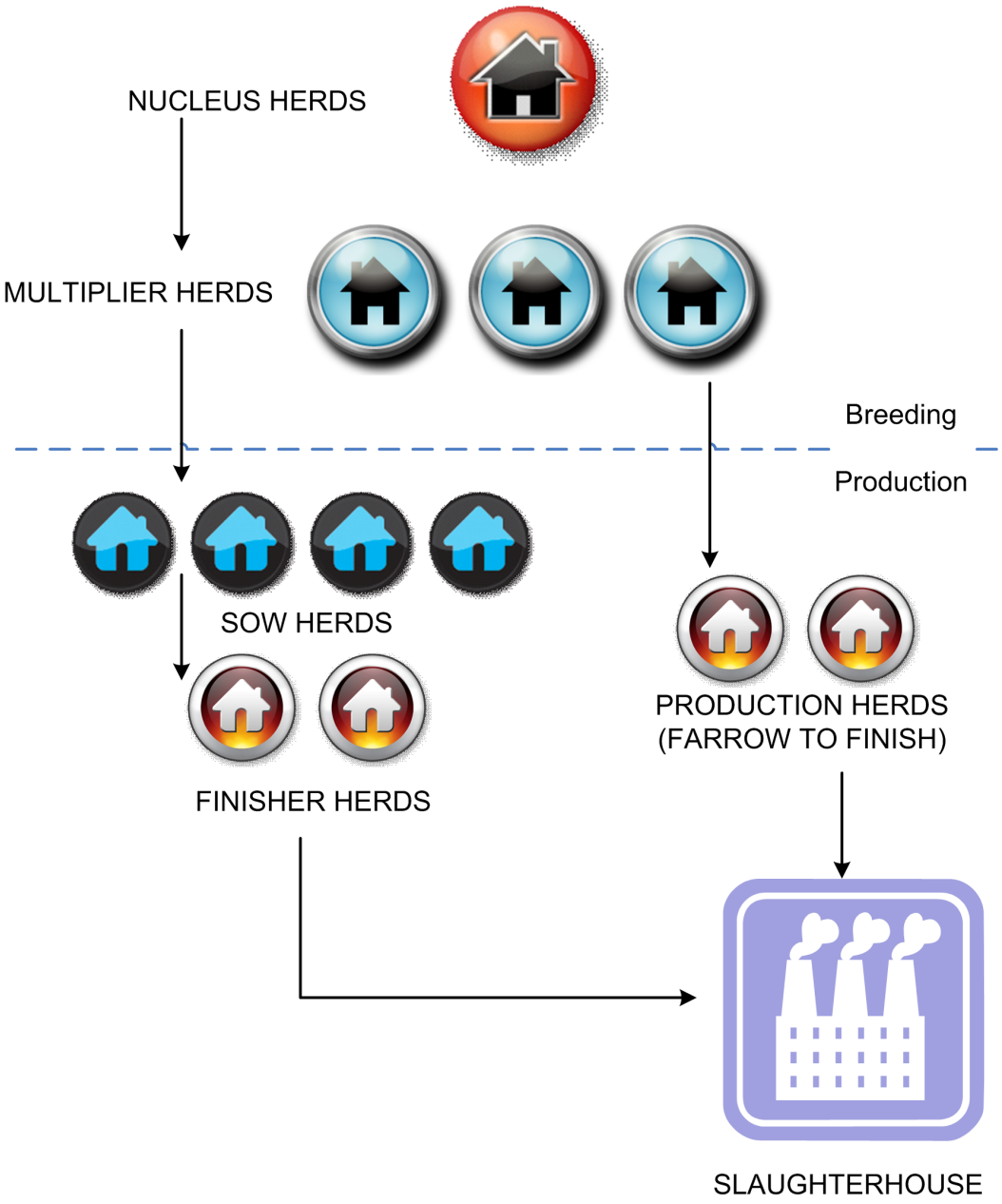

Figure 1.1: Schematic of pig production in the UK. Pig production is split into two distinct categories: breeding and production. Breeding herds (nucleus and multiplier) are specialist units where improvements to the genetic characteristics of the breeds are made; only production herds, and specialist contract finishing herds, rear pigs solely for slaughter to provide meat for human consumption.

1.2), although there are a wide range of systems in place to rear the fattening pig.

The vast majority of production systems can be defined in terms of distinct stages

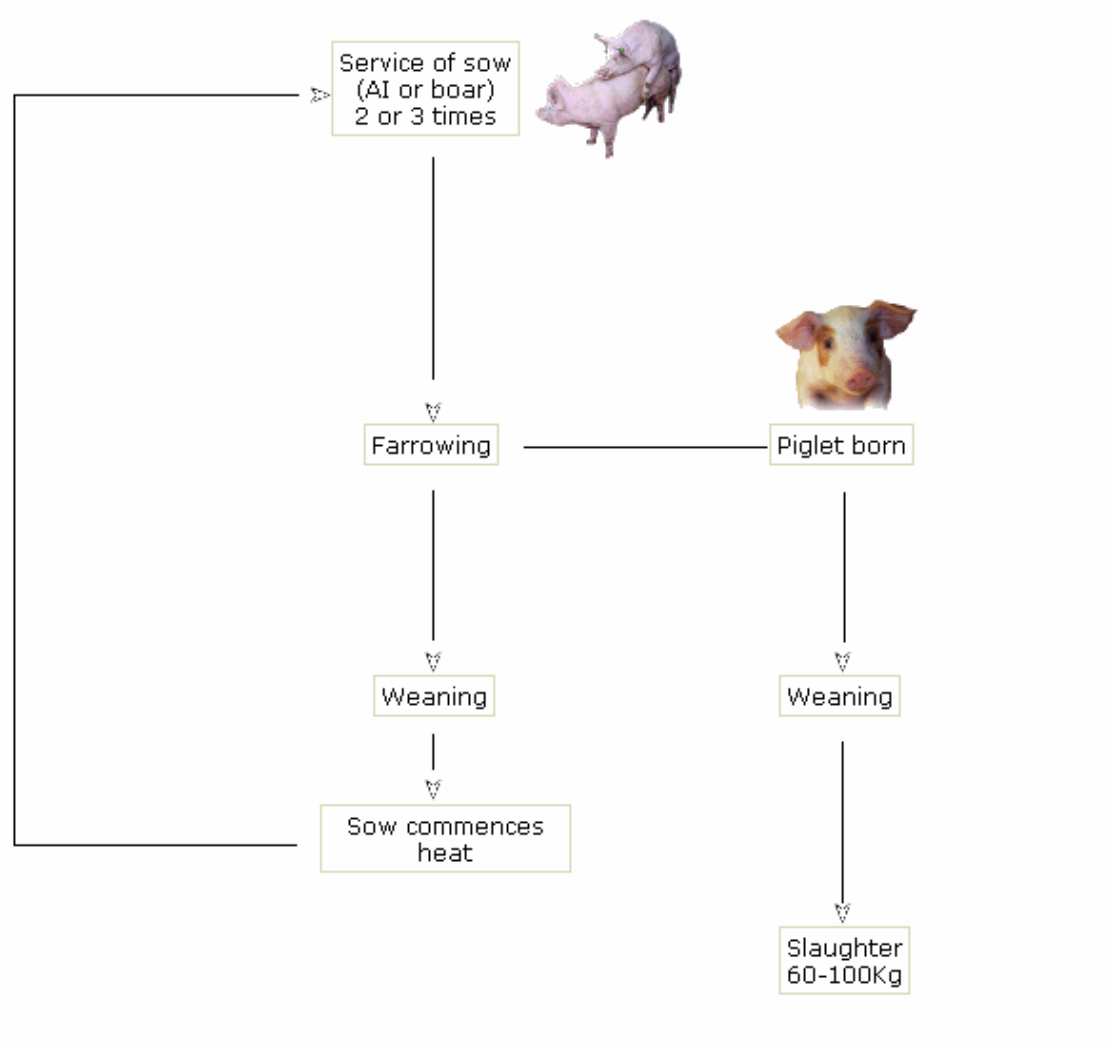

Figure 1.2: Rearing of pigs to slaughter weight. Sows are typically arranged into groups; servicing is staggered such that a group of sows will reach partuition every one or two weeks. Picture taken from www.ukagriculture.com.

of rearing, which are:

- Farrowing: Between 8-15 piglets born to a sow, each sow and litter within its own pen; around 15-50 pens within individual compartments. Piglets weaned between 21-42 days of age.

- Weaning(nursery): Pigs are moved into specialist accommodation for the purpose of weaning the pigs onto feed and growing them to around 30kg; the

ambient temperature is usually strictly maintained as weaners are less able to regulate temperature at this age. Litters of piglets are grouped together into pens of around 10-50 pigs each. Pigs are moved onto either dry or wet feed, and stay within these pens until 8-12 weeks of age.

- Growing: Pigs are moved into bigger pens. Becoming less common in modern systems, this intermediate stage will generally see relatively little mixing of pigs from different pens, and pigs will stay here for approximately 6-8 weeks. (The growing phase may be conjoined with the finishing phase to produce a longer overall finishing period).

- Finishing: Pigs are moved into specialist accommodation. These farms/buildings tend to be larger, as pigs are fattened to slaughter weight over a period of 8-16 weeks. Contract finishing farms may source their stock from a number of weaner (nursery) or grower farms.

Not all farmers will practice all of these stages of rearing, and differences may be found in mixing patterns and the age of pigs within each system. Information relating to the transmission of Salmonella between different ages of pigs is limited, therefore we conclude that it is sufficient to differentiate between these rearing groups rather than specific age groups.

The main management difference between farms relates to how the farmer manages the transfer of pigs through the different stages of rearing. There are many different ways to organise the serving of sows, mixing of pigs etc, but the main difference will be if pigs are raised in an all-in-all-out (AIAO) or a continuous system[1], with

[1]AIAO production is the priniciple of raising pigs as a distinct cohort that have no direct contact with another cohort of pigs. Theoretically, AIAO production should be carried out by building, so there is a distinct period between batches where rigorous cleaning and disinfection will take place. Practically, most AIAO production is conducted by room, not by building. Continuous production captures all other systems of management.

the assumption being that AIAO limits the number of pigs that contact each other, and whether or not there is any movement of pigs between farms.

A special form of AIAO production, and of crucial importance for the Salmonella status, is whether farms apply batch production, and how this is applied through the production chain. Batching is a result of farrowing 20-50 sows simultaneously (i.e. within a few days) in one compartment, such that all of the progeny are very close in age. This cohort of piglets can then be raised as a distinct management group up until slaughter, without introducing or allowing contacts with other pigs. Within that system the piglets from the same litter can also be kept together in the same pen up to slaughter. Batching is perceived as beneficial because of the ability of the farmer to plan ahead and reduce peaks and troughs in labour demands, together with associated productivity gains. Batching of sows into groups can be done on either a 1, 2 or 3 weekly-cycle, such that groups of sows give birth within a defined weekly period. In addition pigs produced in these systems reach slaughter up to one month earlier than in old traditional systems with a continuous production (which is considered to be as a result of improved health status). Of basic importance for the efficacy of this system is that a cleaning and disinfection (C&D) procedure is applied between batches. In discussion with pig farming experts (industry, vets etc) AIAO production will be at a compartment level (where cohorts of similarly-aged pigs are moved into and out of a room/section of a building separately from other cohorts).

Harder to define, but a crucial difference between farms, is biosecurity. We define biosecurity as anything that provides a barrier between the Salmonella-free pig on the farm and the (possibly) Salmonella-positive environment outside (or indeed inside) the pigs' dwelling, including any cleaning and disinfection routines. Biosecurity would include the maintenance of any pig housing, good hygiene during

production (in particular good manure management that decreases pig exposure to contaminated faeces), cleaning and disinfection between batches of pigs, and storage of feed to prevent it being accessed by birds and rodents (e.g. open storage/non silos). Also important, and related to biosecurity, is whether the pig is kept indoors or outdoors. Outdoor production has become more popular for large-scale production within the last couple of decades (especially in the UK) and has particular differences to inside production that could affect Salmonella introduction and transmission; for example exposure to wildlife including birds and rodents, mixing of sows and type of feed. However, according to analysis of the UK data collected as part of the EFSA breeding survey (EFSA, 2009a; Hill, prep) large-scale outside production is still quite rare in the UK beyond the stage of weaning (see Figure 1.3).

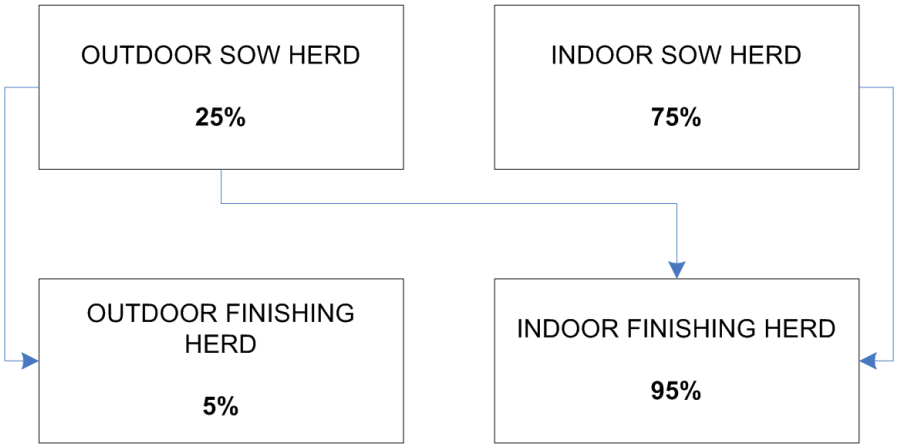

Figure 1.3: Proportion of UK pig production herd (by head) kept indoors and outdoors.

The production system factors identified previously are probably important to consider regardless of the particular infectious organism. However, for Salmonella introduction and transmission we are also interested in two other factors: feed and flooring. Feed can be a source of Salmonella infection in pigs, however it can also be a factor in reducing the level of transmission (Lo Fo Wong and Hald,

2000; O'Connor et al., 2008). Clearly contaminated feed poses a risk to pigs, and has been highlighted as probably the main cause of infection in regions where Salmonella infection in pigs is low (e.g. some Scandinavian countries) (EFSA, 2006, 2008a, 2010c), but the relationship between feed and Salmonella infection in pigs is complex. Within the UK, the serotypes commonly associated with feed contamination (e.g. *S.* Agona, *S.* Mbandaku) are not usually those which are commonly associated with pig infection, such as *S.* Typhimurium and *S.* Derby (EFSA, 2008a). As with management systems, feeding systems are variable between farms. The main factor with relevance to Salmonella transmission appears to be the way in which the feed affects the pH and content of organic acids in the pig gut (O'Connor et al., 2008; Wales et al., 2010). There will be variation in the type of food used, the additives used, and how the feed is presented to the pigs (meal/mash/pellets/grinding). All of these factors affect the ecology of the pig gut. The lower the pH the more hostile the environment for any Salmonella, and hence infection is less likely. Of particular importance is whether the feed is presented as a dry or wet form, or whether it is pelleted or non-pelleted (Lo Fo Wong and Hald, 2000; O'Connor et al., 2008).

While the evidence for flooring type affecting Salmonella transmission is varied (some studies point to it as a risk factor, most don't) (lo fo Wong et al., 2004; Nollet et al., 2004), logical thinking suggests that slatted flooring may well have some effect as it will remove faeces/Salmonella from the pig environment. Again, there are many flooring types (partially slatted, bare concrete, straw-laden), which will all have different characteristics in preventing/aiding exposure of pigs to faecal material. Based on the previous discussion, the five main risk factors considered for large pig farm management are: rearing stages; AIAO vs continuous production; feed; flooring and finally inside vs outside production.

There are other factors that may well influence Salmonella introduction and transmission (e.g. stocking density, age of building, storage of feed). However, while some of these factors have been identified as risk factors in some studies (e.g. stocking density, number of pigs on the farm), the evidence is less clear than for the other factors mentioned above. Most other factors are also less descriptive than the ones considered above. For example, it is not clear what drives the increased risk of infection in pigs on larger farms, but there could be an underlying factor regarding management of these farms which is driving this increased risk (above and beyond that larger farms may have a lower propobability of stochastic fade-out). However, if we do not know the underlying risk factor, we cannot model it. We therefore consider the most appropriate course of action to model the five main factors, and highlight where appropriate where other factors that have not been modelled may contribute to the variation in the likelihood of infection.

1.3 Disease transmission models

This section will provide the rationale for the use of the models chosen in the later chapters. Previous models in the area of Salmonella in pigs will also be reviewed; advantageous characteristics of these models will be used and expanded in later chapters.

1.3.1 Deterministic transmission models

Definition

The main characteristic of a deterministic model is that given a unique set of initial conditions and parameters, the model will always produce the same outcome, with no random variation. Hence, if the initial conditions and model system are known then we can always predict the outcome of the model. For example, $E = MC^2$ is a determinstic model that predicts with extreme precision the energy of an electron given that the mass of an electron is known to high precision and speed of light is known with complete precision.

Overview of determinstic disease transmission modelling

Many biological phenomena can be described by recursion relations, also called difference equations (e.g. $n_{k+2} = n_k + n_{k+1}$), including cell division, plant growth and the logarithmic spirals on the abalone *Haliotis*. Such difference equations have also been applied to epidemic growth of disease in humans and animals. The earliest account of mathematical modelling applied to disease spread (disease transmission modelling) was by Daniel Bernoulli in 1766, on the subject of inoculation against smallpox. One of the most famous advances made by subsequent mathematicians and physicists was by A. G. McKendrick and W. O. Kermack, who proposed a simple (by today's standards) deterministic (compartmental) model which predicted the spread of disease within a closed population (assuming a homogeneous population with no age or social structure), over continuous time. Three population states are considered: Susceptible (S), Infected (I) and Recovered (R). This type of model is hence known as a SIR model. The change in the population of

Susceptible, Infected and Recovered over time is given by

$$\begin{aligned} \frac{dS}{dt} &= -\beta SI \\ \frac{dI}{dt} &= \beta SI - \gamma I \\ \frac{dR}{dt} &= \gamma I \end{aligned} \tag{1.1}$$

where β and γ are constants defining the rate at which humans/animals in Susceptible and Infected states are infected and recover respectively. Many authors also use the term force of infection, which is denoted as λ and is equal to βI.

A key value derived from the above equations is the epidemiological threshold, R_0, and is defined as follows

$$R_0 = \frac{\beta S}{\gamma} \tag{1.2}$$

In equilibrium, this epidemiological threshold is one of the most important measures in epidemiology, and defines the number of secondary infections caused by a single primary infection (before the primary infection's recovery). If $R_0 < 1$, then each infected human/animal produces less than one new infection, so the outbreak will eventually die out. However, when $R_0 > 1$ then the number of new persons/animals infected is one or more, and hence the outbreak will continue and expand.

The basic SIR model described above was not commonly used until two seminal papers by Anderson and May (Anderson and May, 1979; May and Anderson, 1979). They redeveloped the SIR model to include the dynamics of birth and death (i.e. a

changing population) and indirect transmission. Since then, a number of variations of the basic SIR model have been developed. The epidemiological threshold R_0 can be re-formulated for each. However, there are three main categories of SIR model depending on the disease characteristics. They are typically called SIR, SIS and SEIR models (where E represents the number in a population that have been exposed/infected, but are not yet infectious to others). They are shown schematically in Figure 1.4.

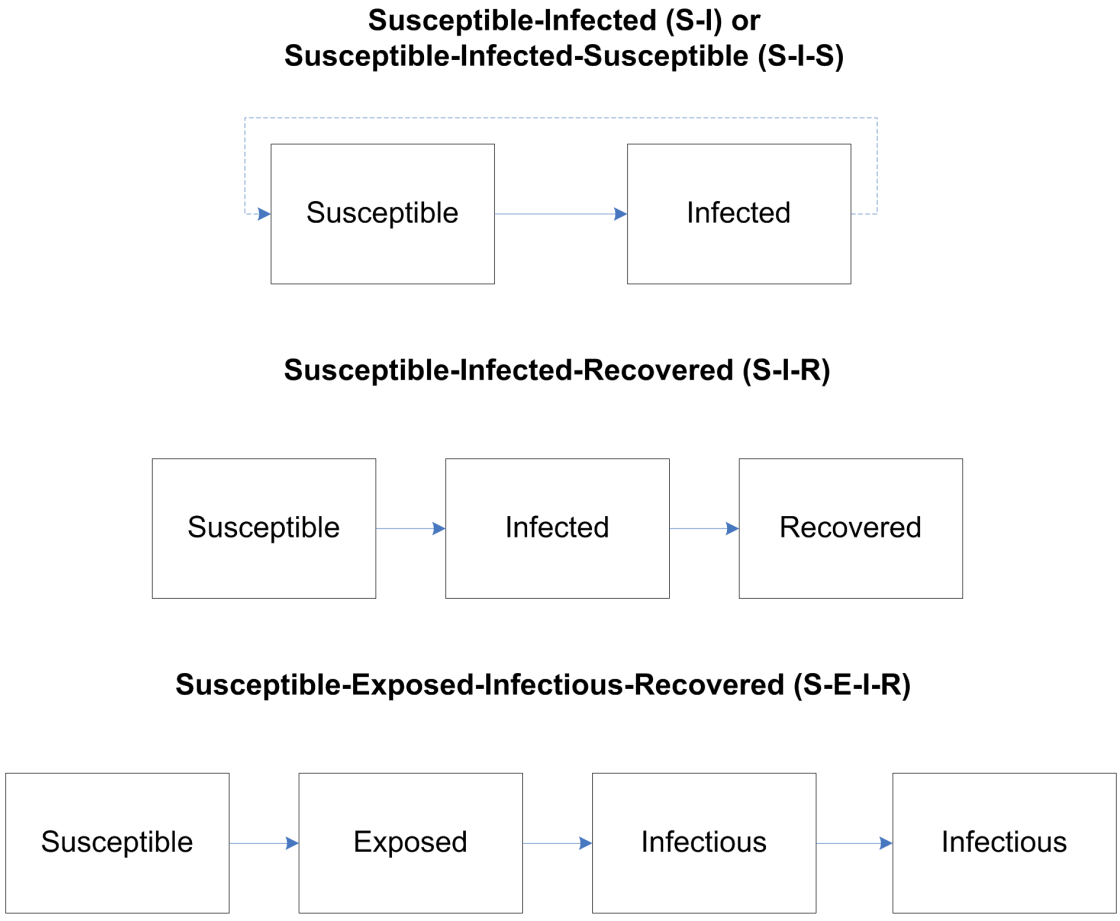

Figure 1.4: Some of the main compartment types for disease transmission models. The model used depends on the assumptions made about the disease characteristics.

The models developed in this thesis are extensions of the broad principles laid down by McKendrick & Kermack and Anderson & May. Previous models in the

area of Salmonella in pigs have also followed similar approaches (see Section 1.3.4).

Discrete and continuous time

Discrete time is the discontinuation of a system's time domain by sampling at a finite level, such that time is measured and sampled in appropriately measurable units, such as seconds, minutes, days or weeks. By contrast, continuous time assumes that time is infinitely divisible. The key difference we are concerned with is that continuous time is represented by the use of differential equations (potentially with other continuous variables), whereas discrete time is associated with difference equations, such as that given in the example at the top of Section 1.3.1.

A simple example is that of radioactive decay, where the number of particles left after time t, N, is given by the formula $N = N_0 e^{-\lambda t}$. As radioactive decay is one of the most perfect examples of random decay known, then the formula can predict N to a high accuracy and in theory we are able to plot N against continuous time. However, while gamma ray detectors are capable of measuring decays occurring less than a nanosecond apart, estimates of λ are usually made by measuring the number of decays per second (in units of bequerels). Hence, an appropriate difference equation to represent the decay of atoms over time is $N_{t+1} = N_t - n_t$, where n_t is the number of decays recorded per second. Reducing the time step to ms or μs will improve the accuracy of the λ estimate, but for many radioactive isotopes with a half-life of more than one hour it is not necessary.

A very simple but compelling reason to use discrete time is that biological phenomena can commonly be most conveniently measured over fixed time intervals: for example, the population of a species on a yearly basis, or the proportion of

individuals with a specific gene in the n^{th} generation. In addition, numerical solutions of difference equations can be used to approximate the solution to a complex differential equation, such as those commonly associated with disease transmission models, where the overarching function is not known, or it is not possible to analytically solve the functions for $S(t)$, $I(t)$ etc....

For deterministic models discrete time difference equations are usually sufficient. However, when dealing with stochastic (probabilistic) models the use of continuous time is more common, as continuous time is an intrinsic property of many probability distributions used in stochastic modelling (see next section).

1.3.2 Linear stability analysis

Equation (1.1) is a set of non-linear partial difference equations. The non-linearity of the term SI can lead to an intractable analytical solution for such a set of equations. However, key properties of a biological system may be investigated by linearising the system to produce a set of linear difference equations. A key analytical method is that of determining steady state solutions, that is when there is no change in the system, for example when $\frac{dS}{dt} = \frac{dI}{dt} = \frac{dC}{dt} = 0$ in Equation (1.1). Generally, a steady state solution satisfies the recursion relation $x_{n+1} = x_n = \bar{x}$, where $\bar{x}$ defines the steady state value of x.

Such a property may seem of marginal interest for systems which describe population growth or disease transmission, but by looking at the stability of such steady states important insight can often be generated into the behaviour of a system. For example, it can be of value to know if a system is unstable so that we may expect change in the near future.

There are two types of steady state: stable and unstable. A steady state is defined as stable if neighbouring states are attracted to it, and unstable if the opposite is true. This property of stable and unstable steady states allows us to investigate the non-linear system in question. We assume a sufficiently small perturbation away from the steady state $\bar{x}$, such that the change in x, dx, is approximated by the linearised version of the non-linear model.

The theory of linear analysis is appropriate for investigating whether the steady state $\bar{x}$ is attractive or repulsive. A recursion relation such as $x_{n+1} = ax_n$ will have solutions of the form

$$x_n = C\lambda^n, \tag{1.3}$$

where λ is the eigenvalue of the system. The theory of linear analysis states that where there are two or more solutions, then any linear combination of these eigenvalues λ_1, λ_2 etc. . . is again a solution. These eigenvalues are fundamental in determining steady states such as $\bar{x}$. As can be seen in Equation (1.3) if $\lambda > 1$ then x_n will become progressively larger as n increases, but will decrease if $\lambda < 1$. This same principle can be applied to the linearised systems of non-linear recursion equations such as Equation (1.1) to identify if small perturbations to steady states of the system will grow ($\lambda > 1$, unstable) or decay back to the steady state ($\lambda < 1$, stable). If there are two or more solutions, the largest valued eigenvalue will tend to govern the dynamics of the system. Further detail on the method for linear stability analysis is given in Chapter 2.

1.3.3 Stochastic transmission models

Definition

The models proposed by McKendrick & Kermack and Anderson & May are deterministic, i.e. the state of the population (number of Susceptibles, Infecteds etc...) at some time t can be predicted with complete accuracy if the prior state of the population at a previous time is known. Such models are useful for large populations, where random effects are averaged out according to the law of large numbers. However, random processes tend to dominate when dealing with small numbers, such as the number of pigs commonly grouped in one pen.

There is some debate over whether the physics of nature is at some base level deterministic or non-deterministic, that is even if all of the processes of a physical system are completely known, whether or not the state of the system can be predicted with complete certainty. If so then randomness is simply an artefact of our incomplete knowledge. However, what is certain is that random processes are especially important in biological mechanisms, as the complexity of such systems means that complete knowledge of the system is virtually impossible (e.g. the height of a human is not only determined by complex genetic factors, but also years of accumulated environmental stresses, the combination of which makes it impossible to know/model with complete certainty the eventual height of any person).

A stochastic model therefore takes into account variability in the model pathway, where the time to the next event, or which event will occur next, is uncertain. In such circumstances the number of the population being modelled at any one time can be modelled by an appropriate probability distribution.

Analytical solutions

In certain circumstances, stochastic models can be solved analytically. One of the simplest and most common examples is of a birth process of single-celled organisms from a starting point of $N(0)$ organisms (see Renshaw (1991)). Treating the problem determinstically, then we can assume a constant birth rate λ, where in a small time interal h there are precisely λh organisms produced. Solving the resultant equations for the number of organisms alive at time t, $N(t)$, leads to

$$N(t) = N(0)e^{\lambda t}$$

.

That is, the population of organisms grows exponentially. However, in a stochastic treatment of the same problem we do not assume that there is a constant predictable production of organisms. Given a population of cells that grow by division we cannot say that within any particular time interval that a particular cell will divide, only that there is a certain probability of division. By using an appropriately small time interval h, we can ensure that the probability of more than one birth is negligible, such that the population size in between $(t, t+h)$ is either $N(t)+1$ (with probability $\lambda h N$) or $N(t)$ (with probability $1-\lambda h N$). The solution of the resultant equation for $N(t)$ is more complicated but can be analytically solved, leading to a negative binomial distribution of the number of organisms at time t, where the probability that the population is of size N at time t, $p(t)$, is given by

$$p(t) = \binom{N-1}{n_0-1} e^{-\lambda n_0 t} \left(1-e^{-\lambda t}\right)^{N-n_0} \quad (N = n_0, n_0+1, \dots) \tag{1.4}$$

Such an analytical solution requires a substantial amount of algebraic manipulation, even given that this is a very simple system considering only idealised growth of organisms, which makes a number of biologically implausible assumptions (e.g. there is no death process, and no maximum capacity of organisms due to nutrient and space contstraints). Analytical solutions are possible for more complicated models including predator/prey and disease transmission models, but in many circumstances any biologically plausible model cannot be solved analytically. When this point is reached it is necessary to use numerical simulation.

Numerical solutions

There are many simulation methods, but all have the same objective: to reconstruct the analytically intractable probability distribution of the output by generating large numbers of indivudal realisations of the system process and then combining the results into a probability distribution that in theory should reflect the variability in the true output.

A simulation typically has the following steps: define the range of inputs; generate inputs randomly from input probability distributions; perform a deterministic computation of the output; aggregate the results into the final probability mass function. The joint probability distribution is estimated by constructing the probability mass function of the output, where the probability of the output lying in the range X is determined by the frequency with which the output from the many distributions lay within the range X. That is, $P(x = X) = \frac{N(x=X)}{N}$, where N is the number of iterations, and $N(x = X)$ is the number of iterations where the output fell within the range X.

One of the most common methods for simulation is Monte Carlo simulation. This

uses a random number generator to determine the random variables for each of the input distributions on each iteration, and constructs the probability mass function directly as described above. A large number of iterations are run in order to ensure the full range of each input probability distribution has been sampled. Convergence criteria are used to ensure that the resulting output probability distribution is stable to additional iteration results. There are no absolute criteria that must be used, but typical criteria used are, for example, less than 1.5% deviation from the mean, or 5th/95th, percentiles of the output distribution after a further 500 iterations runtime.

There are other simulation methods, for example Latin Hypercube sampling, which bin the range of each of the input probability distributions, and then ensures that each section of the probability distribution is sampled at the correct frequency. This method can reduce the number of iterations necessary for convergence of the model, as the model is forced to pick values from all sections of the range, when low-frequency parts of an input distribution may be missed.

The stochastic birth process example in Section 1.3.3 can be simulated numerically by considering the inter-event time, in this case the time between each birth. The time S to the next event is an exponentially distributed random variable where

$$Pr(S \geq s) = e^{-\lambda N s} \ (s \geq 0),$$

To simulate a value of s we select a uniformly distributed random number, Y, in the range (0,1) and put $e^{-\lambda NS} = Y$. Rearranging then

$$s = \frac{-[log_e(Y)]}{\lambda N}.$$

Using this algortihm then a large number of iterations to simulate $N(t)$ (10,000 or more) will then converge upon the anaytically derived mean and variance for $N(t)$ from Equation (1.4) (Renshaw, 1991).

The model above is a continuous time model. However, as described above in Section 1.3.1 discrete time is commonly used in disease transmission models. Stochastic models can also be developed for these discrete time models and numerically simulated, using the formula in Equation (1.5).

Discrete- and continuous-time stochastic models

Discrete and continuous time have the same definitions when applied to stochastic modelling as for deterministic modelling. A common example of a stochastic continuous time model is a simple predator-prey model (as discussed in Murray (2008); Law and Kelton (2000)), which can be analytically solved, e.g. the change in prey population over time, $x(t)$, where one formulation can be given by $\frac{dx}{dt} = rx(t) - ax(t)y(t)$, where $x(t)$ denotes the prey population over time and r and a are random variables describing the growth rate and predation rate of the prey respectively.

The above predator-prey model is theoretically a continuous model, where it is possible to solve for $x(t)$ and $y(t)$ and the outputs will be real numbers. However, in reality the numbers of predator and prey are integers, and therefore discrete. Hence, some rounding function would be required to produce realistic discrete outputs. This is a simple and common example of where both continuous and discrete elements are required in a model to produce realistic outputs. Most reasonably complex simulation models will require a combination of discrete and continuous events occurring (or at least quasi-continuous). For example, the model described

in Chapter 6 has clearly discrete time events (e.g. the number of pigs infected in a timestep of one day), but also arguably continuous time state events (e.g. the shedding of large numbers of Salmonella into the environment reaching some threshold at an indeterminate time where infection of pigs leads to higher magnitudes of shedding). In reality, these combined discrete-continuous models are typically solved numerically, where continuous time is approximated using discrete-event simulation, such as Monte-Carlo simulation. This discrete-event method is used in Chapter 6.

Markov Chains

Both stochastic models described in Chapters 5 and 6 are too complex to be solved analytically and so must be solved with numerical simulation, and specifically are implemented using Markov Chains and Monte Carlo simulation.

In a discrete time model, the state of the system over time can be described by a chain of events based on the probabilities associated with transition. Such a model is called a Markov Chain model, after the Russian mathematician Andrey Markov. A simple graphical representation of a Markov Chain is given in Figure 1.5 for the SIR model. The primary attribute of a Markov Chain is the Markov property, which is that the probability of transition is independent of all that has occurred in previous timesteps, and therefore is only dependent on the current model state.

Common probability distributions used in stochastic disease transmission modelling

There are a range of random, or stochastic, processes that have been mathematically described. Two important processes for disease transmission modelling are

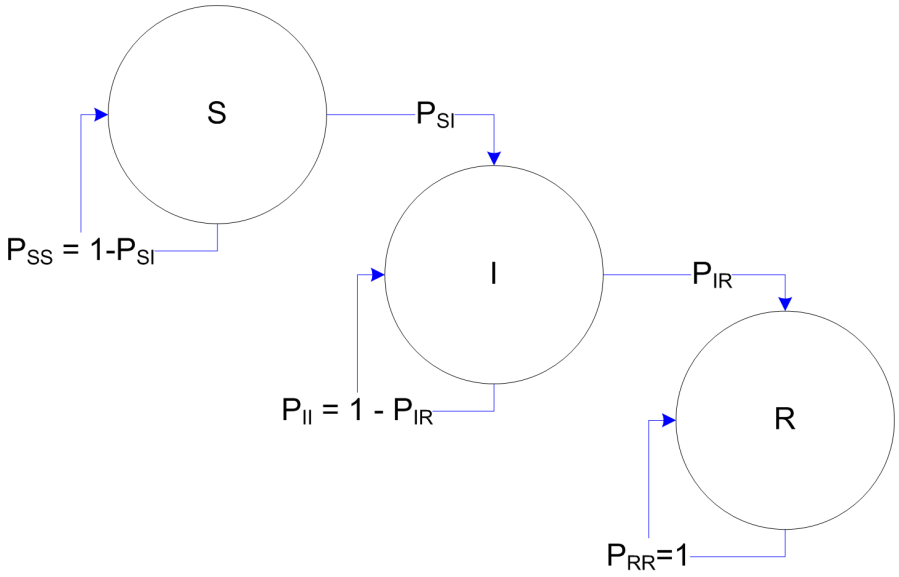

Figure 1.5: A simple example of a Markov Chain applied to the SIR model, where the chain of events is described by the probabilities of transition between states, and S, I and R are the number of individuals in each state.

the Binomial and Poisson processes.

The application of randomness to the SIR models described in Section 1.3.1 was first proposed by Reed & Frost in 1927 (although never formally published) and then re-formulated by Fine (1977). The rate of transition between Susceptible and Infected, $\lambda(t)$, can be given by

$$\lambda(t) = 1 - (1-p)^{I(t)}, \tag{1.5}$$

where p is the probability of an effective contact (i.e. sufficient for infection to occur) between a Susceptible and Infected person/animal, and $I(t)$ is the number of infecteds at time t. If the number of Susceptibles is defined as $S(t)$, then the number of newly Infecteds at the next timestep, $NI(t+1)$, can be described as a Binomial random variable, where

$$NI\left(t+1\right)=B\left(S\left(t\right),\lambda\left(t\right)\right). \tag{1.6}$$

The probability of an event which has two outcomes can be described by the binomial probability, where the probability of obtaining exactly k successes in n trials is

$$P\left(X=k\right)=\binom{n}{k}p^{k}\left(1-p\right)^{(n-k)}, \tag{1.7}$$

where p is the probability of success and $\binom{n}{k}=\frac{n!}{k!(n-k)!}$. Such a system can be used to represent the probability of transition from Susceptible $\rightarrow$ Infected or Infected $\rightarrow$ Recovered etc ... An inherent trait of the Binomial theorem is that it retains no memory of previous timesteps, i.e. the probability of transition depends only on the state of the system at that time point, and is independent of all prior timepoints, which meets the requirement of the Markov property. We can therefore use the Binomial process to determine the number transferring between states in a Markov Chain, and this is indeed the main methodology behind much of the stochastic modelling in this thesis.

The Binomial process produces discrete outcomes from a discrete number of trials (e.g. the number of infected animals and the number of animals respectively). As such, the Binomial process is technically the correct process for the majority of processes that occur in the models in this thesis (e.g. the number of infections per day, the number of organisms transferred between pens). However, the statistical algorithms used to generate random variables from the Binomial process are computationally expensive. When the number of events is sufficiently large, the Poisson process is a very good approximation of the Binomial process (the Pois-

son process is derived from the Binomial process, and letting $t \to 0$). Using the Poisson process to generate random variables is relatively much quicker than the corresponding Binomial calculations. Therefore, where events commonly involve more than 100 'events' we replace the Binomial process with the Poisson process (100 was chosen as a reasonable compromise between speed and accuracy of the calculation).

The probability of obtaining k events in the interval $(t, t+\tau]$ of some continuum (e.g. time) is

$$P\left[N\left(N\left(t+\tau\right)-N\left(t\right)\right)=k\right]=\frac{e^{-\lambda\tau}\left(\lambda\tau\right)^{k}}{k!}$$

where λ is the rate parameter, such that the expected number of events per interval is $\lambda\tau$.

1.3.4 Previous models for Salmonella in pigs

The first dedicated transmission models for Salmonella in pigs were published in 2004 (van der Gaag et al., 2004; Ivanek et al., 2004). Both are based on the traditional SIR model, although Ivanek et al. use a deterministic approach while van der Gaag takes a stochastic approach. The model of Ivanek et al. (2004) describes the transmission of infection in a deterministic manner via the introduction of one pig into a herd of grower-finisher pigs, which are housed in one barn, with no separation by pens. At any time, pigs may be in one of four states: susceptible, latent, infected and carrier. It is a basic SEIR model, dealing with a closed population of pigs over a defined period of time, where the recovered state is replaced with a carrier phase (C). A schematic representation of the model is given in Figure 1.6.

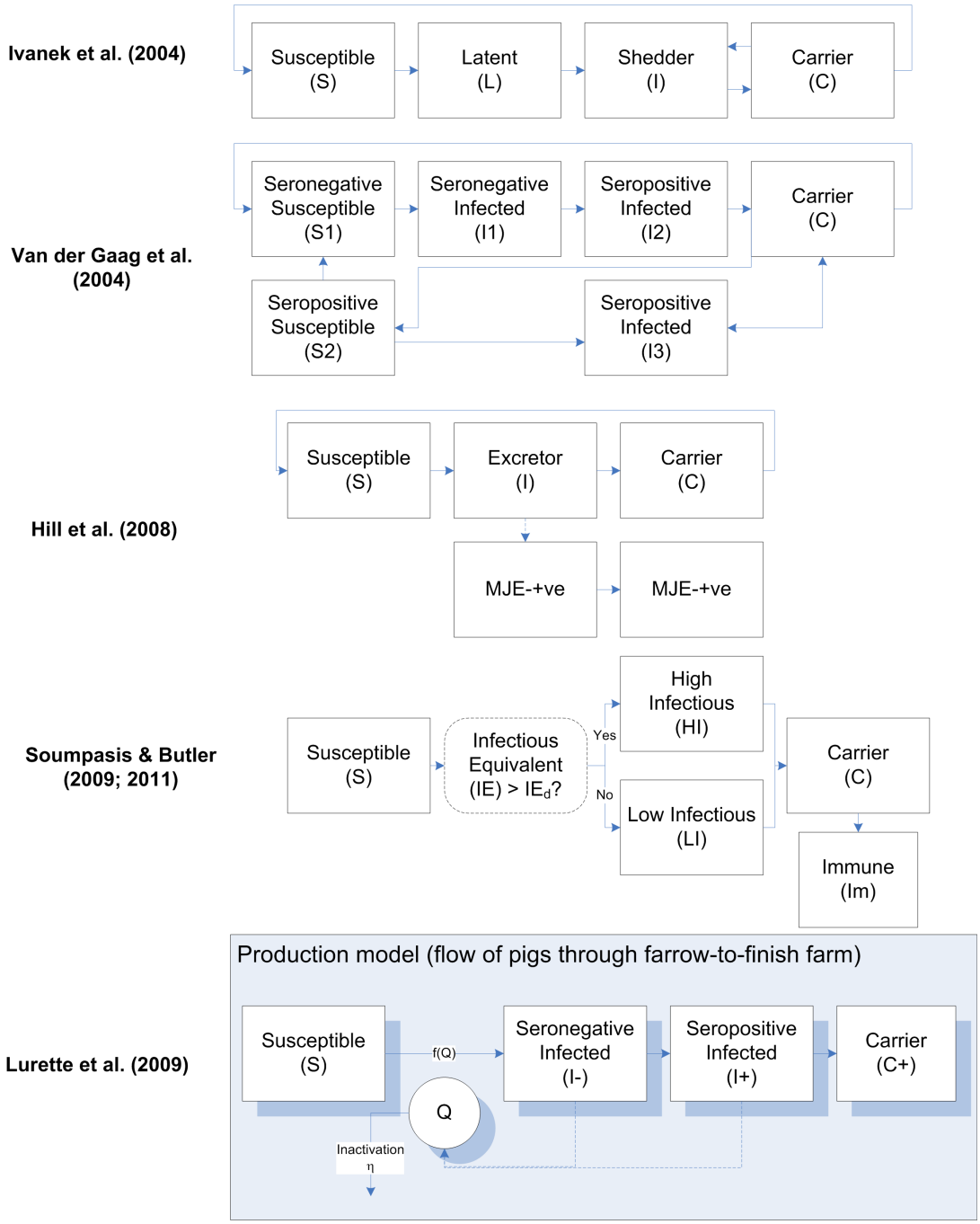

Figure 1.6: State transitions of previous Salmonella in pigs models Ivanek et al. (2004); van der Gaag et al. (2004); Hill et al. (2008); Lurette et al. (2008a); Soumpasis and Butler (2009).

van der Gaag's farm transmission model is part of a larger stochastic farm-to-slaughter model, including both multiplying and finishing herds, and is an individual-

based model, following 100 pigs in one cohort from birth to slaughter (and the subsequent processing of the carcasses). van der Gaag separates infection into four states and susceptibility into two as described in Figure 1.6. Pigs may be susceptible and serologically-negative (S1), infectious and serologically-negative (I1), infectious and serologically-positive (I2), carriers and serologically-positive (C), recovered and susceptible and serologically-positive (S2) and finally re-infected and infectious (I3). There are probabilities associated with transitions between all states, and the probability of initial infection (S1 $\rightarrow$ I1) is assumed to be dependent not only on the number of infected animals in the cohort, but also feed contamination and external sources of infection (wildlife etc...). Sojourn times in each state are assumed to be exponentially-distributed, for example the probability of the transition I1 $\rightarrow$ I2 is governed by the equation $1 - e^{-\delta}$, where $\delta = 1/$seroconversion period (1/day).

These first two models were important steps in the field, especially van der Gaag's, which includes serology and the penning of pigs for the first time. Both produce reasonable results in terms of the number of pigs infected at the point of slaughter (around 10-20%). However, both these models are limited in their applicability to intervention analysis, given their reliance on abstract transmission parameters describing the probabilities of transition. While the van der Gaag model does differentiate between infection from pigs and from the environment, the parameter estimation is necessarily based on expert opinion due to a lack of relevant data to apportion infection between sources.

The next development came from an individual-based model for British grower-finisher production by Hill et al. (2008). This model had a similar scope to van der Gaag et al. (2004), including both serological response and penning of pigs. However, once a pig had been infected, it was assumed that serological conversion was

then independent of the course of infection (see Figure 1.6), whereas van der Gaag et al. (2004) assumed there was a clear dependence between progression of disease and serological response. Analysis of observational data (Kranker et al., 2003) suggests that the exponentially-distributed sojourn time between Infected and Carrier in the van der Gaag et al. (2004) model leads to a much quicker transition than what occurs in reality. The Hill model therefore assumes the sojourn times between Excretor and Carrier, and Carrier and Susceptible are Weibull-distributed. The major difference in assumption is that Hill et al assume that transfer between states becomes more likely as time progresses, whereas Ivanek and van der Gaag assume a constant rate of transfer between states. The assumption of a varying hazard function in the Hill model effectively violates the Markov property, as the probability of transition is no longer memoryless. Another development within the Hill model is the inclusion of continuous production, where pigs are introduced continually over the rearing period. This also removes the simplifying assumption of a closed population of the original SIR model. The removal of the assumptions of a memoryless system and closed population make the model far more complex than preceding models. However, the inclusion of continuous production (very common in Great Britain) and the modelling of a varying hazard function reflects real-world data more realistically. Hill et al. (2008) also attempt to estimate the transmission parameter β from data for the first time. The UK monitoring programme in place at the time (the Zoonoses Action Plan) was a Meat Juice ELISA (MJE) based monitoring programme conducted at the abattoir for a large majority of British pig herds. The model was anchored to fit observational data on the prevalence of MJE-positive pigs, by adjusting the values for the within and between pen transmission parameters.

A regularly updated transmission model for finishing pigs has been developed by

Soumpasis & Butler (Soumpasis and Butler, 2009, 2011). The main difference between this group of models and the models described above is the distinction between high dose and low dose infection. This is a sensible development, given several papers note that pigs shed more salmonellas if they are infected at a higher dose (Fedorka-Cray et al., 1994; Jensen et al., 2006). The Infected class is therefore split into two states, High Infectious (HI) and Low Infectious (LI). Whether pigs are infected with a high or low dose is decided by the "Infectious Equivalent" (IE), which is a proxy for the environmental load of Salmonella. The equation given for IE is

$$IE = \frac{HI + \epsilon * LI}{N}$$

where ϵ is a reduced transmissibility rate to reduce the level of β when the model is governed by Low Infection dynamics. Hence, once IE rises above a certain threshold, IE_d, the model switches to the High Infection dynamics, and all infected pigs after this point transfer to the HI state rather than the LI state. This switching between two dynamics has the result of speeding up the epidemic once infection reaches a certain level. Stochasticity is incorporated into the model via the "τ-leap method". Rather than taking each pig and determining whether it makes a transition from one state to another on any given time step, the number of "events", or pigs that transfer from one particular state to another, is assumed to be Poisson distributed. For example, the number of High Infection events ($S \rightarrow HI$) per day is given by Poisson($\beta * S * IE$) (if $IE > IE_d$). Further work anchored the model to a field study to give more realistic parameter estimates.

Finally, a very detailed model has been developed by Lurette et al. (2008a,b, 2009), which first models the production of pigs through a farrow-to-finish farm (including

the mixing of pigs at weaning, and the mixing of pigs towards the end of finishing when underweight pigs are transferred to a group of pigs of similar weight), and then overlays the transmission of Salmonella on top of this production model. Such a model is much more realistic in mimicking the contacts of pigs with others, if at the expense of complexity. The transmission model is also very complex; Lurette et al assume that pigs will shed a relatively high load of Salmonella while they remain seronegative (transition $S \rightarrow I-$), but much less when the pig seroconverts ($I- \rightarrow I+$) (see Figure 1.6). They also consider the environmental contamination of the pen (Q) by the shedding of the infected pigs. This environmental contamination model is more detailed than the one by Soumpasis & Butler, including a decay function (η) that removes contamination to the pen environment. The probability of infection is dose-dependent (ie. it is a function of Q), although the dose-response function is arbitrarily constructed from expert opinion.

Since the models of van der Gaag et al. (2004) and Ivanek et al. (2004), there has been an obvious improvement and increase in complexity as authors have strived to create more realistic models. Several key issues for intervention analysis have been addressed with varying levels of success, including dose-dependency (in various forms) and modelling of the production system. Several key factors of these models (e.g. dose-dependent shedding, modelling of the environment and the flow of pigs on the farm) should be captured in the models developed in this thesis. However, there is also plenty of scope for advancing the methodology of Salmonella in pig transmission modelling, not least in bringing to bear new data sources to more accurately model the source of infection and parameterise the model using UK production system data.

1.4 Thesis motivation and outline

As discussed in Section 1.1, the presence of Salmonella in pigs at slaughter has been assessed as one of the most important food safety priorities at a national and EU level. While intervention is to be a food-chain wide approach, the EU has made it clear that the focus of intervention is on reducing the prevalence of Salmonella infection in pigs at slaughter. Indeed, the targets to be set by the EU once the evidence gathering phase is complete are to be measured using lymph-node infection at slaughter (at the time of writing, the EU have just received the final piece of required evidence, the cost-benefit analysis for breeding pigs (FCC, 2011)) . Therefore, most National Control Plans, including the UK's, will probably focus on on-farm interventions (whether at the breeding or fattening farm).

The aim of this thesis is to develop a series of transmission models capable of assessing the effect of on-farm interventions on British pig farms. In the previous section models for Salmonella in pigs were briefly reviewed. We conclude that the production/transmission model by Lurette et al. (2008a,b) represents the most relevant model for Salmonella in pig intervention analyses. As such, developments made by Lurette et al have been the main inclusions in the model development described throughout this thesis.

The chapters in this thesis are arranged to demonstrate the natural progression in complexity and accuracy of the transmission models. Chapters 2 and 3 describe progressively more detailed (1-, 2- and multi-pen) deterministic transmission models, building on the original principles set out by Ivanek et al. (2004), and using standard SIR/compartment model methodology. The models developed in these chapters are analysed analytically and numerically. The former has not been carried out in such detail before. The special conditions of local and global stability

at equilibrium are solved analytically for all three models, and allow insight in the dynamics of the transmission via relatively straightforward mathematics. In Chapter 3, concerning the multi-pen model, the model is also analysed spatially to identify the existence of any Turing spatial patterns or the existence of any travelling waves. The epidemic curve for each model is derived numerically and these results are used to check and strengthen the analytical solutions for equilibrium and stability/spatial patterns.

In Chapter 4 the transmission parameters within the standard multi-pen model (Chapter 3) are replaced by explicitly including faecal shedding of Salmonella (the new model is denoted as the "cross-contamination" model). A dose-response function is also incorporated to determine the probability of infection given exposure to environmental contamination. The model is formulated deterministically, and so again stability conditions are determined, and the existence of spatial patterns or travelling waves are investigated. As before, numerical solutions are also found to derive an epidemic curve and strengthen the analytical results.

Chapter 5 re-formulates the standard and cross-contamination multi-pen models into stochastic models. This is carried out by assuming the number of newly infected pigs at each time step can be estimated by an equation similar to that described in Equation (1.6). In addition, the numbers of pigs making the Excretor $\rightarrow$ Carrier state transition are assumed to be distributed according to the Weibull distribution. Numerical simulations are provided and contrasted with the results from the deterministic models. The stochastic version of the standard multi-pen model is a modification of the Hill model described above (Hill et al., 2008).

In Chapter 6 the stochastic environment model is developed further, including a more detailed version of environmental contamination and subsequent pig expo-

sure. Three primary sources of infection are considered: faecal shedding by pigs; feed contamination and external contamination of the environment (by wildlife such as rodents or birds). Similar to the model of Lurette et al. (2008a,b) the transmission model runs on top of a new generic production model describing the flow of pigs, designed to be used by any EU MS (in this thesis it is parameterised for the UK). The production model enables the modelling of 56 farm types, and extends the range of production back to farrowing on the breeding farms, so that the initial time of infection can be modelled, rather than concentrating only on the fattening herd.

The penultimate chapter (Chapter 7) focuses on the use of the final production/transmission model for intervention analysis. As the model from Chapter 6 is designed from the outset to assess interventions, a wide range of interventions can be modelled. The wider results of the intervention analyses were ultimately included and interpreted in an EFSA Scientific Opinion (EFSA, 2010c), which is to be used as a cornerstone of the evidence base for setting the targets each MS will be set to reduce the prevalence of infection in slaughter pigs.

In Chapter 8 a discussion on the advantages and disadvantages of the models developed over the chapters, and where future improvements could be made, is provided. The impact of the results of the models developed in this thesis for policy-making is discussed.

Chapter 2

One- and two-pen deterministic models

2.1 Introduction

The aim of this chapter is to describe the first and second in a series of transmission models for Salmonella in pigs which are suitable for intervention analysis. In Section 1.3 several published transmission models for Salmonella in pigs have been discussed. The simplest of these is by Ivanek et al. (2004), and is proposed as the starting point for the series of models in this thesis (i.e. the 1-pen model discussed directly below in Section 2.2). The model is re-constructed here with some modifications, as the foundation for further model development in later chapters. Following on from Ivanek et al. (2004), the modifications are applicable to the grower-finisher stage of production.

Factors likely to affect the transmission of Salmonella in a grower-finisher herd include whether the pigs are reared indoors or outdoors, the number of sources from

which a farmer buys their pigs, and (importantly for modelling considerations) whether a farm is run on an All-In-All-Out (AIAO) or continuous basis (Berends et al., 1996). Even strict AIAO practices are likely to break the assumption of typical SIR models that the population is closed. This means the closed, singly housed population of the one-pen model described in Section 2.2 is unrealistic. Therefore, two updates to the one-pen model are relevant: first, we model penned housing, which is ubiquitous on UK pig farms; and two, we model continuous production (or the movement of pigs on and off the farm over the time period of the model). The number and placement of pens within a pig house are highly variable, but typically there may be 10-20 pens in one house. Therefore, as a first step to investigating multiple penning beyond the single pen description, and the inclusion of penned populations, a two-pen model is described and then analysed.

2.2 1-pen model

2.2.1 Model definition

The mechanisms of Salmonella transmission between pigs have been discussed in detail in Section 1.1. Briefly, the dominant mechanism is thought to be the faecal-oral route, with some potential for airborne transmission (Fedorka-Cray et al., 1994; Gray et al., 1996; Lo Fo Wong and Hald, 2000; Proux et al., 2001). Hence, an SIR model, where the force of infection, λ, is directly proportional to the number of infected pigs within the pen/herd, is applicable as a first order approximation. Explicitly, $\lambda = \beta I$, where β is the probability of an effective contact between an excreting and susceptible pig and I is the number of excreting pigs within the population (for clarity the term infection is reserved as an all-encompassing term

including both shedding and non-shedding pigs that are infected in the lymph nodes). There will also be some recovery from Salmonella infection over time, first to a carrier state, where pigs remain infected (within the lymph nodes) but do not excrete the organism (equivalent to the Recovered state in a traditional SIR model), and then finally back to the Susceptible state. According to Bailey (1975) the timestep of the model should be equivalent to the average latent period of infection. In the case of Salmonella in pigs, this period of latency is around 24-48 hours (Straw et al., 1999). Using a timestep of 1 day means that there is no need to include the latent state, as it is captured implicitly. Therefore, there are three states: Susceptible (S), Excretor (I) and Carrier (C). The total number of pigs within a pen, n, is assumed to be constant (and is equal to $S + I + C = n$). The number of pigs within each state at time t will be governed by the transition rates between Susceptible-Excretor ($\lambda = \beta I$), Excretor-Carrier (γ) and Carrier-Susceptible (δ). For one pen, Equation (2.1) can be used to describe the change in the number of pigs within each state over time t

$$\begin{aligned} \frac{dS}{dt} &= -\beta SI + \delta C, \\ \frac{dI}{dt} &= \beta SI - \gamma I, \\ \frac{dC}{dt} &= \gamma I - \delta C. \end{aligned} \tag{2.1}$$

For ease of analysis, we non-dimensionalise this set of Ordinary Differential Equations (ODEs), where time t is the independent variable (in units of days) and S, I and C are the dependent variables in units of number of pigs. Replacing each of the variables by writing $S = \tilde{S}\langle S\rangle$, $I = \tilde{I}\langle I\rangle$, $C = \tilde{C}\langle C\rangle$ we get

$$\begin{aligned}
\frac{d\tilde{S}\langle S\rangle}{dt} &= -\beta\tilde{S}\langle S\rangle\tilde{I}\langle I\rangle + \delta\tilde{C}\langle C\rangle, \\
\frac{d\tilde{I}\langle I\rangle}{dt} &= \beta\tilde{S}\langle S\rangle\tilde{I}\langle I\rangle - \gamma\tilde{I}\langle I\rangle, \\
\frac{d\tilde{C}\langle C\rangle}{dt} &= \gamma\tilde{I}\langle I\rangle - \delta\tilde{C}\langle C\rangle.
\end{aligned} \tag{2.2}$$

On setting $\langle S\rangle = \langle I\rangle = \langle C\rangle = n$ and $\tilde{\beta} = \beta n$, Equation (2.2) reduces to

$$\begin{aligned}
\frac{d\tilde{S}}{dt} &= -\tilde{\beta}\tilde{S}\tilde{I} + \delta\left(1 - \tilde{S} - \tilde{I}\right), \\
\frac{d\tilde{I}}{dt} &= \tilde{\beta}\tilde{S}\tilde{I} - \gamma\tilde{I},
\end{aligned} \tag{2.3}$$

where $\tilde{S}$ and $\tilde{I} \in [0, 1]$ are the non-dimensionalised proportions of pigs in either the Susceptible or Excretor state respectively in a pen of n pigs, and we have used $\tilde{C} = 1 - \tilde{S} - \tilde{I}$. For convenience the tilde notation is dropped and S, I etc... are taken to denote the non-dimensionlised versions of the model variables and parameters. The rescaled model is investigated analytically in the next section using stability analysis methods.

2.2.2 Stability analysis

Equilibrium solutions

An equilibrium solution is when the $\frac{d}{dt}$ terms in Equation (2.3) are zero. We denote the equilibrium solutions by $S = S^*$ and $I = I^*$. Setting the $\frac{d}{dt}$ terms in Equation (2.3) to zero and solving the corresponding algebraic equations simultaneously the

following equilibrium points can be found

$$(S^*, I^*) = \begin{cases} (1,0) \\ \left(\frac{\gamma}{\beta}, \frac{\delta(\beta-\gamma)}{\beta(\gamma+\delta)}\right) \end{cases} \tag{2.4}$$

We refer to the first steady state (i.e. $(1,0)$) as the fully-susceptible steady state, and the second steady state (i.e. $\left(\frac{\gamma}{\beta}, \frac{\delta(\beta-\gamma)}{\beta(\gamma+\delta)}\right)$) as the infected steady state.

Local stability

We now explore the stability of these two equilibria, by exploring the linear stability of these states. If any small deviation from the equilibrium points S^*, I^* is considered then the system can be approximated by an appropriately linearised system (Roussel, 2005). Generally, if we have a set of autonomous ODEs, for example

$$\dot{\mathbf{x}} = \mathbf{f}(\mathbf{x}),$$

where $\dot{\mathbf{x}}$ is shorthand notation for $\frac{d\mathbf{x}}{dt}$. If $\mathbf{x}^* = \{x_1^*, x_2^*, \ldots, x_n^*\} \in \mathbb{R}^n$ is an equilibrium point and $\mathbf{dx} = \mathbf{x} - \mathbf{x}^*$ is the displacement from $\mathbf{x}^*$, then the multivariate Taylor expansion of $\mathbf{f}(\mathbf{x})$ is as follows

$$\dot{\mathbf{x}} = \mathbf{f}(\mathbf{x}^*) + \left.\frac{\partial \mathbf{f}}{\partial \mathbf{x}}\right|_{\mathbf{x}^*} (\mathbf{x} - \mathbf{x}^*) + \left.\frac{\partial^2 \mathbf{f}}{\partial \mathbf{x}^2}\right|_{\mathbf{x}^*} \frac{(\mathbf{x} - \mathbf{x}^*)^2}{2!} + \ldots$$

By definition the first term of this equation is zero at equilibrium. For local stability we are only interested in small deviations away from $\mathbf{x}^*$, i.e. when $\mathbf{dx}$ is small. Hence, we assume that only the second term is significant and we can

ignore the subsequent terms as being small. The leading order system can be collected in matrix form to give the Jacobian matrix, $\mathbf{J}$. Given the state vector $\mathbf{x} = (x_1, x_2, \ldots, x_n)$ and rate vector $\mathbf{f} = (f_1, f_2, \ldots, f_n)$ then

$$\mathbf{J} = \left| \begin{array}{ccc} \frac{\partial f_1}{\partial x_1} & \cdots & \frac{\partial f_1}{\partial x_n} \\ \vdots & \cdots & \vdots \\ \frac{\partial f_n}{\partial x_1} & \cdots & \frac{\partial f_n}{\partial x_n} \end{array} \right\|_{\mathbf{x}=\mathbf{x}^*}.$$

The solution of the leading order system can be written as a superposition of terms in the form $e^{\mu t}$, where $\{\mu\}$ are the set of eigenvalues of the Jacobian. If eigenvalues of the Jacobian are complex, then the complex part simply contributes an oscillatory component to the solution. Hence, it is only the real parts of the eigenvalues that are important to determine asymptotic stability, as this shows whether the scale of $d\mathbf{x}$ grows (one or more eigenvalues have a positive real part) or diminishes (all eigenvalues have a negative real part). Hence, if all eigenvalues have negative real parts then $\partial\mathbf{x} \to 0$ as $t \to \infty$ and the equilibrium point $\mathbf{x}^*$ is locally stable; otherwise $\partial\mathbf{x}$ will grow and x^* will be unstable.

Specifically for the system considered in Equation (2.3) then the Jacobian matrix for the 1-pen system is as follows.

$$\mathbf{J} = \left[\begin{array}{cc} -\beta I^* - \delta & -\beta S^* - \delta \\ \beta I^* & \beta S^* - \gamma \end{array} \right].$$

Substituting the equilibrium solutions from Equation (2.4) in turn then gives the following:

Equilibirum 1: $(S^*, I^*) = (1,0)$

$$\mathbf{J_1} = \begin{bmatrix} -\delta & -\beta - \delta \\ 0 & \beta - \gamma \end{bmatrix}.$$

This matrix is upper triangular, hence the diagonal entries of $\mathbf{J_1}$ are the eigenvalues of this first equilibrium point. As both δ and β are real and positive then $-\delta$ is always negative. Therefore, the first equilibrium point will be stable if $\gamma > \beta$. This makes sense intuitively as this means that the fully-susceptible steady state is stable if the rate of recovery is greater than the rate of transmission, which biologically would ensure that infection would die out.

EQUILIBRIUM 2: $(S^*, I^*) = \left(\frac{\gamma}{\delta}, \frac{\delta(\beta-\gamma)}{\beta(\gamma+\delta)}\right)$

The Jacobian at the second equilibrium point is

$$\mathbf{J_2} = \begin{bmatrix} -\frac{\delta(\beta-\gamma)}{(\gamma+\delta)} - \delta & -\gamma - \delta \\ \frac{\delta(\beta-\gamma)}{(\gamma+\delta)} & 0 \end{bmatrix}.$$

$\mathbf{J_2}$ can be converted to a lower triangular matrix by switching rows. Hence,

$$\mathbf{J_2} = \begin{bmatrix} \frac{\delta(\beta-\gamma)}{(\gamma+\delta)} & 0 \\ -\frac{\delta(\beta-\gamma)}{(\gamma+\delta)} - \delta & -\gamma - \delta \end{bmatrix}.$$

Given the row switch, stability is reached when the top diagonal eigenvalue is positive and the lower diagonal eigenvalue is negative. Therefore as the lower diagonal eigenvalue of $\mathbf{J_2}$ is always negative ($-\gamma - \delta < 0$), the second equilibrium is stable if $\frac{\delta(\beta-\gamma)}{(\gamma+\delta)}$, i.e. if $\beta > \gamma$. In summary, the 1-pen system will settle to the fully susceptible steady state if $\gamma > \beta$ and to the infected steady state if $\beta > \gamma$.

Global stability

In the section above we have investigated stability of the 1-pen system in the localised region of the steady state (i.e. for small displacements from (S^*, I^*)). However, for planar systems we can also use phase-plane plots to assess the global stability. Phase plane plots for the 1-pen system can easily be constructed using the direction field plot capability in Maple (Maplesoft, 2010). We investigate global stability of the 1 pen system by constructing phase-plots in (S, I) space with different $(S(0), I(0))$ initial conditions in the Susceptible ($\gamma > \beta$) and infected ($\beta > \gamma$) cases (see Figure 2.1). The yellow curves indicate the trajectory towards the fully-susceptible and infected steady states from the initial conditions (S, I): $(0.4, 0.1)$,$(0, 0.9)$ and $(0.7, 0.3)$ (only three initial points are shown in each case for clarity; similar asymptotic behaviour is observed for all initial conditions investigated.). We therefore conclude that the system appears to be globally stable under the same conditions for local stability.

2.2.3 Numerical solution

The parameter estimates are listed in Table 2.1.

Table 2.1: Parameter estimates for the deterministic models

Notation	Description	Value	Reference
β ($\tilde{\beta}n$)	Probability of an effective contact between a susceptible and infected pig	0.4	Dent et al. (2009)
γ ($\tilde{\gamma}$)	Rate of transition from Excretor to Carrier	0.038 days^{-1}	Kranker et al. (2003); Gray et al. (1995)
δ ($\tilde{\delta}$)	Rate of transition from Carrier to Susceptible	0.022 days^{-1}	Gray et al. (1995)

The values for the probabilities of effective contact are taken from analysis carried

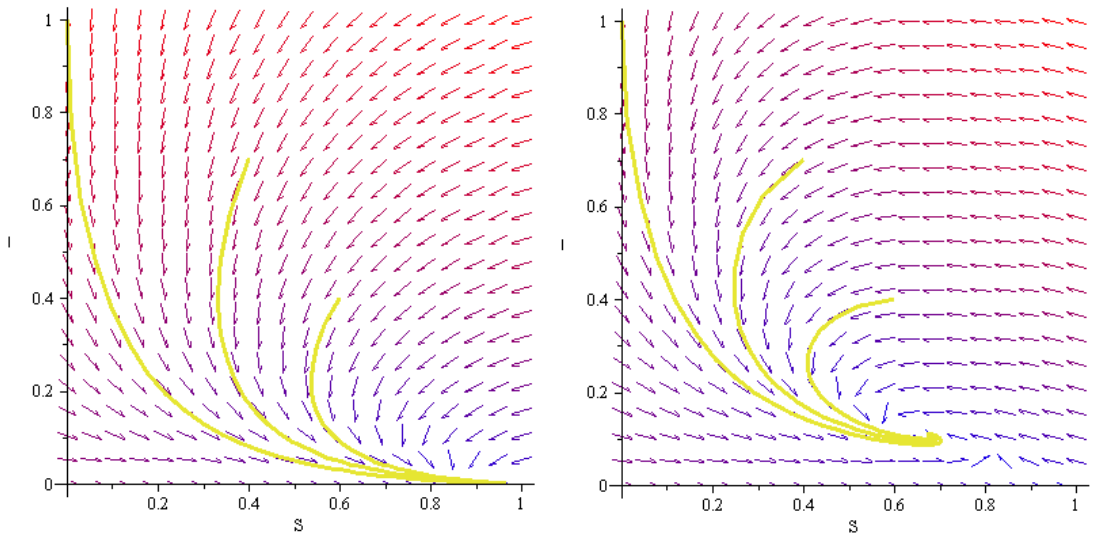

Figure 2.1: Direction field plots for the trivial and non-trivial steady states of the 1-pen system. Both stability conditions are invariant to initial conditions for S and I. For the trivial steady state phase plot (left hand side) then $\beta = 0.2, \gamma = 0.3$ and $\delta = 0.1$, and for the non-trivial steady state (right hand side) then $\beta = 0.3, \gamma = 0.2$ and $\delta = 0.1$.

out on a British longitudinal study of Salmonella in pigs (Dent et al., 2009). The rate of transition between Excretor and Carrier, γ, is the reciprocal of the average duration of shedding Salmonella. Pigs are likely to intermittently shed Salmonella after one-two weeks of infection (Kranker et al., 2003; Nollet et al., 2005). As a simplifying assumption, it is assumed that pigs that intermittently shed Salmonella shed relatively little Salmonella compared to newly infected pigs, and hence can be ignored for the purposes of modelling transmission at this stage. Taking this into account, several studies estimate the average duration of shedding of Salmonella by pigs. Kranker et al. (2003) and Gray et al. (1996) both estimate an approximate duration of shedding of 26 days. Therefore, $\gamma = 1/26 = 0.0385\text{d}^{-1}$.

The rate of transition between Carrier and Susceptible, δ, is the reciprocal of the average duration of Salmonella carriage (i.e. the pig is infected in the lymph node, but not shedding Salmonella). Concordant with the assumption made regarding

intermittent shedding above, it is assumed that the duration of carriage includes the period of intermittent shedding, and any remaining time after complete cessation of Salmonella excretion in which the pig is still infected in the lymph nodes. No data are available for the duration of the intermittent-shedding/carrier status; however, a study by Gray et al. (1995) estimated the average *total* time of infection as 70 days. Since the length of the shedding period is known, an estimate for the duration of carrier status is obtained by subtracting the duration of the infection from the total time of infection, which gives 44 days. Therefore $\delta = 1/44 = 0.022\text{d}^{-1}$.

For simplicity it was assumed that all pigs in a pen are susceptible except the one which has entered the Excretor state, therefore at $t = 0$ then $I = \frac{1}{40}$ and $S = 1 - \frac{1}{40}$ (using the dimensionless versions of I and S).

Given the current parameter estimation then $\beta = 0.40$ ($\tilde{\beta}n = 0.01 * 40$) and $\gamma = 0.038$. Hence, we would expect that the system should settle to the infected steady state ($\tilde{\beta} > \gamma$), where $S^* = \frac{\gamma}{\tilde{\beta}} = 0.095$ and $I^* = \frac{\delta\left(\tilde{\beta}-\gamma\right)}{\tilde{\beta}(\gamma+\delta)} = 0.332$.

The solution curves are obtained by numerically solving Equation (2.3) in MATLAB (MATLAB 2011a, The MathWorks Inc., Natick, MA, 2011) using the ODE45 solver. With the current parameter estimation, the one-pen model produces the epidemic curve as shown in Figure 2.2. As indicated by the linear analysis above, the epidemic reaches an infected equilibrium towards the end of the rearing period (80-90 days).

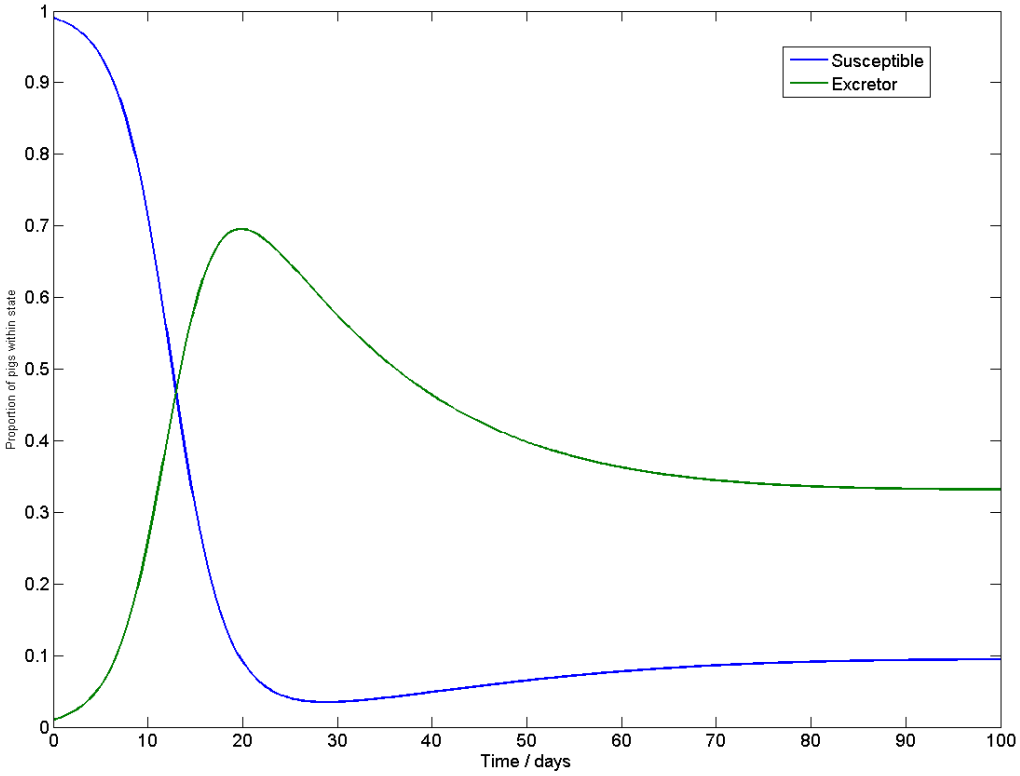

Figure 2.2: Time course of infection within one pen of 40 pigs with no outside force of infection. Parameter values are given in Table 2.1

2.2.4 Summary

The one-pen model is a gross simplification of the reality of pig farming and the spread of Salmonella between pigs, but provides a simple foundation on which to build. Carriers do not contribute to infection in any way; they are not contributing to the level of Salmonella in the environment (represented by β) and are not available for infection. Hence, stability of the system does not depend on Carriers. If the rate of infection (β) is greater than the rate of ceasing shedding (γ), then the dynamics of infection within one pen are of a rapid transmission of infection between pigs in the pen, followed by a steady state of excretion. If $\gamma < \beta$, then

any infection will rapidly fade away.

The one-pen model is identical to that of Ivanek et al. (2004), save for the removal of a latent stage of infection. However, the epidemic curves produced by both models are significantly different, due to the parameter estimation and initial conditions. Ivanek et al. (2004) assume a much higher proportion of Excretors in the initial conditions, a much lower probability of an effective contact (β), and almost double the average duration of shedding. The parameter estimates β and γ were updated in this model due to new longitudinal data (and subsequent statistical analysis) not available at the time of the development of the Ivanek model.

2.3 Two-pen deterministic model

2.3.1 Model definition

The inclusion of multiple pens means there must be consideration of the interaction between pigs from different pens. As transmission predominantly occurs via the faecal-oral route, it was considered reasonable as a first assumption that faecal material from excreting pigs will largely remain within the pen that contains the pigs from which the contaminated faeces originate, but that there will be leakage of contamination via some process (for example, airborne contamination, cleaning of pens, farmer incursion). For a two-pen system Equation (2.1) can be modified to give the system in Equation (2.5)

$$
\begin{aligned}
\frac{dS_1}{dt} &= -\beta_1 S_1 I_1 - \beta_2 S_1 I_2 + \delta C_1, \\
\frac{dS_2}{dt} &= -\beta_1 S_2 I_2 - \beta_2 S_2 I_1 + \delta C_2, \\
\frac{dI_1}{dt} &= \beta_1 S_1 I_1 + \beta_2 S_1 I_2 - \gamma I_1, \\
\frac{dI_2}{dt} &= \beta_1 S_2 I_2 + \beta_2 S_2 I_1 - \gamma I_2, \\
\frac{dC_1}{dt} &= \gamma I_1 - \delta C_1, \\
\frac{dC_2}{dt} &= \gamma I_2 - \delta C_2,
\end{aligned}
\tag{2.5}
$$

where β_1 and β_2 denote the probability of an effective contact between a susceptible and excreting pig within the same pen, and an excreting and susceptible pig within adjacent pens respectively, we expect that $\beta_1 > \beta_2$. The variables S_1, I_1, C_1, S_2, I_2 and C_2 represent the number of pigs within each state within the first (subscript 1) and second (subscript 2) pens. The force of infection for this 2-pen system is for pen 1,2 $\lambda_1 = \beta_1 I_1 + \beta_2 I_2$, $\lambda_2 = \beta_1 I_2 + \beta_2 I_1$ respectively.

Re-scaling Equation (2.5) in a similar fashion as for the one-pen system (where $\langle S_1 \rangle = \langle I_1 \rangle = \langle C_1 \rangle = \langle S_2 \rangle = \langle I_2 \rangle = \langle C_2 \rangle = n$) then

$$
\begin{aligned}
\frac{d\tilde{S}_1}{d\tilde{t}\langle t\rangle} &= -\frac{\beta_1}{n}\tilde{S}_1\tilde{I}_1 - \frac{\beta_2}{n}\tilde{S}_1\tilde{I}_2 + \delta C_1,\\
\frac{d\tilde{S}_2}{d\tilde{t}\langle t\rangle} &= -\frac{\beta_1}{n}\tilde{S}_2\tilde{I}_2 - \frac{\beta_2}{n}\tilde{S}_2\tilde{I}_1 + \delta C_2,\\
\frac{d\tilde{I}_1}{d\tilde{t}\langle t\rangle} &= \frac{\beta_1}{n}\tilde{S}_1\tilde{I}_1 + \frac{\beta_2}{n}\tilde{S}_1\tilde{I}_2 - \gamma\tilde{I}_1,\\
\frac{d\tilde{I}_2}{d\tilde{t}\langle t\rangle} &= \frac{\beta_1}{n}\tilde{S}_2\tilde{I}_2 + \frac{\beta_2}{n}\tilde{S}_2\tilde{I}_1 - \gamma\tilde{I}_2,\\
\frac{dC_1}{d\tilde{t}\langle t\rangle} &= \gamma\tilde{I}_1 - \delta C_1,\\
\frac{dC_2}{d\tilde{t}\langle t\rangle} &= \gamma\tilde{I}_2 - \delta C_2.
\end{aligned}
\tag{2.6}
$$

Setting $\tilde{\beta}_1 = \beta_1 n$, $\langle t\rangle = \frac{1}{\beta_1 n}$, $\tilde{\beta}_2 = \frac{\beta_2}{\beta_1}$, $\tilde{\delta} = \frac{\delta}{\beta_1 n}$ and $\tilde{\gamma} = \frac{\gamma}{\beta_1 n}$ leads to Equation (2.7)

$$
\begin{aligned}
\frac{d\tilde{S}_1}{dt} &= -\tilde{S}_1\tilde{I}_1 - \tilde{\beta}_2\tilde{S}_1\tilde{I}_2 + \tilde{\delta}\left(1 - \tilde{S}_1 - \tilde{I}_1\right),\\
\frac{d\tilde{S}_2}{dt} &= -\tilde{S}_2\tilde{I}_2 - \tilde{\beta}_2\tilde{S}_2\tilde{I}_1 + \tilde{\delta}\left(1 - \tilde{S}_2 - \tilde{I}_2\right),\\
\frac{d\tilde{I}_1}{dt} &= \tilde{S}_1\tilde{I}_1 + \tilde{\beta}_2\tilde{S}_1\tilde{I}_2 - \tilde{\gamma}\tilde{I}_1,\\
\frac{d\tilde{I}_2}{dt} &= \tilde{S}_2\tilde{I}_2 + \tilde{\beta}_2\tilde{S}_2\tilde{I}_1 - \tilde{\gamma}\tilde{I}_2.
\end{aligned}
\tag{2.7}
$$

As for the one-pen model the criteria for linear stability are investigated using the non-dimensionalised form of the system in Equation (2.7). Again, for convenience, tildes are dropped from the notation.

2.3.2 Stability analysis

Equilibrium solutions

We denote the equilibrium values by $S_1 = S_1^*, S_2 = S_2^*, I_1 = I_1^*, I_2 = I_2^*$. Setting the $\frac{d}{dt}$ terms in Equation (2.7) to zero, solving the corresponding algebraic equations simultaneously, the following set of equilibrium points are found:

$$(S_1^*, S_2^*, I_1^*, I_2^*) = \begin{cases} (1, 1, 0, 0) \\ \left(\frac{\gamma}{\beta_2+1}, \frac{\gamma}{\beta_2+1}, \frac{\delta(\beta_2-\gamma+1)}{(\beta_2+1)(\delta+\gamma)}, \frac{\delta(\beta_2-\gamma+1)}{(\beta_2+1)(\delta+\gamma)}\right) \\ \left(1 - \frac{I_1^*(\delta+\gamma)}{\delta}, 1 - \frac{I_2^*(\delta+\gamma)}{\delta}, \frac{\delta((1-\beta_2)(1-\beta_2-\gamma)\pm\sqrt{a})}{2(1-\beta_2)(\delta+\gamma)}, \frac{I_1^*((\delta+\gamma)I_1^*-\delta+\delta\gamma)}{\beta_2(\delta-(\delta+\gamma)I_1^*)}\right), \end{cases} \tag{2.8}$$

where $a = (1-\beta_2)^2(1-\beta_2-\gamma)^2 + 4(\beta_2(1-\beta_2)(1-\beta_2-\gamma)$.

Local stability

For the system considered in Equation (2.7), the Jacobian matrix for the 2-pen system is as follows.

$$\mathbf{J} = \begin{bmatrix} -I_1^* - \beta_2 I_2^* - \delta & 0 & -S_1^* - \delta & -\beta_2 S_1^* \\ 0 & -I_2^* - \beta_2 I_1^* - \delta & -\beta_2 S_2^* & -S_2^* - \delta \\ I_1^* + \beta_2 I_2^* & 0 & S_1^* - \gamma & \beta_2 S_1^* \\ 0 & I_2^* + \beta_2 I_1^* & \beta_2 S_2^* & S_2^* - \gamma \end{bmatrix}.$$

As before we now explore linear stability of the equilibria, by exploring the eigenvalues of $\mathbf{J}$ for each equilibrium point in turn.

EQUILIBIRUM 1: $(S_1^*, S_2^*, I_1^*, I_2^*) = (1, 1, 0, 0)$, which we will refer to as the non-infection state.

The Jacobian becomes

$$\mathbf{J}_1' = \begin{bmatrix} -\delta & 0 & -1-\delta & -\beta_2 \\ 0 & -\delta & -\beta_2 & -1-\delta \\ 0 & 0 & 1-\gamma & \beta_2 \\ 0 & 0 & \beta_2 & 1-\gamma \end{bmatrix}.$$

The eigenvalues of $\mathbf{J_1}$ are $(-\beta_2+1-\gamma, \beta_2-\gamma+1, -\delta, -\delta)$. Given that by definition δ is a real and positive number then the third and fourth eigenvalues will always be negative. Hence for the fully susceptible solution $(1, 1, 0, 0)$ to be stable we then require that $-\beta_2 + 1 - \gamma < 0$ and $\beta_2 + 1 - \gamma < 0$. In other words, $\beta_2 > 1 - \gamma$ and $\beta_2 < \gamma - 1$. The non-shaded area in Figure 2.3 represents the region in (β_2, γ) space where these two expressions both hold (in the region $\beta_2 > 0$).

EQUILIBRIUM 2: $(S_1^*, S_2^*, I_1^*, I_2^*) = \left\{ \frac{\gamma}{\beta_2+1}, \frac{\gamma}{\beta_2+1}, \frac{\delta(\beta_2-\gamma+1)}{(\beta_2+1)(\delta+\gamma)}, \frac{\delta(\beta_2-\gamma+1)}{(\beta_2+1)(\delta+\gamma)} \right\}$
, which represents an infection state in which the level of infectivity is the same in both pens.

From which, we obtain the Jacobian

$$\mathbf{J}_2 = \begin{bmatrix} -\psi-\delta & 0 & -\frac{\gamma}{\beta_2+1}-\delta & -\frac{\beta_2\gamma}{\beta_2+1} \\ 0 & -\psi-\delta & -\frac{\beta_2\gamma}{\beta_2+1} & -\frac{\gamma}{\beta_2+1}-\delta \\ \psi & 0 & \frac{\gamma}{\beta_2+1}-\gamma & \frac{\beta_2\gamma}{\beta_2+1} \\ 0 & \psi & \frac{\beta_2\gamma}{\beta_2+1} & \frac{\gamma}{\beta_2+1}-\gamma \end{bmatrix},$$

where $\psi = \frac{\delta(\beta_2+1-\gamma)}{(\delta+\gamma)(\beta_2+1)} + \frac{\beta_2\delta(\beta_2+1-\gamma)}{(\delta+\gamma)(\beta_2+1)}$. The eigenvalues of $\mathbf{J_2}$ are:

$$\lambda_{1,2} = \frac{1}{2(\delta+\gamma)}\left(-\delta\left(\beta_2+1+\delta\right) \pm \sqrt{\delta^2(\beta_2+1+\delta)^2 - 4\delta(\delta+\gamma)^2\left(\beta_2-\gamma+1\right)}\right),$$
$$\lambda_{3,4} = \frac{1}{2(\beta_2+1)(\delta+\gamma)}\left(\Omega \pm \sqrt{\Omega^2 - 4\delta\left(\beta_2+1\right)\left(\beta_2^2+\beta_2\gamma+2\beta_2+1-\gamma\right)\left(\delta+\gamma\right)}\right),$$

where $\Omega = -\left(\delta + \delta\beta_2^2 + 2\beta_2\delta\gamma + \delta^2\beta_2 + 2\gamma^2\beta_2 + \delta + 2\delta\beta_2\right)$.

Since both Ω and $-\delta\left(\beta_2+1+\delta\right)$ are negative then both negative roots of $\lambda_{1,2}$ and $\lambda_{3,4}$ are negative. Inspection of the first term in $\lambda_{1,2}$ highlights that the positive root of $\lambda_{1,2}$ will be negative if the square root term is less than $\delta(\beta_2+1+\delta)$, which will hold if $\beta_2 > \gamma - 1$. Similarly, the positive root of $\lambda_{3,4}$ will be negative if $\beta_2^2 + \beta_2\gamma + 2\beta_2 + 1 - \gamma > 0$. Solving this last quadratic inequality gives:

$$\beta_2 > -\frac{(2+\gamma)}{2} \pm \frac{1}{2}\sqrt{\gamma\left(\gamma+8\right)} = \beta_2^*$$

.

The second equilibrium will therefore be stable provided that $\beta_2 > \beta_2^*$ and $\beta_2 > \gamma - 1$. The region of stability is indicated by the shaded region in Figure 2.3.

Equilibrium 3:

$(S_1^*, S_2^*, I_1^*, I_2^*) = \left(1 - \frac{I_1^*(\delta+\gamma)}{\delta}, 1 - \frac{I_2^*(\delta+\gamma)}{\delta}, \frac{\delta((1-\beta_2)(1-\beta_2-\gamma)\pm\sqrt{a})}{2(1-\beta_2)(\delta+\gamma)}, \frac{I_1^*((\delta+\gamma)I_1^*-\delta+\delta\gamma)}{\beta_2(\delta-(\delta+\gamma)I_1^*)}\right)$, where $a = (1-\beta_2)^2(1-\beta_2-\gamma)^2 + 4(\beta_2(1-\beta_2)(1-\beta_2-\gamma)$. This represents an infection state in which infectivity is different in pens 1 and 2.

Inspection of the steady state equations can shed light on the validity of this third steady state solution. Recall that S_1^*, S_2^*, I_1^*, I_2^* must all lie between 0 and 1, and $\delta, \gamma \geq 0$. We also expect $\beta_2 \in [0,1]$ since this is the rescaled inter-pen infectivity

with respect to β_1 and we assume that $\beta_1 > \beta_2$. We first make an observation about the numerator of I_1^*, which is

$$\delta\left[(1-\beta_2)(1-\beta_2-\gamma) \pm \sqrt{a}\right] =$$
$$\delta(1-\beta_2)(1-\beta_2-\gamma) \pm \sqrt{\delta^2(1-\beta_2)^2(1-\beta_2-\gamma)^2 + 4\delta^2(\beta_2(1-\beta_2)(1-\beta_2-\gamma))}.$$

The square root term will always be greater than $\delta(1-\beta_2)(1-\beta_2-\gamma)$, since $\beta_2 < 1$ and $\beta_2 > 1-\gamma$, hence the negative square root value for I_1^* will be less than zero, which violates the condition that $I_1^* \geq 0$. Thus the negative root is not a valid solution.

We also require that $S_1^* \geq 0$ and $I_1^* \geq 0$. Solving these two inequalities using the equilibrium points for S_1^* and I_2^* as shown above (i.e. $S_1^* = 1 - \frac{I_1^*(\delta+\gamma)}{\delta} > 0$ and $I_2^* = \frac{I_1^*((\delta+\gamma)I_1^* - \delta + \delta\gamma)}{\beta_2(\delta-(\delta+\gamma)I_1^*)} > 0$), after some rearranging gives

$$\frac{\delta}{\delta+\gamma} \geq I_1^* \geq \frac{\delta(1-\gamma)}{\delta+\gamma}. \tag{2.9}$$

Substituting the positive square root expression for I_1^* into Equation (2.9) we then have

$$\begin{aligned} \frac{\delta}{\delta+\gamma} &\geq \frac{\delta\left((1-\beta_2)(1-\beta_2-\gamma)+\sqrt{a}\right)}{2(1-\beta_2)(\delta+\gamma)} \\ &\geq \frac{\delta(1-\gamma)}{\delta+\gamma}. \end{aligned} \tag{2.10}$$

Deleting similar terms from each side of Equation (2.10) and rearranging, we have from the first inequality

$$
\begin{aligned}
2\left(1-\beta_2\right)-\left(1-\beta_2\right)\left(1-\beta_2-\gamma\right) &> \sqrt{a} \\
\Rightarrow \left(1+\gamma-\beta_2^2-\beta_2\gamma\right)^2 &> a \\
\Rightarrow \left(\beta_2-1\right)^2\left(\gamma+\beta+1\right)^2 &> \left(\beta_2-1\right)^2\left(\gamma+\beta+1\right)^2-4\gamma\left(1-\beta_2\right) \\
\Rightarrow 4\gamma\left(1-\beta_2\right) &> 0.
\end{aligned}
$$

Performing a similar rearrangement for the second inequality, we have

$$
\begin{aligned}
\left(\beta_2-1\right)^2\left(\gamma-\beta-1\right)^2 &\leq \left(1-\beta_2\right)^2\left(1-\beta_2-\gamma\right)^2+4\beta_2\left(1-\beta_2\right)\left(1-\beta_2-\gamma\right) \\
\Rightarrow \left(\beta_2-1\right)^2\left(\gamma-\beta-1\right)^2 &\leq \left(\beta_2-1\right)^2\left(\gamma-\beta-1\right)^2+-4\gamma\beta_2^2\left(\beta_2-1\right) \\
\Rightarrow 4\gamma\beta_2^2\left(\beta_2-1\right) &\geq 0.
\end{aligned}
$$

In summary, we have $4\gamma\left(1-\beta_2\right)>0$ and $4\gamma\beta_2^2\left(\beta_2-1\right)\geq 0$. By definition $\gamma>0$ and so the first condition implies that $\beta_2<1$. However employing this in the second condition gives $\beta_2\geq 1$, which is a contradiction and therefore this final steady state solution must be invalid.

Since the third state is not valid, both pens must converge to the same state; either they both settle to the fully-susceptible steady state, or they both settle to an identical infected steady state. That is, there appears to be no capacity in this case for the pens to settle to a steady state where the infection level is different in the pens.

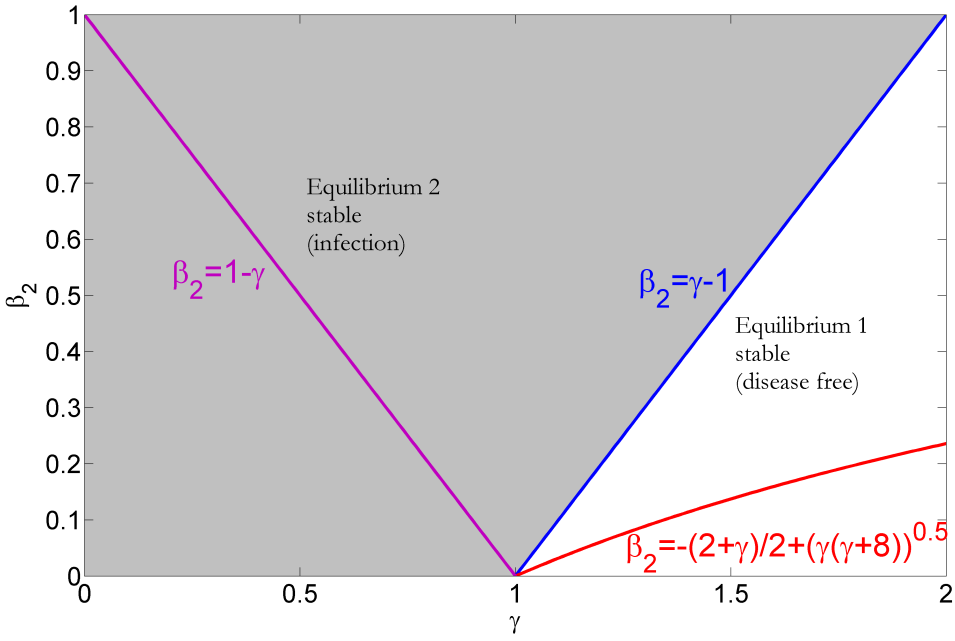

Figure 2.3: The area enclosed by the lines $\beta_2 = 0$ and $\beta_2 = \gamma - 1$ represents the parameter space of $[\beta_2, \gamma]$ when the 2-pen system settles to the non-infected steady state, and the shaded area represents the parameter space when the 2-pen system settles to the infected steady state (Equilibrium 2).

Comparison of stability analysis results against R_0

We can also think of the above result for the stability of the 1-pen and 2-pen systems in terms of the reproductive ratio R_0, which equals:

$$R_0 = \text{ rate of infection } \times \text{ the duration of infection } \times \text{ the number of contacts .}$$

In the unscaled case, the rate of infection is either β or $\beta_1 + \beta_2$, and the average duration of infection is $\frac{1}{\gamma}$. Therefore the basic reproductive ratios for the 1- and 2-pen systems, $R_0(1)$ and $R_0(2)$, are equal to $\frac{\tilde{\beta} n}{\gamma}$ and $\frac{(\tilde{\beta}_1 + \tilde{\beta}_2) n}{\gamma}$ respectively. For an epidemic to continue $R_0(1)$ or $R_0(2)$ must be greater than one, which will only

occur if $\tilde{\beta}n > \gamma$ or $\left(\tilde{\beta}_1 + \tilde{\beta}_2\right) n > \gamma$, which we find are identical to the conditions for the infected steady state in our system.

Phase space plots

The variation in the value of the steady state $\{S_1^*, S_2^*, I_1^*, I_2^*\}$ in the parameter space $[\beta_2, \gamma]$ is shown in Figure 2.4. The transition between the fully-susceptible system and infected steady state occurs at $\beta_2 = \gamma - 1$, represented by the black lines in Figure 2.4 - the susceptible steady state occurs when $\beta_2 < \gamma - 1$. The first thing to observe is that the phase space plots for both pens are identical, confirming that if the pens are to settle to equilibrium they must be at the same level of infection. There is a much steeper gradient in the change of the steady state values for I_1^* and I_2^* than there is S_1^* and S_2^*. The values for I_1^* and I_2^* in the infected steady state are very close to zero for much of the $[\beta_2, \gamma]$ parameter space, whereas there is much more gradual increase in the infected steady state values for S_1^* and S_2^*. This occurs because γ determines the proportion in the Carrier state (C). Hence, as γ increases, so the proportion of Excretors is reduced as most pigs transfer to the Carrier state by the stage of equilibrium. The proportion of Susceptibles is unaffected by this dynamic.

Examples of the dynamics over time as the solutions tend to these two steady states are given in Figure 2.5, where values of β_2 and γ have been selected from the appropriate part of the parameter space of $[\beta_2, \gamma]$. Parameter values for the fully-susceptible graph are $\gamma = 1.8$ and $\beta_2 = 0.8$, and for the infected steady state graph $\gamma = 1.0$ and $\beta_2 = 1.0$. The damped oscillatory pattern as the system settles down to the non-infected state in the left hand plot is apparent (corresponding to complex eigenvalues with negative real components).

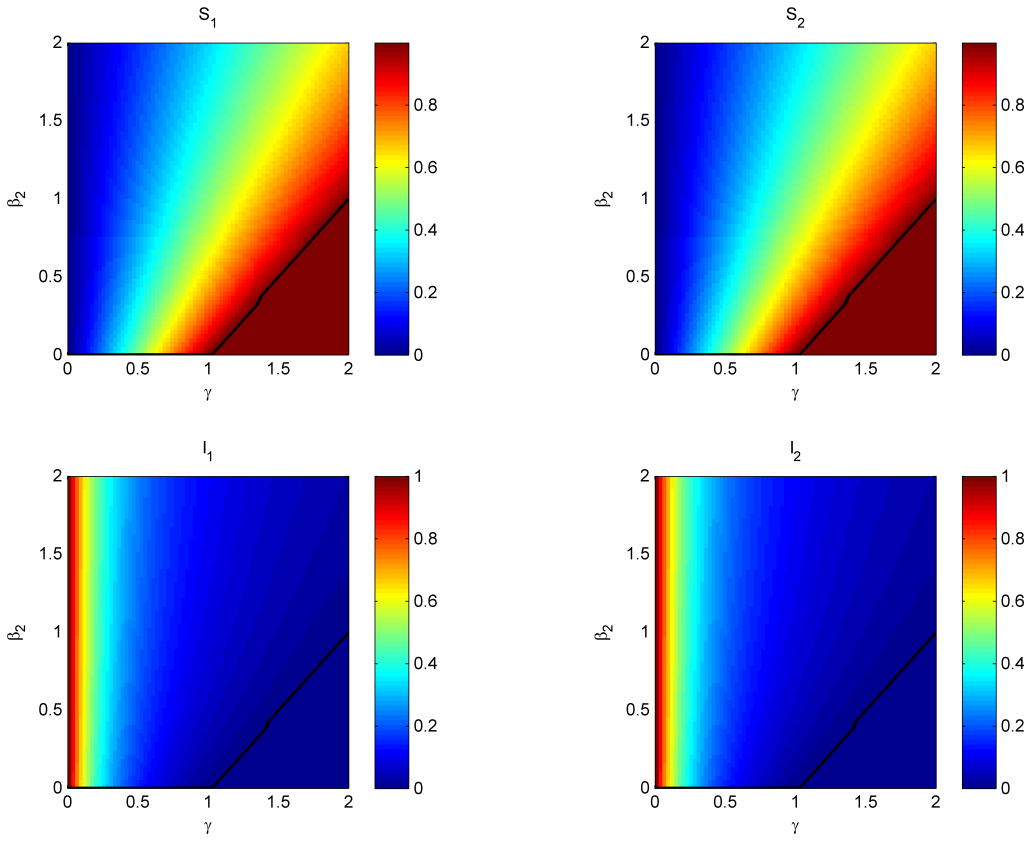

Figure 2.4: Change in the steady state values for $\{S_1^*, S_2^*, I_1^*, I_2^*\}$ over parameter space $[\beta_2, \gamma]$. The black lines represent the intersection $\beta_2 = \gamma - 1$. Parameter values are given in Table 2.1

Global stability

Numerical analysis of the 2-pen system shows that the stability conditions are independent of initial starting conditions for S_1, S_2, I_1 and I_2 (see Figure 2.6 for an example). The contour colour of the surface plots represents the value of I_1^* (top) and I_2^* (bottom) after 200 days. We see that for $\gamma < \beta_2 + 1$ the infected steady state is reached, regardless of the initial level of infecteds, but for $\gamma \geq \beta_2 + 1$ the same susceptible state is reached - again, independent of the intitial state of the system. Direction field plots showing the trajectory of the epidemic curve from

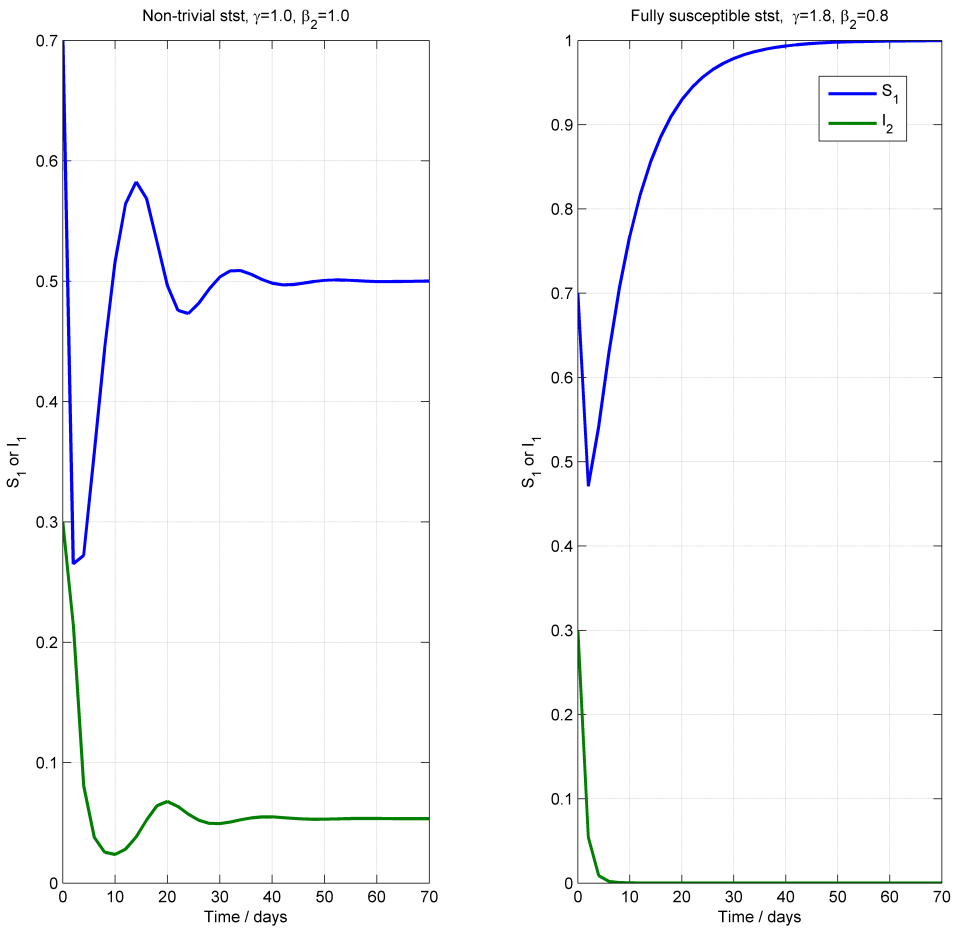

Figure 2.5: Examples of epidemic curves settling down to one of two distinct steady states (fully susceptible or infected) over time, given appropriate values of β_2 and γ. LHS $\gamma = 1$ and $\beta_2 = 1$, RHS $\gamma = 1.8$ and $\beta_2 = 0.8$. The remaining parameters are as in Table 2.1.

initial starting conditions to either the fully-susceptible or infected steady states are shown in Figure 2.7. For the non-infected steady state phase plot (left hand side) then $\beta = 0.1, \gamma = 1.2$ and $\delta = 0.1$, and for the infected steady state (right hand side) then $\beta = 1.2, \gamma = 0.1$ and $\delta = 0.1$. In both cases, the curves all converge to the same suceptible state, for the LHS and RHS respectively, suggesting that the 2-pen system is globally stable under the same conditions as for local stability.

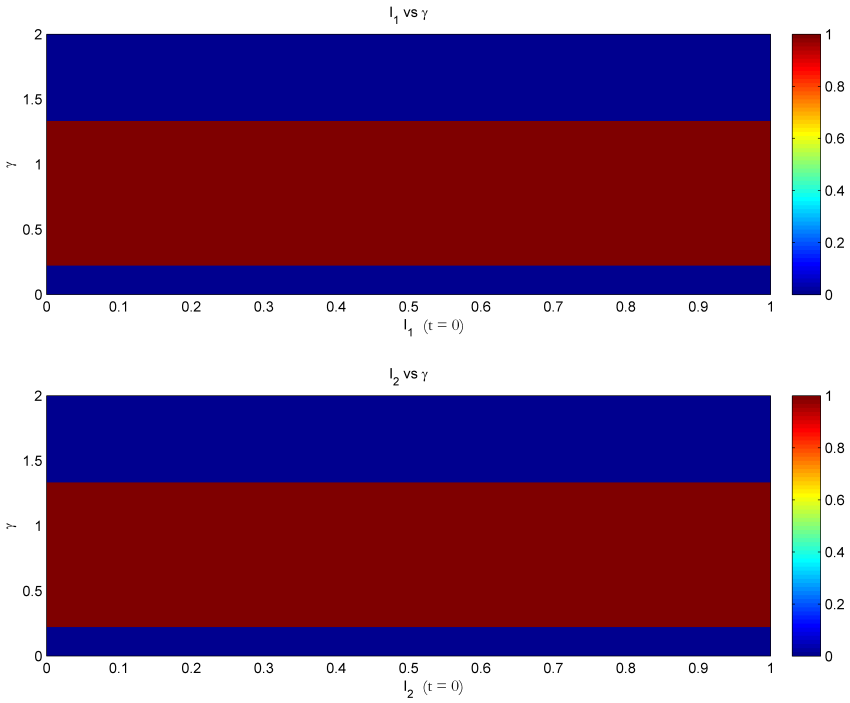

Figure 2.6: Stability conditions are invariant to intitial conditions for S_1, S_2, I_1 and I_2; the particular steady state which the system tends to depends on the value of γ alone. The parameters β_2 and δ determine where the transition from one steady state occur. For these particular simulations $\beta_2 = \delta = 0.2$.

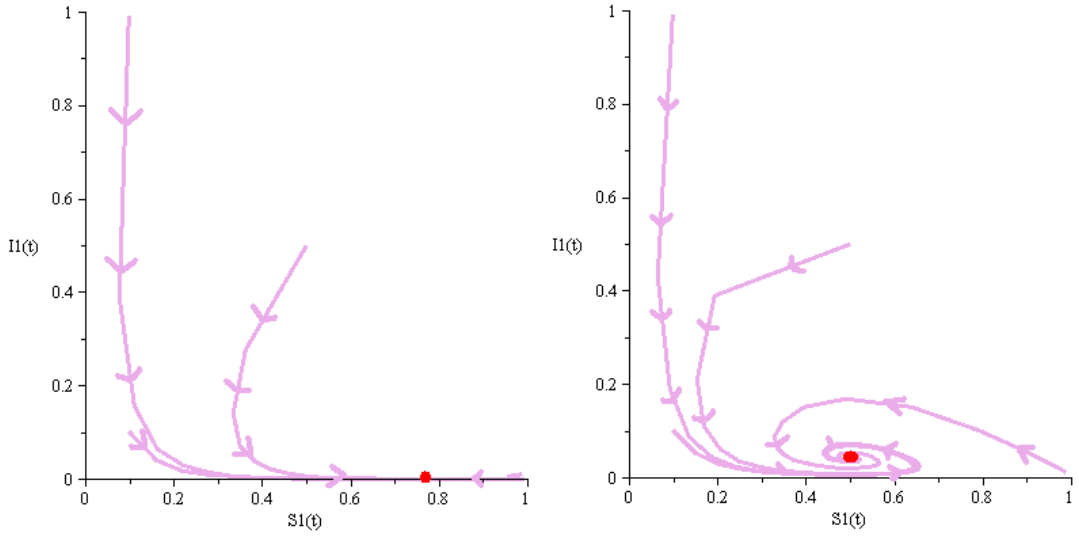

Figure 2.7: The purple lines represent the trajectories of the proportion of susceptible and infected pigs to the steady states in both the trivial (LHS) and non-trivial (RHS) plots. Both stability conditions are invariant to initial conditions for S_1, S_2, I_1 and I_2. The steady state values are represented by red circles. For the non-infected steady state phase plot (left hand side) then $\beta = 0.1, \gamma = 1.2$ and $\delta = 0.1$, and for the infected steady state (right hand side) then $\beta = 1.2, \gamma = 0.1$ and $\delta = 0.1$.

2.3.3 Numerical solution

The parameter estimates are listed in Table 2.2.

Table 2.2: Parameter estimates for the 2-pen deterministic model

Notation (non-scaled)	Description	Value	Reference
β_1	Probability of an effective contact between a susceptible and infected pig in the same pen	0.01	Estimate
β_2 $(\frac{\beta_2}{\beta_1})$	Probability of an effective contact between a susceptible and infected pig between pens	0.1	Estimate
γ $(\frac{\gamma}{\beta_1 n})$	Rate of transition from Excretor to Carrier	0.095 days^{-1}	Kranker et al. (2003); Gray et al. (1995)
δ $(\frac{\delta}{\beta_1 n})$	Rate of transition from Carrier to Susceptible	0.055 days^{-1}	Gray et al. (1995)

For the numerical solution, we take $\beta_2 = 0.1$, where β_2 is an approximation in the absence of data (and is taken to be a tenth of the value of β).

The two-pen model produces an epidemic curve as shown in Figure 2.8. As for the one-pen model, then the majority of pigs will become infected during the 84 day grower-finisher period. Again, as for the infection case in the one-pen model, the epidemic appears to be reaching equilibrium towards the end of the rearing period.

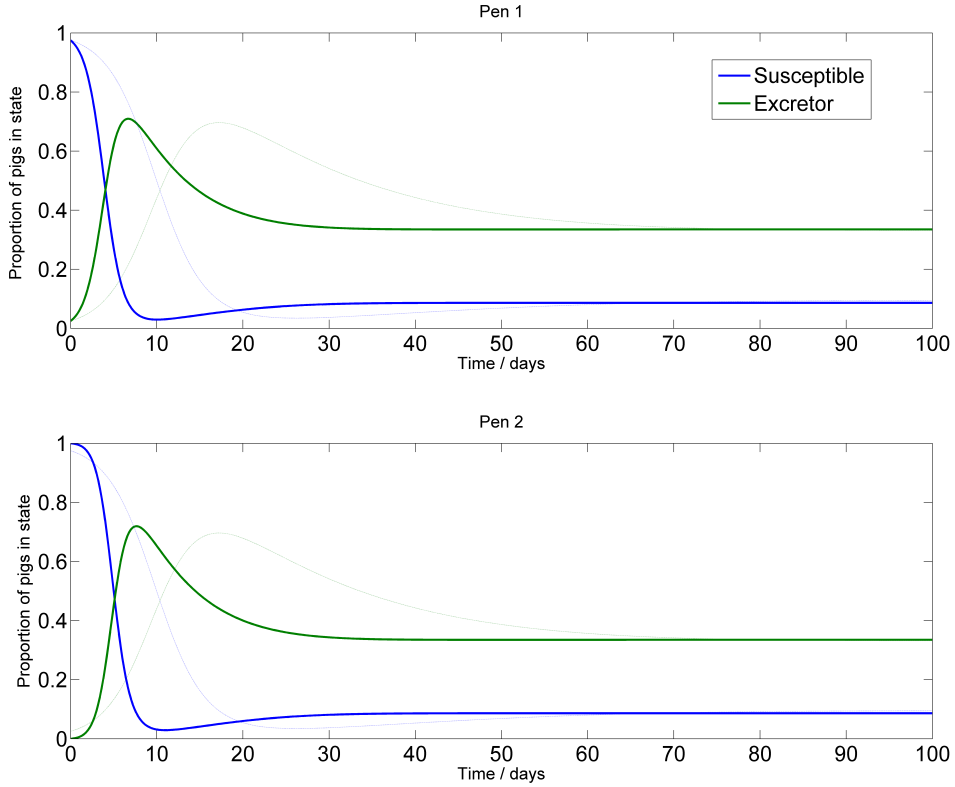

Figure 2.8: Time course of infection within two pens pigs with a force of infection between pens ten times lesser than the force of infection within a pen. The 2-pen model reaches a very similar steady stae value as for the 1-pen model (the 1-pen epidemic curve is shown as dashed lines).

2.3.4 Discussion

We show that as with the 1-pen system, the 2-pen system will always converge to either an infection state (with the infection levels the same in both pens) or a disease-free state in both pens. The steady state to which the system converges to depends only on the rate of infection (in the case of the 1-pen system, β, and in the case of the 2-pen system, β_2) and the rate of recovery γ.

For each system (1-pen and 2-pen) there is a subdivision of phase space of $\{\beta, \gamma\}$ or $\{\beta_2, \gamma\}$,respectively for 1-pen and 2-pen cases, below which the system settles to the fully-susceptible steady state, and above which the system settles to the infected steady state. If the rate of recovery is greater than the rate of infection then the system will settle to the fully-susceptible steady state. If vice versa, then the system will settle to the infected steady state. This result is biologically consistent, as it would be expected that if more pigs are recovering than becoming infected, then infection should eventually die out.

Despite the simplicity of the one-pen and two-pen models, much can be learnt about the dynamics of infection from the stability analysis techniques above. The results suggest that once infection is introduced it will continue indefinitely, having reached the infected steady state. Of interest is the fact that this result appears to hold no matter what the initial conditions are, i.e. that the steady state is globally stable. If such a result were to hold in reality, then it has significance for the interventions that can be effective in reducing Salmonella in pigs. For example, if rodent control is only effective in reducing the numbers of initially infected pigs, rather than eliminating infection, then the benefit of such an intervention may well be cancelled out, as the infected pigs will still continue to transmit infection.

Chapter 3

Multi-pen determinstic model

3.1 Introduction and farm setup

As described in Chapter 1, British pig farming is typified by penned housing and continuous production (i.e. pigs of different ages live within the same house, and hence there are 'continuous' introductions to and departures from the house over the course of one rearing stage period). The ways in which farmers employ penned housing and continuous production are many and varied, and hence in order to reduce the complexity of the initial multi-pen model (and thus much of the farm to farm variability present in the UK) the 'most common' approach to grower-finisher production in the UK is considered. Expert opinion (Rob Davies, VLA; Paul Blanchard, BASF, personal communication) is used to define a typical farm, within which the majority of pigs in the UK will be produced. This typical farm has the following attributes: inside production; exclusive grower-finisher herd; single site/house; continuous system of production; pens used to segregate the herd into smaller groups.

There are a range of penning systems used, but for simplicity it is assumed that pig pens are typically arranged as in Figure 3.1. In this particular case, there are two rows ($I_r = \{1, 2\}$) each with 6 pens ($J = \{1, 2.., 6\}$). To facilitate the investigation of continuous production as a risk factor, it is assumed that pens are depopulated/repopulated on a weekly basis. The times (t) at which each pen is depopulated/repopulated is given in Figure 3.1. Initial conditions are that the model starts when a pen of weaner pigs is transferred into Pen ($i = 1$,$j = 1$) at $t = 1$, where i can be any element from the set I_r and j can be any element of the set J. The rearing period is set at 84 days, such that all other pens have been depopulated/repopulated by the time the pigs in Pen (1,1) reach slaughter weight and are sent to slaughter ($t = 85$).

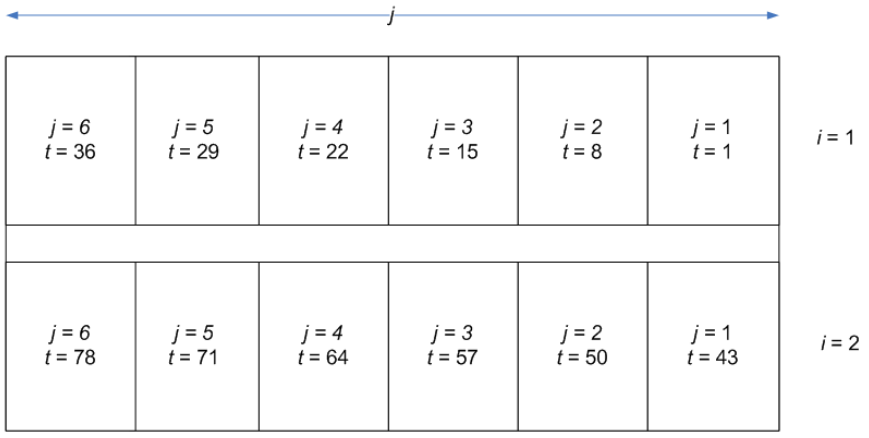

Figure 3.1: Schematic diagram of pen layout for the multi-pen determinstic model. The t indicated denotes the time of depopulation/repopulation of that pen in the model.

3.2 Model description

Expanding to the 12-pen system described in Figure 3.1 then the force of infection must include all potential contamination from each pen. Hence, the set of

differential equations for the 12-pen farm system described above can be written in general terms as

$$\begin{aligned}
\frac{dS_{i,j}}{dt} &= -\lambda_m S_{i,j} + \delta C_{i,j}, \\
\frac{dI_{i,j}}{dt} &= \lambda_m S_{i,j} - \gamma I_{i,j}, \\
\frac{dC_{i,j}}{dt} &= \gamma I_{i,j} - \delta C_{i,j}, \\
\lambda_m &= \sum_{k=1}^{2} \sum_{l=1}^{6} \beta_{k,l} I_{k,l},
\end{aligned} \tag{3.1}$$

where $\beta_{k,l}$ is the probability of an effective contact between an excreting pig in pen (k,l) and a susceptible pig in Pen (i,j). For simplicity the probability of an effective contact is split into within-pen, within-row and between-row terms, that is

$$\beta_{k,l} = \begin{cases} \beta_1 & \text{if } i = k \ \& \ j = l, \\ \beta_2 & \text{if } i = k \ \& \ j \neq l, \\ \beta_3 & \text{if } i \neq k. \end{cases}$$

Such a model is intractable for analytical solutions, and so a slightly modified version is defined for the analytical methods used in the following sections. Defining a continuous, infinite string of compartments (in this case pens) is a common method to allow analytical solutions, which avoid additional complexity caused by boundary conditions. The inclusion of a simpler spatial framework allows for more analytical methods to be used: we can investigate spatially heterogeneous stability conditions (using the specific method of Turing stability analysis) and determine the existence of travelling waves, where the speed of transmission between pens

can be deduced.

3.3 Stability analysis

For the stability analysis, we assume an infinitely long string of pens, equivalent to one row of pens in Equation (3.1). However, the assumption that within-row between-pen transmission is equal across all pens in an infinite pen system would be biologically implausible. Therefore, we limit between-pen transmission to adjacent pens only. Using the same non-dimensionalisation as for the 2-pen system (see Equation (2.7)) the dynamics of the n-pen system can be described as:

$$\begin{aligned} \frac{dS_j}{dt} &= -S_j I_j - \beta_2 S_j \left(\frac{I_{j-1} + I_{j+1}}{2} \right) + \delta \left(1 - S_j - I_j \right), \\ \frac{dI_j}{dt} &= S_j I_j + \beta_2 S_j \left(\frac{I_{j-1} + I_{j+1}}{2} \right) - \gamma I_j. \end{aligned} \tag{3.2}$$

where S_j and I_j are the proportions of Susceptibles and Excretors in pen j at time t respectively, β_2, γ and δ are defined as before in the 2-pen system, and $j \in \mathbb{Z}$.

Homogeneous steady state

By definition, a spatially uniform homogeneous steady state of the n-pen system will have $S_j = S^* \, \forall \, j$ and $I_j = I^* \, \forall \, j$, i.e. all pens will settle to the same values of Susceptibles and Excretors. Therefore, in a homogeneous equilibrium Equation (3.2) at steady state will reduce to

$$
\begin{aligned}
0 &= -S^*I^* - \beta_2 S^*I^* + \delta\left(1 - S^* - I^*\right), \\
0 &= S^*I^* + \beta_2 S^*I^* - \gamma I^*.
\end{aligned}
\tag{3.3}
$$

Solving for S^* and I^* we have

$$
\begin{aligned}
S^* &= \frac{\gamma}{1+\beta_2}, \\
I^* &= \frac{\delta\left(1+\beta_2-\gamma\right)}{\gamma+\beta_2\gamma+\delta+\delta\beta_2}.
\end{aligned}
\tag{3.4}
$$

Given S^* and I^* are positive real numbers then the homogeneous steady state is only valid when

$$
\gamma < \beta_2 + 1. \tag{3.5}
$$

This condition is the same as for the stability of the 2-pen infected steady state, and again the combined within- and between-pen force of infection must be greater than the rate of transition from Excretor to Carrier (γ) in order for the infected steady state to remain stable.

Examining the existence of spatial patterns (Turing stability analysis)

A well-documented area of research in mathematical biology is the study of patterns, typically in determining the development of form and shape during development (morphogenesis). One of the most important contributions to this field was by Alan Turing with his seminal paper on the potential for diffusion to lead

to chemical morphogenesis (Turing, 1952). Briefly, Turing assumed a uniform, positive stable steady state when two chemicals are well-mixed (i.e. in the absence of diffusion), and showed that small inhomogeneous perturbations may lead to the formation of spatial patterns in the presence of diffusion of the two chemicals. Diffusion-driven spatial patterns have been recognised as playing a crucial role in many aspects of chemical morphogenesis. For example, the prepattern of chemical concentration produced by inhomogeneous perturbations may determine the cell type into which embryonic cells will form (Edelstein-Keshet, 1988).

While the system of infection dynamics described in this chapter is clearly very different to chemical morphogenesis, the mathematics of Turing pattern formation is applicable, as the spread of infection between pens of pigs is analogous to the diffusion process. The conditions for a stable homogeneous steady state that is then unstable to inhomogeneous perturbations are found by linearising the non-linear system in question and choosing an appropriate form of spatially varying perturbation. Interpreting this mathematical process biologically (for the particular case of Salmonella in pig pens), then as shown for the 1-pen and 2-pen models an infected steady state is reached if the rate of infection is greater than the rate of recovery. However, small perturbations in the level of infection in a pen may come from inhomogeneous environmental transfer of Salmonella between wildlife and pigs in different pens, or from infected pigs shedding Salmonella at slightly different rates in different pens. These perturbations are entirely plausible, and indeed would be expected to be the norm, rather than the exception.

We linearise Equation (3.2) using

$$
\begin{aligned}
S_j &= \bar{S}_j + S^* \\
I_j &= \bar{I}_j + I^*
\end{aligned}
\tag{3.6}
$$

where $\bar{S}_j$ and $\bar{I}_j$ denote perturbations of S_j and I_j from their respective equilibria.

Substituting Equation (3.6) into Equation (3.2) and ignoring higher order terms (e.g. $\bar{S}_j^2$, since we assume that $\bar{S}_j$ and $\bar{I}_j$ are small) we get

$$
\begin{aligned}
\tfrac{d\bar{S}_j}{dt} &= -\bar{S}_j I^* - S^* \bar{I}_j - \beta_2 S^* \left(\tfrac{\bar{I}_{j-1}+\bar{I}_{j+1}}{2}\right) - \beta_2 \bar{S}_j I^* - \delta\left(\bar{S}_j + \bar{I}_j\right), \\
\tfrac{d\bar{I}_j}{dt} &= \bar{S}_j I^* + S^* \bar{I}_j + \beta_2 S^* \left(\tfrac{\bar{I}_{j-1}+\bar{I}_{j+1}}{2}\right) + \beta_2 \bar{S}_j I^* - \gamma \bar{I}_j.
\end{aligned}
\tag{3.7}
$$

Now we look for spatially varying solutions of the form $\bar{S}_j = \hat{S} e^{\mu t + i\lambda j}$ and $\bar{I}_j = \hat{I} e^{\mu t + i\lambda j}$, where $\hat{S}$ and $\hat{I}$ are constants, μ is the temporal growth rate of spatial modes of wavelength λ. The constant μ determines whether the inhomogeneous perturbation will grow to lead to instability (and potentially spatial patterns), or simply settle back to the steady state. The latter part of the exponential, $i\lambda j$ is a complex term that contributes a spatial oscillatory part to the perturbation; j is the number of a pen.

Rearranging we have

$$
\begin{aligned}
\left(\mu\hat{S} + \hat{S}I^* + S^*\hat{I} + \beta_2 S^* \hat{I}\left(\tfrac{e^{i\lambda}+e^{-i\lambda}}{2}\right) + \beta_2 \hat{S} I^* + \delta\left(\hat{S} + \hat{I}\right)\right) \cdot e^{\mu t + i\lambda j} = 0 \\
\left(\mu\hat{I} - \hat{S}I^* + S^*\hat{I} - \beta_2 S^* \hat{I}\left(\tfrac{e^{i\lambda}+e^{-i\lambda}}{2}\right) - \beta_2 \hat{S} I^* + \gamma\hat{I}\right) \cdot e^{\mu t + i\lambda j} = 0.
\end{aligned}
$$

Dividing through by $e^{\mu t + i\lambda j}$ and converting into matrix form we then get

$$\begin{bmatrix} \mu + I^* + \beta_2 I^* + \delta & S^* + \beta_2 S^* k(\lambda) + \delta \\ -I^* - \beta_2 I^* & \mu - S^* - \beta_2 S^* k(\lambda) + \gamma \end{bmatrix} \cdot \begin{bmatrix} \hat{S} \\ \hat{I} \end{bmatrix} = \begin{bmatrix} 0 \\ 0 \end{bmatrix}. \tag{3.8}$$

where $k(\lambda) = \cos(\lambda) \equiv \frac{e^{i\lambda}+e^{-i\lambda}}{2} \in [-1, 1]$. The characteristic equation of the matrix is of the form $\mu^2 + a_1\mu + a_2 = 0$, the roots of which have negative real parts if $a_1 > 0$ and $a_2 > 0$. Expanding the determinant in Equation (3.8) and collecting terms then gives

$$\begin{aligned} a_1 &= \frac{\delta{\beta_2}^2 - \beta_2\gamma^2 k(\lambda) - \beta_2\gamma k(\lambda)\delta + \gamma\delta\beta_2 + \beta_2\gamma^2 + 2\delta\beta_2 + \delta^2\beta_2 + \delta + \delta^2}{(1+\beta_2)(\gamma+\delta)}, \\ a_2 &= \frac{\delta(\beta_2^2 - \beta_2\gamma k(\lambda) + 2\beta_2 + 1 - \gamma)}{(1+\beta)}. \end{aligned} \tag{3.9}$$

Note that a_1 and a_2 are linear functions in $k(\lambda)$. We can determine the fixed gradients of a_1 and a_2 in terms of the remaining parameters by differentiating, namely:

$$\frac{da_1}{dk} = -\frac{(\beta_2\gamma^2 + \gamma\delta\beta_2)}{(1+\beta_2)(\gamma+\delta)}, \tag{3.10a}$$

$$\frac{da_2}{dk} = -\frac{\delta\beta_2\gamma}{(1+\beta_2)}. \tag{3.10b}$$

Since these are both strictly negative and $a_1(k=1)$ and $a_2(k=1)$ are both assumed to be strictly positive so that S^* and I^* are stable to homogeneous perturbations, this means that $a_1, a_2 > 0 \ \forall \ k \in [-1, 1]$, and so Turing spatial patterns are not predicted. Hence, we may expect that even in a large n-pen system that all pens will eventually settle to the same level of infection over a sufficient period

of time.

3.4 Travelling wave analysis

In the previous section no Turing spatial patterns were found, suggesting that the multi-pen model solutions will eventually settle to one of the uniform steady states. Therefore, of interest is the speed of the spread of infection between pens, and how fast the system will settle to the chosen steady state.

For many physical and chemical processes, the formation of waves is crucial in transferring energy, mass and/or information, and the same can be said for a vast array of biological phenomena, for example wound healing and epidemic spread. A travelling wave can be defined as a wave which travels with constant speed and shape, and the mathematics associated with these types of waves were formalised in the first half of the 20th Century. A classic pedagogical example is given by Fisher (1937), who described by the formation of travelling waves the spatial spread of a favoured gene in a population.

As for the homogeneous stability analysis and formation of Turing spatial patterns, the method for travelling wave analysis involves linearisation of the non-linear system. In addition, the analytical system of ODEs can be simplified by transferring to a moving frame of reference in which the wave will appear stationary, i.e. a moving frame of reference that moves at same fixed speed as the wave.

The spatially homogeneous steady state of the n-pen system $\{I^*, S^*\}$, and its conditions for stability has already been described in Section 3.3. To investigate the existence of any travelling waves, we start with Equations (3.2) and (3.7).

As described in Edelstein-Keshet (1988), a travelling wave is a function that moves

along some spatial axis over time t at a constant speed, c, whilst retaining a fixed shape. It is useful to convert from the stationary observer frame of reference (in j and t) to the frame of reference of the moving observer, where both space and time dependence are described by one parameter, z. Conversion to z in our infinite pen system is achieved by the following relation.

$$z = j - ct$$

where c is the wave speed. Therefore, we write

$$S(z) = S(j,t),\ I(z) = I(j,t).$$

This change of reference frame is depicted visually in Figure 3.2. The top panel depicts the movement of the travelling wave in the (j,t) frame of reference. At some initial starting point j_0 infection spreads out from this pen into fully susceptible pens, moving further along the string of pens in time, at speed c. The wavefront, followed by a wave of fixed shape, moving at some constant speed c, initially introduces a small amount of infection into a pen, but as time moves forward the infection level within the pen increases to the infection steady state (I^*).

Changing into the moving frame of reference (bottom panel of Figure 3.2) the observer moves along with the wave at the same speed as the wave, c, and so observes a static wave. Therefore, instead of having both time and space dependency, the moving frame of reference incorporates both time and space into one dependent variable, z. We can use the general case in Figure 3.2 to explicitly consider what happens to S^* and I^* over time. In the non-stationary frame of reference (top

panel), then at time t_0, $I(0,0)$ is positive but small, and $S(0,0) \approx 1$. At time t_0, as $j \to \infty$ then $I(j,t_0) \to 0$ and $S(j,t_0) \to 1$. As t increases, the level of infection in pen j_0 increases to I^*, and infection spreads out into the adjacent pens, until eventually as $t \to \infty$, $I(j,t) \to I^*$ and $S(j,t) \to 0$. In the stationary frame of reference (the bottom panel of Figure 3.2) as $z \to \infty$, $I(z) \to 0$ and $S(z) \to 1$, i.e. infection has yet to reach pens far away from z_0. Conversely, as $z \to -\infty$, $I(z) = I^*$ and $S(z) = S^*$, i.e. the pens in negative z have all reached the homogeneous steady state.

In summary, as $z \to \pm\infty$ the following limits apply.

$$\lim_{z \to -\infty} S(z) = S^*$$

$$\lim_{z \to -\infty} I(z) = I^*$$

$$\lim_{z \to \infty} S(z) = 1$$

$$\lim_{z \to \infty} I(z) = 0.$$

Taking the general result above and applying it to the system described in Equation (3.2), then $S((j,t)$ and $I(j,t)$ can be transformed into the z frame of reference, giving

$$\begin{aligned} \frac{dS_j(t)}{dt} &= \frac{dS(z)}{dt} \\ &= \frac{dS_j}{dz} \cdot \frac{dz}{dt} = -c \cdot \frac{dS(z)}{dz}. \end{aligned} \tag{3.12a}$$

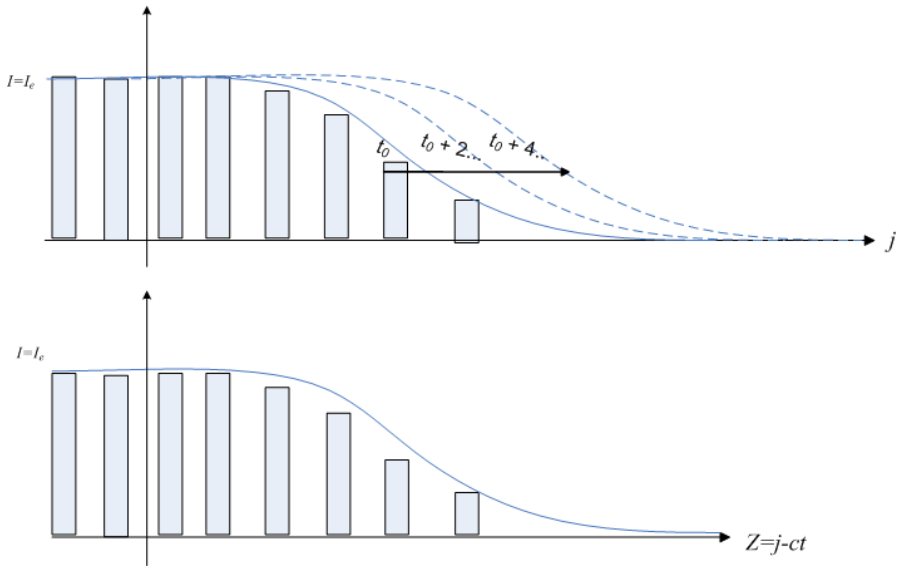

Figure 3.2: Travelling wave of infection spreading through string of pens as viewed from stationary frame of reference (top) and moving frame of reference (bottom). Bars denote level of infection in pens. Converting to the moving frame of reference (bottom) creates a static wave as a function of z, which can be described as the distance along the wave from some arbitrary point, z_0.

Similarly

$$\frac{dI_j}{dt} = -c \cdot \frac{dI(z)}{dz}. \tag{3.12b}$$

Substituting Equations (3.12a) and (3.12b) into Equation (3.2) we obtain

$$\begin{aligned} -c \cdot \frac{dS(z)}{dz} &= -S_z I_z - \beta_2 S_z \left(\frac{I(z-1) + I(z+1)}{2} \right) + \delta \left(1 - S_z - I_z\right), \\ -c \cdot \frac{dI(z)}{dz} &= S_z I_z + \beta_2 S_z \left(\frac{I(z-1) + I(z+1)}{2} \right) - \gamma I_z. \end{aligned} \tag{3.13}$$

We now perform a similar linearisation of the system as for the n-pen stability analysis. Defining similar perturbations as in Equation (3.6), that is

$$
\begin{aligned}
S_z &= \bar{S}_z + S^* \\
I_z &= \bar{I}_z + I^*
\end{aligned}
\tag{3.14}
$$

where $\bar{S}_z$ and $\bar{I}_z$ are the perturbations of S_z and I_z respectively and we again assume these perturbations are small. I_z is a positive real number, and so travelling wave solutions cannot have an oscillatory approach to $I_z = 0$ (as otherwise I_z would become negative as it approached zero - we will refer to this point again later). We linearise about the steady state as $z \to \infty$, i.e. $(S, I) = (1, 0)$. Using $S(z) = 1 - \bar{S}(z)$ and $I(z) = \bar{I}(z)$ we get

$$
\begin{aligned}
-c \cdot \bar{S}' &= -\bar{I}_z - \beta_2 \left(\frac{\bar{I}(z-1) + \bar{I}(z+1)}{2} \right) - \delta \left(\bar{S}_z + \bar{I}_z \right), \\
-c \cdot \bar{I}' &= \bar{I}_z + \beta_2 \left(\frac{\bar{I}(z-1) + \bar{I}(z+1)}{2} \right) - \gamma \bar{I}_z.
\end{aligned}
\tag{3.15}
$$

Given that we now have linear ODEs in terms of z then an appropriate form of solution we have

$$
\bar{u} = \hat{u} e^{\lambda z} \quad \text{for } \bar{u} = \bar{S} \text{ and } \bar{I} \tag{3.16}
$$

for some wavenumber λ and constants $\hat{S}$ and $\hat{I}$. In other words

$$
\begin{aligned}
\bar{S}_z &= \hat{S} e^{\lambda z}, \\
\bar{I}_z &= \hat{I} e^{\lambda z}.
\end{aligned}
\tag{3.17}
$$

Substituting the perturbations $\bar{S}(z)$ and $\bar{I}(z)$ from Equation (3.17) in Equation (3.15) and transferring all components to the LHS we derive the following

$$\begin{aligned}\left(-c\lambda\hat{S}+\hat{I}+\beta_2\hat{I}\left(\frac{e^{\lambda}+e^{-\lambda}}{2}\right)+\delta\left(\hat{S}+\hat{I}\right)\right)\cdot e^{\lambda z}=0,\\ \left(-c\lambda\hat{I}-\hat{I}-\beta_2\hat{I}\left(\frac{e^{\lambda}+e^{-\lambda}}{2}\right)+\gamma\hat{I}\right)\cdot e^{\lambda z}=0.\end{aligned} \tag{3.18}$$

Dividing through by $e^{\lambda z}$ and converting to matrix form

$$\underbrace{\begin{bmatrix}-c\lambda+1+\delta & 1+\beta_2 k(\lambda)+\delta\\ 0 & -c\lambda-1-\beta_2 k(\lambda)+\gamma\end{bmatrix}}_{\mathbf{A}}\cdot\begin{bmatrix}\hat{S}\\ \hat{I}\end{bmatrix}=\begin{bmatrix}0\\ 0\end{bmatrix}, \tag{3.19}$$

where this time $k(\lambda)=\cosh(\lambda)\equiv\frac{e^{\lambda}+e^{-\lambda}}{2}$. For equations of the general form of Equation (3.19), i.e. $\mathbf{A}\cdot\mathbf{x}=0$, then a non-trivial solution can only occur if the determinant of $\mathbf{A}$ is equal to zero. Evaluating the determinant at zero we then have

$$\det\mathbf{A}=-(c\lambda-\delta)(-c\lambda-1-\beta_2\cosh(\lambda)+\gamma)=0. \tag{3.20}$$

Therefore, either $c=\frac{\delta}{\lambda}$ or c is given by

$$(c\lambda+1+\beta_2\cosh(\lambda)-\gamma)=0. \tag{3.21}$$

Kolmogorov et al. (1937) showed that it is always true that propagating-wave solutions of PDEs (should they exist) must satisfy some minimum wave speed if

certain initial conditions are satisfied. Generally, these initial conditions are of the form of the wavefront for the system given here (i.e. compact initial conditions; just one pen being infected at $t = 0$). As mentioned above, complex roots for the function $(c\lambda + 1 + \beta_2 \cosh(\lambda) - \gamma) = 0$ are not realistic. It turns out that this gives a restriction on c, namely there exists a minimum wave speed, c_{min}. Plotting $(c\lambda + 1 + \beta_2 \cosh(\lambda) - \gamma) = 0$ gives a unimodal functon in $[c, \lambda]$ space with a minimum at c_{min}.

An example is given in Figure 3.3, using $\beta_2 = 0.6$ and $\gamma = 1$. The boundary between red $((c\lambda + 1 + \beta_2 \cosh(\lambda) - \gamma) > 0)$ and blue $((c\lambda + 1 + \beta_2 \cosh(\lambda) - \gamma) < 0)$ represents the values in $[c, \lambda]$ parameter space where $(c\lambda + 1 + \beta_2 \cosh(\lambda) - \gamma) = 0$. Hence, solutions for Equation (3.21) in the blue regions involve complex roots of λ are are therefore not valid. The minimum wavespeed is located at the value for c where there is one real repeated root for λ. According to Kolmogorov et al. (1937), for sufficiently compact initial conditions, all waves with these chosen parameter values in our system will move at exactly this minimum speed.

Plotting the minimum wavespeed over a range of β_2 and γ values we obtain Figure 3.4 for c_{min} in units of pens/timestep. Travelling waves will lead to the infected steady state when $\beta_2 > \gamma - 1$, hence there are no valid travelling waves for $\beta_2 \leq \gamma - 1$, indicated on the graph by the white shaded area.

Indicated by a white dot on Figure 3.4 is the combination of β_2 and γ which are used for the numerical solutions shown below in Section 3.5. We therefore estimate that the travelling wave should move with a speed of roughly 1 pen per timestep.

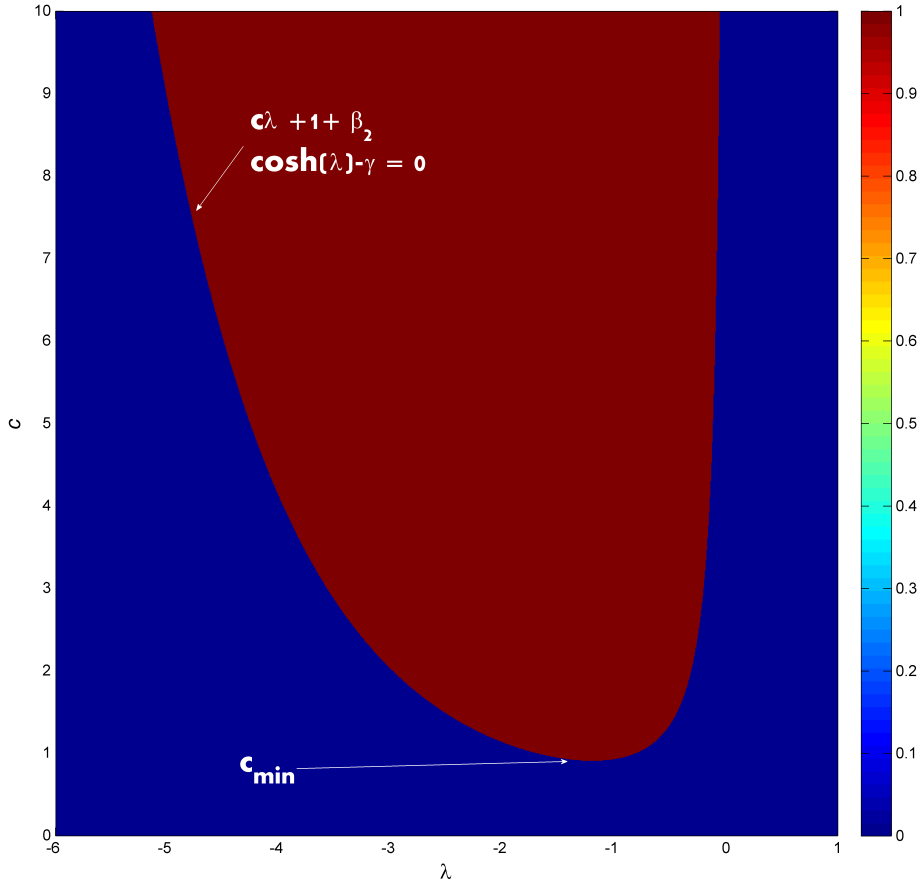

Figure 3.3: Solutions of Equation (3.21) have been found and plotted in over (c, λ) parameter space. Complex roots for λ occur in the blue region and are not valid. The minimum valid wavespeed occurs at the value for c for where there is one real repeated root for λ. $\beta_2 = 0.6$ and $\gamma = 1$.

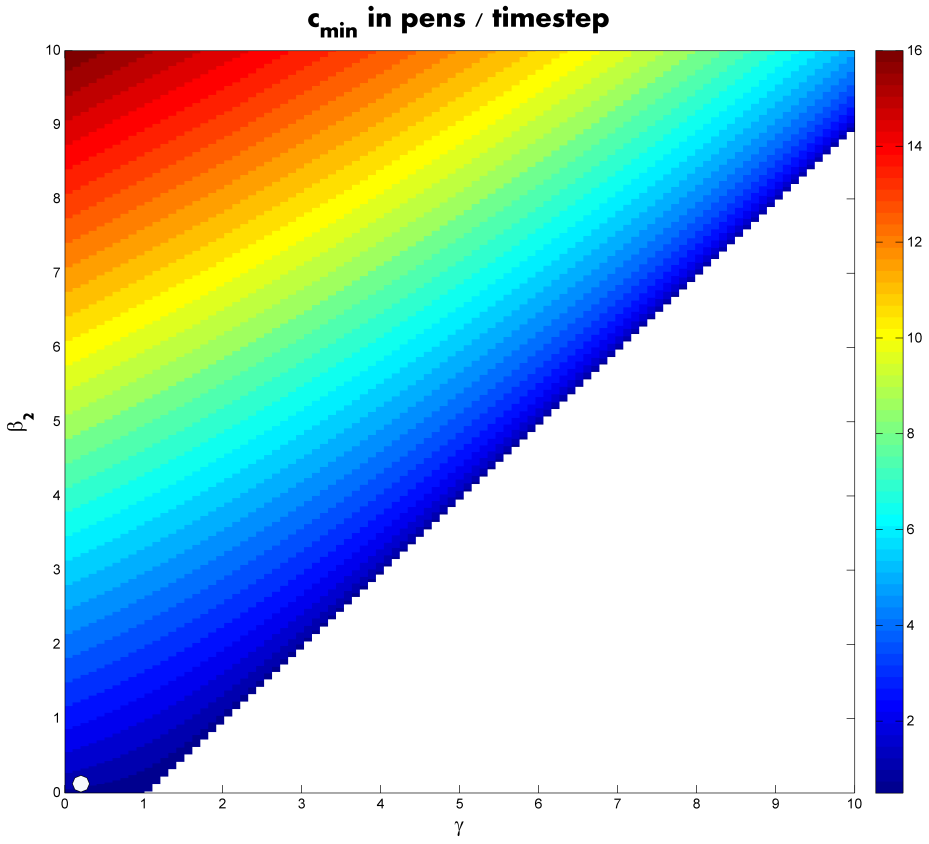

Figure 3.4: Surface plot indicating minimum wavespeed, c_{min}, over $[\beta_2, \gamma]$ parameter space, using a timestep of 1 day. The white dot represents the combination of γ and β_2 used in the numerical solution shown in Figure 3.5.

3.5 Numerical solution

As for the one- and two-pen models it was assumed that one newly excreting pig enters the farm at $t = 1$ along with other new stock. Therefore, $S_{1,1} = 1 - \frac{1}{40}$ and $I_{1,1} = \frac{1}{40}$. For all other pens we assume all pigs are in the Susceptible state.

We numerically solve both formulations of the multi-pen model, i.e. the 12-pen model (Equation (3.1)) and a much longer 1-dimensional string of pens (to mimic the infinite string case) (Equation (3.2)), to highlight the interesting dynamics that occur based on the assumptions made.

The output for each pen of the 12-pen model is very similar to the one and two-pen model epidemic curves (see Pen (1,1) in Figure 3.5). The only difference is the epidemic curves within adjacent pens to the initially infected pen (Pen (1,1)) because of the repopulation/depopulation at varying times. Peaks of infection are higher in pens restocked with susceptible pigs at the point when other pens around it are reaching peak infection (as the value of λ_m is higher at this timepoint, around 10-20 days). However, the epidemic curve in Pen(1,1), where pigs are slaughtered on day 85, is very similar to the one and two pen models.

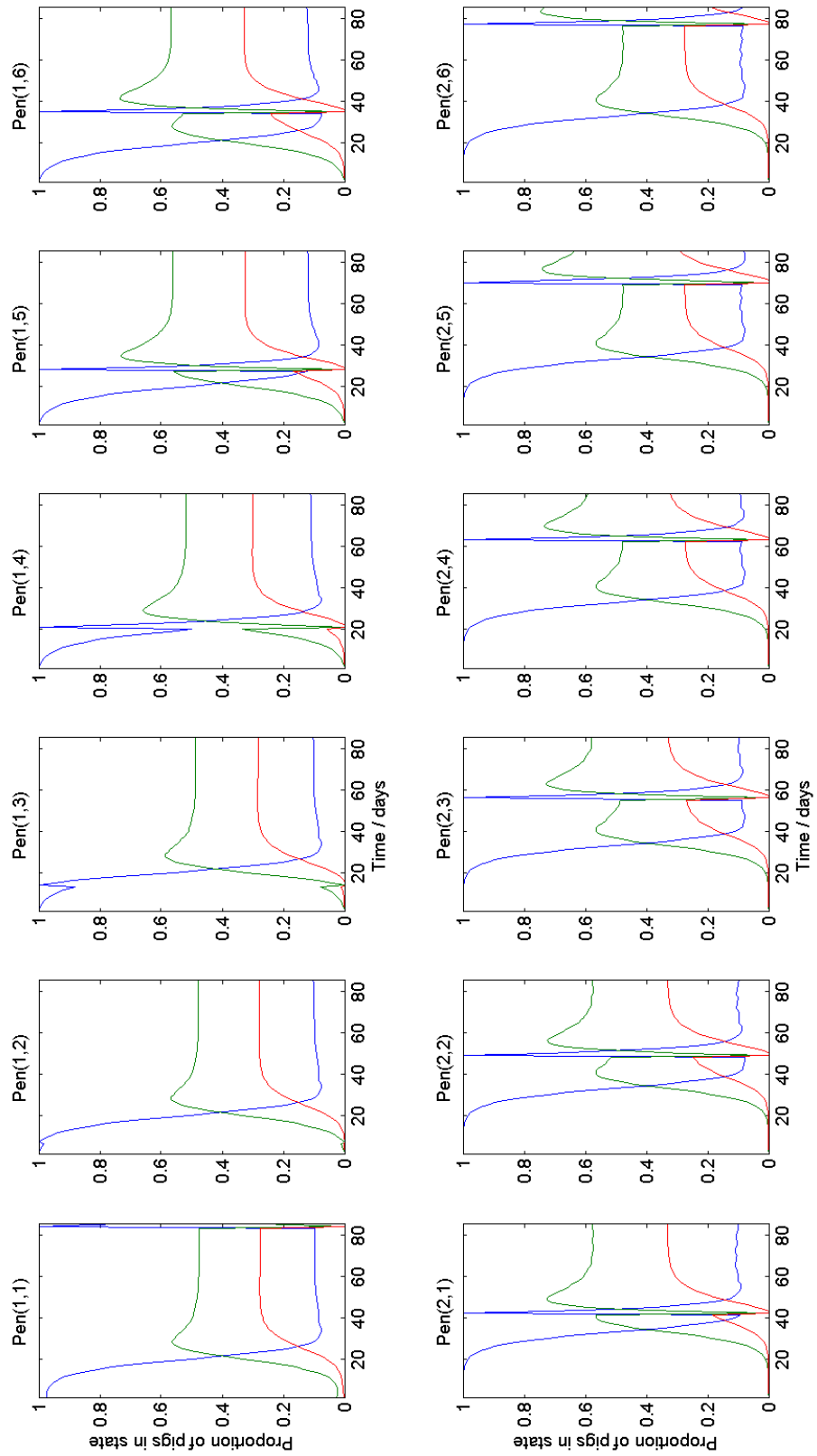

Figure 3.5: Time course of infection within the 12-pen setup using continuous production.

Naturally, the hypothetical infinite string of pens cannot be solved for an infinite number of pens. Instead, it is solved for a large number of pens, such that the interactions between the first pen infected at $t = 0$ (Pen 1) is sufficiently removed from that of the last uninfected pen. Three hundred pens was judged sufficient to meet this criterion and to allow us to numerically estimate the travelling wave speed. The numerical solution of the epidemic curve is shown for the first twelve pens for ease of comparison against the 12-pen model (see Figure 3.6). This system does not have the feature of continuous production, and so the similarity in the epidemic curves between pens (and to the epidemic curves of the one and two pen models) can clearly be seen. Another dynamic that becomes apparent is the progressive delay in the peak of infection and equilibrium as the pen number increases, explicitly showing the travelling wave. We can estimate the speed of the travelling wave across the 300 pens by subtracting the time it takes for pen q to settle to the steady state from the time it takes pen $q + 1$, and then taking an average over all 300 pens. The speed of the travelling wave for a string of pens governed by realistic parameter estimation is around 1.6 pens/timestep. This compares relatively well with the estimate from the travelling wave analysis of around 1 pen per timestep. In non-scaled terms, the travelling wavespeed is estimated to be around 0.4 and 0.6 pens per day for the analytical solution and numerical solution estimates respectively.

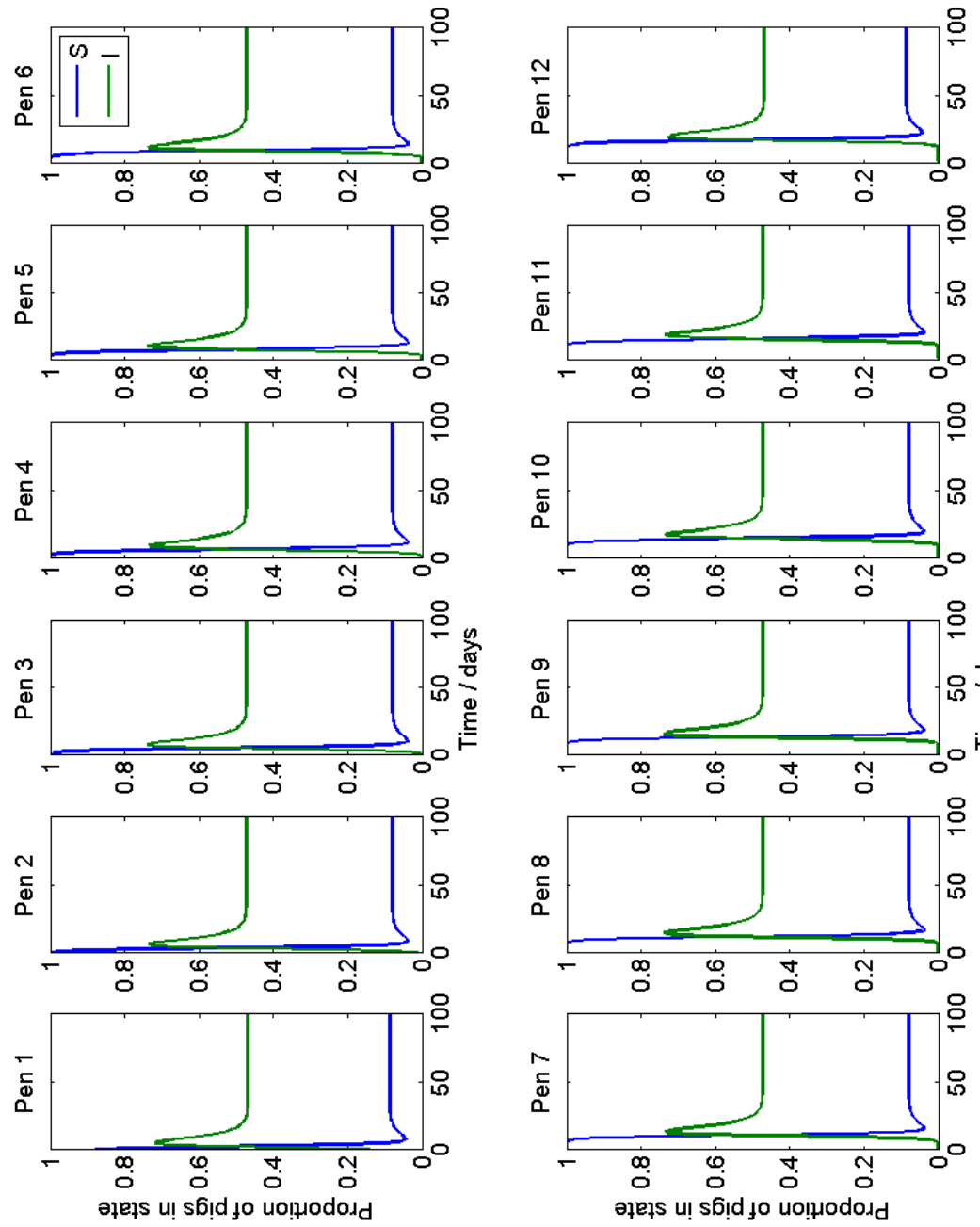

Figure 3.6: Time course of infection within the string of pens setup.

3.6 Discussion

The stability conditions for the multi-pen model are the same as for the two-pen model. This is expected, as the multi-pen model analysed for stability is a generalisation of the 2-pen model to an infinite string of pens. The infinite string of pens model allows analysis of spatial characteristics; the first we investigated is the possibility of Turing spatial patterns. Spatial patterns are not predicted analytically, and numerical analysis confirmed this. Given that the system always settles to an homogeneous steady state then it is relevant to investigate the speed of transmission between pens; for this, we used travelling wave analysis. Analytical and numerical solutions suggests the minimum wavespeed is around 0.4-0.6 pens per day, when $\beta_2 = 0.1$ and $\gamma = 0.095$.

Numerical analysis of the more realistic farm setup described in Equation (3.1) includes allowance for continuous production, where batches of pigs would be sent to slaughter weekly. As discussed in Section 2.3.4, if $\beta_2 \ll \beta_1$ then β_2 effectively provides no more than a small load of infection into adjacent pens, at which point the within-pen transmission component (β_1) dominates. Hence, the epidemic curves in all pens are almost identical, except for the weekly slaughtering of pigs from alternate pens. Therefore, the use of continuous production with the current modelling framework, for deterministic models at least, seems to be a complication that adds little to the essential dynamics of the system, apart from momentarily disrupting the equilibrium of each pen.

Travelling wave analysis shows that every pen will eventually settle to the same infected steady state. Variation in the initial conditions did not change this result (analysis not shown). Hence, again, if these results are applicable in reality then pigs will sustain infection independent of other sources such as rodents or feed.

Each of the pens in the numerical solution are only approaching equilibrium towards the end of the rearing period (1 timestep $\sim$ 2.5 days, finishing period 84 days). Hence, the relevance of the equilbirium situation is limited for commercial pig production (although may well be much more relevant for premium, slower-growing breeds). Several observational studies confirm that infection on pig farms is extremely heterogeneous (VLA, 2009; Jensen et al., 2006; Kranker et al., 2003). Not only is infection often found only in a small number of pens, but there is little equilibrium in infection between pens over time. Indeed, infection appears to be extremely intermittent. The sampling methods used may well explain a large proportion of the variation in infection over space and time on a pig farm (the sensitivity of faecal sampling is known to be very poor, and so it is likely that infection in pigs/pens is simply missed on a large number of occasions). However, given the sheer variation found in observational studies, and that Salmonella is ubiquitous in the environment and found in a number of sources, it is likely that there is more of a dynamic 'peak and trough' of infection on an infected pig farm as new infected pigs enter the finishing house and disturb any equilibrium between pens.

The slow rate of transmission between pens (given current parameter estimation) would explain some of the variation in pen infection. If the rate of transmission between pens is very slow, then other modes of infection may dominate over faecal-oral transmission. For example, rodent or feed contamination may introduce infection independently of faecal-oral transmission; this would explain the heterogeneity observed in many observational studies.

Therefore, the next step is to start to build into the model a more realistic consideration of important variables on the farm. Two major contributions to variability in infection dynamics are varying and multiple sources of infection on any one

farm, and the environmental contamination of the environment due to variable shedding of Salmonella by pigs (and wildlife) and variable efficiency of removing the Salmonella in the pig pen environment by cleaning and disinfection (C&D).

To consider both the source of infection and variable shedding rates, and how these two factors determine the dynamics of Salmonella transmission, we must consider the dose-response of the pig to exposure through various sources of infection. The source of infection will determine the level of exposure (e.g. contaminated faeces contain a far greater concentration of Salmonella organisms than contaminated feed) and hence the likelihood of infection, and the level of exposure, will play an important role in the eventual level of shedding from an infected pig (Jensen et al., 2006; Osterberg and Wallgren, 2008; Osterberg et al., 2009). The source of infection and variable shedding responses to infection will be taken into account with more complex stochastic models in later chapters, but in the next chapter we modify the multi-pen model and explicitly introduce the modelling of environmental contamination and dose-response. The model described in this chapter did not display any heterogeneity or dynamics other than each pen eventually settling to the same infected homogeneous steady state; however, the introduction of added complexity of bacterial shedding may well produce markedly different dynamics, for example by producing Turing patterns in the level of pen infection. Hence, we investigate this new environmental 'cross-contamination' model using the same techniques as described in this chapter (Turing stability analysis, travelling wave propagation).

Chapter 4

Multi-pen determinstic model with contamination

4.1 Modelling faecal-oral transmission explicitly

The models described above in the previous chapters have the advantage of being analytically amenable and simple. However, these models produced very similar dynamics of infection in each pen, where infection in each pen always settled to the same homogeneous steady state. One of the main disadvantages of this form of deterministic model, and a potential cause of the over-simplified dynamics described in previous chapters, is that transmission is governed by just one parameter, the probability of an effective contact, β or β_1 etc. The probability of an effective contact is determined by many factors, including the type of housing/flooring, the type of production system used and the feed type (Berends et al., 1996). However, formulating and parameterising a model that splits the transmission parameter into all of its contributing parts (e.g. for all the different farm types in Great

Britain, and then for intervention modelling) is impractical.

Therefore, in this chapter, we develop a model that explicitly accounts for two of the major components of the transmission parameter: first, the level of shedding of Salmonella by pigs and the subsequent contamination of the pen and wider farm environment, and second the resulting (dose-response) exposure of susceptible pigs. The amount of Salmonella in the environment is largely determined by the following main factors: how much Salmonella is shed by pigs, the rate of decay of Salmonella in the pen environment and the rate of cross-contamination of Salmonella between pens (cleaning and disinfection is also important when depopulating/repopulating). The susceptibility of a pig to infection given exposure to Salmonella can be modelled using a standard dose-response function. Such a "cross-contamination" model is much more amenable to intervention analysis, as the farm environment can be modified via the pen level contamination parameter to describe interventions including cleaning and disinfection and biosecurity (including effective barriers between pens), and the dose-response model can be modified to investigate interventions such as vaccination, organic acids or the use of wet/fermented feed instead of dry feed.

For the multi-pen model described in the previous chapter, neither continuous production or multiple rows of pens had a significant effect in changing the overall epidemic curve within a pen. Therefore, for simplicity, we modify the theoretical string of pens model in Equation (3.2) to include cross-contamination. Combining all of the factors described above for a pen j we get:

$$\begin{aligned}
\frac{dS_j}{dt} &= -D\left(f_j\right) S_j + \delta C_j, \\
\frac{dI_j}{dt} &= D\left(f_j\right) S_j - \gamma I_j, \\
\frac{dC_j}{dt} &= \gamma I_j - \delta C_j, \\
\frac{df_j}{dt} &= p_f I_j - d_f f_j + \eta\left(f_{j+1} + f_{j-1} - 2f_j\right).
\end{aligned} \tag{4.1}$$

where f_j is the amount of Salmonella contained within faecal material within pig pen j, p_f is a parameter describing the magnitude of pig excretion, d_f is the rate of decay (per day) for Salmonella in the pen environment, η is the rate of cross-contamination between pens and $D\left(f_j\right)$ is a dose-response function. An appropriate sigmoidal function has been chosen so that

$$D\left(f_j\right) = \frac{c_1 f_j^m}{{c_2}^m + f_j^m},$$

where c_1, c_2 and m are real and positive parameters describing the shape of the dose-response curve. Such a sigmoidal function has a form as shown in Figure 4.1. When m is non-zero and positive, then the dose-response function has some key characteristics: first, there is a monotonically increasing probability of infection with increasing dose; second, the dose-response function approaches an asymptote at c_1 as dose becomes large. The value of m determines the shape of the function and represents the important dynamics of infection: as m increases, so the 'influential' range of doses decreases. For example, in Figure 4.1, when $m = 1$ there is a broad range of doses where the probability of infection markedly increases, and so a change in all but the lowest and highest doses can have a significant effect on the probability of infection. However, for $m > 1$ then there is a much more

distinct three-phase dose-response curve; a shallow gradient at low doses (representing where a pig's immune response may overcome a small exposure), a steeper gradient at medium doses (where the dose ingested could sufficiently challenge the immune response and infection becomes more likely as more and more salmonellas are ingested), and finally a shallower gradient as the dose approaches the asymptote (representing where the immune response could be completely overwhelmed and infection is all but certain). The scale parameter c_2 determines how quickly the probability of infection reaches the asymptote; as c_2 increases a larger dose is required to reach the asymptote.

To ease analysis, Equation (4.1) is re-scaled in a similar fashion as for the standard n-pen model in Chapter 3. We define $S = \tilde{S}\langle S\rangle$, $I = \tilde{I}\langle I\rangle$, $f = \tilde{f}\langle f\rangle$ and $t = \tilde{t}\langle t\rangle$, and then set $\langle S\rangle = \langle I\rangle = \langle C\rangle = n$. Therefore $\tilde{S} + \tilde{I} + \tilde{C} = 1$, and $\tilde{C} = 1 - \tilde{S} - \tilde{I}$. Also setting $\langle t\rangle = 1/\tilde{\delta}$, $\langle f\rangle = c_2$, $\tilde{c}_1 = c_1\langle t\rangle = c_1/\delta$, $\tilde{\gamma} = \gamma/\delta$, $\tilde{p_f} = p_f/\delta$, $\tilde{d}_f = d_f/\delta$ and $\tilde{\eta} = \eta/\delta$ then gives

$$\frac{d\tilde{S}_j}{d\tilde{t}} = \left(1 - \tilde{S}_j - \tilde{I}_j\right) - D_f(\tilde{f}_j)\tilde{S}_j, \tag{4.2a}$$

$$\frac{d\tilde{I}_j}{d\tilde{t}} = D_f(\tilde{f}_j)\tilde{S}_j - \tilde{\gamma}\tilde{I}_j, \tag{4.2b}$$

$$\frac{d\tilde{f}}{d\tilde{t}} = \tilde{p}_f\tilde{I}_j - \tilde{d}_f\tilde{f}_j + \tilde{\eta}\left(\tilde{f}_{j+1} + \tilde{f}_{j-1} - 2\tilde{f}_j\right), \tag{4.2c}$$

$$D_f(\tilde{f}_j) = \frac{\tilde{c}_1\tilde{f}_j^m}{1 + \tilde{f}_j^{\,m}}. \tag{4.2d}$$

As for previous re-scalings, the tilde notation is dropped from now on for notational simplicity.

As for the multi-pen model described in Chapter 3, we analyse the system under

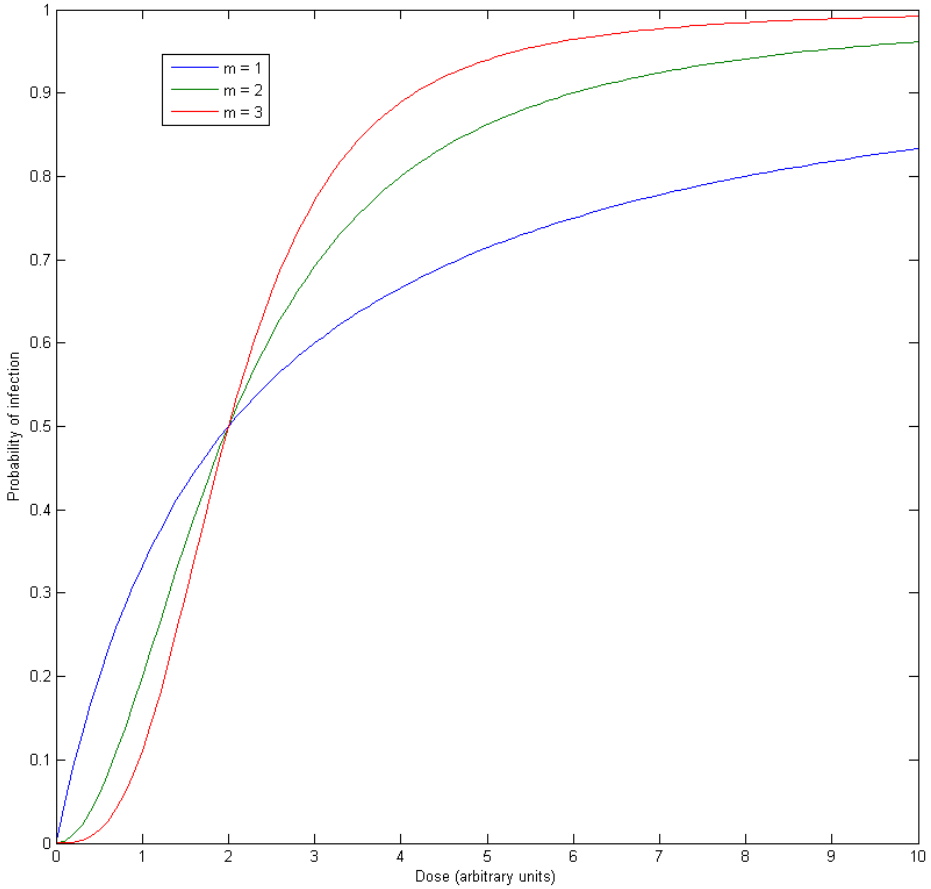

Figure 4.1: Shape of the dose-response function for $m = 1, 2, 3$. $c_2 = 1$. The value of c_1 in this specific example is 1, hence the maximum probability of infection tends to 1 as dose gets large.

both homogeneous and spatially varying perturbations.

4.2 Stability analysis

4.2.1 Homogeneous steady state

The system described in Equation (4.2) is at a spatially uniform equilibrium when $S_j = S^*$, $I_j = I^*$ and $C_j = C^*$ so that

$$(1 - S^* - I^*) - D_f(f^*)S^* = 0, \tag{4.3a}$$

$$D_f(f^*)S^* - \gamma I^* = 0, \tag{4.3b}$$

$$p_f I^* - d_f f^* = 0. \tag{4.3c}$$

Algebraic manipulation of Equation (4.3b) gives

$$D_f(f^*) = \frac{\gamma I^*}{S^*}. \tag{4.4a}$$

Substituting Equation (4.4a) into Equation (4.3a) and then rearranging for S^* gives

$$S^* = 1 - (1 + \gamma)\, I^*. \tag{4.4b}$$

Hence,

$$D_f(f^*) = \frac{\gamma I^*}{S^*} = \frac{\gamma I^*}{1 - (1 + \gamma)\, I^*}. \tag{4.4c}$$

Now, using the expression for $D_f(f^*)$ then gives

$$\frac{c_1 f_j^m}{{c_2}^m + f_j^m} = \frac{\gamma I^*}{1-(1+\gamma)\,I^*}. \tag{4.4d}$$

In addition, we can use Equation (4.3c) to give

$$f^* = \frac{p_f}{d_f} I^*. \tag{4.4e}$$

Therefore f^* is directly proportional to I^*, by a scale factor p_f/d_f, which we will from here on after refer to as c_3. Substituting Equation (4.4e) into (4.2d), the following must then hold at the homogeneous steady state

$$\frac{\gamma I^*}{1-(1+\gamma)\,I^*} = \frac{c_1 {c_3}^m {I^*}^m}{1+c_3^m {I^*}^m}. \tag{4.5}$$

The number of solutions to Equation (4.5) is dependent on the parameter values, especially m, which determines the shape of the dose-response curve. Solving for steady states rapidly becomes intractable above $m > 2$. Straightforward algebraic manipulation of Equation (4.5) when $m = 1, 2$ shows that

$$(S^*, I^*) = \begin{cases} (0,1) & \text{if } m = 1,2, \text{ fully susceptible s.s.,} \\ \left(\frac{\gamma(c_3+1+\gamma)}{c_3 b}, -\frac{(\gamma - c_1 * c_3)}{c_3 b}\right) & \text{if } m = 1,2 \text{ infected s.s.,} \\ \left(1 - \frac{(1+\gamma)(c_1 c_3 \pm a)}{2c_3 b}, \frac{c_1 c_3 \pm a}{2c_3 b}\right) & \text{if } m = 2, \text{ an additional infected s.s..} \end{cases}$$

where $a = \sqrt{c_1^2 c_3^2 - 4\gamma^2 - 4c_1\gamma - 4c_1\gamma^2}$ and $b = (\gamma + c_1 + c_1\gamma)$.

For the cases when $m > 2$, we can also numerically solve Equation (4.4c) in order

to determine the number of steady states that occur in different parts of parameter spaces. An example of how the number of steady states vary as c_1 and m varies is shown in Figure 4.2. Figure 4.3 shows the results of numerically solving the LHS and RHS of Equation (4.5) to determine the number of possible solutions over parameter space (γ, c_1) when $m = 1$.

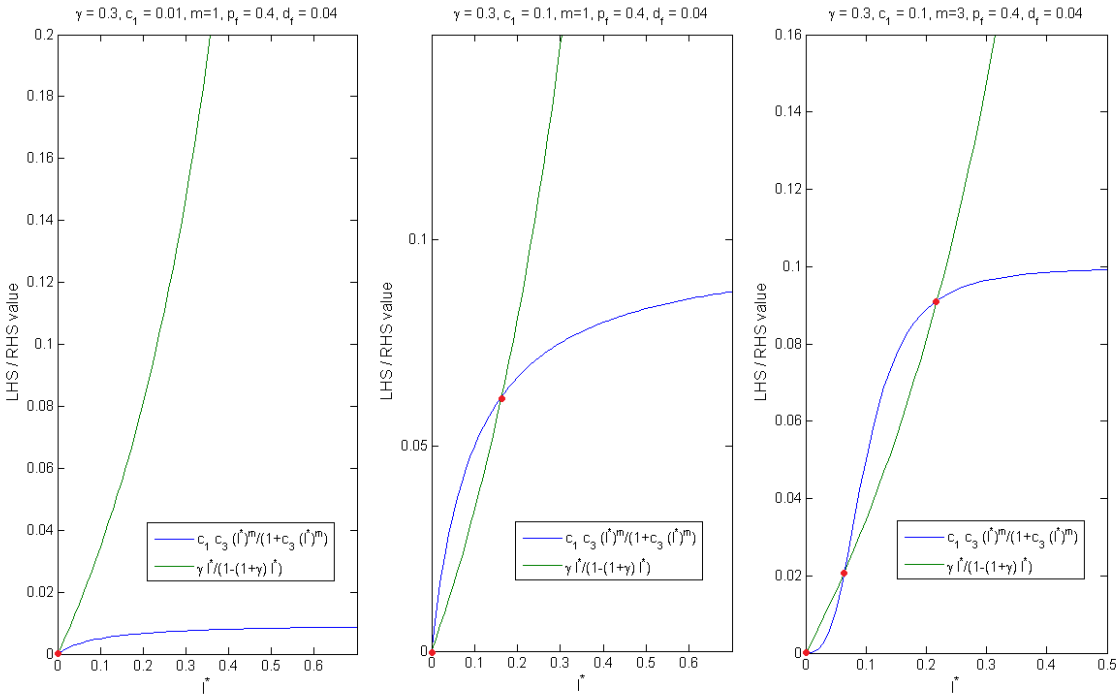

Figure 4.2: Each subplot shows the number of solutions for specific combinations of parameter values γ, c_1 and m. Each intersection represents one solution for a homogeneous steady state (represented by red dots).

4.2.2 Stability to homogeneous steady state

We can investigate the stability of the multiple steady states identified above by phase plane analysis, where an example is shown in Figure 4.4. The blue lines

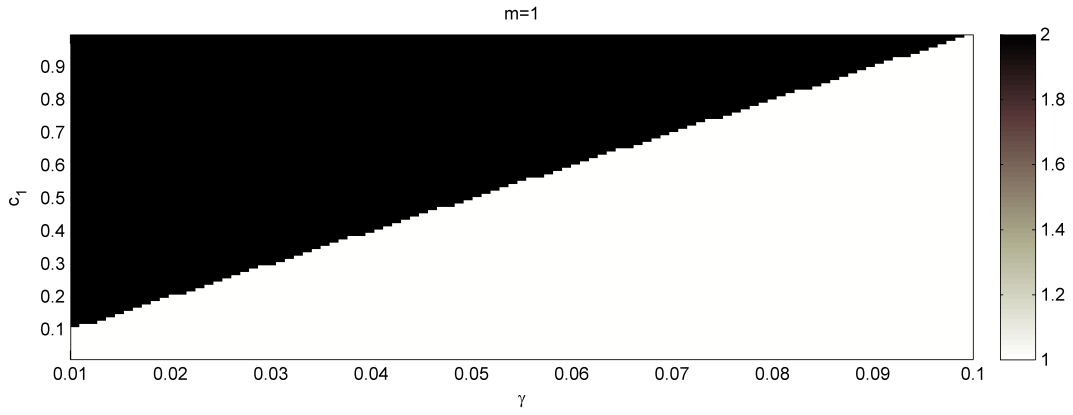

Figure 4.3: Number of steady states over parameter space (γ, c_1) when $m = 1$. The number of steady states is one when $d_f\gamma > c_1 p_f$ (trivial non-infected steady state), and two when $c_1 p_f > d_f\gamma$ (infected steady state). We have $d_f = 0.04$, $p_f = 0.4$.

describe the trajectory in (S, I) space over time from various initial conditions for the parameter values used in Figure 4.2. The red circles indicate a stable steady state, and the green circle represents an unstable steady state. We note that $I^* = 0$ is always a stable steady state in the first and second case, and the maximum possible infected steady state is also always stable.

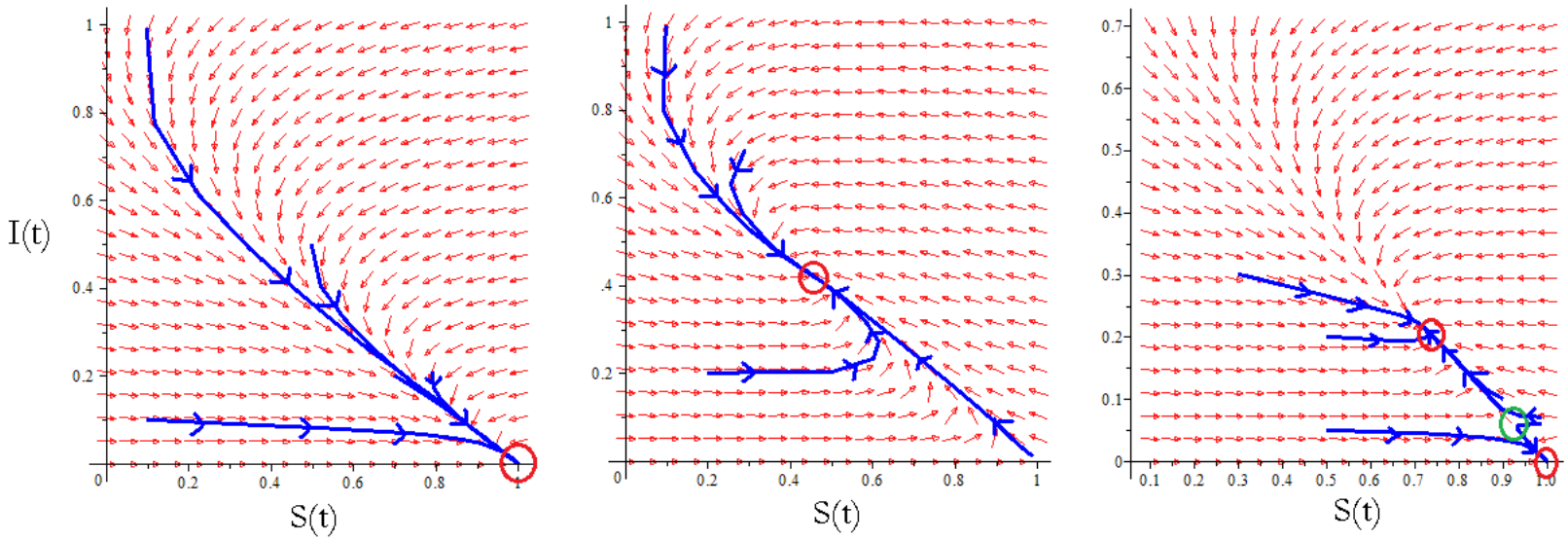

Figure 4.4: Phase plane plots corresponding to the panels in Figure 4.2. A red circle denotes a stable homogeneous steady state and a green circle denotes an unstable homogeneous steady state.

Analytically determining the stability of steady states rapidly becomes intractable for $m > 1$. However, it is possible to analytically determine the stability of the steady states for $m = 1$ by evaluating the sign of the eigenvalues of the Jacobian. When $m = 1$ then $D_f(f^*) = \frac{c_1 f}{1+f}$ and $D'_f(f) = \frac{c_1}{1+f} - \frac{c_1 f}{(1+f)^2}$, and the Jacobian evaluated at $(S^*, I^*, f^*) = (1, 0, 0)$ is

$$\mathbf{J_0} = \begin{bmatrix} -1 & -1 & -c_1 \\ 0 & -\gamma & c_1 \\ 0 & p_f & -d_f \end{bmatrix}$$

The eigenvalues of $\mathbf{J_0}$ are $\left(-1, -\frac{d_f}{2} - \frac{\gamma}{2} + \frac{\sqrt{a}}{2}, -\frac{d_f}{2} - \frac{\gamma}{2} - \frac{\sqrt{a}}{2}\right)$, where $a = {d_f}^2 - 2\gamma d_f + \gamma^2 + 4c_1 p_f$. The real parts of the first and third eigenvalues are always negative. The second eigenvalue will be negative if

$$-\frac{d_f}{2} - \frac{\gamma}{2} + \frac{\sqrt{{d_f}^2 - 2\gamma d_f + \gamma^2 + 4c_1 p_f}}{2} < 0$$

Rearranging this gives

$$\begin{aligned} \sqrt{{d_f}^2 - 2\gamma d_f + \gamma^2 + 4c_1 p_f} &< d_f + \gamma \\ {d_f}^2 - 2\gamma d_f + \gamma^2 + 4c_1 p_f &< (d_f + \gamma)^2 \\ {d_f}^2 - 2\gamma d_f + \gamma^2 + 4c_1 p_f &< {d_f}^2 + 2d_f\gamma + \gamma^2, \\ \Rightarrow c_1 p_f &< d_f \gamma \end{aligned}$$

Hence, the fully-susceptible steady state will be stable (in the case $m = 1$) if $d_f\gamma > c_1 p_f$. Both d_f and γ are parameters describing removal of within-pen

contamination, where γ is the rate of transition from Excretor to Carrier, and d_f describes the rate of decay of Salmonella in the pen environment. The product of these two parameters must be greater than the product of two "contamination" parameters, where c_1 determines the magnitude of the dose-response function, and p_f describes the magnitude of contamination produced by excreting pigs. This is analogous to the one, two and multi-pen homogeneous steady states, where the fully-susceptible steady state is only stable if the recovery rate is greater than the probability of an effective contact.

Consequently, the fully susceptible steady state is unstable when $c_1 p_f > d_f \gamma$. The plot in Figure 4.3 describes both cases where $d_f \gamma > c_1 p_f$ and $d_f \gamma < c_1 p_f$. When $d_f \gamma > c_1 p_f$ then there is only one (susceptible only state) steady state and when $d_f \gamma < c_1 p_f$ there are two steady states, where the fully-susceptible steady state is unstable, and the infected steady state is stable.

When $m > 1$ then three steady states may exist depending on the other parameter values (see for example Figure 4.3). In this case we must adopt a more general treatment. The Jacobian for general m is

$$\mathbf{J_{0_m}} = \begin{bmatrix} -1 - D_f(f^*) & -1 & -\frac{\partial D(f^*)}{\partial f} S^* \\ D_f(f^*) & -\gamma & \frac{\partial D(f^*)}{\partial f} S^* \\ 0 & p_f & -d_f \end{bmatrix}.$$

The detererminant is $|\lambda \mathbf{I} - \mathbf{J}|$, where $\mathbf{I}$ is the identitiy matrix. The resulting determinant is then

$$\begin{bmatrix} \lambda + 1 + D_f(f^*) & 1 & \frac{\partial D(f^*)}{\partial f} S^* \\ -D_f(f^*) & \lambda + \gamma & -\frac{\partial D(f^*)}{\partial f} S^* \\ 0 & -p_f & \lambda + d_f \end{bmatrix} = 0.$$

We now determine the Routh-Hurwitz criteria to investigate whether the multiple steady states are stable or not. The general characteristic equation for a 3x3 matrix with eigenvalues λ is $\lambda^3 + a_2\lambda^2 + a_1\lambda + a_0 = 0$. The coefficients of a_2, a_1 and a_2 in this specific case are

$$a_2 = D_f(f^*) + 1 + \gamma + d_f, \tag{4.6a}$$

$$a_1 = d_f + D_f(f^*)\left(d_f + \gamma + 1\right) + \gamma d_f + \gamma - \frac{\partial D\left(f^*\right)}{\partial f} S^* p_f, \tag{4.6b}$$

$$a_0 = \left(\gamma + D_f(f^*)\right) d_f - \frac{\partial D\left(f^*\right)}{\partial f} S^* p_f + D_f(f^*)\gamma d_f. \tag{4.6c}$$

The Routh-Hurwitz criteria for stable steady states for a cubic polynomial are $a_0 > 0$, $a_2 > 0$ and $a_1 a_2 - a_0 > 0$. As all parameters are real and positive the coefficient a_2 is always greater than zero (Equation (4.6a)). Using the chain rule then gives

$$\frac{\partial D_f\left(I^*\right)}{\partial I} = \frac{\partial D_f\left(f^*\right)}{\partial f}\frac{\partial f}{\partial I} = \frac{\partial D_f\left(f^*\right)}{\partial f}\frac{p_f}{d_f}, \tag{4.7}$$

so that

$$\frac{\partial D_f\left(f^*\right)}{\partial f} = \frac{d_f}{p_f}\frac{\partial D_f\left(f^*\right)}{\partial I}. \tag{4.8}$$

Substituting Equations (4.4c), (4.4b) and (4.7) into (4.6c) then gives

$$a_0 = \left(\gamma + \frac{\gamma I^*}{1-(1+\gamma)\,I^*}\right) d_f - \frac{\partial D_f\,(I^*)}{\partial I}\frac{(1-(1+\gamma)\,I^*)\,d_f}{p_f} + \frac{\gamma I^*}{1-(1+\gamma)\,I^*}\gamma d_f. \tag{4.9}$$

For a steady stable state we require that $a_0 > 0$. Solving this inequality for $\frac{\partial D_f(I^*)}{\partial I}$ then gives

$$\frac{\partial D_f\,(I^*)}{\partial I} < \frac{\gamma}{(1-(1+\gamma)\,I^*)^2}. \tag{4.10}$$

The RHS of the inequality (4.10) is the gradient of $\frac{\gamma}{(1-(1+\gamma)I^*)^2}$. The inequality (4.10) then shows that if the slope of $D_f\,(I^*)$ is more shallow than that of $\frac{\gamma}{(1-(1+\gamma)I^*)^2}$ at the homogeneous steady state then that state may be stable (we would still need to confirm that $a_1a_2 - a_0 > 0$). But, importantly, inequality (4.10) demonstrates that if $D_f\,(I^*)$ is steeper than the curve $\frac{\gamma}{(1-(1+\gamma)I^*)^2}$ at the steady state then $a_0 < 0$ at that state and so it must be unstable. This then shows that in the two steady state case (e.g. panel 2 in Figure 4.2) the susceptible only state is unstable and in the 3 steady state case (e.g. panel 3 in Figure 4.2) the intermediate infection state is unstable. The condition $a_1a_2 - a_0 > 0$ is analytically intractable but we find from numerical investigation that the remaining states in the 2,3 steady state cases are always stable.

As for the 'standard' multi-pen model in Chapter 3 the system can be linearised to indicate the stability of the above steady state solutions when perturbed homogeneously and heterogeneously to explore the existence of Turing patterns.

4.2.3 Existence of Turing spatial patterns

Linearising about the steady state by setting $S_j = \bar{S}_j + S^*$, $I_j = \bar{I}_j + I^*$ and $f_j = \bar{f}_j + f^*$ and substituting into Equation (4.2) gives

$$\begin{aligned}
\bar{S}_j{}' &= 1 - \bar{S}_j - S^* - \bar{I}_j - I^* - D_f\left(\bar{f}_j + f^*\right)\left(\bar{S}_j + S^*\right) \\
\bar{I}_j{}' &= D_f\left(\bar{f}_j + f^*\right)\left(\bar{S}_j + S^*\right) - \gamma\left(\bar{I}_j + I^*\right) \\
\bar{f}_j{}' &= p_f\left(\bar{I}_j + I^*\right) - d_f\left(\bar{f}_j + f^*\right) + \eta\left(\left(\bar{f}_{j+1} + f^*\right) + \left(\bar{f}_{j-1} + f^*\right) - 2\left(\bar{f}_j + f^*\right)\right)
\end{aligned} \tag{4.11}$$

As we assume that $\bar{S}_j$, $\bar{I}_j$ and $\bar{f}_j$ are small then any combination of terms such as $\bar{S}_j\bar{I}_j$ will be considered to be negligible. Expanding $D_f\left(\bar{f}_j + f^*\right)$ using a Taylors series expansion about f^*, namely $D_f\left(\bar{f}_j + f^*\right) = D_f\left(f^*\right) + \frac{dD_f}{df}\Big|_{f=f^*}\bar{f}_j + \underbrace{D\left(f_j^2\right)}_{small} \approx D_f\left(f^*\right) + D_f'\left(f^*\right)\bar{f}_j$. Removing negligible terms and using the steady state conditions (Equation (4.3)) then gives

$$\begin{aligned}
\bar{S}_j{}' &= -\bar{S}_j - \bar{I}_j - \mathcal{A}\bar{f}_j S^* - D_f(f^*)\bar{S}_j, \\
\bar{I}_j{}' &= \mathcal{A}\bar{f}_j S^* + D_f(f^*)\bar{S}_j - \gamma\bar{I}_j, \\
\bar{f}_j{}' &= p_f\bar{I}_j - d_f\bar{f}_j + \eta\left(\bar{f}_{j+1} + \bar{f}_{j-1} - 2\bar{f}_j\right),
\end{aligned} \tag{4.12}$$

where $\mathcal{A} = \frac{dD_f(f^*)}{df}$. Similar to the n-pen system the spatial perturbations $\bar{S}$, $\bar{I}$ and $\bar{f}$ can be written as $\hat{S}e^{\mu t + i\lambda j}$, $\hat{I}e^{\mu t + i\lambda j}$ and $\hat{f}e^{\mu t + i\lambda j}$ respectively, where $\hat{S}$, $\hat{I}$ and $\hat{f}$ are constants, λ is the spatial wavenumber and μ is the growth rate of the perturbations. Substituting these expressions into Equation (4.12) and then

rearranging

$$\begin{aligned}\left(\mu\hat{S}+\hat{S}+\hat{I}+\mathcal{A}\hat{f}_j S^*+D_f(f^*)\hat{S}_j\right)e^{\mu t+i\lambda j}&=0,\\ \left(\mu\hat{I}-\mathcal{A}\hat{f}S^*-D_f(f^*)\hat{S}_j+\gamma\hat{I}\right)e^{\mu t+i\lambda j}&=0,\\ \left(\mu\hat{f}-p_f\hat{I}+d_f\hat{f}-2\eta\hat{f}\left(\cos\lambda-1\right)\right)e^{\mu t+i\lambda j}&=0.\end{aligned}\tag{4.13}$$

Dividing by $e^{\mu t+i\lambda j}$ and converting to matrix form gives

$$\underbrace{\begin{bmatrix}\mu+1+D_f(f^*) & 1 & \mathcal{A}S^*\\ -D_f(f^*) & \mu+\gamma & -\mathcal{A}S^*\\ 0 & -p_f & \mu+d_f-2\eta\left(\mathcal{K}-1\right)\end{bmatrix}}_{\mathbf{A}}\cdot\begin{bmatrix}\hat{S}\\ \hat{I}\\ \hat{f}\end{bmatrix}=\begin{bmatrix}0\\ 0\\ 0\end{bmatrix}$$

where $\mathcal{K}=k\left(\lambda\right)=\cos\lambda$. For non-trivial solutions $\hat{S}$, $\hat{I}$ and $\hat{f}$ are non-zero, in which case the determinant of $\mathbf{A}$ must be zero. We use the Routh-Hurwitz criteria to determine the roots of the determinant and whether spatial (Turing) patterns will occur. The determinant in this case is of the form $\mu^3+a_1\mu^2+a_2\mu+a_3\mu=0$. The Routh-Hurwitz criteria are $a_1>0$, $a_3>0$ and $\Delta=a_1a_2-a_3>0$. As discussed in Chapter 3, spatial patterns occur when the homogeneous steady state is stable to homogeneous perturbations, but when one or more of the Routh-Hurwitz criteria are violated for the steady state when there are heterogeneous perturbations. The coefficients of a_1, a_2 and a_3 in this case are

$$
\begin{aligned}
a_1 =& 2\eta\left(1-\mathcal{K}\right)+1+d_f+D_f(f^*)+\gamma,\\
a_2 =& -\mathcal{A}S^*p_f+2D\eta\left(1-\mathcal{K}\right)+2\gamma\eta\left(1-\mathcal{K}\right)+2\eta\left(1-\mathcal{K}\right)\\
&+D_f(f^*)d_f+D_f(f^*)\gamma+\gamma d_f+d+D_f(f^*)+\gamma,\\
a_3 =& -\mathcal{A}S^*p_f+2\gamma\eta\left(1-\mathcal{K}\right)+2D_f(f^*)\gamma\eta\left(1-\mathcal{K}\right)+\gamma d_f+D_f(f^*)d_f\\
&+2D_f(f^*)\eta\left(1-\mathcal{K}\right)+D_f(f^*)\gamma d_f.
\end{aligned}
\tag{4.15}
$$

Therefore, for homogeneous perturbations (where $\mathcal{K}=1$, i.e. where $\lambda=0$ and the perturbations have the form $ue^{\mu t}$ for $u=S,\ I,\ f$), then conditions (4.15) reduce to

$$a_1\left(\mathcal{K}=1\right)=1+d_f+D_f(f^*)+\gamma, \tag{4.16a}$$

$$a_2\left(\mathcal{K}=1\right)=\gamma d_f+\gamma+D_f(f^*)+D_f(f^*)\left(d_f+\gamma\right)-\mathcal{A}S^*p_f+d_f, \tag{4.16b}$$

$$a_3\left(\mathcal{K}=1\right)=-\mathcal{A}S^*p_f+\gamma d_f+D_f(f^*)\gamma d_f+D_f(f^*)d_f. \tag{4.16c}$$

As all parameters are real and positive then $a_1\left(\mathcal{K}=\infty\right)$ will always be positive. Inspection of $a_1\left(\mathcal{K}\right)$ shows that, since $a_1\left(\mathcal{K}\right)>0$, and $\mathcal{K}\in[-1,1]$, then $a_1\left(\mathcal{K}\right)>0$ $\forall\,\mathcal{K}\in[-1,1]$. Therefore, Turing patterns will only occur when both $a_3\left(k=1\right)>0$ and $\Delta\left(k=1\right)>0$, and either $a_3\left(k=[-1,1)\right)<0$ or $\Delta\left(k=[-1,1)\right)<0$.

Stability to homogeneous perturbations ($\mathcal{K}=1$)

The remaining two conditions, a_3 and Δ, define two lines which delimit the relevant regions of $(\mathcal{A},\ p_f)$ parameter space into stability or instability to homogeneous

perturbations. These are found by solving for $\mathcal{A}$ when $a_3(\mathcal{K}=1)=0$ and $\Delta(\mathcal{K}=1)=0$.

First, the two conditions $a_3\left(\mathcal{K}=1\right)$ and $\Delta\left(\mathcal{K}=1\right)$ can be specified in terms of only I^*. Using the chain rule we can write $\mathcal{A}$ in terms of I^*, i.e. $\mathcal{A}_{I^*}=\frac{\partial D_f(f^*)}{\partial f}\frac{\partial f}{\partial I}=\mathcal{A}\frac{p_f}{d_f}$. From Equation (4.4b) we have $S^*=1-\left(1+\gamma\right)I^*$ and from Equation (4.4c) we have $D_f\left(f^*\right)=\frac{\gamma I^*}{1-(1+\gamma)I^*}$. Therefore, solving $a_3(\mathcal{K}=1)=0$ and $\Delta(\mathcal{K}=1)=0$ respectively, gives

$$H_1:\mathcal{A}=\frac{\gamma}{\left(1-\left(\gamma+1\right)I^*\right)^2}, \tag{4.17a}$$

$$H_2:\mathcal{A}=\frac{a\left[d_f\left(\gamma^2+\gamma\left(1+d_f\right)+1+d_f\right)I^*-\left(1+d_f\right)\left(d_f+\gamma\right)\right]}{d_f\left(1-\left(1+\gamma\right)I^*\right)^2\left(\left(d_f+\gamma d_f+\gamma^2\right)I^*-d_f-\gamma\right)}, \tag{4.17b}$$

where $a=\left[\left(\left(\gamma+1\right)^2-\gamma\right)I^*-\gamma-1\right]$. As we are unable to identify general solutions for I^* for all m we fix I^* at a biologically reasonable value (we find that our results are insensitive to our choice of $I^*\in(0,1)$). In doing this we also fix the value of γ through Equation (4.5). Rearranging Equation (4.5) for γ then gives

$$\gamma=\frac{-c_1(\frac{p_f}{d_f})^m I^{*m}\left(I^*-1\right)}{I^*\left(1+(\frac{p_f}{d_f})^m I^{*m}+c_1(\frac{p_f}{d_f})^m I^{*m}\right)}.$$

Substituting in appropriate values for free parameters (I^*, p_f, d_f, m) we can plot the two lines (H_1 and H_2 in $(\mathcal{A},p_f)$ parameter space). From numerical solutions in previous chapters the infection steady state is usually reached when around 20-30% of pigs in a pen are infected. Hence we set $I^*=0.2$; we also set $d_f=0.04$ (Gray and Fedorka-Cray, 2001; Tannock and Smith, 1972) and $m=1.5$ (value chosen to produce bistable kinetics, see later). The resulting plot is shown in Figure 4.5,

where the Routh-Hourwitz conditions, $a_3(k=1) > 0$ and $\Delta(k=1) > 0$ are met in the parameter space below the red and green curves respectively (green shaded area). Hence, the steady state $I^* = 0.2$ is stable under homogeneous perturbations in the green shaded area.

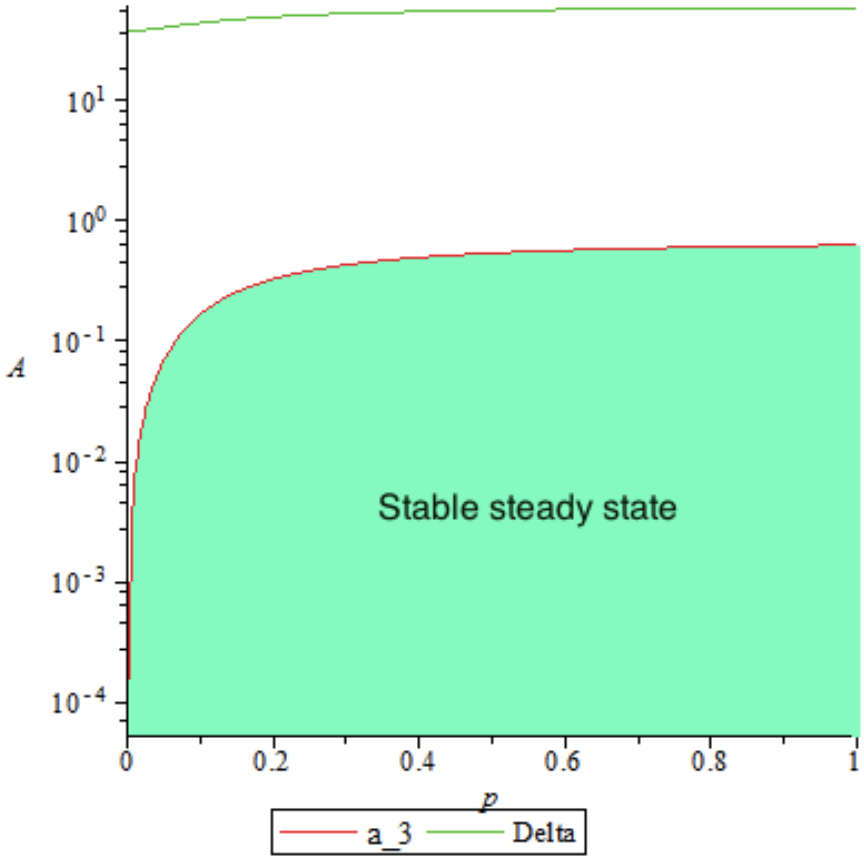

Figure 4.5: The green shaded area represents when both criteria $a_3(\mathcal{K}=1) > 0$ (red) and $\Delta(\mathcal{K}=1) > 0$ (green) are met in $(\mathcal{A}, p_f)$ parameter space, and the steady state is stable to homogeneous perturbations.

Stability to heterogeneous perturbations ($k \in [-1, 1)$

Generally, $a_3 > 0$ and $\Delta > 0$ can be solved for $\mathcal{A}$ to give

$$H_3 : \mathcal{A} = \frac{\gamma\left(2\eta\left(1-\mathcal{K}\right)+d_f\right)}{d_f\left(1-\left(\gamma+1\right)I^*\right)^2},$$
$$H_4 : \mathcal{A} = \frac{ab}{d_f\left(1-\left(\gamma+1\right)I^*\right)g},$$

where

$$b = \left(\mathcal{K}-1\right)\left(2\gamma\eta+2\eta+4\eta d_f\right)+\left(1-\mathcal{K}\right)\left(2\eta I^*\right)\left(1+2d_f+\gamma+\gamma^2+2d_f\gamma\right)$$
$$-\left(4\eta^2\right)\left(\mathcal{K}^2+1\right)\left(I^*+1\right)+4\gamma\eta I^*\left(1-2\mathcal{K}\right)+4\eta^2\mathcal{K}\left(2\left(1+\left(1+\mathcal{K}\right)I^*\right)\right),$$

and

$$g = \left(2\eta\left(\mathcal{K}-1\right)+2\eta I^*\left(\gamma+1\right)\left(1-\mathcal{K}\right)-\gamma-d_f+d_f I^*+\gamma I^* d_f+\gamma^2 I^*\right). \tag{4.18}$$

The gradient of H_3 as a function of $\mathcal{K}$ is negative, hence if H_1 is positive then H_3 will also be positive over the domain of $\mathcal{K} = [-1, 1]$. That is, it is not possible to violate the Routh-Hurwitz criterion (i.e. $a_3 < 0$) in this case. For the criterion H_4 we make some observations about its characteristics, and how these compare against the criteria for Turing patterns to occur, that is for $H_4 < 0$ when $H_2 > 0$.

We first note that Δ is a quadratic in $\mathcal{K}$, i.e. it has the form $a\mathcal{K}^2 + b\mathcal{K} + c$. The coefficient of $\mathcal{K}^2$ is $4\eta^2\left(\gamma + D\left(f^*\right) + 1\right)$. As all parameters are real positive numbers then this coefficient is always positive, and hence we know that $\frac{d\Delta}{d\mathcal{K}} = 0$ is the minimum value of the quadratic equation.

To reiterate, the criteria for Turing patterns to occur is for a steady state to be stable to homogeneous perturbations but unstable to heterogeneous perturbations.

Taking this knowledge and knowing that we have a positive $\mathcal{K}^2$ coefficient we can sketch some conditions that must be met for Turing patterns to occur ($H_2 > 0, H_4 < 0$), see Figure 4.6. The black curves signify when the criteria for Turing pattern formation are met, and the grey curves when the criteria are not met.

The key criteria are: that $\Delta(\mathcal{K} = 1) > 0$, and that either $\Delta(\mathcal{K}) < 0$ when $\frac{d\Delta}{d\mathcal{K}} = 0$ for some $\mathcal{K} \in [-1, 1]$, or $\Delta(\mathcal{K} = -1) < 0$ given $\frac{d\Delta}{d\mathcal{K}} = 0$, $\mathcal{K} \notin [-1, 1]$.

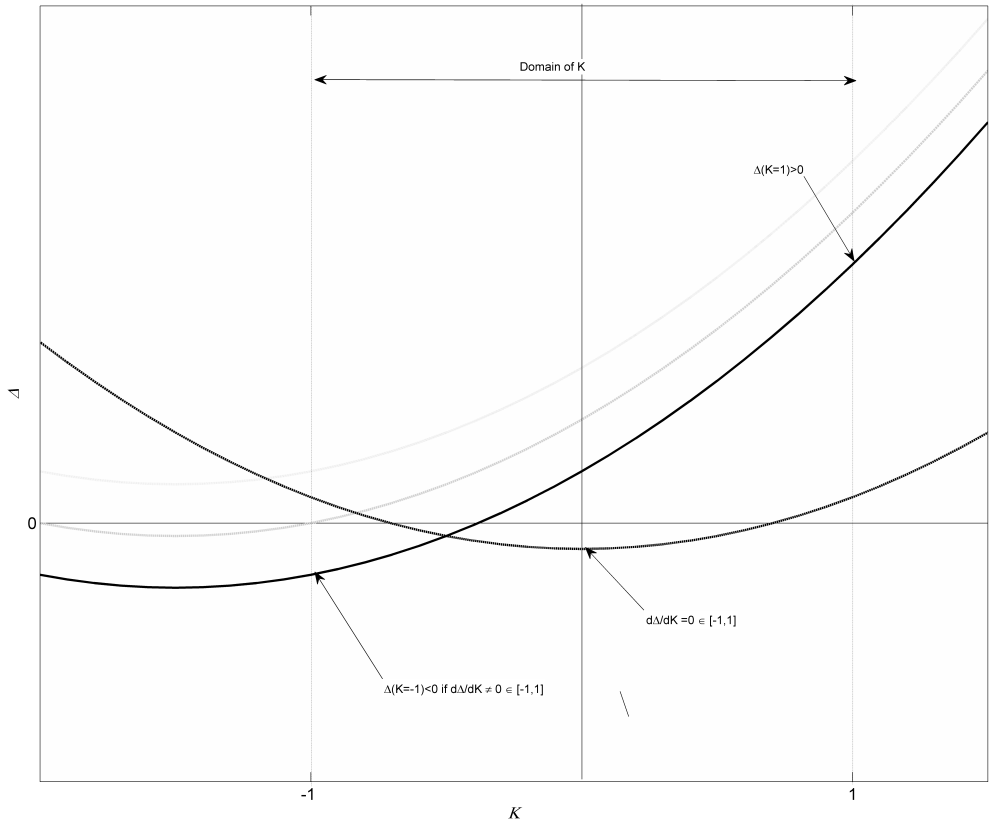

Figure 4.6: Sketch of conditions for Turing patterns to occur for condition H_4 over the domain of $\mathcal{K} \in [-1, 1]$. Black lines represent curves which allow the formation of Turing patterns, grey lines when Turing patterns cannot form.

If H_1 is positive then H_3 can never be negative due to its negative gradient over the domain of $\mathcal{K}\,[-1, 1]$. Therefore we perform a similar check for H_4 by evaluating

the slope of Δ at $\mathcal{K} = 1$. Differentiating Equation (4.18) $(H - 4)$ and substituting in $\mathcal{K} = 1$ gives

$$\left.\frac{d\Delta}{d\mathcal{K}}\right|_{\mathcal{K}=1} = -\frac{\left(\gamma^2 I^* - 1 + gI^* + I^* - \gamma\right) q}{\left(\left(-1 + I^* + \gamma I^*\right)^3 d_f\right)}, \tag{4.19}$$

where $q = (\gamma^2 I^* + 2\gamma I^* d_f + \gamma I^* + 2d_f I^* + I^* - \gamma - 2d_f - 1)$.

As for the homogeneous perturbation analysis in the previous section, we can delineate between regions of $(\mathcal{A}, p_f)$ parameter space (or whichever parameter space we choose). Taking the same values as for the fixed parameters in the previous analysis for homogeneous perturbations we get the graph in Figure 4.7. The red curve denotes $\Delta(\mathcal{K} = 1) = 0$, where below the curve $\Delta(\mathcal{K} = 1) > 0$ and above it $\Delta(\mathcal{K} = 1) < 0$. The green curve denotes $\left.\frac{d\Delta}{d\mathcal{K}}\right|_{\mathcal{K}=1} = 0$, where above the curve $\left.\frac{d\Delta}{d\mathcal{K}}\right|_{\mathcal{K}=1} > 0$ (i.e. H_4 has a positive gradient at $\mathcal{K} = 1$) and below the curve $\left.\frac{d\Delta}{d\mathcal{K}}\right|_{\mathcal{K}=1} < 0$ (i.e. H_4 has a negative gradient at $\mathcal{K} = 1$). Hence, for the parameter space where $\Delta(\mathcal{K} = 1) > 0$ (homogeneous steady state is stable) then $\left.\frac{d\Delta}{d\mathcal{K}}\right|_{\mathcal{K}=1} < 0$ (that is the gradient of the curve for $\Delta(\mathcal{K} = 1)$ is negative. Therefore, as $\Delta(\mathcal{K})$ is a quadratic with a positive $\mathcal{K}^2$ coefficient, then $\frac{d\Delta}{d\mathcal{K}} < 0 \;\forall\; \mathcal{K} \leq 1$. Hence, Turing patterns cannot form as there is a negative gradient of $\Delta(\mathcal{K})$ along the valid domain of $\mathcal{K}\imath\,[-1, 1]$, and therefore if H_2 is positive then H_4 must always be positive in the valid range of $\mathcal{K}$.

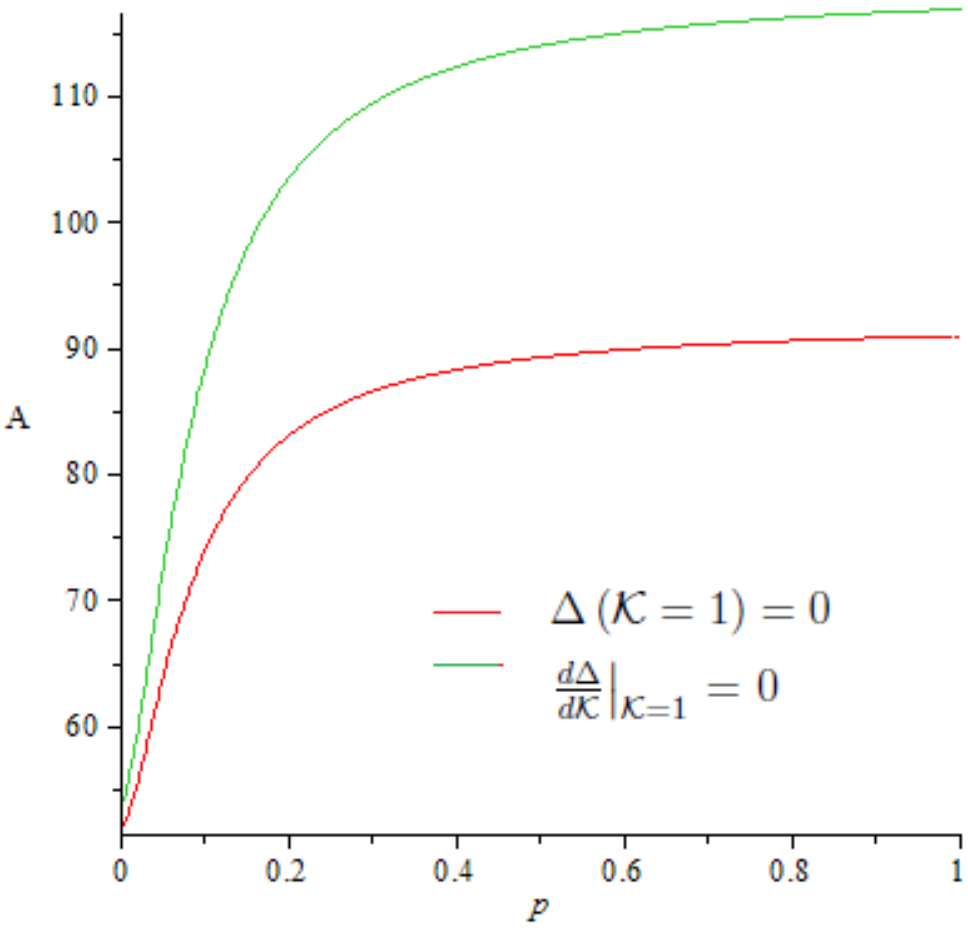

Figure 4.7: The red curve denotes the equation $\Delta(\mathcal{K}=1)=0$ in $(\mathcal{A}, p_f)$ parameter space. The steady state is stable to homogeneous perturbations in the region below this curve. The green curve denotes the equation $\frac{d\Delta}{d\mathcal{K}}\big|_{\mathcal{K}=1}=0$, where below the line represents a negative gradient to H_4 over the domain of $\mathcal{K}$.

4.3 Solutions for travelling wave of cross contamination model

The analysis above on Turing patterns suggests that the n-pen cross-contamination system of ODEs settles to the homogeneous steady state and no Turing patterns are possible. Therefore, as for the standard n-pen system, we look for travelling

waves to assess the speed at which the system settles to the infected homogeneous steady state. In addition, with the potential of bistability that may occur with the cross-contamination model, we can also investigate regions of parameter space that will lead to more complex wave dynamics, e.g. the possibility of pinning. Pinning is where the travelling wave is stationary and two infection levels stably exist in pens either side of the pinned wave. Therefore, when examining the system, we also examine parameter ranges that will lead to the existence of two infected steady states and hence bistable kinetics.

The frame of reference transformations of $S'_j(t)$ and $I'_j(t)$, as described in Equations (3.12a) and (3.12b) in Section 3.4, are still applicable to the cross-contamination model. A similar transformation can be made for $f'_j(t)$. Substituting these transformations into the linearised form of the cross-contamination model in Equation (4.12) gives

$$\begin{aligned} -c \cdot \frac{d\bar{S}(z)}{dz} &= -\bar{S}_z - \bar{I}_z - \mathcal{A}\bar{f}_z S^* - D_f(f^*)\bar{S}_z \\ -c \cdot \frac{d\bar{I}(z)}{dz} &= \mathcal{A}\bar{f}_z S^* - \gamma \bar{I}_z + D_f(f^*)\bar{S}_z \\ -c \cdot \frac{d\bar{f}(z)}{dz} &= p_f \bar{I}_z - d_f \bar{f}_z + \eta\left(\bar{f}_{z+1} + \bar{f}_{z-1} - 2\bar{f}_z\right) \end{aligned} \tag{4.20}$$

where $z = j - ct$ as shown in Section 3.4. Now setting the spatial perturbations $\bar{S}_z$, $\bar{I}_z$ and $\bar{f}_z$ to $\hat{S}e^{\lambda \mathbf{z}}$, $\hat{I}e^{\lambda \mathbf{z}}$ and $\hat{f}e^{\lambda \mathbf{z}}$ respectively, where $\hat{S}$, $\hat{I}$ and $\hat{f}$ are constants and λ is the spatial decay rate, and substituting $\bar{S}$, $\bar{I}$ and $\bar{f}$ into Equation (4.20) and rearranging gives

$$\begin{aligned}\left(\left(-c\lambda+1+D_f(f^*)\right)\hat{S}+\hat{I}+\mathcal{A}\hat{f}S^*\right)e^{\lambda\mathbf{z}}&=0\\ \left(\left(-c\lambda+\gamma\right)\hat{I}-\mathcal{A}S^*\hat{f}-D_f(f^*)\hat{S}\right)e^{\lambda\mathbf{z}}&=0\\ \left(\left(-c\lambda+d_f-2\eta\left(\mathcal{K}-1\right)\right)\hat{f}-p_f\hat{I}\right)e^{\lambda\mathbf{z}}&=0\end{aligned}\tag{4.21}$$

where $\mathcal{K}=k\left(\lambda\right)=\frac{e^{\lambda}+e^{-\lambda}}{2}=\cosh\lambda$.

Dividing through by $e^{\lambda\mathbf{z}}$, and converting into matrix form then gives

$$\begin{bmatrix}-c\lambda+1+D_f(f^*) & 1 & \mathcal{A}S^*\\ -D_f(f^*) & -c\lambda+\gamma & -\mathcal{A}S^*\\ 0 & -p_f & d_f-c\lambda-2\eta\left(\mathcal{K}-1\right)\end{bmatrix}\cdot\begin{bmatrix}\hat{S}\\ \hat{I}\\ \hat{f}\end{bmatrix}=\begin{bmatrix}0\\ 0\\ 0\end{bmatrix}.$$

As before for the n-pen system, we consider the case where the state ahead of the infection travelling wave (i.e. $I^*=0$ and $S^*=1$ as $z\to\infty$) and we consider $\bar{S}$, $\bar{I}$ and $\bar{f}$ to be perturbations of this state so that Equation (4.23) reduces to

$$\underbrace{\begin{bmatrix}-c\lambda+1 & 1 & 0\\ 0 & -c\lambda+\gamma & 0\\ 0 & -p_f & d_f-c\lambda-2\eta\left(\mathcal{K}-1\right)\end{bmatrix}}_{\mathbf{A}}\cdot\begin{bmatrix}\hat{S}\\ \hat{I}\\ \hat{f}\end{bmatrix}=\begin{bmatrix}0\\ 0\\ 0\end{bmatrix}.$$

For non-trivial solutions $\hat{S}$, $\hat{I}$ and $\hat{f}$ are all non-zero, and the determinant of $\mathbf{A}$ must then be equal to zero. Hence,

$$\left(1-c\lambda\right)\left(\gamma-c\lambda\right)\left(d_f-2\eta\left(\cosh\lambda-1\right)-c\lambda\right)=0.$$

Solutions of which are $c = \frac{1}{\lambda}, \frac{\gamma}{\lambda}, \frac{d_f - 2\eta(\mathcal{K}-1)}{\lambda}$. The first two solutions only result in forward waves (i.e. $c > 0$). Pinning can only occur when $c = 0$ and this can only occur with the third solution. A plot of the third solution for c against λ is shown in Figure 4.8. As can be seen there is no real minimum wavespeed as c decreases monotonically as λ increases with a vertical asymptote at $\lambda = 0$, which corresponds to the homogeneous solution. In this case the local dynamics are bistable, and in this case the speed and direction of travelling wave speed are often determined by the non-linearities of the system.

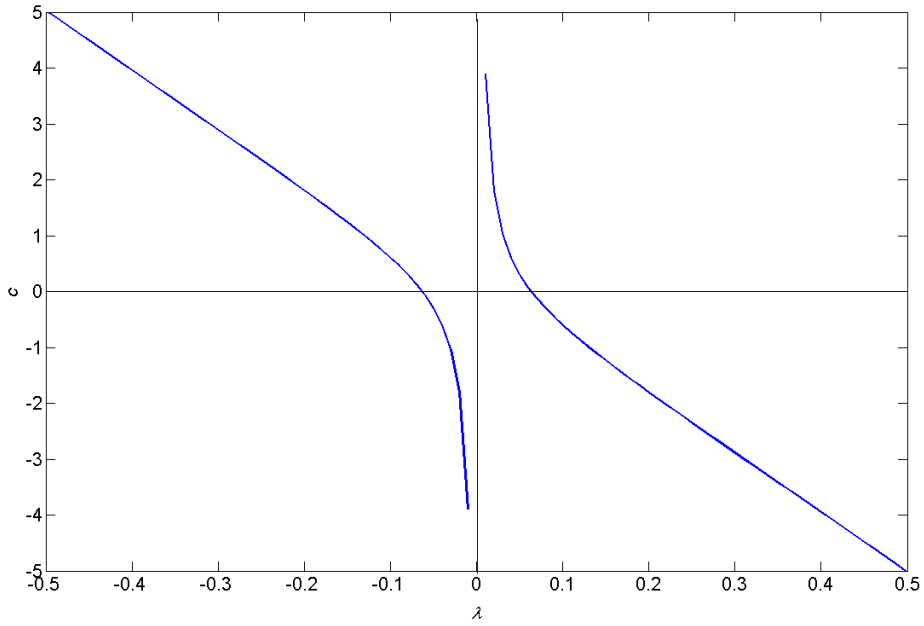

Figure 4.8: Plot of wavespeed c against λ; $\eta = 10$ and $d_f = 0.04$.

4.4 Numerical solutions

The same principle is used to numerically solve the cross-contamination model as for the standard string of pens model described in Section 3.5; i.e. we model the

transmission of infection between a string of 300 pens, where Pen 1 is infected at $t = 0$ and the remaining pens are all in the non-infection steady state.

4.4.1 Parameter estimation

Where relevant, the same parameter estimates are used for the cross-contamination model as for the non-contamination models in previous chapters. Parameter estimates for p_f, η and c_1 are not available from the literature, hence biologically plausible values have been chosen to produce an epidemic curve that results in a similar steady state value for I^* as possible to the n-pen model in Chapter 3[1]. Choosing parameter values that produce a similar epidemic curve as the standard model will allow comparison of the dynamics between the standard and cross-contamination models.

Table 4.1: Parameter estimates for the cross-contamination model

Notation	Description	Value[1]
p_f	Shedding rate parameter	18.8
d_f	Rate of Salmonella decay in pen environment	1.9
c_1	Dose-response parameter	3
η	Faecal cross-contamination parameter	1
m	Dose-response shape parameter	3

4.4.2 Cross-contamination model epidemic curve

The resulting epidemic curve for the cross-contamination model is shown in Figure 4.9. Despite the more complicated interactions of faecal shedding and dose-response included in the cross-contamination model, similar dynamics of infection

[1]More detailed parameter estimation will be undertaken for the dose-response and shedding parameters of the more sophisticated stochastic model in Chapter 6.

can be seen in this model as for the standard multi-pen model (Figure 3.5). The value of η was set to explicitly demonstrate the progressive delay in equilibrium being reached as pen number increases. As can be seen in Figure 4.9 when η is set to 1 (meaning the non-scaled value of η is 0.02 - hence $\sim 2\%$ of contaminated faecal material is cross-contaminated between pens each day) spread of infection is fairly slow at the scale of the non-dimensionalised timestep, at approximately 1 pen per timestep. However, the timestep used in the non-scaled version of the cross-contamination model is $\frac{1}{\delta}$, or approximately 50 days. Therefore, spread between pens is relatively much slower when compared to the length of the growing-finishing period (84-116 days). Detailed numerical analysis of the travelling wavespeed is presented in the next section.

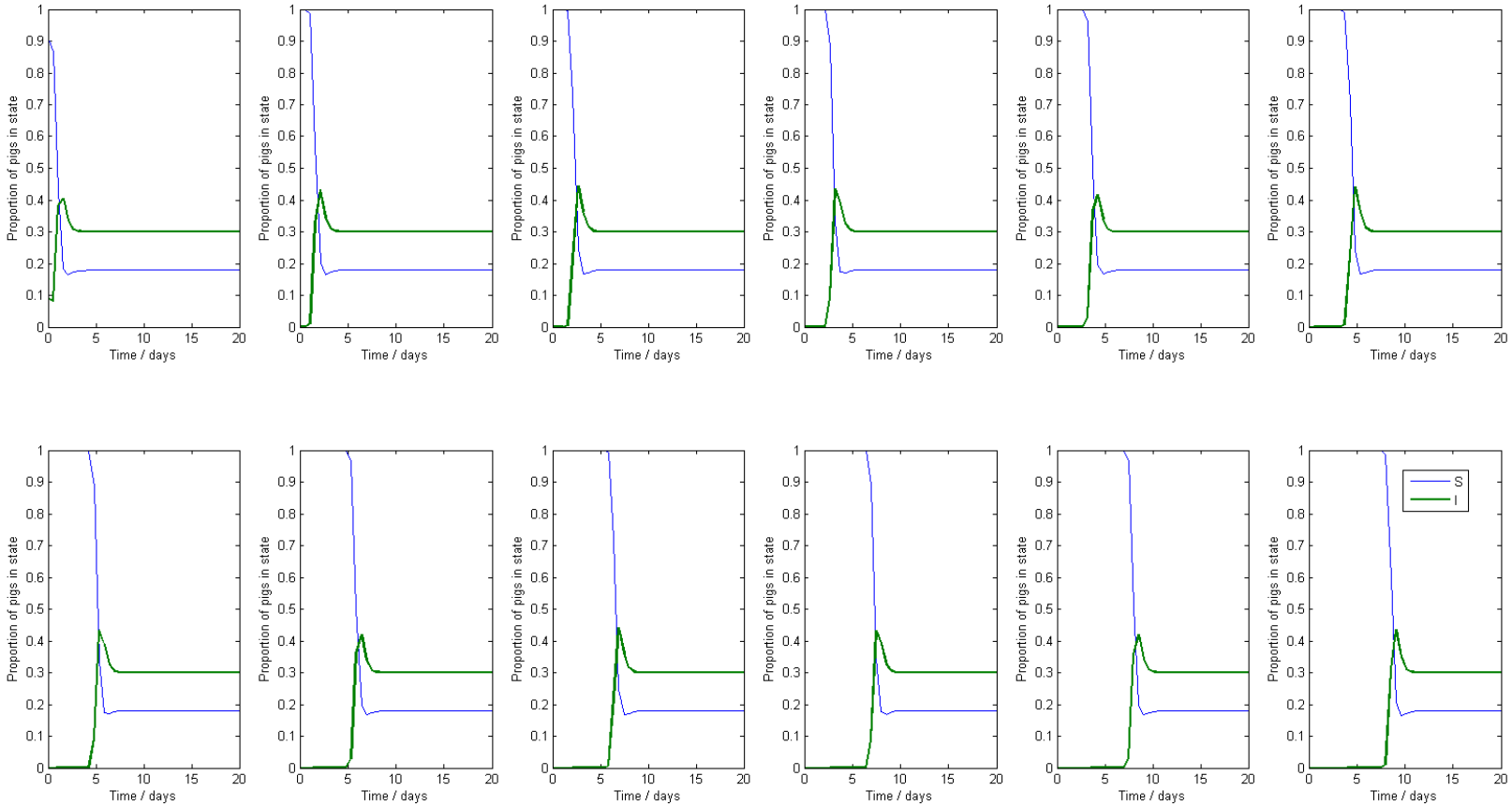

Figure 4.9: Time course of infection in 12 pens of the string of (300-) pens model. Parameter estimates are chosen to give a similar infection profile as for the standard dynamic models in previous chapters. See Table 4.1.

Numerical investigation of the wave speed and the existence of pinning

Using the same numerical technique for evaluating the wavespeed of the travelling wave as described in Section 3.5 the precise speed of the wavefront for the cross-contamination parameterised as above is 1.6 pens per timestep (see Figure 4.9). In non-scaled terms this is equivalent to 0.032 pens per day (1.6 pens per 50 days), far slower than the equivalent standard model. While we cannot compare precise numerical quantities of wavespeed (as the standard and cross-contamination models are not entirely equivalent and use different parameter estimates), we can qualitatively compare the trend for how wavespeed differs for given parameter values. For example, the cross-contamination model parameter c_1 is comparable to the probability of an effective contact, β_2. The variation in the travelling wavespeed for β_2 versus γ (see Figure 4.11) is qualitatively similar to the variation of wavespeed for c_1 versus γ in Figure 3.4. Both have similar curved contours and both have the maximum wavespeed when γ and either c_1 or β_2 are at their largest values. Hence, while the standard and cross-contamination models are markedly different in terms of how infection is modelled, they still have similar qualitative behaviour in terms of their wavespeeds.

Of interest is the situation where two infected steady states exist, i.e. where there is the potential for pinning through bistable kinetics. It is proposed that in order to produce bistability there are three main criteria: (i) a positive feedback loop, (ii) a mechanism for filtering out small stimuli and (iii) a mechanism for preventing explosion (Willhelm, 2009). It is thought that, of prime importance, any automonous differential system (such as the cross-contamination model equations described here) requires a positive feedback mechanism to induce bistability (Cinquin and Demongeot, 2002). The positive feedback process should have hys-

teresis, allowing the process to retain its activity without a persistent signal. In the cross-contamination model, the contaminated faecal material is produced by pigs, which infects more pigs, causing more production of faecal material and so on. However, the faecal material is still able to infect pigs even if the pigs that originally produced the contaminated material recover or are moved away (fulfilling the criterion of hysteresis). The decay of Salmonella in the contaminated material may serve to fulfil both the second and third criteria described above. The decay of material over a timestep is sufficient enough to cancel out any small stimuli such as environmental contamination; it also prevents a runaway increase in contaminated material. Bistability only occurs when the dose response parameter $m > 1$, but yet all of the above criteria are met when $m \leq 1$. However, one other criterion is also presupposed to be necessary in some circumstances for bistability to occur: that there is "some type of non-linearity" (Willhelm, 2009). Of course, the cross-contamination system is already non-linear, but when $m > 1$ the non-linearity is magnified (allowing for three equilibrium states to occur). It is possible that the non-linearity of the dose-response model drives the bistability in this case, as when the two infected steady states are sufficiently stable, the perturbation from contamination from adjacent pens may well be insufficient to change the steady states and hence the travelling wave will stop.

We first identify combinations of parameter values that will produce two infected steady states, by a similar process as for that carried out to produce Figures 4.3. From Equation (4.5), m, c_1 and γ all determine the number of steady states. Solving Equation (4.5) in (m, γ), (m,c_1) and (c_1,γ) parameter space, we can identify the combination of parameter values where two infected steady states exist, and their associated minimum and maximum values for I^* (illustrated in Figure 4.10). For the fixed parameters we choose values, $m = 3$, $c_1 = 0.1$, $\gamma = 1.9$, $p_f = 18.8$

and $d_f = 1.9$.

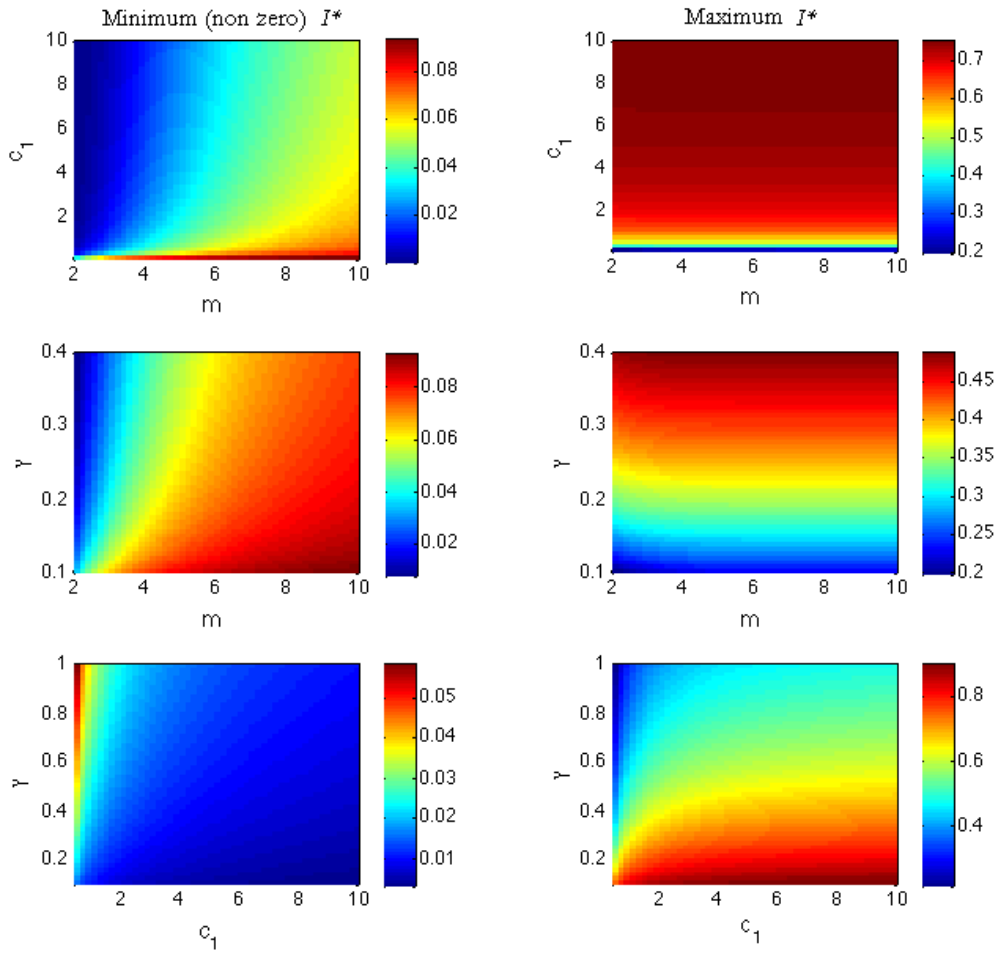

Figure 4.10: Minimum and maximum values of infected steady states over regions of parameter space where there are two infected steady states, unless otherwise stated $m = 3$, $c_1 = 0.1$, $\gamma = 1.9$, $p_f = 18.8$ and $d_f = 1.9$.

The wavespeed for all parameter spaces can be found in a similar fashion as described in Section 3.4. Iterating over all regions of the parameter space described above. The contour plots show the variation in wavespeed for each combination of the dsecribed parameter regions (see Figure 4.11).

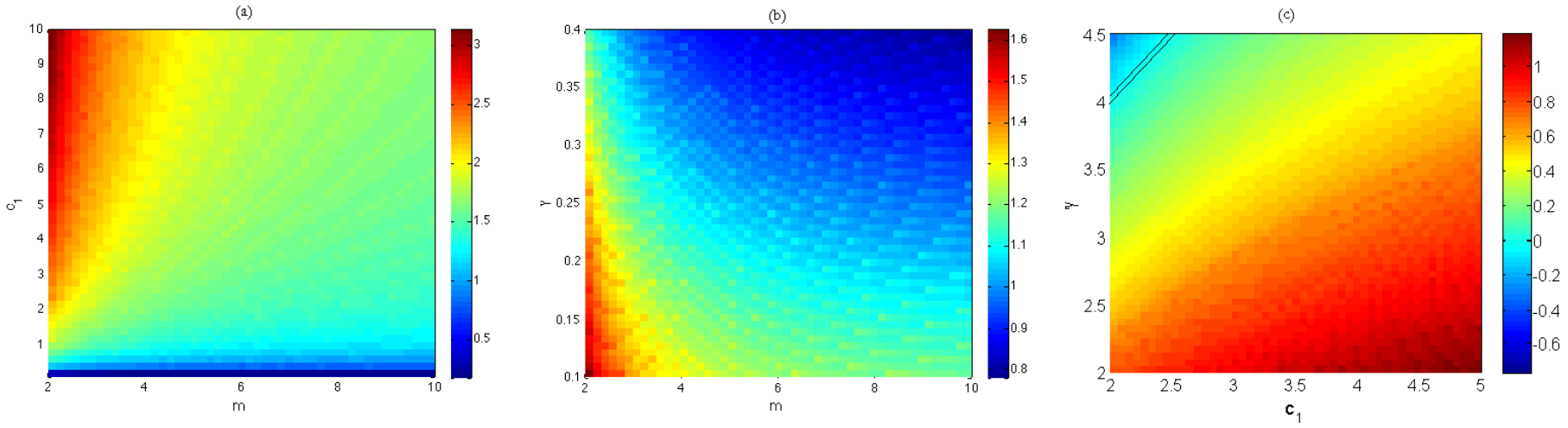

Figure 4.11: Speed of travelling wave in parameter spaces that give two infected steady states. The region bounded by black lines in (c_1, γ) space (part (c)) produces a pinned wave (i.e. wave speed $c = 0$).

Using relevant values for the maximum and minimum infected steady states as shown in Figure 4.10, we set the level of infection I in the first 150 pens of the 300-pen string model to halfway between the minimum and maximum infected steady states, and the remaining pens to halfway between zero and the minimum infected steady state. The level of Susceptibles is set using Equation (4.4b). These initial conditions ensure that the level of infection is not accidentally set at any of the steady states, so we can be certain that the absence of a travelling wave is due to pinning and not numerical artifacts. It is assumed that there is no contaminated faecal material in any pens at $t = 0$. Keeping all other parameters at the same value as above in Table 4.1, and setting $c_1 = 2$, then we vary γ between 3.5 and 4.5. The effect on the travelling wave speed is displayed in Figure 4.12.

For large γ, we observe an advancing wave of infection. For small γ, the infection recedes and the travelling wave eventually restores each pen to the susceptible only state. However, for γ values in the bounded 'pinning' region (see panel (c) in Figure 4.12), we observe a static wavefront. Here, both infection and susceptible only states are homogeneously stable, and the spatially heterogeneous stable solution is the static solution, in which the pens which were initially in the basin of attraction of the infection/susceptible stabe states evolve to and stay in these states and a pinned wave is observed.

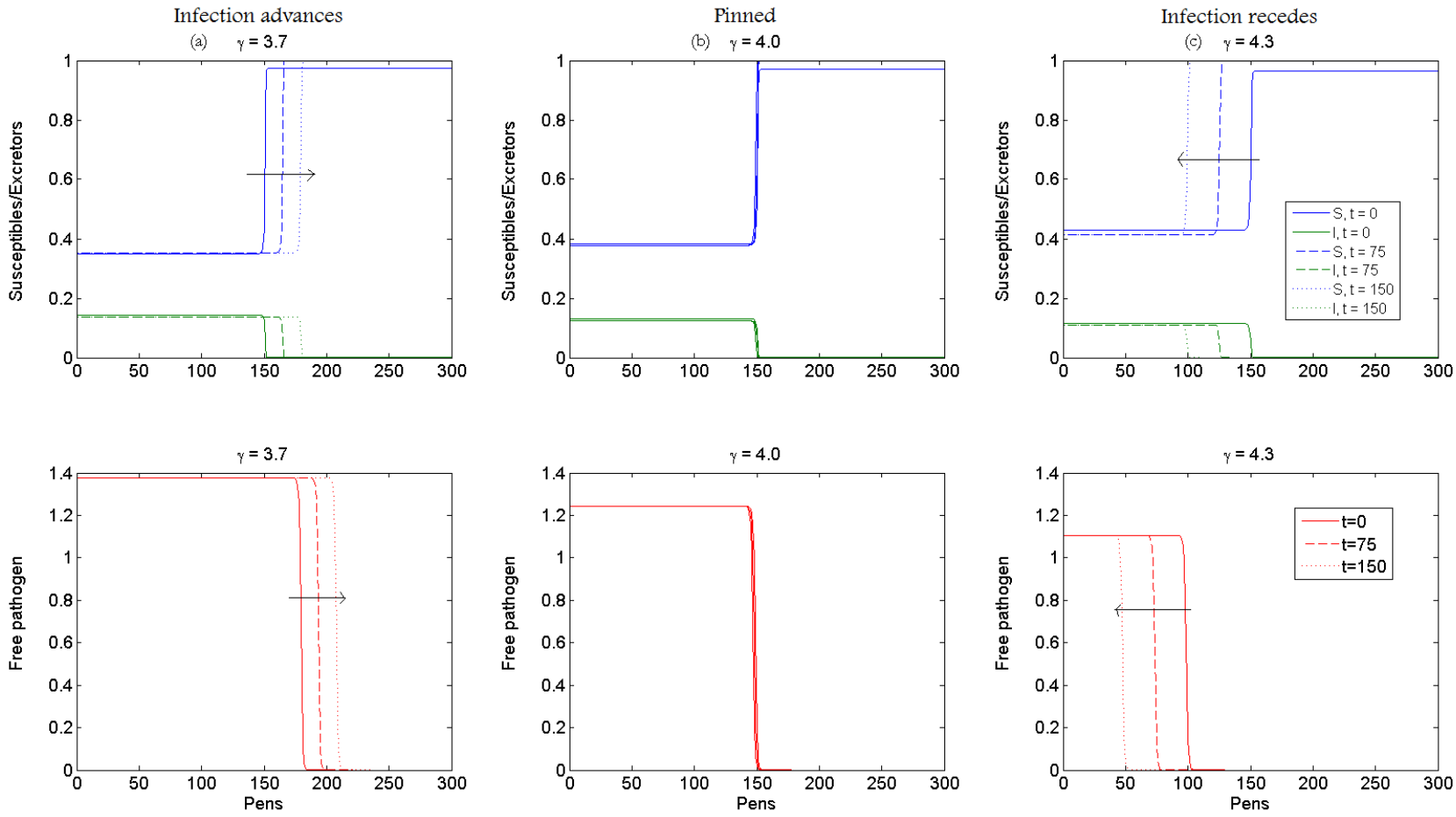

Figure 4.12: Direction of travelling wave in (c_1, γ) parameter space. The arrows represent the direction of the travelling wave. In all panels $p_f = 18.8$, $d_f = 1.9$, $c_1 = 2$, $\eta = 1$ and $m = 3$. In panel (a) $\gamma = 3.7$, panel (b) $\gamma = 4.0$ and in panel (c) $\gamma = 4.3$.

4.5 Discussion

The cross-contamination model is significantly more complex than the standard n-pen model, but provides several advantages over the latter. The cross-contamination model explicitly includes faecal contamination and dose-response, rather than incorporating both implicitly into one transmission parameter. This provides a model that is much more amenable to intervention analysis and parameter estimation. However, we find that the system still settles to the same infectious behaviour as we observe for the standard model in Chapter 3. However, we find the additional feature of pinning as described in Section 4.4.2.

The cross-contamination model takes significantly longer to reach overall equilibrium (i.e. the time when infection in all pens is at the infected steady state) than the standard model for the parameters chosen for the numerical solutions. Here, we predict a cross-contamination travelling wave speed of around 0.02 pens per day, compared to the standard model speed of 0.4-0.6 pens per day. It is hard to directly compare the two travelling wave speeds, as the cross-contamination parameters associated with each model, η and β_2, are estimates in the absence of data. However, if the true value of η should lie near the current estimate ($\eta = 1$) then the infected steady state is unlikely to be reached in many pens (if any), over the timeframe of the growing-finishing period (between 84-116 days). Hence, the heterogeneity between pen infection observed in studies on pig farms may well simply be reflecting the fact that the infection levels within pens have not had chance to increase towards the predicted equilibrium. Accompanied with continuous production and heterogeneous exposure to environmental Salmonella burden, then it is highly unlikely that pig populations remain constant enough for equilibrium to be reached in normal grower-finisher rearing periods.

The stability analysis conducted in this and previous chapters represent a way to highlight some key dynamic principles of a complex non-linear system such as Salmonella infection between pigs. With current parameter estimation, the within-pen infected steady state will be reached fairly quickly, within the timeframe of grower-finisher production (84-116 days). Our best guess at estimating between-pen transmission suggests that infection will travel slowly between pens (assuming it only depends on the direct spread of faecal material between adjacent pens), at a rate which means that infection will be unlikely to spread significantly before the end of grower-finisher production. This suggests that one potential opportunity to reduce Salmonella infection in pigs is to prevent cross-contamination between pens, which would further slow the process of cross-contamination.

Infection in pig pens tends to be extremely heterogeneous, with clustering of infection within one or two pens (VLA, 2009). This would support the conclusion above that between-pen transmission is slow, but also it supports the hypothesis that the introduction of Salmonella into a herd is also very heterogeneous (e.g. the continual introduction of new, stressed, and possibly infected, weaners onto the farm). This spatially heterogeneous introduction of Salmonella, or the precise source of infection, has not been considered in the models developed so far, in order to simplify the model dynamics. As reducing the contamination of sources of Salmonella includes several prime intervention candidates (e.g. cleaning and disinfection of pens between depopulation and re-population, decontamination of feed) then this is an important factor to consider, and is dealt with in Chapter 6.

The cross-contamination model introduced complex dynamics that we thought may have led to the potential for Turing patterns. However, no Turing patterns are predicted, and all pens tended to the stable infected homogeneous steady state once infection is introduced. Under certain parameterisations of the model

bistability occurs, where there are two possible infected steady states, one stable and one unstable. Pinning may occur under certain combinations of c_1 and γ. In this case, the infection levels are held at their initial state almost indefinitely, for a time much longer than the period of rearing (see Figure 4.12). In order to produce such a situation in reality would mean intervening to change the dose-response of pigs (perhaps through vaccination or the use of organic acids), or by changing the duration of infection, in order to 'pin' the infection within a certain part of the farm. If intervention is sufficient, then the values of the parameters can also be modified such that the level of infection in pens can be rolled back to zero (see Figure 4.12). The cross-contamination model described in this chapter is the final deterministic model developed in this thesis. Additional complexity would almost certainly mean analytical solutions for steady states and stability become intractable. Instead, in the next chapter we turn to stochastic (numerical) simulation models to develop models that contain further important factors for Salmonella transmission, such as considering explicit sources of infection.

Chapter 5

Stochastic versions of standard SIR and cross-contamination models

5.1 Introduction

In the previous two chapters a deterministic multi-pen model based on standard SIR model dynamics (here called the 'standard' model) and a deterministic cross-contamination model, where the shedding of contaminated faeces is explicitly described, were developed. Analysis of these models highlighted key dynamics of infection, for example if infection is introduced, it is probable that an infected steady state will be reached, rather than infection dying out. In addition, this steady state appears to be globally stable, such that the steady state is reached independent of initial conditions. However, it is noted that the similarities of infection dynamics between pens is not easily explained when compared to ob-

servational studies (Kranker et al., 2003; Jensen et al., 2006; VLA, 2009). Also, the small number of pigs within each distinct population group (i.e. within each pen) means that overall infection dynamics are vulnerable to stochastic variation, which are not captured in determinstic models. The modelling methodologies available for stochastic modelling have been described in Chapter 1. Therefore, in this chapter, we investigate the development of two stochastic models, building on the deterministic models previously described in Chapters 3 - 4, in order to better describe the natural variability inherent in pig infection dynamics.

5.2 Model development

5.2.1 Further development of standard SIR model

The non-scaled multi-pen deterministic model was defined in Chapter 3 as

$$\begin{aligned}
\frac{dS_{i,j}}{dt} &= -\left(\sum_{k=1}^{2}\sum_{l=1}^{6}\beta_{k,l}I_{k,l}\right)S_{i,j} + \delta C_{i,j},\\
\frac{dI_{i,j}}{dt} &= \left(\sum_{k=1}^{2}\sum_{l=1}^{6}\beta_{k,l}I_{k,l}\right)S_{i,j} - \gamma I_{i,j},\\
\frac{dC_{i,j}}{dt} &= \gamma I_{i,j} - \delta C_{i,j},
\end{aligned} \tag{5.1}$$

where the subscripts i and j represent the pen where susceptibles are exposed to infection, as defined in Chapter 3, $i \in I_r = \{1, 2\}$, and $j \in J = \{1, \ldots, 6\}$, and k and l represent the position and row of where the force of infection originates, $k \in K = \{1, 2\}$ and $l \in L = \{1, \ldots, 6\}$.

The stochastic transmission model has the same aims as the deterministic model

described in Chapter 4: to describe the epidemic curve in a 12 pen pig grower-finisher house given the initial introduction of Salmonella in one pig in pen (1,1) at time $t = 0$.

The methods for stochastic modelling were outlined in Chapter 1; we apply these methods, and further develop them, for the specific case of the 12-pen model described above in Equation (5.1). In particular, we first replace the rate of tranmission (β, β_1, β_2 etc...) with a stochastic probability of infection, as first described by Reed & Frost in 1927 and formalised in the literature by Fine (1977). Second, we replace the assumption of constant rates of transistion between Excretor and Carriers (γ), and Carriers and Susceptibles (δ) with probabilistic parameters defining the length of duration in each state for each individual infected pig. The end result is an indiviudal-based stochastic SIRS model, which incorporates large amounts of variability. We now take the reformulation of each transition in turn.

Transistion: Susceptible → Excretor

The standard form of the Reed-Frost model was described by Fine (1977), and the rate of transistion between Susceptible and Excretor, $\lambda(t)$, can be given by

$$\lambda(t) = 1 - (1 - p)^{I(t)}, \tag{5.2}$$

where p is the probability of an effective contact (i.e. sufficient for infection to occur) between a susceptible and excreting pig, and in this case $I(t)$ is the number of excreting pigs at time t. If the number of susceptible pigs is defined as $S(t)$, then the number of newly excreting pigs at time t, $NI(t)$, is

$$NI(t) = \lambda(t) S(t). \tag{5.3}$$

The deterministic formulation of this model can easily be transformed into a stochastic version by considering each contact between Susceptible and Excretor as a binomial trial, with $S(t)$ trials and $\lambda(t)$ probability of "success" (infection). Therefore, the number of newly infected pigs at time t is a random variable determined by

$$NI(t) \sim B(S(t), \lambda(t)), \tag{5.4}$$

where B denotes a binomial distribution. The stochastic probability of an effective contact, p, is equivalent to the deterministic probability of an effective contact, β, β_1 etc.... As for $\beta_{k,l}$ in Equation (5.1) we can assume that p will vary according to where the susceptible and excreting pigs are placed relative to each other. We can therefore describe the multi-pen system by modifying Equation (5.2) using similar assumptions as proposed in Section 3.

The stochastic, multi-pen force of infection for pen (i,j) , $\lambda_{i,j}$ is thus

$$\lambda_{i,j}(t) = 1 - \prod_{m=1}^{3} (1 - p_m)^{I_m(t)}, \tag{5.5}$$

where $m = \{1, 2, 3\}$ and p_1, p_2 and p_3 denote the probability of an effective contact between a susceptible and excreting pig in the same pen, different pens within the same row and different pens within different rows respectively. The number of excreting pigs applicable to each p are defined by the following equation

$$I_m(t) = \begin{cases} I_{i,j}(t) & \text{if } m{=}1, \\ \sum_{l \in L: l \neq L} I_{k,l} & \text{if } m{=}2,\ i = k, \\ \sum_{l \in L} I_{k,l} & \text{if } m{=}3,\ i \neq k. \end{cases} \tag{5.6}$$

We can write similar expressions for the addition of newly infected pigs to pen (i, j) within one timestep, $NI_{i,j}(t)$, as for Equation (5.4)

$$NI_{i,j}(t) \sim B\left(\lambda_{i,j}(t), S_{i,j}(t)\right). \tag{5.7}$$

Transitions: Excretor → Carrier & Carrier → Susceptible

As for the transition between Susceptible and Excretor pigs, the duration of infection and carriage will be variable between pigs. Assuming independence between the individual duration of excretion and carriage then we can define a function for each to describe the variation between pigs. For each pig q infected at time t a duration of excretion, $\gamma_s(q)$, and a duration of carriage, $\delta_s(q)$, are defined. The appropriate choice of function for, and the subsequent parameter estimation, depends on the data available, and both are therefore described in more detail in Section 5.2.2.

Algorithms for the stochastic model

The initial conditions are set the same as for the multi-pen deterministic model (i.e. one excretor pig enters pen (i, j) at $t = 0$). Each iteration of the discrete-time model is updated at every timestep using the following alogrithm.

- The number of newly infected pigs in each of the 12 pens in the time period $[t, t+1)$, $NI_{i,j}(t)$, is calculated using Equation (5.7).
- For each newly infected pig q in pen (i,j) random variables, $\omega_{i,j}(q)$ and $\mu_{i,j}(q)$ are generated from appropriate probability distributions for the durations of excretion ($\gamma_s(q)$) and carriage ($\delta_s(q)$) respectively. The times at which each infected pig q transitions from Excretor to Carrier, t_C, and from Carrier to Susceptible, t_S, are $t+\omega_{i,j}(q)$ and $t+\mu_{i,j}(q)$ respectively.
- The number of pigs transitioning at each timestep (i.e. $t = t_C$ or $t = t_S$) is stored in memory. The number of pigs in pen(i,j) making the transition $E \to C$ and $C \to S$ at time t are defined as $NC_{i,j}(t)$ and $NS_{i,j}(t)$ respectively.

The number of pigs within each state in pen (i,j) at time $t+1$ is therefore given by

$$\begin{aligned} S_{i,j}(t+1) &= S_{i,j}(t) - NI_{i,j}(t) + NS_{i,j}(t), \\ I_{i,j}(t+1) &= I_{i,j}(t) + NI_{i,j}(t) - NC_{i,j}(t), \\ C_{i,j}(t+1) &= C_{i,j}(t) + NC_{i,j}(t) - NS_{i,j}(t). \end{aligned} \tag{5.8}$$

Each iteration of the model is run using the algorithm for stochastic simulation in Section 1.3.3, using Monte Carlo simulation techniques. At 5000 iterations standard convergence criteria were used to ensure the model had converged sufficiently (i.e. the mean and 5th and 95th percentiles of the output change less than $\pm 1.5\%$ over 500 iterations. The output is taken to be the proportion of pigs in each state at the last timestep).

The model is implemented in MATLAB 2010b (©Mathworks Inc., USA). Each simulation consists of 5000 iterations.

5.2.2 Parameter estimation

The parameter estimates for the stochastic standard SIRS model are given in Table 5.1. The parameter estimates for p_1, p_2 and p_3 are the same as for β_1, β_2 and β_3 within the deterministic model. The duration of shedding and duration of carriage are derived individually for each pig in the stochastic model, and are random variables from the functions $\gamma_s(q)$ and $\delta_s(q)$.

Table 5.1: Parameter estimates for the stochastic model

Notation	Description	Value	Reference
n	Number of pigs within a pen	40	MLC (2009)
p_1	Probability of an effective contact between a susceptible and infected pig within the same pen	0.01	Dent et al. (2009)
p_2	Probability of an effective contact between a susceptible pig in pen$q$ and an infected pig within a different pen in row i	0.001	Dent et al. (2009)
p_3	Probability of an effective contact between a susceptible pig in pen$q$ and an infected pig within a different pen in opposite row i	$p_2/3$	Expert opinion
$\gamma_s(q)$	Duration of shedding	Weibull(35.32,1.50)	Kranker et al. (2003)
$\delta_s(q)$	Duration of carriage	LogNorm(134,90) - $\gamma_s(q), \delta_s(q) \geq 0$	Ivanek et al. (2004)

There are several (experimental or observational) studies that investigate the dynamics of infection in pigs (Kranker et al., 2003; Jensen et al., 2006; Osterberg

et al., 2009). Kranker et al. (2003) is the only observational study, and hence we choose this study for parameter estimation. Kranker et al. (2003) took monthly faecal and blood samples from 180 pigs in three herds over a period of up to 140 days. The faecal results for each individual pig are shown in Figure 5.1(a). Data of such form, especially where the dataset is right-censored (i.e. several of the culture-positive pigs were slaughtered before a culture-negative sample was taken) are appropriate for the development of a survival function. We therefore conduct survival analysis on the dataset to estimate the probability density function (PDF) for the duration of shedding, $\gamma_s(q)$.

The raw dataset from Kranker et al. (2003) was obtained from the authors. To conduct the survival analysis we make the same assumptions as were made by the authors for their own analysis:

- Shedding began 1 week prior to the first isolation and lasted, uninterrupted, until 1 week after the last isolation, unless;
- If an individual pig was found to be culture negative, or one sample was missing between two culture-positive samples, then the pig was considered to be shedding for the entire time period between the two positive samples;
- If an individual pig that had previously tested culture positive was found to be culture negative on two or more successive sampling occasions then the pig was assumed to have recovered from the shedding stage of infection; further culture-positive samples were assumed to indicate re-infection.

Suvival analysis involves the modelling of time to event data, which in this case is the time from initial infection until a pig ceases to shed Salmonella in its faeces. Typically, a survival function, $S_f(t)$, is constructed, describing the probability that the time of an event (in this case ceasing shedding), T, is greater than the

time since infection, t_{inf}. Mathematically, $S_f(t) = P(T > t_{inf})$; this function has the form of a complementary cumulative density function (CCDF). An initial plot, treating censored datapoints as uncensored, shows the preliminary survival function for the Kranker dataset (Figure 5.1(b)).

Two common distributions fitted to "time-to-failure" data (in this case, time to ceasing shedding) are the Exponential and Weibull, and examples of the respective CCDFs are shown in Figure 5.2. The Exponential CCDF is dependent on one variable, λ, which results in a constant hazard function, i.e. the probability of a failure occurring is independent from the time since infection. The Weibull CCDF contains two parameters, λ and κ, the latter being a shape parameter. This shape parameter determines whether the probability of failure decreases over time ($\kappa < 1$), stays constant ($\kappa = 1$, equivalent to the Exponential function), or increases over time ($\kappa > 1$).

Biologically, it would appear more realistic that the probability of ceasing shedding should increase as time since infection increases. That is, a suitable function would be a Weibull function with $\kappa > 1$. The shape of the survivial function in Figure 5.1(b) supports this assumption. Therefore, we fit the data from the Kranker study to a Weibull CCDF. The forms of the Weibull CCDF (F_c) and PDF (f) for a random variable X are as follows

$$f(t;\lambda,\kappa) = \frac{\kappa}{\lambda}\left(\frac{t}{\lambda}\right)^{\kappa-1} e^{-(t/\lambda)^k} \qquad t \geq 0, \;\; \kappa,\lambda > 0,$$
$$F_c(t;\lambda,\kappa) = e^{-(t/\lambda)^k}.$$

.

Defining a right censored datapoint as one where the pig was still shedding Salmonella

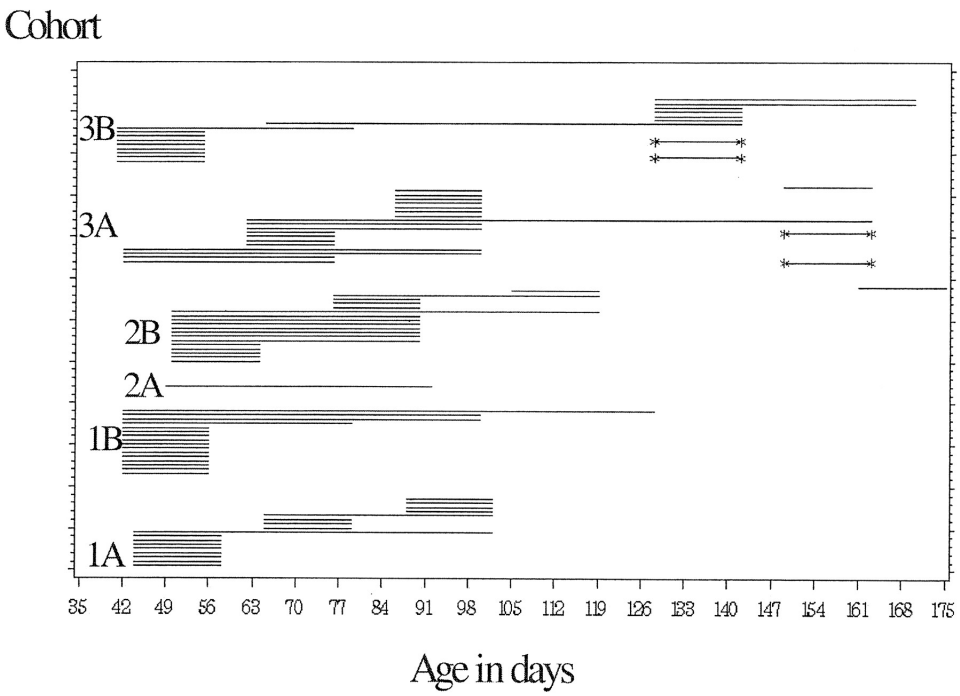

(a) Estimated shedding times of *Salmonella* Typhimuirim in 88 pigs (of 180) that tested positive on at least one occasion during the 140 day period of the Kranker et al study. Individuals represented by bars with asterisks are assumed to be reinfected. Figure taken from Kranker et al. (2003) .

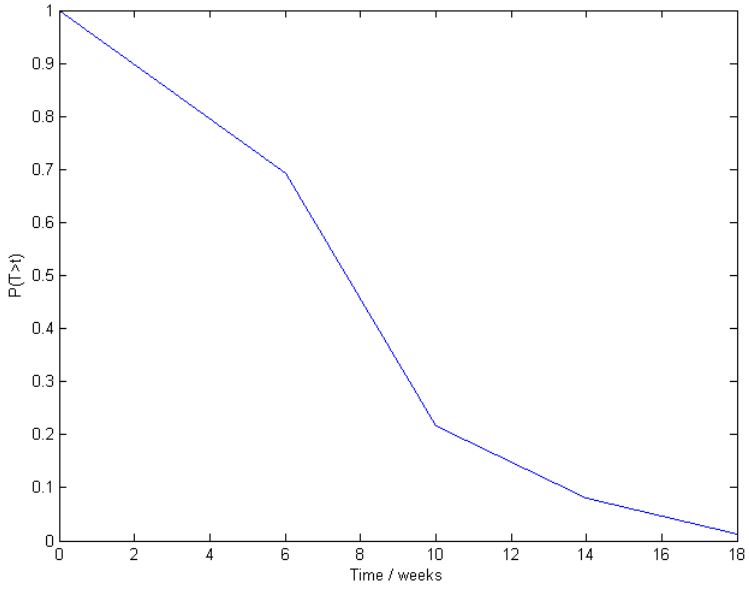

(b) A plot of the survival function for the data shown in Figure 5.1(a)

Figure 5.1:

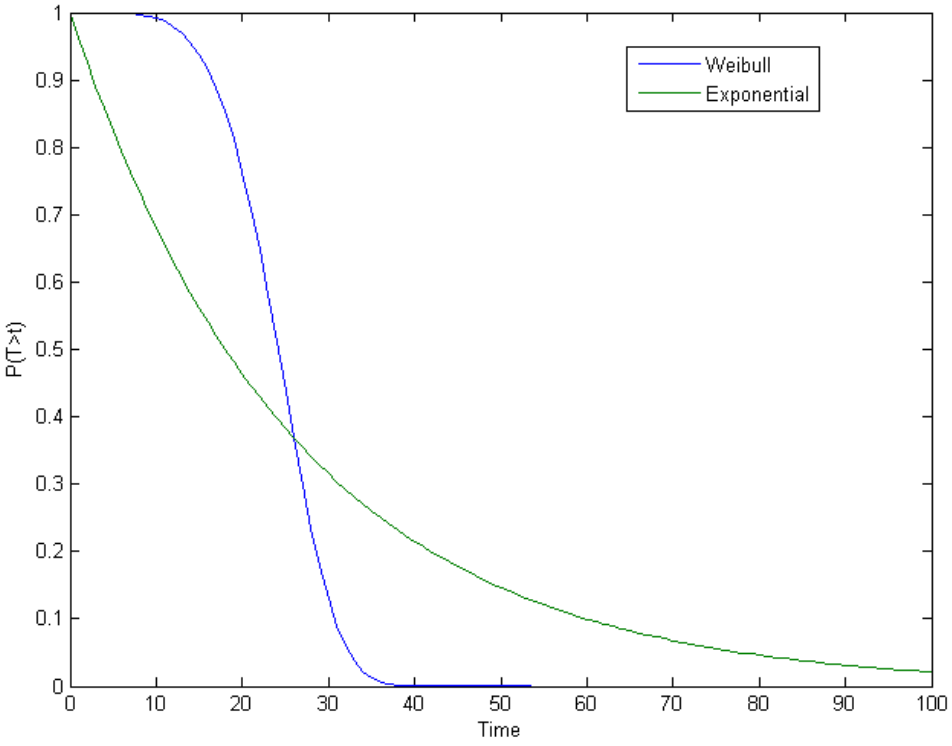

Figure 5.2: Comparison of Complementary Cumulative Distribution Functions for the Exponential ($\lambda = 26$) and Weibull ($\lambda = 26$ and $\kappa = 5$).

when the last sample was taken, then 24 of the 88 pigs identified as shedding at one or more sampling points were right censored. No pigs were found to be shedding Salmonella at the first sample point, therefore there was no left censoring of the data. Using the assumptions for time of infection listed above and the distribution fitting tool in MATLAB 2010a then Maximum likelihood Estimates (MLEs) for λ and κ are 35.32 and 1.50 respectively. The resulting CCDF and PDF are shown in Figure 5.3. Other distributions, for example the Exponential and Gamma, were fitted to the censored Kranker dataset but none fitted as well as the Weibull distribution. We therefore have

$$\gamma_s(k) \sim Weibull(35.32, 1.50). \tag{5.9}$$

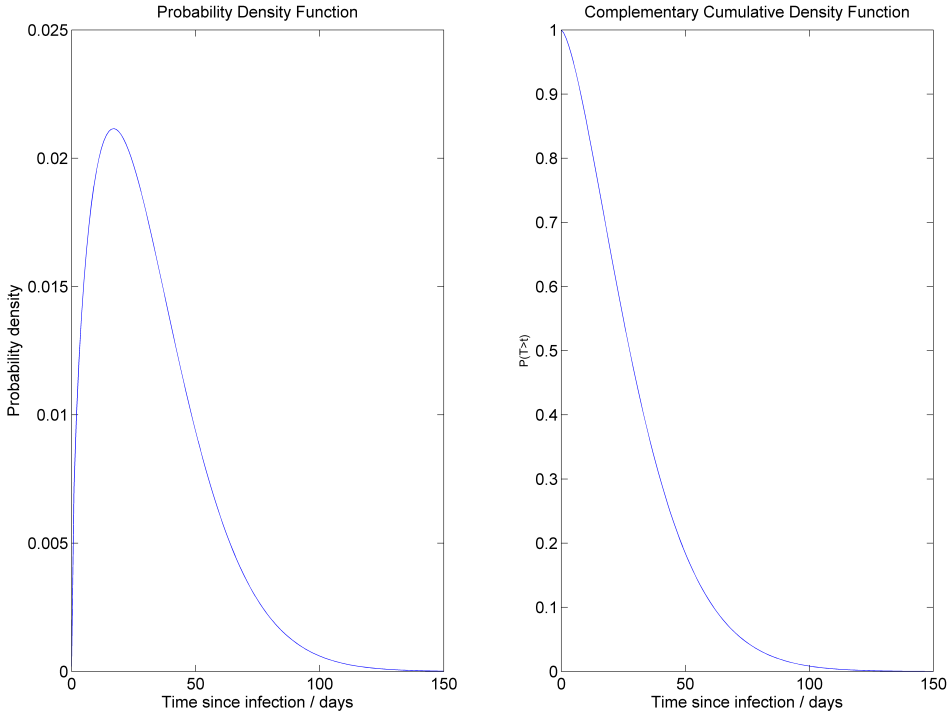

Figure 5.3: PDF and CCDF for the Weibull distribution fitted to the censored Kranker dataset ($\lambda = 35.32$ and $k = 1.50$). The average time of shedding is 31.89 days. As $\kappa = 1.5$ then the survival function is not too disimilar from that of the Exponential survival function ($\kappa = 1$) and there is steep gradient of decline in the first 50 days.

A number of studies have investigated the time course of overall Salmonella infection in pigs by sampling various organs/lymph nodes (Fedorka-Cray et al., 1994; Gray et al., 1996; Kranker et al., 2003). Of the lymph nodes and organs sampled, there is a trend across all studies that the most commonly infected sites are the ileo-caecal lymph nodes and cecum, which also tend to remain infected the longest. We therefore define the Carrier state as the period where a pig has ceased shedding of Salmonella in its faeces, but is still infected in the ileo-caecal lymph node (as

this was also the site chosen for sampling for the slaughter pig survey conducted by the European Food Safety Authority (EFSA) in 2008 (EFSA, 2009a)). As lymph nodes can only be sampled once the pig has been slaughtered, it is not possible to collect individual longitudinal data as for faecal shedding. There is further discussion of parameterisation for the duration of the carrier stage in Chapter 6, but for the purposes of this preliminary stochastic model we assume the same parameter estimation for the duration of carriage for an individual pig q, $\delta(q)$, as in Ivanek et al. (2004) (see Table 5.1).

5.2.3 Standard dynamic model results

The epidemic curve that results from infection of one pig in pen $(1,1)$ at $t = 0$ (averaged over all iterations) is shown in Figure 5.4 (there are very similar curves for each pen, with only a small delay in the epidemic peaks of other pens due to between-pen transmission). The first observation is that the *average* epidemic curve is very similar to that of the equivalent pen in the deterministic model in Figure 3.6. However, as shown in Figure 5.5 the epidemic curve for individual iterations vary, although this variation does not markedly change the overall shape and timing of the epidemic curve. The probability of stochastic fade-out[1] is very low ($6 * 10^{-4}$), with only one iteration of the model resulting in no transmission of infection either within- or between-pen. The epidemic curves in each of the other pens are similar to that in pen (1,1), with a very similar probability of stochastic fade-out.

[1]Stochastic fade-out is defined as when there are no infected pigs on the farm. This can be defined at any point in the 150 day period, but given the average duration of shedding is 26 days, the probability of stochastic fade-out was calculated at 50 days, as the initially infected pig should then have recovered to Carrier status, and no longer be infectious.

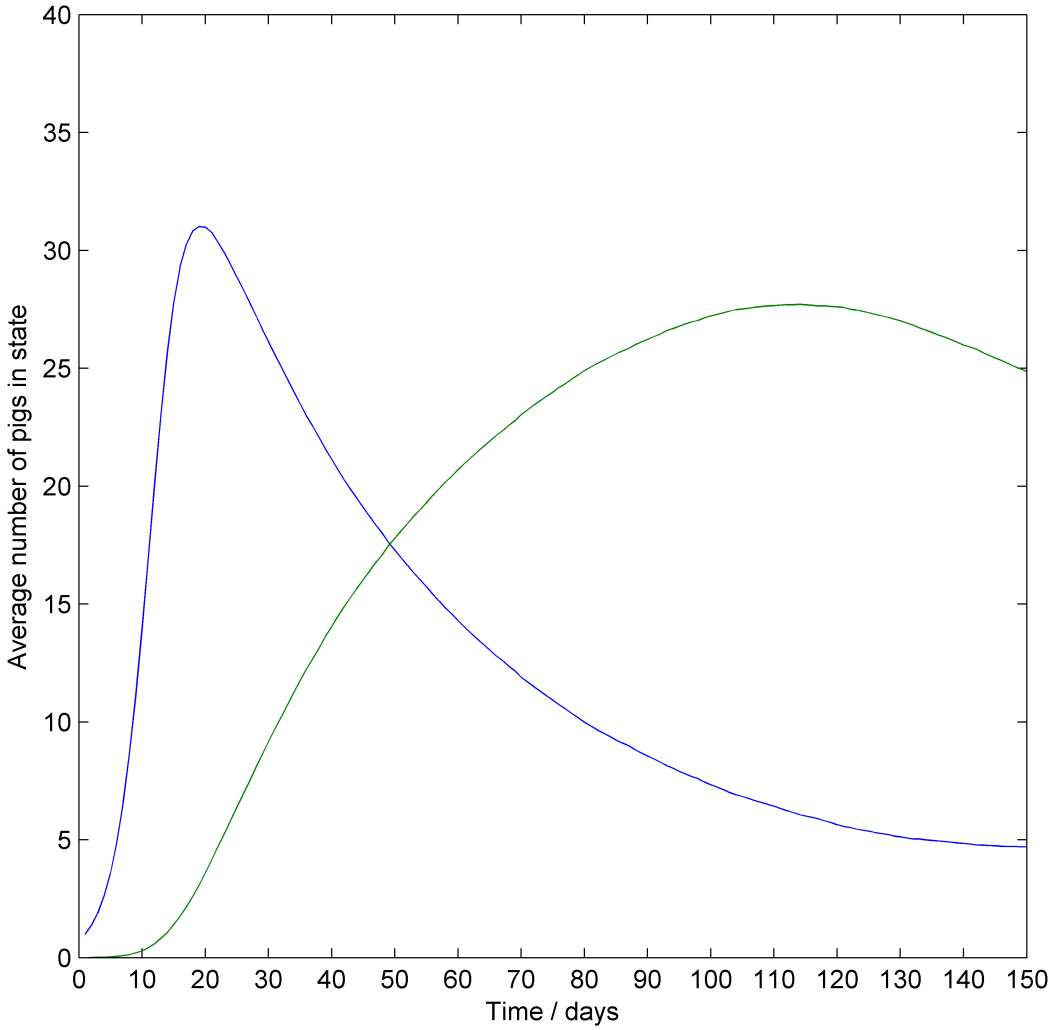

Figure 5.4: Plot of average epidemic curves for Excretors and Carriers from the 1500 iterations of the model.

5.3 Cross-contamination model

5.3.1 Transistion: Susceptible → Excretor

The rate of infection in the standard stochastic SIRS model above is governed by the probability of an effective contact, p_1, p_2 etc ..., which encapsulates all factors

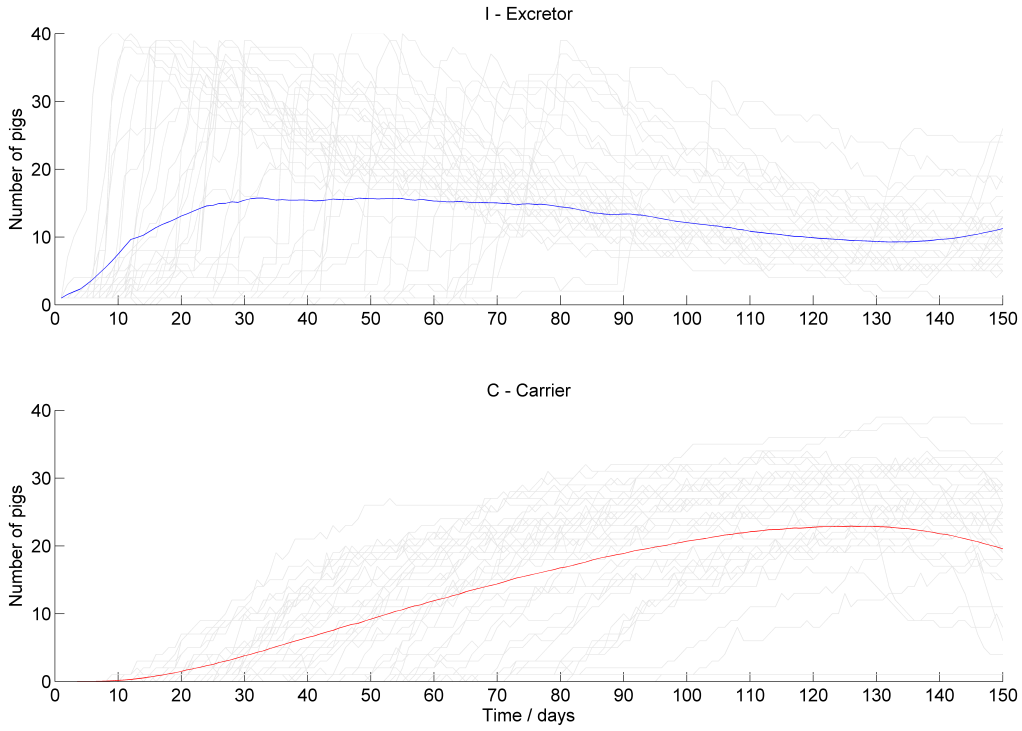

Figure 5.5: Plot of 1000 randomly selected epidemic curves from the 5000 iterations of the model (grey lines). The average number of Excretors (blue) and Carriers (red) over time is also displayed.

that affect transmission (e.g. the amount of *Salmonella* in the environment, the type of feed being fed to the pigs). The cross-contamination model proposed in Chapter 4 is a preliminary step towards separating out these individual factors, by explicitly incorporating faecal contamination of the pig pen environment. As for the standard SIR model we can incorporate stochastic effects within the cross-contamination model. The deterministic model equations are as follows

$$
\begin{aligned}
\frac{dS_j}{dt} &= -D_f\left(f_j\right) S_j + \delta C_j, \\
\frac{dI_j}{dt} &= D_f\left(f_j\right) S_j - \gamma I_j, \\
\frac{dC_j}{dt} &= \gamma I_j - \delta C_j, \\
\frac{df_j}{dt} &= p_f I_j - d_f f_j + \eta\left(f_{j+1} + f_{j-1} - 2f_j\right),
\end{aligned}
\tag{5.10}
$$

where f_j is the amount of *Salmonella* in the pig pen j, p_f is a parameter describing the magnitude of pig excretion, d_f is the rate of decay (per day) for Salmonella in the pen environment, η is the rate of cross-contamination between pens and $D_f\left(f_j\right)$ is a dose-response function. An appropriate sigmoidal function has been chosen and so

$$
D_f(f_j) = \frac{c_1 {f_j}^m}{{c_2}^m + {f_j}^m},
$$

where c_1, c_2 and m are real and positive dose-response parameters.

The dose-response parameter $D_f(f_j)$ is the equivalent of the Reed-Frost force of infection, λ. The inclusion of the explicit faecal parameter f directly describes the amount of cross-contamination that occurs between pens, so there is no need to sum the probabilities of effective contacts from different pens (as in Equation (5.2)). Similar equations for the transition between Susceptible and Excretor in pen j can be written as for the standard model described in Equation (5.6), except λ_{ms} is replaced by the value of the dose response parameter $D_f(f_j, t)$ in pen j at time t.

$$NI_j\left(t+1\right) = B\left(S_j\left(t\right), D_f\left(f_j, t\right)\right), \tag{5.11}$$

where the amount of contaminated faecal material in pen j at time t is given by

$$f_j\left(t+1\right) = f_j^*\left(t\right) + \tau_{j-1} + \tau_{j+1} - \tau_{bj}. \tag{5.12}$$

The parameter $f_j^*\left(t\right)$ is the amount of contaminated material left in the pen after decay and cross-contamination are accounted for. The terms τ_{j-1} and τ_{j+1} represent the amount of faecal contamination that are cross contaminated during the timestep from pen j to pens $j-1$ and $j+1$ (within the same row) respectively. For end-of-row pens then only the terms relating to the single adjacent pen are used. The term τ_{bj} denotes the amount of faecal material spread to the neighbouring row of pens during the timestep from pen j.

The amount of faecal material left in the pen after decay and cross-contamination, $f_j^*\left(t\right)$, is described by a multinomial distribution. This then provides the values for τ_{j-1}, τ_{j+1} and τ_{bj} etc. . . , which can then be used in subsequent calculations for pens $j-1$ and $j+1$.

$$\left\{f_d, \tau_{j-1}, \tau_{j+1}, \tau_{bj}, f_j^*\left(t\right)\right\} = MN\left(f_j\left(t\right), \left\{d_f, p_{j-1}, p_{j+1}, p_{bj}, \left(1-p_{j-1}-p_{j+1}-p_{bj}\right)\right\}\right),$$

where f_d is the amount of Salmonella that decays reducing the total amount of contaminated material. Hence, the term f_d is not re-assigned to any pen and means that without any excreting pigs the total amount of contamination will reduce over time. The terms d_f, p_{j-1}, p_{j+1} and p_{bj} are the probabilities of an amount of faecal

material decaying or being cross-contaminated to pens $j-1$, $j+1$ or the opposite row of pens. The amount of faecal material cross-contaminated to the oppositie row is randomly assigned to one of the pens in the opposite row (hence, at any given timestep, a pen may receive none or 1 to 6 times τ_{bj} amounts of contaminated faecal material from pen j).

5.3.2 Transistions: Excretor → Carrier & Carrier → Susceptible and implementation of model

The transistions Excretor-Carrier and Carrier-Susceptible, and how the model is implemented, are identical to the standard SIRS model (see Sections 5.2.1 and 5.2.1).

5.3.3 Algorithm for cross contamination model

The algorithms for each iteration and the overall simulation are the same as for the standard model.

5.3.4 Parameter estimation

We use the same parameter estimates for the dose response function $D(f_j)$, the magnitude of faecal shedding and decay of *Salmonella*, $(p_f,\ d_f)$ as have been given in Table 4.1 for the deterministic model. As cross-contamination between adjacent pens will not necessarily cancel out in a stochastic model as it will for the deterministic model, we also need parameter estimates for the cross-contamination factors, p_{j+1}, p_{j-1} and p_{bj}. There are no data available to estimate the rate of cross-

contamination between pens or between rows. We have therefore chosen values which appear biologically plausible.

Table 5.2: Parameter estimates for the stochastic cross-contamination model

Notation	Description	Value	Reference/Notes
p_{j-1}, p_{j+1} for all j	Proportion of contaminated faecal material in pen j at time t that is cross-contaminated to adjacent pen	0.06	Author's best guess
p_{nj}	Proportion of contaminated faecal material in pen j at time t that is cross-contaminated to a pen in another row in one timestep	0.009	Author's best guess

5.3.5 Cross-contamination model results

The average epidemic curve over all iterations for all pens is given in Figure 5.6. The first observation is that there is some variation between pens as there is a delay between the initital infection time of each pen. Also, the *average* epidemic curve peaks at a far lower level than for the deterministic model in Figure 4.9 (and hence the standard stochastic model result above). The reason for this is that, given the initial conditions (one infected pig in Pen (1,1)), the probability of stochastic fade-out of infection is high (0.785). The epidemic curves in each of the other pens are similar to that in Pen (1,1), with a very similar probability of stochastic fade-out over all pens (0.804) as for Pen (1,1) (although there is a time delay for between-pen infection, which produces a corresponding time delay in the peak of infection in each pen). The similarity between the two probabilities of stochastic fade-out reflects the fact that should infection be maintained in the initially infected pen then between-pen transmission is highly likely to occur (conversely if stochastic fade-out occurs, then between-pen transmission is extremely

unlikely). The probability of stochastic fade-out across the pig house is almost constant no matter where it is measured (t =50 days - 0.8036, t =100 days - 0.8056, t =150 days - 0.8104), hence very few, less than 0.2% of iterations, result in stochastic fade-out of infection if within and between-pen transmission occurs.

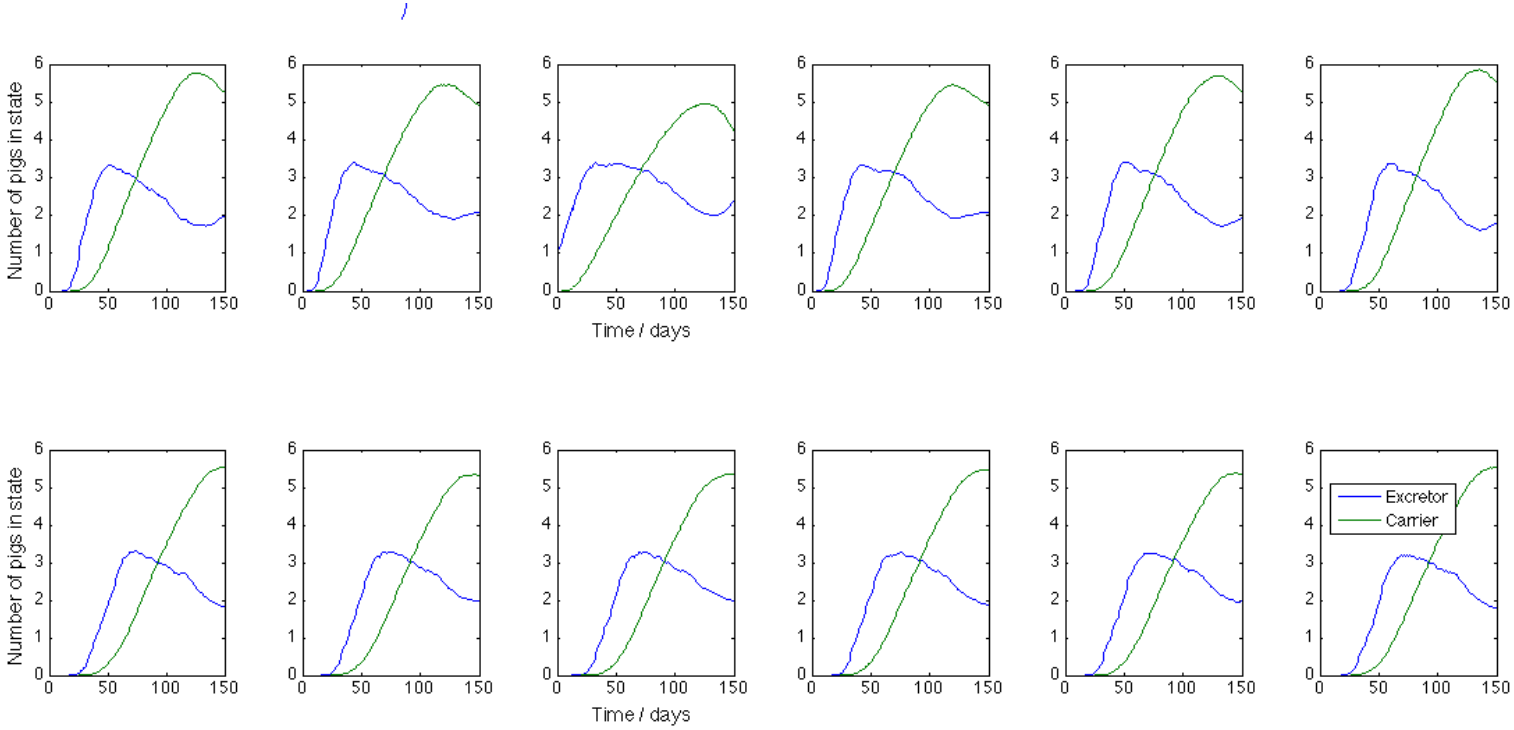

Figure 5.6: Plot of the average epidemic curves in all 12 pens of the cross-contamination model (blue - Excretor, red - Carrier).

The reason for the much greater probability of stochastic fade-out in the cross-contamination model compared to the standard model is clear from Figure 5.7, where only the iterations with no stochastic fade-out are plotted. The average epidemic curve for these iterations (blue - Excretor, red - Carrier) is also shown. The variation between iterations is far more pronounced in the cross-contamination model, and indeed most iterations result in no transmission of infection at all, with the initially infected pig recovering before transmission occurs. Where infection does occur the timing of the epidemic varies, which also flattens the average epidemic curve and lowers the average peak of infection. These new dynamics are generated by the inclusion of dose-response and explicit faecal shedding. The magnitude of faecal shedding is a function of the number of infected pigs in a pen, but because of stochastic variation and variable shedding, the dose-response functon is more variable than the equivalent force of infection from the standard model.

We have attempted to make the comparison of results between the standard and cross-contamination models as valid as possible, by using the same parameter estimates and initial conditions where possible, and attempting to produce similar rates of transmission through the force of infection $\lambda_{i,j}(t)$ (standard model) and the dose-response relationship for the cross-contamination model. Hence, any differences in the model results should be as much a reflection of the model structure as possible, rather than changes in parameter estimation. The key difference in dynamics, that is of far more variability in the epidemic curve of individual iterations (and the peak of infection) for the cross-contamination model compared to the standard model, is generated through the stochastic nature of faecal contamination of adjacent pens, and the more variable dose-response function (which is dependent on the variable faecal contamination).

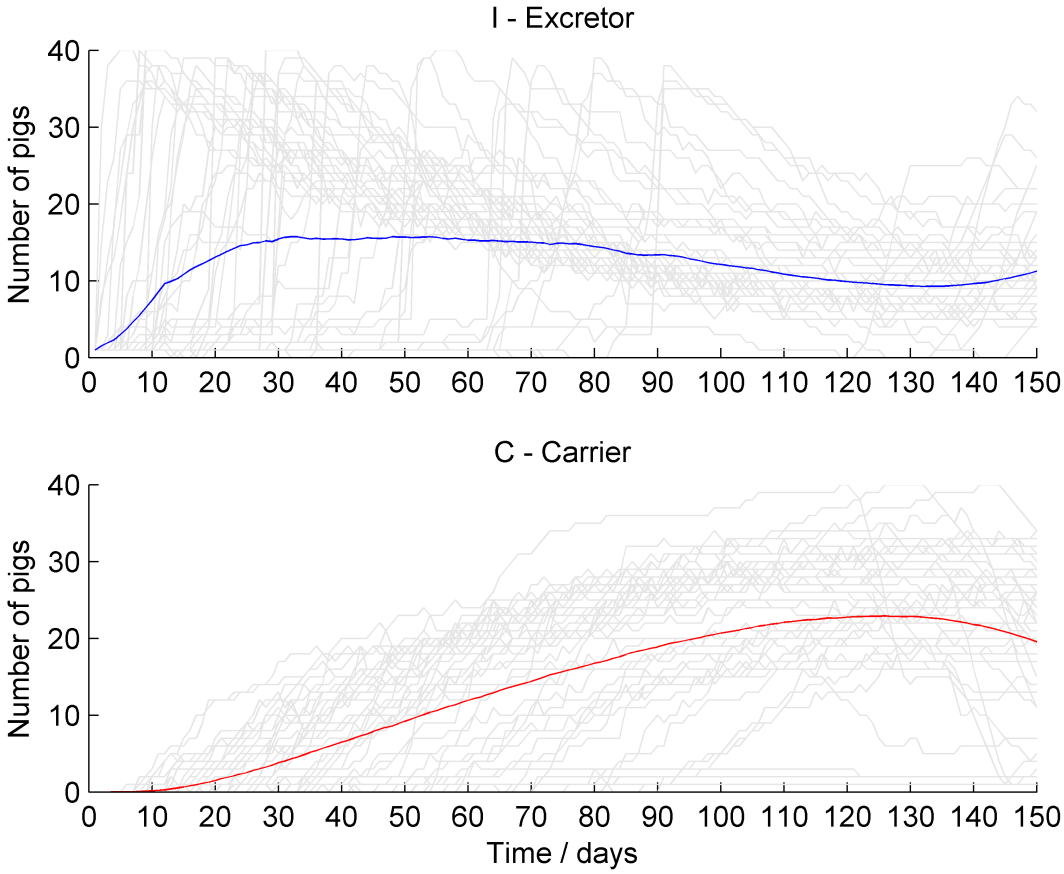

Figure 5.7: Plot of the average epidemic curve over all 1500 iterations of the cross-contamination model (blue - Excretor, green - Carrier).

5.4 Discussion

The stochastic models presented in this chapter are modifications of the previous deterministic models. The main differences are the use of the Reed-Frost/explicit faecal shedding models to create individual-based models that describes stochastic transmission, along with the inclusion of individual parameter estimation of duration of shedding/carriage. When infection is maintained, the average epidemic curves produced by both the standard and cross-contamination models are very similar to those from the deterministic models. However, there is a high propob-

ability of stochastic fade-out for the stochastic cross-contamination model, hence over all iterations the average epidemic curve for this model peaks at a much lower level of infection than for the equivalent deterministic model. At an individual iteration level, the stochastic effects of the standard model did not produce markedly different results. However, the stochastic effects included in the cross-contamination model mean that the infection dynamics between pens can be very different; for example, the exact timing of the epidemic within a farm is very variable. However, when an epidemic occurs, most iterations of the model produce an epidemic curve that is similar in shape to the average epidemic curve, even if the peak of infection is lower/higher than average, and/or the timing of that peak is delayed. The stochastic fade-out introduces an interesting dynamic where the average prevalence of infection at slaughter is dominated by a few farms that are highly infected, while the rest of the farms are not infected or infected at a very low level. This particular result replicates observational studies much better than the deterministic models, and suggests that stochastic fade-out of infecton is an important dynamic to consider.

Of note is that when transmission does occur, then the stochastic models still tend to produce an equilibrium of sorts, especially if the average epidemic curve is considered. Hence, the stochastic models suggest that once infection is established in 2 or more pigs then the pen will tend to remain infected until the end of the finishing period. Thus, the stochastic models suggest only subtle differences in the conclusions of the determinstic models: that infection will, by and large, sustain itself once it has spread between 2 or more pigs. In terms of intervention, the results of the stochastic models would not produce any dramatically different conclusions than the deterministic ones; faecal-oral transmission is more than likely to sustain itself, so completely preventing the infection of pigs within a cohort (e.g. pen,

building) is the only reliable and effective way to reduce spread of the organism with current parameter estimates.

All of the models described up until now have been for grower-finisher production. Initial conditions of numerical simulations have been set without thought to realism in order to investigate the basic dynamics of infection. However, as the previous investigation of continuous production highlighted, the time of infection is very important in determining the prevalence of infection at the point of slaughter. Therefore, greater attention must be paid to this factor. Given most observational studies point to initial infection between farrowing and reaching the grower-finisher stage, then these stages of rearing should be included in a more realistic model. The source of infection is also likely to influence infection dynamics as well. Hence, in the next chapter we develop the stochastic cross-contamination model described in this chapter, to include earlier stages of rearing and the source of infection. The cross-contamination model also allows the inclusion of farming management specific parameter estimation (as these farming practices are reflected in the level of contamination of the farm, and the dose-response of pigs to Salmonella exposure), and so this is also captured.

Chapter 6

Stochastic model from birth to slaughter and including sources of infection

6.1 Introduction

The models in previous chapters dealt with transmission of Salmonella once introduced into a typical grower-finisher pig house. However, many interventions depend on preventing introduction of infection from farrowing onwards (biosecurity, rodent control), and the introduction/transmission of Salmonella has been shown to be dependent on farm management factors not currently included in the model (e.g. feed type, flooring type) (Nollet et al., 2004; VLA, 2005; O'Connor et al., 2008). The model dsecribed in this chapter therefore incorporates features to deal with these factors.

The developments described in this chapter are motivated not only by this thesis,

but also for the production of a farm model capable of assessing interventions between EU Member States (MSs), for the EFSA QMRA described in Chapter 1. While there are many factors (such as climate) that may affect the transmission of Salmonella within a MS, the primary difference that is amenable to modelling is the management of the farm; hence differences in the effect of interventions between MSs can best be identified by differentiating between management types within MSs.

The farm model described in this chapter is a direct continuation of the methodological progress described in the previous chapters, and is intended to a) describe as realistically as possible how transmission dynamics differ according to different pig farming management practices, and b) assess the contribution of different sources of infection to transmission and the eventual prevalence of infection in slaughter-age pigs. Such developments are applicable for describing the difference between farm management systems in the UK (the main subject of this thesis), but also for the differentiation of dynamics between MSs (the focus of the EFSA QMRA). While we discuss the model results in the context of the UK situation (a high-prevalence country, where the prevalence of lymph-node infection at slaughter was recorded as 21.2% in the slaughter pig baseline survey conducted by EFSA (EFSA, 2009a)), we also include the results of a farm model developed for a much lower-prevalence country than the UK (for political reasons we cannot name this MS, and label it MS1) in order to highlight some of the important dynamics and sources of infection under different scenarios.

Such aims described above require a large extension and modification of the stochastic cross-contamination model described in Chapter 5, which are detailed in the next section.

6.2 Methods

6.2.1 Model algorithm and overview

For clarity we define a distinct difference between the use of the terms 'sow' and 'pig'. Pigs are explicitly defined as those animals which are raised only for slaughter and progress through all the rearing stages of farrowing, weaning, growing and finishing. Sows are explicitly those animals producing the pigs raised for slaughter in farrow-to-finish or production herds (as opposed to breeding sows in multiplier or nucleus herds).

In order to explicitly include management systems, sources of infection and a more realistic accounting of the contamination of the environment, several extensions of the cross-contamination model described in Chapter 4 have been made:

- We initially model the flow of pigs through a pig farm from birth to slaughter, much like the model of Lurette et al. (2008a). Hence, we are able to model the contacts, and transmission of Salmonella, between cohorts.
- Three sources of infection are included (at the following stages of production); the sow (farrowing), feed contamination (weaning to finishing) and "external" contamination, e.g. by rodents/birds (all stages).
- Dose-response and faecal shedding are explicitly modelled with a focus on detailed parameter estimation, in order to capture mechansitically the effects of different farm management practices (e.g. C&D) on environmental contamination.
- Difference in farm types is captured by a combination of changes to the production flow framework and/or parameter estimation of model parameters.

Such a model is far more complex than the models described in previous chapters, and hence the model algortihm is also correspondingly more complex. We outline the following chronology of the model process in the following schematic (Figure 6.1).

The farm model is an individual-based stochastic Susceptible-Infected-Susceptible (SIS) model, adapted to take account of i) multiple changing populations, rather than a single closed population and ii) intermittent shedding of Salmonella. The model is implemented using Monte-Carlo simulation, where each iteration represents production from one farm over a 500 day period, incorporating farrowing, weaning, and grower and finisher production. Over this 500-day cycle of production batches of pigs are sent to slaughter each week. Two outputs are generated for each batch of pigs sent to slaughter: the prevalence of lymph-node infection and a distribution for the concentration of Salmonella shed within the faeces of infected pigs.

For each iteration there are a large number of spatial and temporal events that can occur at random, including the seeding of infection into the farm, the response to exposure (in terms of whether or not infection occurs) and subsequently the shedding rate. All farms are set to be Salmonella-negative at the start of an iteration (day 1). There are three assumed sources of infection that will lead to pig infection: sows, feed and wildlife. All pigs born are assumed to be susceptible, and hence the first infection of a pig must occur because of one of the three sources; only then can pig-to-pig transmission take place. Following initial infection of the herd, which can occur at any time, transmission is described by an individual-based environmental infection model, which tracks i) the shedding and inactivation/movement of Salmonella in the environment and ii) the dose-response of pigs exposed to environmental contamination.

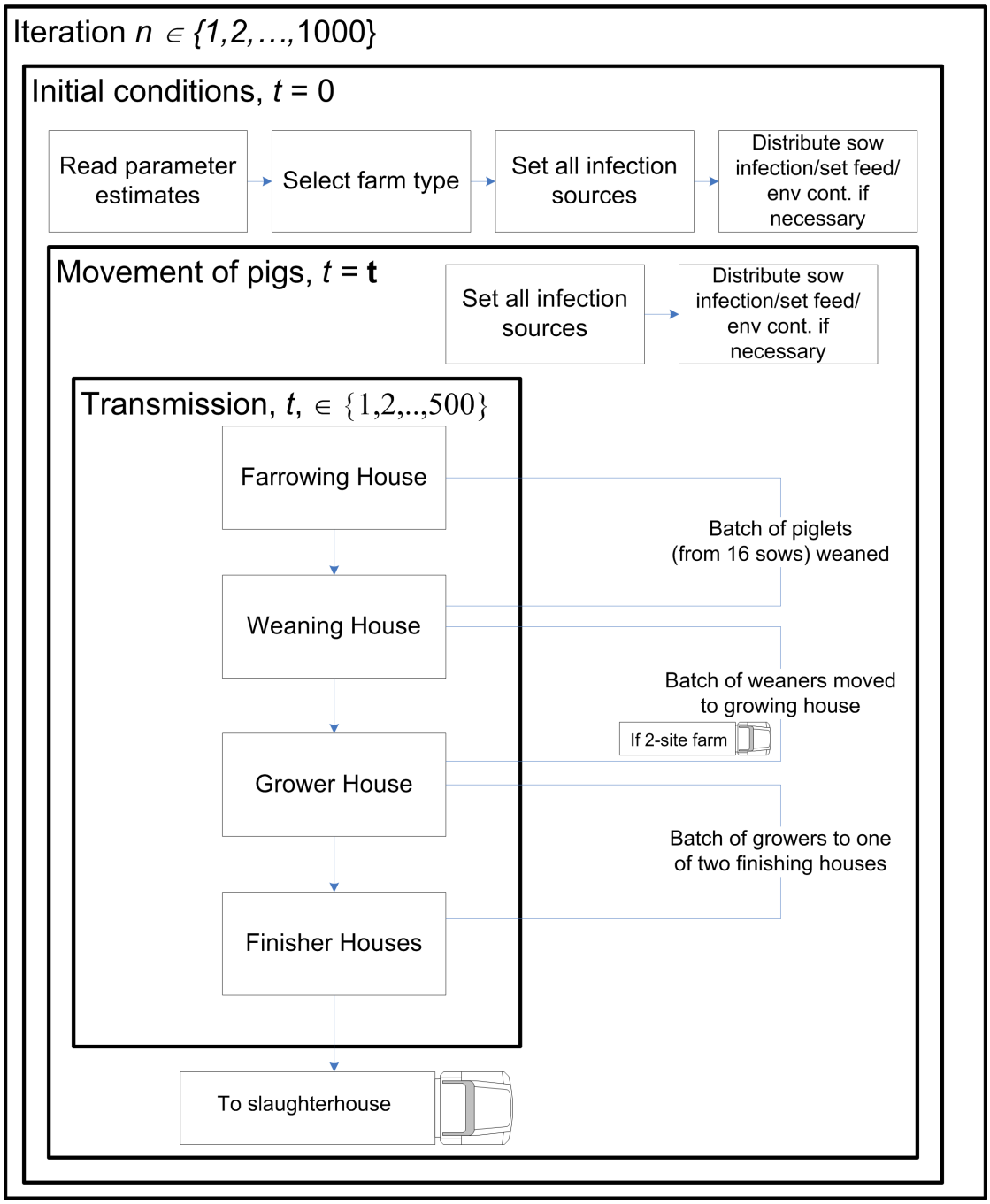

Figure 6.1: Model algorithm.

There are 32 farm types included in the model, depending on the combination of factors such as feed type, flooring type and whether the farm is a farrow-to-finish or multi-site farm (see Section 6.2.2). The farm type is selected randomly

at the beginning of an iteration based on the relative proportions of each farm type (derived from various data sources). The initial condition routine determines which sows shed Salmonella and which batches of feed are contaminated over the entire period of modelling. All three sources of infection are "static", i.e. they are not affected by the dynamic transmission of Salmonella between pigs, hence these initial conditions will remain the same over the whole timeframe considered.

The baseline model is run for 1000 iterations (representing 1000 farms). Management factors (for example flooring, feed type used) are used to define farm types, for which more description is given later. Farm types are allocated proportionally to the 1000 farms to represent the national structure of the pig herd within a particular MS (see Section 6.2.4). Hence, it is assumed that summing the predicted number of lymph-node positive pigs over all batches/farms and dividing by the total number of pigs within the batches provides an estimate for the prevalence of lymph-node positive pigs being sent to slaughter (i.e. leaving the farm gate) for a particular MS.

6.2.2 Management of farms

Large variability in breeding herd and slaughter pig prevalence across EU MSs is apparent from two baseline surveys carried out in 2006-8 (EFSA, 2008b, 2009a). While some of this variability can be assumed to originate from topography and climate, the majority will result from the types of production systems used by farmers. We included management systems and practices for which there was sufficient evidence to show a direct effect on transmission of Salmonella. Individual farms within the model are assigned a farm type based on these relevant characteristics. The options modelled are described in Table 6.1.

Table 6.1: Description of management factors included within the farm model.

Management factor	Description
One site or two-site farm	Two types of farm are considered: farms rearing slaughter pigs from birth to slaughter weight (breeder-finisher) or farms rearing birth to approximately 8 weeks old and then transferring pigs to a specialist finisher site (breeder-weaner and finisher only).
All-in-all-out versus continuous production	All-in-all-out (AIAO) production has been shown to be a protective factor for Salmonella infection (lo fo Wong et al., 2004; Nollet et al., 2004). AIAO production as modelled is the theoretical ideal; batches of pigs are kept together in one room for each of the weaning, growing and finishing stages without any direct contact with any other batches all the way through rearing. All other systems are termed "continuous".
Indoor versus outdoor production	According to data from the EFSA baseline survey for breeding pigs (EFSA, 2009a) large-scale outside production is still quite rare for pigs beyond the stage of weaning, and therefore only the farrowing stage is included as a possible outside production stage.
Feed type	Feed can be both a source of Salmonella infection in pigs and a factor in determining the level of transmission. Of particular importance is whether the feed is presented in a dry or wet form, or whether it is pelleted or non-pelleted ((lo fo Wong et al., 2004; Farzan and Friendship, 2005; O'Connor et al., 2008). Only the distinction between wet or dry feed is assumed because there is some information on the relative effect of wet/dry feed on the prevalence of Salmonella infection in pigs and good information on whether a farmer uses wet/dry feed from the EFSA baseline survey for breeding pigs (EFSA, 2009a).
Flooring type	While the evidence for flooring type affecting Salmonella transmission is varied, logical thinking suggests that properly maintained slatted flooring may well have some effect as it will remove faeces/Salmonella from the pig environment. There are many flooring types (partially slatted, bare concrete, straw-laden), but with current data we can only differentiate between slatted and solid flooring.

It is assumed that all slaughter pigs will go through four main stages of rearing: farrowing, weaning, growing and finishing (fattening) and will be moved into spe-

cialist accommodation for each stage of rearing (pigs can be transported between farms at the end of weaning if a two-site system is used). Pigs will be batched in some way, such that there are distinct age cohorts that move through the system at well-identified times. A batch cohort is defined as one group of sows that all give birth at the same time in one of the five farrowing houses (see Figures 6.2 and 6.3). Given current parameter estimation (see Table 6.3) then there are 16 sows within each farrowing house cohort, producing 10 piglets each; these 160 piglets are grouped into pens of 40 at weaning (28 days). As each group of piglets reach weaning age the group of sows is replaced with another group of sows reaching parturition, after a week of the pen being empty for cleaning and disinfection (C&D). From the farrowing building, each batch cohort will spend 4 weeks in the weaning house, 6 weeks in the growing house and 12 weeks in one of the two finishing houses. If the system is multi-site, there there will be a stage of transport between weaning and growing. The model explicitly tracks pens, rather than batches, over the 500 day production cycle. Batch cohorts are moved between these pens over time as shown. Over a 500 day cycle of production, there are 67 batches of finishing pigs sent to slaughter.

Pigs will spend sa days in the farrowing house before being weaned, wa days in the weaning accommodation, and then ga and fa days in the growing and finishing stages respectively, before being sent to slaughter on a weekly basis at times $\mathbf{t} = \{1, 8, 15, \ldots, 498\}$. There are n_{pig} pigs in pen j, n_{pen} pens in room l, and n_{room} rooms in a building. At the beginning of the model (t=1) each pen/room/building is populated with pigs (except for one farrowing building, which is left empty for cleaning and disinfection for one week). The system is relatively flexible, and differences between rearing stage, inside/outside and AIAO/continuous production are captured via parameter estimation of the farm management system factors.

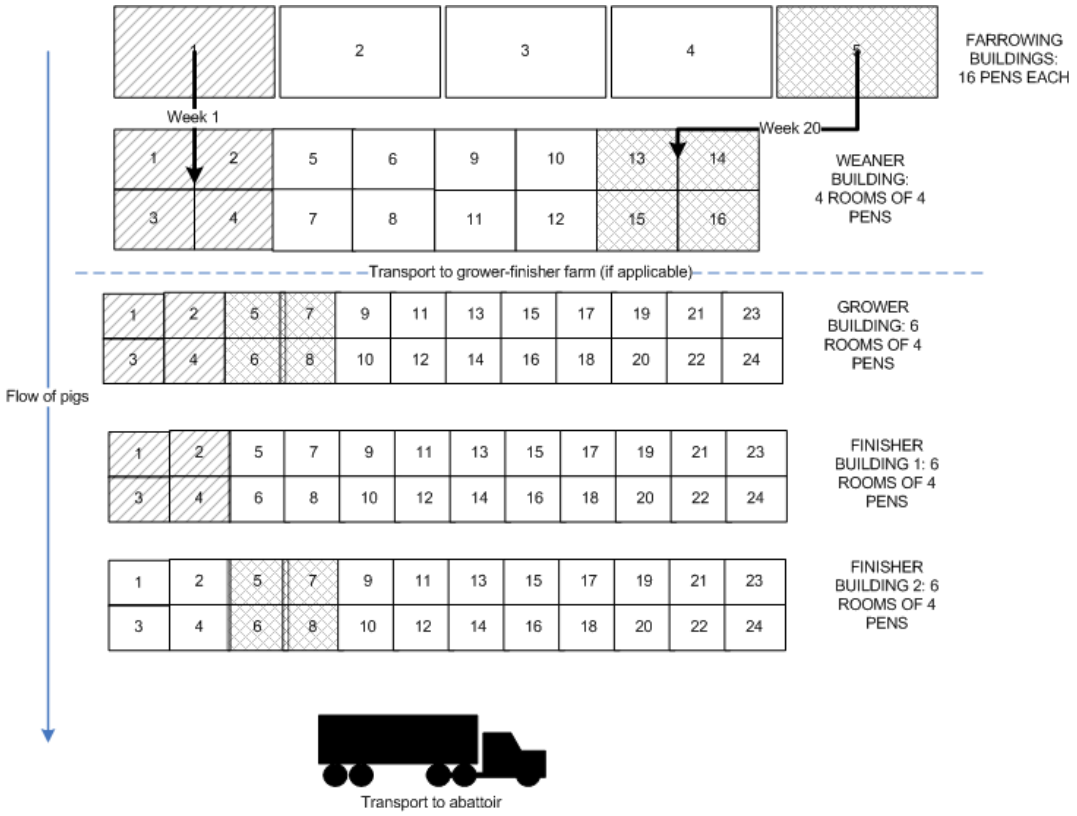

Figure 6.2: Schematic of pig flow through generic large farm system as modelled. Examples of flow are given by shaded annotations: i) single-hatched; piglets are weaned and grouped into batch of 4 pens within one weaner room at the start of Week 1, moved to growing accommodation on Week 5, finishing accommodation on Week 11 and slaughtered on Week 23; ii) double-hatched; new group of sows moved into vacated farrowing building 5 on Week 16; piglets are weaned at start of Week 20 and pass through rooms in subsequent accommodation as they become empty at the time where movement occurs.

For computational efficiency it was also assumed that pig movement is regimented and efficient, such that the pens containing the individual batch of pigs sent to slaughter at times $\mathbf{t}$ are filled immediately with the group of pigs within the growing house that have reached finishing weight, and that group is replaced by the batch of pigs reaching the required growing weight etc. . . (with the exception of the farrowing house, where there is a week's delay before re-population with the next batch of sows reaching partuition). For slaughter pigs that are finished on

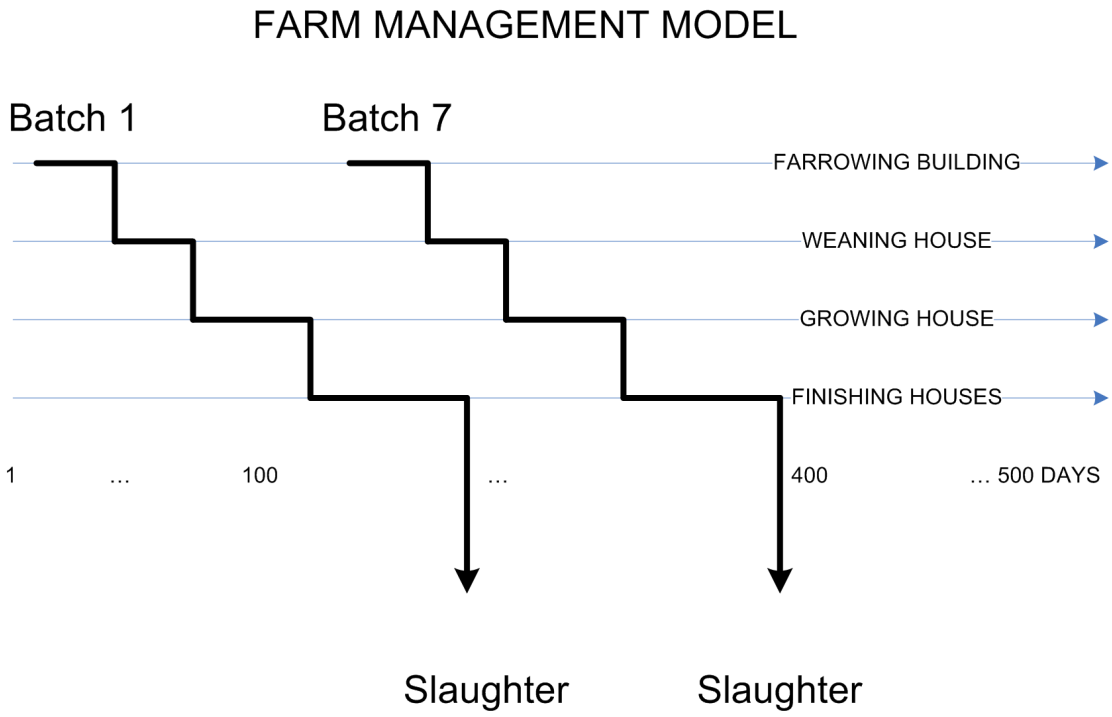

Figure 6.3: The model explicitly tracks pens over the 500 day production cycle. Batch cohorts are moved between these pens over time as shown. Over a 500 day cycle of production, there are 67 batches of finishing pigs sent to slaughter.

a grower-finisher farm, it is assumed that they were reared on a breeder-weaner farm and transported to the grower-finisher farm. Transport has been highlighted as a risk factor for Salmonella transmission between pigs (Berends et al., 1996), hence Salmonella transmission during transport is included in the model if this farm type is selected. Transport between farms is assumed to be almost identical to transport between the finishing house and abattoir, hence the model we use here is largely based on a Transport & Lairage model (Simons et al., prep), except it is assumed only one cohort (batch) is transported at a time.

6.2.3 Transmission model

Model states

Rather than the SIRS compartment model of the previous models, a more complex system is used in this model in order to account for intermittent and variable shedding of Salmonella. This is necessary, as Salmonella is a dose-dependent, faecally-transmitted infection, and in order to capture the effect of farm management practices on the environmental contamination of the farm, we must model in more detail the shedding of Salmonella by infected pigs. Therefore, we introduce variability into the infectious state I, such that pigs may or may not be shedding (intermittent shedding) and if they do shed that shedding is variable. These traits have been observed in a number of studies (Kranker et al., 2003; Jensen et al., 2006; Nollet et al., 2005). Inspection of the time of excretion (as determined by faecal sampling) and infection (as determined by presence of Salmonella in various organs) suggests that pigs are able to shed intermittently throughout the duration of being infected (Gray et al., 1996; Jensen et al., 2006), hence the assumption of intermittent shedding effectively removes the need for the Carrier status. This is because pigs are no longer assumed to cease shedding at the end of the infectious period, but rather could cease/restart shedding a number of times before the infection is finally cleared. The model is therefore classed as an SIS model, see Figure 6.4.

Therefore, it was assumed that a pig will be in one of two states at time t; Susceptible or Lymph-node positive (specifically infection in the ileo-caecal lymph node). Similar to the principle introduced by Soumpasis and Butler (2009) the concentration of Salmonella shed by Lymph-node positive pigs is dependent on whether the pig is infected by a 'low' ($< 10^6$ CFUs) or 'high' ($\geq 10^6$ CFUs) dose.

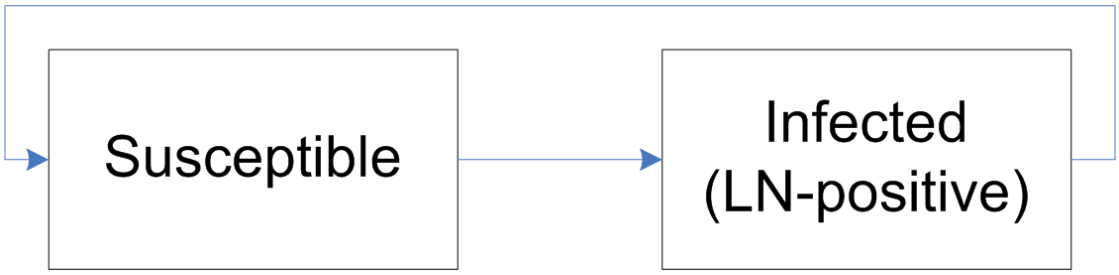

Figure 6.4: Schematic of SIS compartment model used in this model. This transmission model is overlaid on top of the production flow model described in Section 6.2.2

Lymph-node positive status was used to determine infection as it is an ideal characteristic at the point of slaughter for which to validate the model (given the ileocaecal lymph node was the primary sample type for the EFSA baseline slaughter pig survey (EFSA, 2008b)). However, being lymph-node positive does not necessarily mean that the pig will be actively excreting Salmonella. Rather, it is an indication of the fact that the pig still has a Salmonella infection and can *potentially* shed Salmonella. Therefore, it is important to note that at some timepoints no shedding of Salmonella may occur, even if a pig is lymph-node positive (i.e. 'intermittent shedding'). As no data were available, it was assumed that pigs immediately return to the 'Susceptible' state following recovery from being lymph-node positive. Recovery from the 'Lymph-node positive' state takes t_{LN} days.

Introduction of Salmonella into pig herd

The sources of infection were based on the opinion of EFSA (2006), which are: other infected pigs (sows/new stock/mixing of cohorts), feed and wildlife. The herd prevalence for Salmonella infection in breeding sows, p_{herd}, is estimated for each of the case study MSs (UK and MS1) from the EFSA breeding herd survey

(EFSA, 2009a). At the start of each iteration, the infection status of the breeding herd/farm is assigned according to the value of p_{herd}. The within-herd prevalence of Salmonella shedding on breeding herds, p_w, will vary between farms, as well as MSs. The number of sows shedding Salmonella within a batch cohort, b, is binomially distributed according to p_w and the number of sows within the cohort, n_{sow}, that is $I_{sow}(j,t) \sim B(n_{sow}, p_w)$. Once the piglets of the current batch of sows in the farrowing house are weaned, the building stays empty for a week to allow effective cleaning and disinfection, before a new cohort of sows is brought into the building to farrow. The number of infected sows in a new group is recalculated using the same process as before.

Each sow in pen j will produce $f_{sow}(j,t)$ faeces per day. If the sow is currently shedding it will excrete Salmonella into the environment at a rate $c_s(j,t)$ (CFUs per gram of faeces). Note that sows are treated as a 'static' source of infection within the model: they are not infected by either of the other sources considered, or by the shedding of their neighbours. We assume each sow remains in the same infection state for the duration of farrowing.

For simplicity, it was assumed that feed can be broken down into two major types: wet (w) and dry (d). Pigs will consume $g(k,j,t)$ grams of feed per day and it is assumed that pigs consume from a new batch of feed every 7 days. We define the prevalence of feed batch contamination as p_{feed}, and randomly select whether each batch of feed is contaminated with Salmonella. The concentration of Salmonella within contaminated feed is denoted as $c_f(k,j,t)$ per gram of feed (equal to zero if feed batch is Salmonella-negative). The Salmonella shed by sows is incorporated into the overall environmental contamination calculations described in Section 6.2.3.

There are little data to quantify the frequency and magnitude (and the associated variability over time and between farms) of any external contamination of the farm. However, there are some data on wildlife incursions onto farms and the amount of Salmonella rodents or birds contaminate the environment with via defecation (Davies and Wray, 1995; Skov et al., 2008). While recognising other external sources of infection exist, it is assumed that only wildlife (specifically rodents and birds) contributes as a source of external contamination of the farm/infection of the pigs.

Skov et al. (2008) investigated the transmission of Salmonella between wildlife and pigs; the study results suggest that wildlife within the vicinity of farms are more commonly infected with Salmonella if the pigs themselves are infected. Therefore, it is assumed that the Salmonella status of the wildlife is equivalent to the status of the farm, i.e. infected or not infected. Rodents and birds are then assumed to contribute $\lambda_e(k, j, t)$ salmonellas to the exposure dose of each pig for each time step onwards from when infection occurs on a farm (assuming, in the absence of any other data, each pig will ingest roughly 1g of rodent/bird faeces per day). Studies have shown that prevalence within rodents/birds on an infected pig farm (p_{wild}) are fairly low, around 1-5% (Davies and Wray, 1995; Skov et al., 2008). Therefore a Bernoulli random variable (with $p = 0.03$) was used to indicate whether a pig would ingest contaminated wildlife faeces such that pig ingestion of Salmonella through external contamination occurs relative to the prevalence of infection within the wildlife. The concentration of Salmonella within wildlife faeces appears to be similar to that within pigs (Davies and Wray, 1995). Hence, in the absence of rigorous quantitative data, a Lognormal distribution for $\lambda_e(k, j, t)$ was assumed, as visual inspection suggested it provided a biologically plausible fit (see Table 6.3).

Transmission of infection via the contaminated environment

There are two major routes of transmission assumed within the model: by the faecal-oral route via the shedding of contaminated faeces (whether pigs, sows or wildlife) or the ingestion of Salmonella from contaminated feed. Observational studies (Kranker et al., 2003; Jensen et al., 2006; Nollet et al., 2005) show intermittent shedding by infected pigs at low levels (usually less than 100 CFU/g of faeces) and a fairly low incidence of infection. A schematic diagram of this dynamic is shown in the transmission model framework for one pen (relevant to all pens, buildings and stages of production), given in Figure 6.5.

The total faecal material in the pen, $F(j,t)$, is added to each day by Susceptibles ($S(j,t)$), Lymph-node positive pigs ($I(j,t)$), infected and non-infected sows (in the farrowing house,) as well as from cross-contamination from other pens (F_{xc}). The faecal material in pen j is simultaneously reduced each day via cross-contamination (F_{xc}) or removal (F_{old}). This faecal material contains $E(j,t)$ salmonellas, which are added to each day from the infected group via shedding in their faeces and reduced each day as a result of decay, δ, and cross-contamination E_{xc}. Pigs ingest λ_i organisms per day via the amount in the faeces, λ_f via feed and λ_e via the environment (and λ_s, organisms from sow faeces if piglets during farrowing). This process results in $e(j,t)$ new infections according to the dose ingested and the dose-response relationship applied.

Shedding and removal of faeces

Salmonella is primarily transmitted via the faecal-oral route (Heard and Linton, 1966; Proux et al., 2001) and infection is dependent on the dose ingested (Loynachan and Harris, 2005). In order to examine a range of specific interventions (for example vaccination, changing feed type, cleaning) the amount of Salmonella

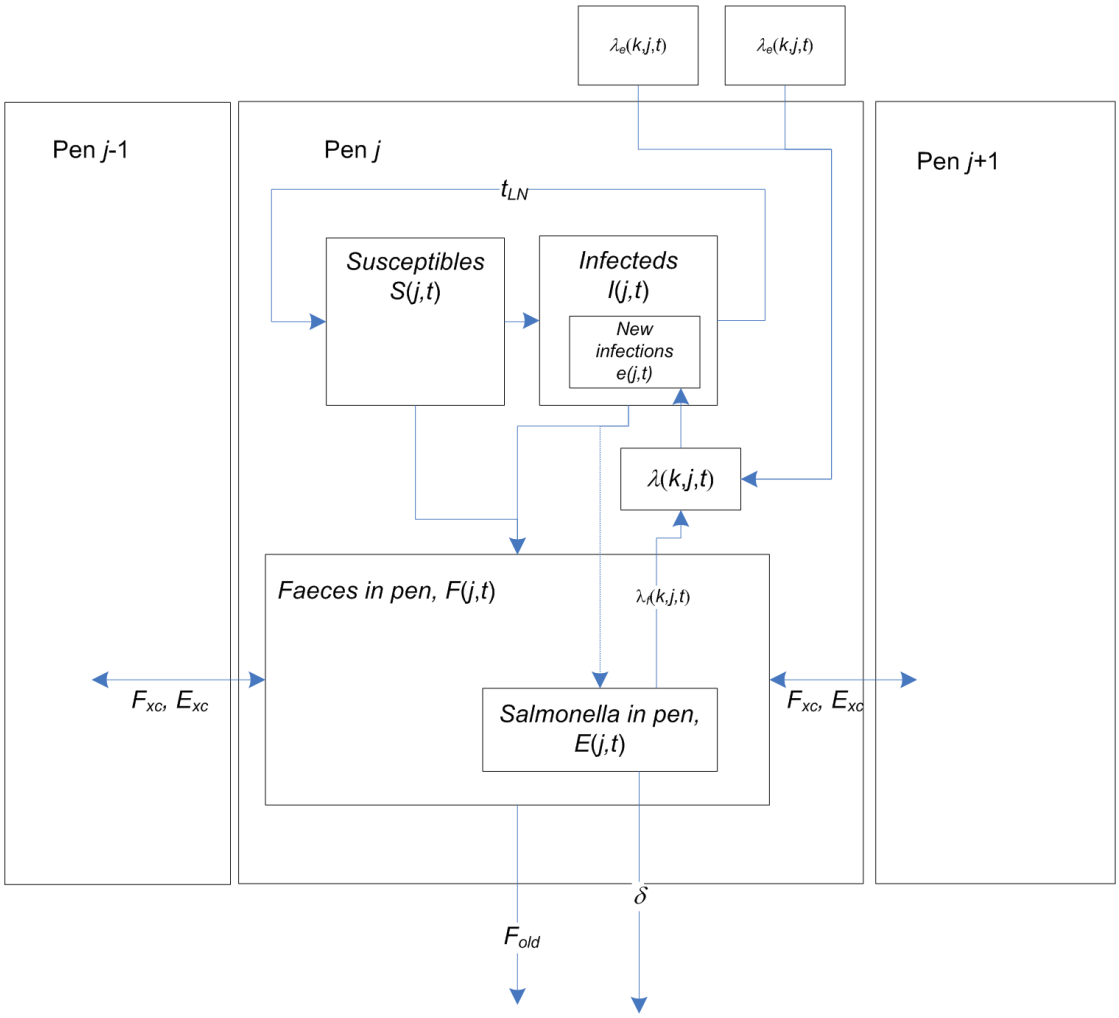

Figure 6.5: Schematic diagram of transmission model. Only the interactions associated with pen j are shown.

ingested by a pig and the subsequent dose-response must be considered. The methods used in previous models (Hill et al., 2008; Lurette et al., 2008a) have been expanded; in particular shedding and the subsequent movement/ingestion of faecal material. For the rest of this section a general parameter definition is used for all stages of production (farrowing, weaning etc...) unless explicitly stated.

The total amount of faecal material in pen j of room l at time t is defined as $F(j,t)$. The amount of faecal material shed by a pig, k, during any one timestep (one day) is defined as $f(k,j,t) \sim N\left(\mu_f, \sigma_f^2\right)$. Similarly, $f_{sow}(j,t) \sim N(\mu_s, \sigma_s^2)$

for sows. It is assumed that fresh faeces (i.e. those shed on day t) will be more viscous than older faeces and will hence be more amenable to fall through slatted flooring. The proportions of faecal material shed on day t in pen j of house l and removed that day via slatted flooring and cross-contamination to an adjacent pen are given by $\beta_{F,day}(j,t)$ and $\beta_{xc}(j,t)$ respectively. Regarding faecal material shed prior to day t, that is faecal material present on day t-1, the proportion removed via slatted flooring is $\beta_{F,old}(j,t)$. The amount of faecal material present in pen j of house l at the end of day t is calculated using Equations (6.1) - (6.4) as follows:

The total amount of faecal material shed by pigs on day t is

$$F_{pig}(j,t) = \sum_{k=1}^{n_{pig}} f(k,j,t), \tag{6.1}$$

except in the farrowing building where $F_{pig}(j,t) = \sum_{k=1}^{n_{pig}} f(k,j,t) + f_{sow}(j,t)$

The amount of faecal material shed on day t removed from pen j is given by

$$F_{day}(j,t) = F_{pig}(j,t) \cdot (1 - \beta_{F,day}(j,t) - \beta_{xc}(j,t)). \tag{6.2}$$

The amount of faecal material shed before day t and removed via slatted flooring on day t is given by

$$F_{old}(j,t) = F(j,t-1) \cdot \beta_{F,old}(j,t). \tag{6.3}$$

The amount of faecal material shed before day t and cross-contaminated to either pen j-1 or j+1 or day t is given by

$$F_{xc}(j,t) = F(j,t-1) \cdot \beta_{xc}(j,t). \tag{6.4}$$

Finally, the amount of faecal material left in the pen at time t is given by

$$\begin{aligned} F(j,t) =& F(j,t-1) + F_{day}(j,t) + F_{xc}(j-1,t)/2 \\ &+ F_{xc}(j+1,t)/2 - F_{old}(j,t) - F_{xc}(j,t). \end{aligned} \tag{6.5}$$

For pens at the end of a row ($j = 1, 6$), then the redundant cross-contamination is removed, either $F_{xc}(j-1,t)/2$ or $F_{xc}(j+1,t)/2$.

The set of pens depopulated through each production stage are assumed to be cleaned out before new pigs are moved in. We assume cleaning out of faecal material at this depopulation time is efficient, therefore $F(j,\mathbf{t}) = 0$, for all rooms which are depopulated/re-populated at times $\mathbf{t}$. In contrast, it is assumed that Salmonella removal will not be 100% efficient (as Salmonella may be released from the faecal material and reside in biofilms or hard-to-clean areas such as feeder tube nipples). This inefficient removal is mathematically described below.

Dissemination of Salmonella into pig envrionment

The amount of Salmonella shed onto the pen environment each day by each pig ($\gamma(k,j,t)$) or sow ($\gamma_s(j,t)$) can be given by

$$\gamma(j,t) = \begin{cases} \sum_{k=1}^{n_{pig}} c_p(k,j,t) \cdot f(k,j,t) & \text{if wean, grow or finishing stage,} \\ \sum_{k=1}^{n_{pig}} \left(c_p(k,j,t) \cdot f(k,j,t)\right) + c_s(j,t) \cdot f_{sow}(j,t) & \text{if farrowing stage,} \end{cases} \tag{6.6}$$

where $c_p(k,j,t)$ and $c_s(k,j,t)$ are the concentrations of Salmonella per gram of faeces shed by a pig and sow respectively. The concentrations $c_p(k,j,t)$ or $c_s(k,j,t)$ are zero for susceptible pigs/sows ($c_p(k,j,t)$ and/or $c_s(k,j,t)$ may also be zero for infected pigs/sows that are intermittently shedding). Similar equations for the total number of Salmonella in the pen environment, as for faecal material ((6.1) - (6.4)), can be defined. Therefore,

$$E_{day}(j,t) = \gamma(j,t) \cdot (1 - \beta_{f,day}(j,t) - \beta_{xc}(j,t)), \tag{6.7a}$$

$$E_{old}(j,t) = E(j,t-1) \cdot \beta_{f,old}(j,t), \tag{6.7b}$$

$$E_{xc}(j,t) = E(j,t-1) \cdot \beta_{xc}(j,t), \tag{6.7c}$$

where E_{old} and E_{xc} are the amounts of Salmonella present at day $t-1$ and removed during day t via slatted flooring and cross-contamination respectively. Therefore, the total amount of Salmonella in pen j at the end of day t, $E(j,t)$ is given by

$$E(j,t) = \begin{cases} \left(10^{\log(E(j,t-1))-\delta}\right) + E_{day} - E_{old}(j,t) - \\ E_{xc}(j,t) + E_{xc}(j-1,t)/2 + E_{xc}(j+1,t)/2 & \text{if } t \neq \mathbf{t} \\ \\ 10^{\log(E(j,t-t_c)\cdot\beta_C)-\delta\cdot t_c} & \text{if } t = \mathbf{t} \end{cases} \tag{6.8}$$

where δ is the decay rate of Salmonella (in logs) per day, t_C is the time in between depopulation and repopulation of the pen (7 days in a farrowing house, zero in all other stages of production) and $\beta_C \sim \text{Beta}(\alpha_{\beta_c}, \beta_{\beta_c})$ and is the fraction of Salmonella remaining in the pen environment after cleaning. For end pens, either

the $E_{xc}(j-1,t)/2$ or $E_{xc}(j-1,t)/2$ terms are removed from the equation.

For simplicity it was assumed that Salmonella is homogeneously mixed within all faecal material in the pen. Therefore the average concentration of Salmonella within a gram of contaminated faecal material, c, is given by

$$c(j,t) = \frac{E(j,t)}{F(j,t)}. \tag{6.9}$$

It was assumed that all (Salmonella-negative and positive) pigs ingest some faecal material each day. Therefore, each pig will ingest $\lambda_i(k,j,t)$ organisms through faecal ingestion, where

$$\lambda_i(k,j,t) = Poisson(\mu \cdot c(j,t)), \tag{6.10}$$

and μ is a random variable describing the mass of faeces ingested by a pig. The total number of Salmonella ingested by each pig on day t, $\lambda(k,j,t)$ can therefore be given as

$$\lambda(k,j,t) = \lambda_i(k,j,t) + \lambda_f(k,j,t) + \lambda_e(k,j,t) \tag{6.11}$$

where $\lambda_i(k,j,t)$, $\lambda_e(k,j,t)$ and $\lambda_i(k,j,t)$ represent the amount of Salmonella ingested by pig k through ingestion of faeces, envrionmental contamination (rodent, bird faeces) and feed respectively.

From experimental data (Loynachan and Harris, 2005), the probability of a pig becoming infected through ingesting $\lambda(k,j,t)$ organisms, $p_{inf}(k,j,t)$, was shown to follow a Beta-Binomial dose-response relationship. Hence, at the individual pig

level

$$p_{inf}\left(k,j,t\right)=1-\left(\left(1-Beta\left(\alpha_{DR},\beta_{DR}\right)\right)^{\lambda(k,j,t)}\right), \tag{6.12}$$

where α_{DR} and β_{DR} are the shape and scale parameters of the Beta-Binomial dose response model, and are dependent on feed type. The number of newly infected pigs in pen j, $e\left(j,t\right)$, can therefore be defined as

$$e\left(j,t\right)=\sum_{1}^{S(j,t)}B\left(1,p_{inf}\left(k,j,t\right)\right). \tag{6.13}$$

The transition of newly infected pigs through the infection states is similar to the stochastic models of Chapter 4. Each of the newly infected pigs are assigned a duration for being lymph-node positive, t_{LN}. Hence, at time $t_{inf}+t_{LN}$ (time of infection + duration of infection) a pig will return to the Susceptible status (if it has not been transported to slaughter first). We define $w\left(j,t\right)$ to be the sum of infected pigs in pen j of room l, that have reached the end of their infection period at time t. Therefore, the number of susceptible ($S\left(j,t\right)$) and infected ($I\left(j,t\right)$) pigs within a pen at the end of day t is calculated as follows:

$$I\left(j,t\right)=I\left(j,t-1\right)+e\left(j,t\right)-w\left(j,t\right), \tag{6.14a}$$

$$S\left(j,t\right)=S\left(j,t-1\right)-e\left(j,t\right)+w\left(j,t\right). \tag{6.14b}$$

where at $t=1$, $S\left(j,t\right)=n_{pig}$ and $I\left(j,t\right)=0$. The prevalence of infection within each pen at time t, $p\left(j,t\right)$ is equal to

$$p\left(j,t\right)=\frac{I\left(j,t\right)}{n_{pig}}. \tag{6.15}$$

The output of the model is the prevalence of infection (as defined as lymph-node positive) within batches of pigs placed on transport to slaughter. Transport to slaughter occurs weekly, i.e. one finishing room (4 pens, 160 pigs) from one of the finishing buildings is emptied on each of the movement timesteps $\mathbf{t}$ discussed above.

Therefore, the prevalence of lymph-node positive pigs at slaughter within a batch of pigs sent to slaughter at times $\mathbf{t}$, $p_i\left(\mathbf{t}\right)$, is given by

$$p_i\left(\mathbf{t}\right)=\frac{\sum_{j=1}^{4} I(j,\mathbf{t})}{4*n_{pig}}. \tag{6.16}$$

6.2.4 Parameter estimation

The weightings for apportioning farm types were taken from data collected from the EFSA baseline survey for breeding pigs (EFSA, 2009a). For farms which the EFSA baseline survey data did not cover (i.e. farms with no breeding herd) other relevant sources were used (see Table 6.2). There are little or no data to measure the variation across EU MSs caused by some of the management factors in terms of Salmonella introduction/transmission (for example number of pigs in a pen), and hence for simplicity these parameters are assumed to be equal across each case study MS (see Table 6.3). All other parameter estimates are detailed in Tables 6.4 and 6.5.

Table 6.2: Structure of case study MS pig populations reflected using the percentage of slaughtered head production that is reared through each farm type (raw data provided from EFSA breeding pig survey EFSA (2009a) and a GB research project (VLA, 2009)).

Farm type	**Case study Member State**					
	MS1			UK		
	Breeder-Finisher	Breeder-Weaner	Finisher only [1]	Breeder-Finisher	Breeder-Weaner	Finisher only [2] [3]
I -A So - D	0.00%	0.00%	0.00%	8.09%	4.94%	52.26%
I - A - So - W	3.30%	3.85%	3.30%	2.73%	0.21%	11.56%
I - A - Sl - D	3.30%	5.13%	3.30%	20.50%	15.05%	18.59%
I - A - Sl W	20.88%	28.21%	20.88%	6.91%	0.63%	4.28%
I C - So - D	0.00%	0.00%	0.00%	11.89%	3.86%	7.91%
I C - So - W	10.99%	7.69%	10.99%	4.01%	0.16%	1.82%
I C - Sl - D	1.10%	3.85%	1.10%	30.12%	11.77%	2.93%
I C - Sl - W	45.05%	35.90%	60.43%	10.15%	0.49%	0.67%
O - A - So - D	0.00%	1.28%	0.00%	0.48%	8.37%	0.00%
O - A - So - W	1.10%	0.00%	0.00%	0.16%	0.35%	0.00%
O - A - Sl - D	0.00%	0.00%	0.00%	1.22%	25.51%	0.00%
O - A - Sl W	5.49%	3.85%	0.00%	0.41%	1.06%	0.00%
O C - So - D	0.00%	0.00%	0.00%	0.71%	6.55%	0%
O C - So - W	4.40%	5.13%	0.00%	0.24%	0.27%	0.00%
O C - Sl - D	0.00%	0.00%	0.00%	1.79%	19.96%	0.00%
O C - Sl - W	4.40%	5.13%	0.00%	0.60%	0.83%	0.00%

The breeding herd prevalence of each case study MS is taken from the EFSA breeding pig survey and assumed to be directly equivalent to p_{herd}. In the absence of data for all case study MSs, it is assumed that, as a worse case scenario, the within-herd prevalence is equal to the UK estimate. The prevalence of Salmonella contamination has been identified to be between 1-10% for samples from feed types commonly used for pigs (EFSA, 2008a). However, there are many issues with sampling of feed for determining prevalence (EFSA, 2006; Cannon and Nicholls, 2002). Of concern is the extremely small sample mass relative to the tonnage produced, meaning that it is highly likely that positive batches are missed if contamination is heterogeneous. Therefore, a conservative estimate of $p_{feed} = 10\%$ is used for both case study MSs.

Assuming that pigs excrete intermittently during the whole time period of infection (as defined by presence of Salmonella in lymph-node), survival analysis methods were used to estimate the duration of lymph-node positivity (Kranker et al., 2003; Jensen et al., 2006). A recent longitudinal study of outdoor pigs (Jensen et al., 2006) enumerated Salmonella at the individual pig level for six weeks (six weekly samples). Two cohorts of pigs (one high and one low dose group) were seeded with experimentally infected pigs on outdoor paddocks, before these cohorts were removed and two new cohorts placed on the vacated paddocks. There were significantly greater concentrations shed by the high dose group (between 0-10^6 CFU/g faeces) than by the low dose group (0-100 CFU/g faeces). Pigs in the second experiment cohorts were then infected quasi-naturally from the contaminated faecal material shed by the first cohorts, and again, the pigs infected in the high dose group shed far larger amounts of Salmonella than the low-dose group.

Within the model we assume that once a pig k has been infected then the magnitude of shedding is randomly assigned from 0 - 8 log CFU/g faeces, according

Table 6.3: Description of management factors included within the farm model. For more detail refer to (ref).

Notation	Description	Stage	Unit	Value	Source
n_{pig}	Number of pigs within a pen	Far W/G/Fin	-	11 40	Far - 1 sow, 10 piglets (Commission, 2010)
n_{pen}	Number of pens within a room/building	Far W G/Fin	-	16 AIAO 4 Cont 16 AIAO 6 Cont 24	Assumed
n_{room}	Number of rooms within a building	Far W G/Fin	-	1 AIAO 4 Cont 1 AIAO 6 Cont 1	Assumed
wa	Age at weaning		Day	28	Commission (2010)
wa	Growing period		Day	42	Commission (2010)
fa	Finishing period		Day	42	Commission (2010)

Table 6.4: Description of parameters related to the sources of infection.

Notation	Description	Unit	Value	Source
p_{herd}	National prevalence of Salmonella-positive breeding herds	-	UK: 0.44; MS1: 0.059	EFSA (2009a)
p_w	Prevalence of infection with a breeding herd	-	0.21	EFSA (2009a)
p_{feed}	Prevalence of feed batch contamination	-	0.10	Assumed from VLA (2008), Cannon and Nicholls (2002) and EFSA (2008a)
$f_{sow}(j,t)$	Mass of faeces defacated by sow per day	g	N(3000,150)	Brent (1986)
g	Amount of feed consumed per day	g	Wean: 500; Grow: 1620; Fin: 3200	Carr (1998)
c_s	Concentration of Salmonella in contaminated sow faeces	CFU/g	LogNormal(2.36,4.39)	VLA (2009)
c_f	Concentration of Salmonella in pig feed	CFU/g	Genarlised Pareto(0.001,0,1)	Sauli et al. (2005)
λ_e	Amount of Salmonella ingested from the external environment per day	CFU	LogNormal(0.1,3)	Davies and Wray (1995)

Table 6.5: Description of biological parameters related to transmission of Salmonella between pigs.

Notation	Description	Unit	Value	Source
f	Mass of faeces defacated per day	g	Piglet: N(100,10); Wean: N(753,50); Grow: N(1194,50); Fin: N(2580,50)	Carr (1998), Leek et al. (2005)
c_p	Concentration of Salmonella in contaminated pig faeces	CFU/g	$0 - 10^7$ (see text)	Jensen et al. (2006)
$\beta_{F,day}$	Removal coefficient for fresh faeces in contaminated pig faeces	-	Beta(40,10)	Assumed
$\beta_{F,old}$	Removal coefficient for old faeces in contaminated pig faeces	-	Beta(2,10)	Assumed
β_c	Cleaning coefficient for flooring	-	Solid: Beta(3,2); Slatted: Beta(1,2)	Assumed
β_{xc}	Cross-contamination coefficient	-	Beta(1,10)	Assumed
δ	Decay constant	day^{-1}	0.04	Gray and Fedorka-Cray (2001), Tannock and Smith (1972)
μ	Mass of faeces ingested by pig per day	g	Piglet: U(0,21); other: U(0,100)	Sansom and Gleed (1981), Gleed and Sansom (1982)
α_{DR}, β_{DR}	Parameters of dose-response model	-	Wet: 0.1766, 50235; Dry: 0.1766, 20235	Loynachan and Harris (2005), Tenhagen et al. (2009)
t_{LN}	Duration of intermittent shedding	day	Weibull(44.94,1.68)	Jensen et al. (2006)

Table 6.6: Low-dose correlation matrix describing the probability of shedding x log CFU/g faeces given pig was shedding y log CFU/g faeces the previous week. Data taken from (Jensen et al., 2006).

Mag. at week w	Probability of shedding at magnitude y during week $w+1$			
	0	2	4	6
Newly infected	0	1	0	0
0	0.44	0.56	0	0
2	0.14	0.64	0.19	0.028
4	0	0.84	0.16	0
6	0	0	1	0

to the dose with which the pig was infected. For every proceeding week after initial infection that a pig remains within the Lymph-node positive state then the magnitude of shedding is determined based on the previous week's magnitude. On each day an infected pig may shed up to x log CFU/g faeces, therefore $c_p(k,j,t) \sim U\left(10^{x-2}, 10^x\right)$ if $x > 0$, else $c_p(k,j,t) = 0$. Correlation matrices have been generated from the dataset describing the magnitude of shedding (either 0, 2, 4, 6 log CFU/g faeces) from infected pigs in the second, quasi-naturally infected, cohort, see Tables 6.6 and 6.7. There is one matrix for each dose group ('low', $1 - 10^6$ CFU, or 'high', $\geq 10^6$ CFU). Hence these correlation matrices give the probability of a pig shedding x log CFU/g faeces one week, given it had shed y log CFU/g faeces the previous week.

In order to derive the dose response parameters, α_{DR} and β_{DR}, a Beta-Poisson model is fitted to experimental dose-response data for pigs fed on dry feed (from ileo-caecal lymph-nodes) (Loynachan and Harris, 2005). The α_{DR} and β_{DR} parameters from the Beta-Poisson model are equivalent to the α_{DR} and β_{DR} parameters of the Beta-Binomial model. Pigs on wet feed will have a greater resistance to infection, due to the lowering of pH within the gut making it a more hostile environment for Salmonella (Wales et al., 2010). The wet feed parameters were

Table 6.7: High-dose correlation matrix describing the probability of shedding x log CFU/g faeces given pig was shedding y log CFU/g faeces the previous week. Data taken from (Jensen et al., 2006).

Mag. at week w	Probability of shedding at magnitude y during week $w+1$				
	0	2	4	6	8
Newly infected	0	0.6	0.39	0	0.01
0	0.37	0.63	0	0	0
2	0.15	0.60	0.20	0.05	0
4	0	0.67	0.22	0.11	0
6	0	0	0.33	0.67	0
8	0	0	1	0	0

estimated by anchoring the relative change in slaughter pig prevalence between dry and wet-feed farms produced by the model to the relative change in prevalence observed within a German risk factor study using data collected through the EFSA baseline survey for slaughter pigs (Tenhagen et al., 2009).

6.2.5 Sensitivity analysis and model interrogation

An Analysis of variance (ANOVA) method was used for sensitivity analysis (Frey et al., 2004). The inputs (or 'factors') were grouped by quartiles and the resultant F-value from ANOVA indicates the confidence that a given factor has an effect on the output mean, i.e. the prevalence of infection within a batch of pigs sent to slaughter ($p_i(t)$). ANOVA decomposes the response variable into an overall mean, main factor effects, interaction effects, and an error term. ANOVA uses the F-test to determine whether a statistically significant difference exists among mean responses for main effects or interactions between factors. The F-test can used to test the significance of each main and interaction effect (although here it is just used to test main effects of the parameters included. The relative magnitude of F values can be used to rank the factors for sensitivity analysis (Mokhtari and

Frey, 2005; Carlucci et al., 1999). Many of the distributions used within the model are sampled many times during one iteration of the model. In order to use the ANOVA method then the mean of the random variable samples drawn from each distribution of one iteration is used to describe the variability between batches. For example the relationship between $p_i(\mathbf{t})$ and the amount of Salmonella ingested via external contamination, $\lambda_e(k, j, t)$, is determined by investigating how the value of $p_i(\mathbf{t})$ is influenced by the mean value of all the individual values of $\lambda_e(k, j, t)$ drawn from the distribution described in Table 6.3 for the relevant pigs (k), pens (j), building (l) and time (t).

The relative contribution of each source of infection (sow, feed, external contamination) was investigated by setting, in turn, the contribution of each source to zero. Analysis of individual iterations was used to investigate complex dynamics, such as comparing the distribution of doses ingested against the contamination of the pig environment. Finally, the output was stratified by management factors (for example feed type, flooring type) and by farm type to elucidate any potentially significant differences between farm types.

6.3 Results

6.3.1 Baseline results

The average within-batch prevalence of lymph-node positive pigs at slaughter age is estimated to be 0.007 (5th percentile 0, 95th percentile 0.031) for MS1, and 0.176 (0, 0.813) for the UK, which apply relatively well compared to a recent EFSA baseline survey of lypmh node samples of pigs at slaughter (21.2% for the UK, and 1.3% for MS1) (EFSA, 2008b). The percentage of positive batches for MS1

and the UK are estimated to be 38% and 62.9% respectively. The distribution of within-batch prevalence (showing only positive batches) is shown in Figure 6.6. It is clear that most batches being sent to slaughter are either Salmonella-negative, or infected at a low prevalence. Batches with a high within-batch prevalence are rarely sent to the slaughterhouse, but it is these high-infection events that determine the magnitude of the estimated national MS prevalence.

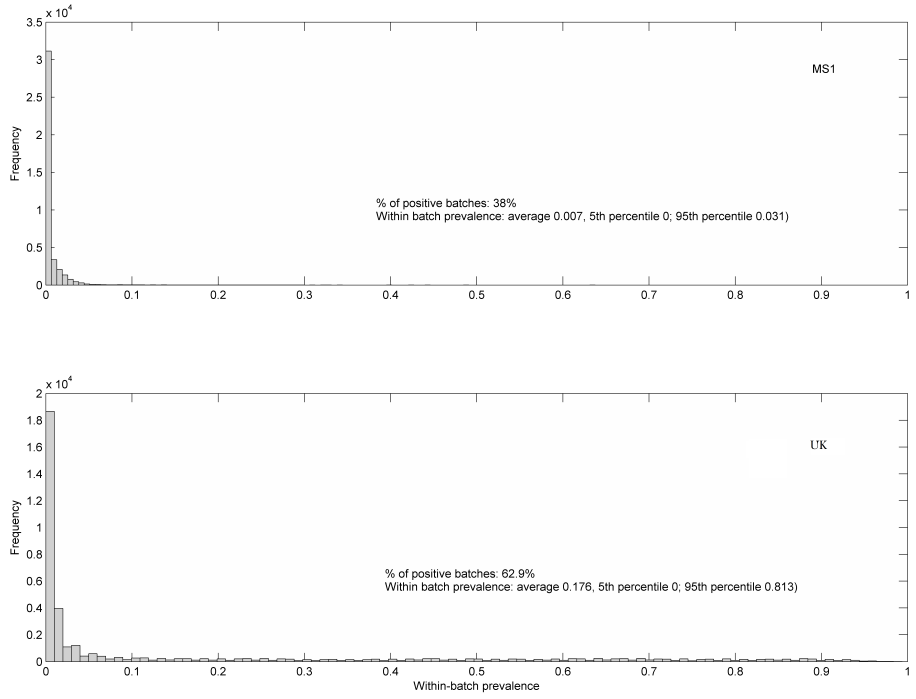

Figure 6.6: Distribution of within-batch prevalence at the point of pigs being loaded onto slaughterhouse transport. The majority of batches are either Salmonella-negative or infected at a low prevalence.

6.3.2 Sensitivity analysis and model interrogation

Sensitivity Analysis

The results of the sensitivity analysis are shown in Figure 6.7. The response

variable is the prevalence of infection within a batch of pigs being sent to slaughter. The notation given to each bar denotes each of the following parameters in the model:

- Sow – average number of Salmonella shed by sows that gave birth to pigs within batch.
- Piglet Weaner, Grower, Finisher – average number of Salmonella shed by piglets, weaners, growers and finisher pigs respectively.
- Wean feed, Grow feed, Fin feed – average number of Salmonella contaminating feed during weaning, growing and finishing periods of the batch.
- Ext cont – average external contamination dose ingested by pigs during rearing period of batch.

For the UK the average load of Salmonella shed by sows is dominant (to the point where the other parameters make little difference). However, for MS1 feed and external contamination parameters are relatively much more important than the load shed by the sows (although ultimately the variability associated with the within-batch prevalence is still largely driven by the average load shed by piglets and weaners within the batch). Further investigation (not shown) supports the results of the sensitivity analysis; if a sow/pig sheds Salmonella the relative contribution of the sow/pig to the dose ingested by susceptible pigs is typically much larger than that contributed by contaminated feed and/or contaminated wildlife faeces.

Source attribution

Figure 6.8 summarises the impact of each source of infection in determining the slaughter pig prevalence within the two case study MSs. Within the UK reducing

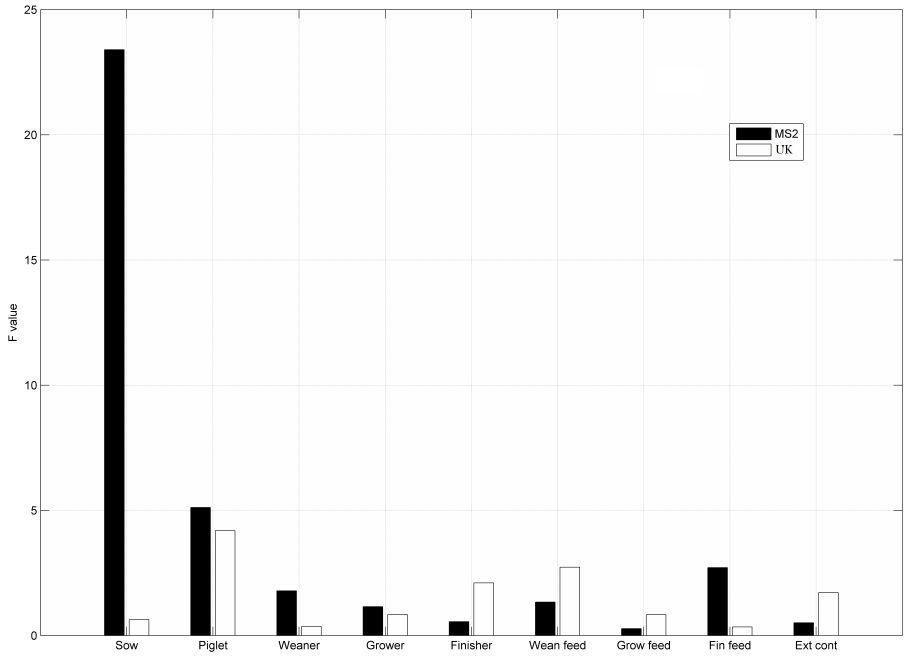

Figure 6.7: Sensitivity analysis for the UK (high prevalence) and MS1 (low prevalence).

breeding herd prevalence to zero (i.e. $p_{herd} = 0$) removes the vast majority of infections at depopulation; conversely, removing feed or external contamination as sources does little to change the national pig prevalence. Again, this result suggests that the sow is a major source of infection; only when sow infection is rare (as in MS1), does feed play an important role in determining slaughter pig prevalence.

The results above overwhelmingly suggest that the breeding herd is a major source of infection for slaughter-age pigs. However, caution must be taken when interpreting this result, especially as it is assumed that the strain of Salmonella infecting the sows is the one which infects the piglets all the way through to slaughter (longitudinal studies suggests a much more complex dynamic of competing strain

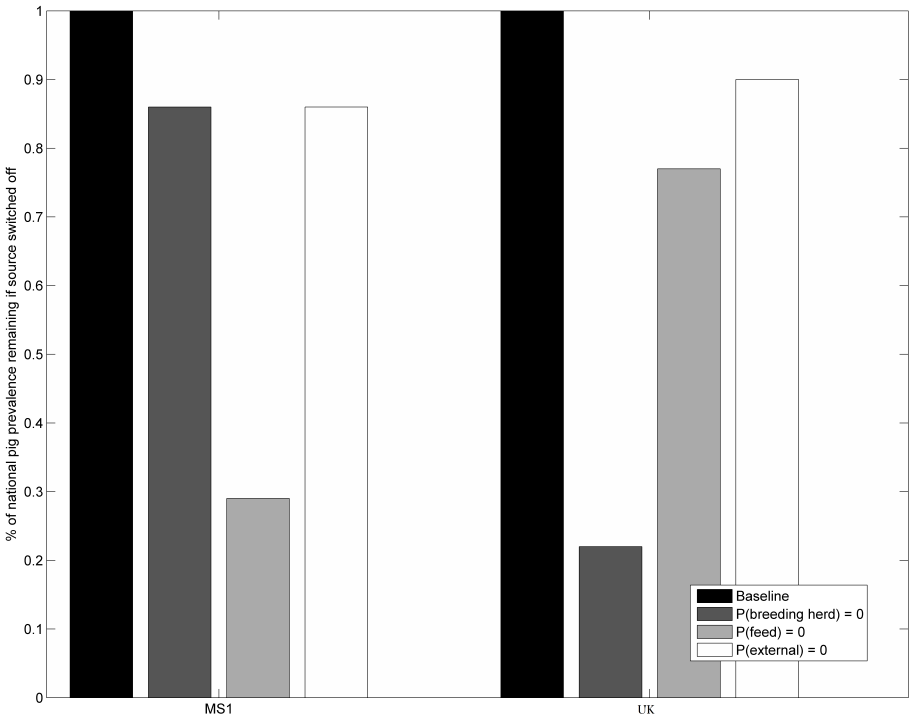

Figure 6.8: Relative impact on national pig prevalence for each MS if each source of infection is set to zero. Baseline (black), breeding herds all negative (dark grey), feed all negative (light grey), no external contamination events (white).

colonisation (Kranker et al., 2003; Jensen et al., 2006)). However, comparison of breeding and slaughter pig prevalence for each MS from the respective EFSA baseline surveys suggests that there is at least some correlation between slaughter and breeding pig prevalence at a MS level (correlation coefficient 0.457) (EFSA, 2008b, 2009a).

Pen contamination rates

The dynamics which produce the distributions of within-batch prevalence as shown in Figure 6.6 were also considered by analysing pen contamination rates and the subsequent Salmonella doses ingested by pigs.

Pen contamination is highly variable, regardless of production stage (farrowing,

weaning, growing or finishing), ranging between $0 - 10^9$ CFUs within a farrowing pen on a single day, and $0 - 10^8$ CFUs in weaning/growing/finishing. Examples of pen contamination for each stage of production are shown in Figures 6.9 and 6.10.

The positive breeding herd has a large effect in increasing the contamination rates within pens at all stages of production relative to negative breeding herds (Figure 6.9). This is because sows shed proportionally more salmonellas than pigs if infected (as they shed more faeces). This means that relatively more piglets are likely to be infected with 'high' doses ($> 10^6$ CFUs), and these piglets will go on to shed significantly more Salmonella into the environment (at all stages of production) than pigs infected at 'low' doses. The consistently higher contamination levels within all stages of production occur because high dose infection is self-sustaining: piglets are initially infected at high doses, and then shed large amounts of Salmonella into the environment across the farrowing and weaning stages, leading to more highly-infected pigs. Hence, while the initially infected piglets may recover sometime around the weaning/growing stage, high-infection transmission can be sustained long after.

It is difficult to validate such results from the literature, primarily because enumeration of pen contamination is rarely done, and because the studies that are available are small, meaning that the rare high levels of contamination are probably missed. However, contamination levels of between $1.8 - 550$ CFUs per 100cm^2 have been isolated from pens in lairage (Boughton et al., 2007). This is within the range commonly estimated by the model given high shedding rates (which might be assumed for pigs during transport and lairage).

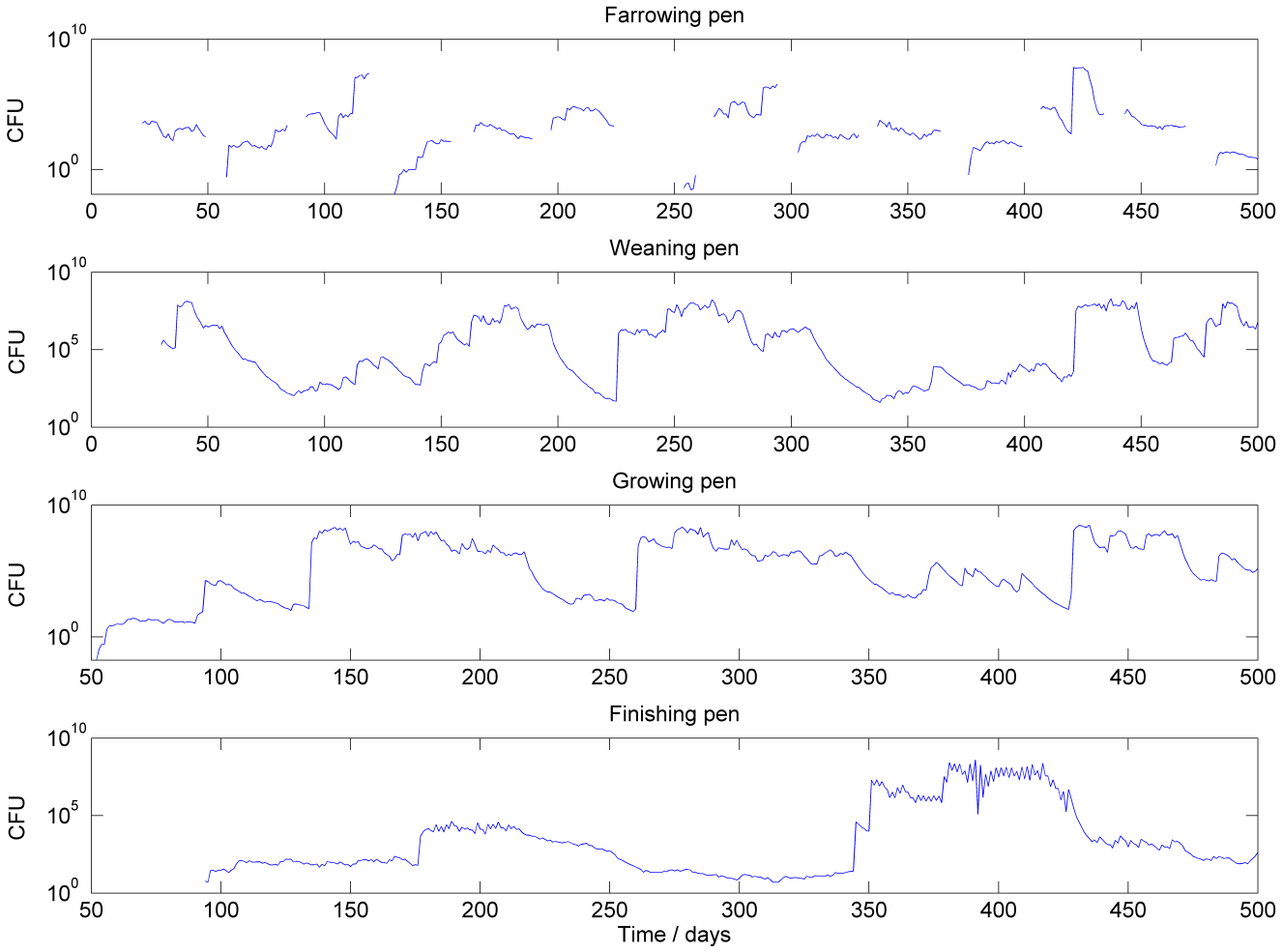

Figure 6.9: Individual pen contamination given positive breeding pig herd profiles over time. Pens are picked to show examples of wide variation only, and are not representative over UK.

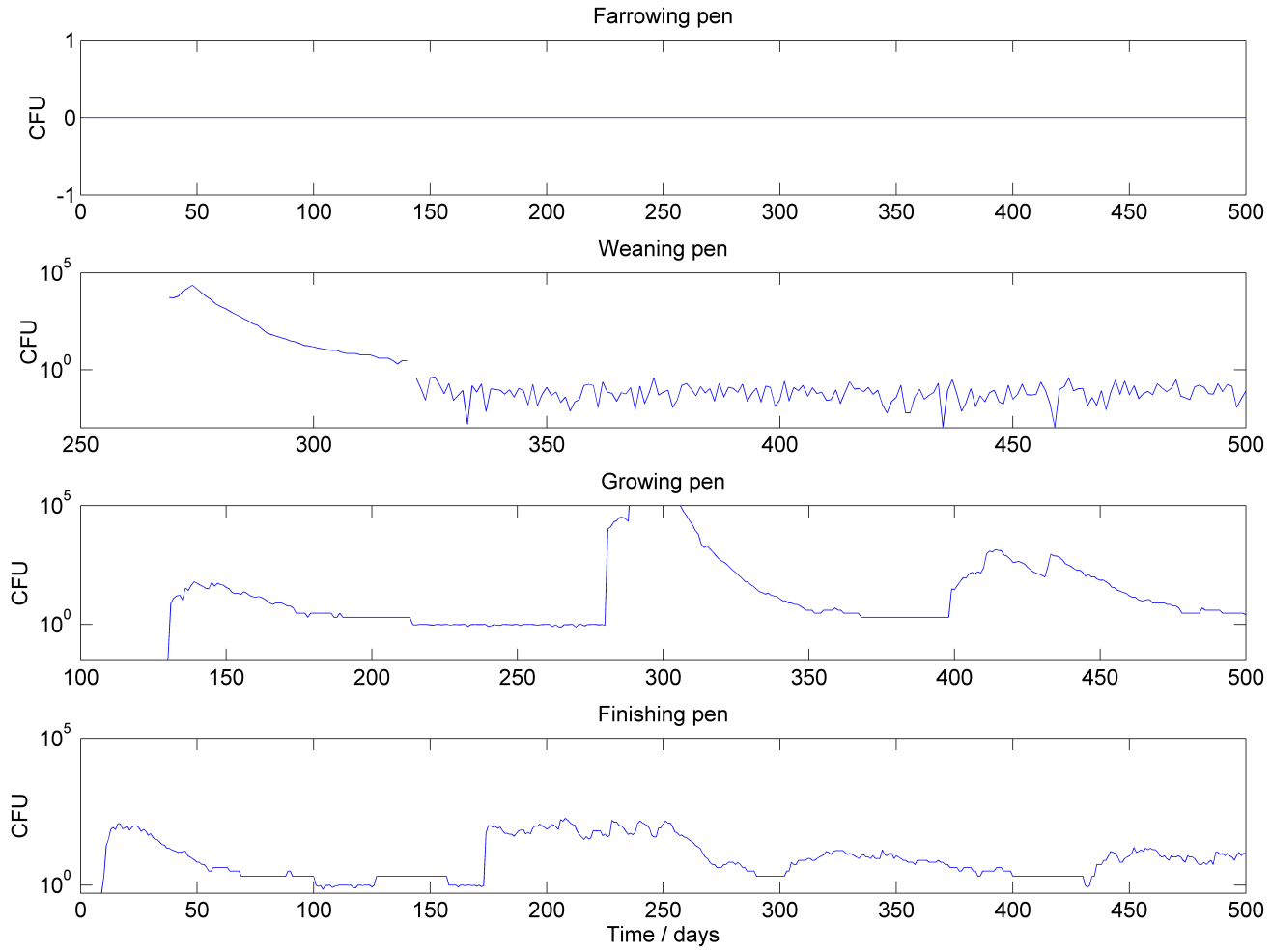

Figure 6.10: Individual pen contamination given negative breeding pig herd profile over time. Pens are picked to show examples of wide variation only, and are not representative over UK.

Doses ingested by pigs

Comparison of the non-zero doses ingested by pigs on infected farms with the average dose-response curve for Salmonella infection is shown for one iteration of the model in Figure 6.11. Infection is, on average, only more likely to occur than not occur (i.e. $p_{inf} > 0.5$) for a very small proportion of exposure events (those above 10^6CFUs). This dynamic corresponds to the results of Figure 6.6, where the vast majority of batches sent to slaughter are infected at a very low prevalence level, despite fairly consistent low-level pen contamination.

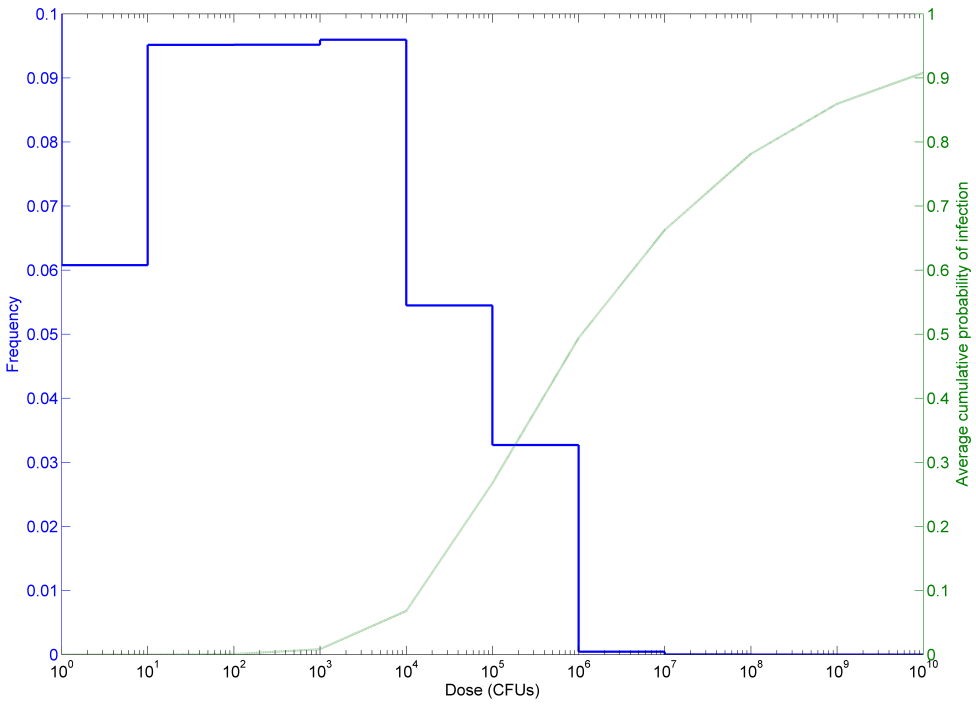

Figure 6.11: Comparison of doses ingested by pigs (from all stages of production) against the average probability of infection (using only non-zero doses from the model). The majority of doses ingested by pigs (from faeces, feed and external contamination) are unlikely to result in infection at the average probability of infection. Note different scales of two y axes.

Farm management influence

A novel aspect of this model is the inclusion of a number of farm types, based on the characteristics of the five main management factors (feed, flooring, production system, inside/outside production, number of sites). Preliminary analysis shows that there are significant confounding factors with the management data (for example within the UK, dry feed was far more common on AIAO farms than on continuous production farms). Therefore, reliable insight can only be generated by observing the results stratified by farm type as a package of management factors (see Figure 6.12). The significant result is that one management factor, the production system (AIAO versus continuous), dominates the risk by farm type. AIAO production reduces risk to approximately one third of that for continuous production. The impact of other management factors is negligible by comparison (or at least is swamped by confounding factors).

6.4 Discussion

The objective of developing this transmission model was to describe the dynamics of Salmonella transmission in pigs in sufficient detail to a) differentiate between the dynamics of infection at a farm and MS level, b) investigate the sources of infection and the link, if any, between the breeding herd and infection at slaughter and c) investigate interventions. The latter objective is discussed in the next chapter 7. In order to meet these objectives the methodology presented in previous chapters has been modified and advanced (including modelling of the environment in much more detail than has been attempted before). Varying management practices have also been considered for the first time in a model of this type. A recent model explicitly included the pig environment, but they did not attempt to differentiate between farm types (Lurette et al., 2008a). In addition, parameterisation of the

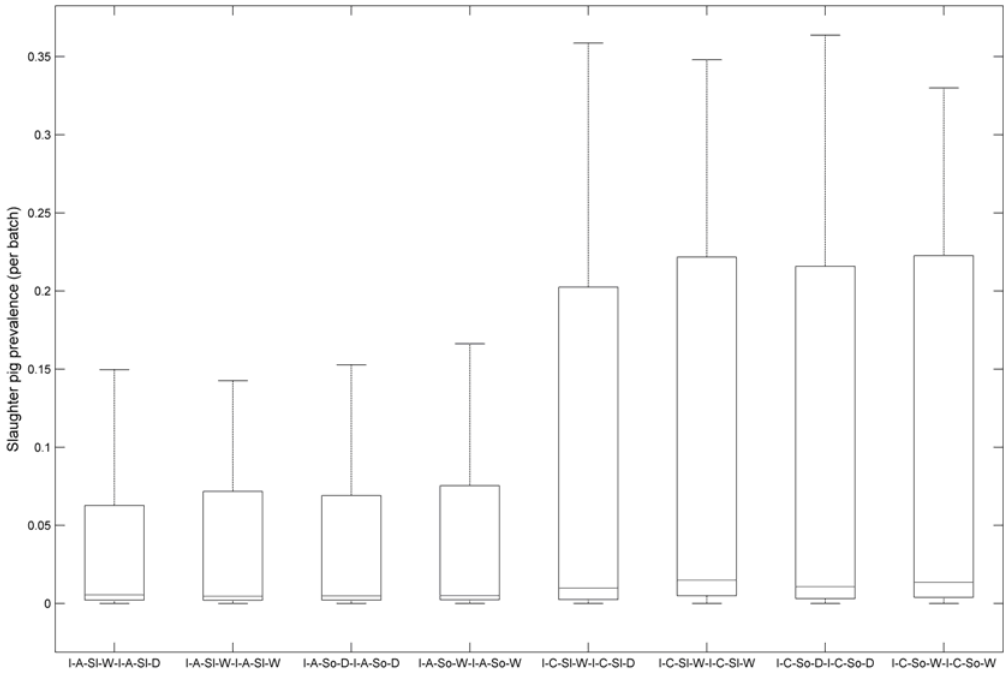

Figure 6.12: Stratification of output (prevalence of within-batch infection) by farm type (for clarity only UK inside breeder-finisher herds shown, however results apply to all types). Key: I — Inside, A — AIAO production, C — Continuous production, So — Solid floor, Sl — Slatted floor, D — Dry feed, W — Wet feed.

model has been improved, especially the dose-response component, including a two-stage shedding component, advancing on that proposed by Soumpasis and Butler (2011).

Exposure to Salmonella, and the response to Salmonella infection in pigs, is incredibly variable, as evidenced by a number of observational and longitudinal studies (Lo Fo Wong and Hald, 2000; Kranker et al., 2003; Jensen et al., 2006). The model reflects this variability, hence contamination of the pen can vary between 10-10^9 organisms over short time periods; such large variation in contamination unsurprisingly leads to large variation in the amount of Salmonella ingested by a pig and subsequently the incidence of Salmonella infection. However, in the

majority of situations contamination of the pig environment will result in exposure at a level insufficient to cause infection. It is only in rare cases, where a sow sheds a high level of Salmonella numbers (or rarer still when feed or the environment is contaminated at a very high level) that a high incidence of infection within a batch is predicted. Accordingly, the results of the model suggest that within-batch prevalence is typically relatively low. It is the relative contribution of highly-infected batches that determine whether a MS has a low or high slaughter pig prevalence. Highly-infected batches t slaughter overwhelmingly originate from farrowing batches where the sow shed a high level of Salmonella. The effect of highly-infected batches is even more heavily weighted given that shedding rates in the model are higher if pigs are infected with doses above 10^6 CFUs, for which doses of this magnitude are much more likely to occur in highly-infected batches originating from a highly infected sow. This is an extremely important result, as it suggests that controlling the shedding rate of sows/pigs may be just as effective at controlling the final slaughter pig prevalence for GB or another MS, if not more so, than reducing prevalence by a significant degree. Interventions, such as vaccination or organic acids, are likely to reduce shedding rates even if infection is not fully prevented.

Management factors applied to each MS are confounded, for example in GB dry feed is more likely to be fed on AIAO farms than continuous ones. Hence, analysis of management factors was only possible at a broader farm type level. This analysis (shown in Figure 6.12) clearly demonstrates that AIAO production is by far the most important risk factor of the management factors considered. Indeed, there were negligible differences between all other farm management factors (for example feed, flooring). It must be pointed out that the AIAO production system assumed in the model is a theoretical description unlikely to be achieved in reality on all but

the most strict systems of AIAO production. Of note is that it was not so much that cleaning and disinfection that makes AIAO farms less of a risk, but rather the strict segregation of pigs minimising the opportunity for spread of infection between concurrent cohorts.

Piglets are able to become infected while still suckling from their mother, although the evidence is mixed for whether (sero-) positive pigs make the progeny more or less likely to be infected at the point of weaning (Lo Fo Wong and Hald, 2000; Nollet et al., 2005). Within these studies there is the indication that infection in piglets could be under-estimated because of a high likelihood of false negatives. Indeed, the studies referenced were relatively small given the number of animals followed; there is certainly the probability they simply didn't sample any highly-infected piglet groups because these are relatively rare. However, the broad consensus from these studies is that it is not until weaning (when piglets are faced with the double stresses of being weaned and mixed with other unfamiliar pigs) that a significant proportion of pigs may become infected with Salmonella. Comparing the model and these findings, the broad trends are certainly the same as observed in these studies. Infection in piglets is rare and usually at a low incidence rate. While stress/feed change during weaning is not modelled, pigs are mixed together. The larger amount of Salmonella shed by weaners relative to piglets, and the fact there are more pigs directly exposed to this Salmonella, means that the peak prevalence of infection is usually observed during the weaning period. There is generally a diminishing prevalence of infection at the point of slaughter. This agrees with most current observational data (Kranker et al., 2003; VLA, 2009).

While the model mathematically describes more variability than most equivalent models, not all factors that describe variability in Salmonella risk in individual slaughter pigs between farms or between MSs have been included. Indeed, the

variability included is limited to the data available for quantitative modelling. For example, most management factors have been split into dichotomous options: wet/dry feed, solid/slatted flooring, AIAO/continuous production. However, in reality the options available for each factor are multiple and complex. The following potentially important factors have not been included in the farm model: further differentiation between feed types (for example pelleted versus non-pelleted), clustering of Salmonella in faeces, varying growth rate (such that pigs are held back in production), and transmission dynamics between sows. Further differentiation between feed types would have been difficult to parameterise, but could potentially be important. However the difference in risk between wet/dry feed was assessed to be the largest of all potential feed type combinations, and this difference in risk was negligible when compared to the difference in risk between AIAO and continuous production. Clustering of Salmonella in faecal material has been modelled before (Arnold and Cook, 2009), but would also require a more complex model. The effect of clustering in faeces would be to vary (even more so) the daily exposure of pigs to Salmonella, where some pigs would ingest considerably more organisms than currently modelled, and some considerably less. The vast majority of pigs ingest no Salmonella, but there is a relatively broad distribution of the numbers ingested given exposure occurs. Further variability would probably mean that most farms would be infected at very very low levels, but the remaining high-prevalence farms would be infected at even higher levels. The slaughter pig prevalence would not change significantly, but we would probably expect to see average shedding rates go up as more pigs would ingest higher levels of Salmonella, creating mre "high-dose" pigs. The implications for public health would probably be that less people would be exposed, but those who are exposed may face higher concentrations. The overall risk assessment model developed for EFSA could be used to

investigate the effect of different levels of clustering on salughter pig prevalence and human health. Over the large number of pigs and timesteps used in the current model, it can be hypothesised that the effect of this clustering averages out, but this cannot be stated with certainty. An important simplifying assumption is that all pigs born into the same cohort will be slaughtered at the same time. In reality, a varying growth rate of individual pigs means pigs may need to be kept back behind their cohort before reaching the correct weight to be moved into a different stage of production or sent to slaughter. This has not been included because of the difficulty in including any variation in pig group size (computationally pig cohorts are represented as matrices, and matrix manipulation is only possible with identical or compatible matrices). Keeping certain pigs back and allowing more mixing between cohorts would almost certainly increase the spread of infection within the model, as the allowance for contact between cohorts in continuous production systems within the model is one of the greatest upward pressures on prevalence for the prevalence of infection in slaughter pigs. Also, there may well be correlation between high shedding levels and being kept back as a result of poor condition due to heavy Salmonella infection, which could also mean any spread was greater than average transmission.

Important data gaps highlighted by the model development were the (variation in) dose-response of pigs to infection, the movement of faecal material and the amount of Salmonella that might be present in the environment due to feed or other external sources of contamination (rodents, birds etc). However, for all information gathered for this model, the trend was that regardless of the type of data needed, it was unlikely that current observational, experimental, longitudinal or survey data would be sufficient to be confident that all the variability had been accurately captured (for example the amount of Salmonella shed by a sow is based

on one study that shows high variation between pigs – but did the study capture the entire range of variation?). Hence, as with all models, the results produced must be viewed in conjunction with the simplifying assumptions made, which were necessary both because of the need to reduce the complexity of a highly variable pig production system across the EU and the data gaps that result because of this complex system.

It is difficult to quantitatively validate the current farm transmission model, as quantitative data are scarce. However, qualitatively the farm transmission model appears to agree well with observed data, and replicates a number of important trends observed in the field (for example the relationship between breeding herd prevalence and MS-level slaughter pig prevalence, peaks and troughs in prevalence at meaning and finishing, extremely variable nature of infection, and the difference between AIAO and continuous production). The results of this model, combined with a Transport & Lairage model for slaughter pigs, were well-validated for three of four case study MSs modelled, using lymph node prevalence data from the EFSA slaughter pig baseline survey (EFSA, 2008b; Simons et al., prep). In summary, given the need to balance potentially myriad risk factors against the need for a parsimonious model that uses reliable data, we are of the opinion that the model provides a useful summary of the variation that is sufficient to describe the relative importance of different risk factors between farms and MSs and provides a strong platform for investigating on-farm interventions.

Analysis of the model pointed to one overwhelming conclusion: the level of infection within a MS's breeding herd largely determines the slaughter pig prevalence for that MS. The analysis showed that if the sow is infected and shedding at high levels, then commonly (although not always) this will mean one or more piglets will become infected: when this occurs then the shedding of Salmonella by infected

pigs, at the farrowing stage or later, dominates the risk (as once a slaughter pig is infected, the subsequent shedding of Salmonella more than outweighs the contribution of contamination within the environment provided by feed and/or the external environment). Such a phenomenon is also hypothesised as a major risk factor for cattle 'super-shedding' VTEC O157 (Pearce et al., 2004; Arthur et al., 2009). However, in low prevalence MSs of which MS1 is typical, infection of the sow is relatively rare (such that it is unlikely that a 'super-shedder' sow will occur in the 500 days of production modelled) and the proportion of initial infections of a piglet, weaner etc... via either feed or external contamination are relatively much higher. This result of breeding herd prevalence determining slaughter pig prevalence is supported by data from the EFSA Salmonella in pig surveys; breeding herd prevalence was correlated, at least to some degree, with slaughter pig prevalence (EFSA, 2008b, 2009a). Incoming infected pigs are also considered to be a primary source of infection for weaning and finishing houses (EFSA, 2006). In summary, breeding herd prevalence is likely to be a strong predictor of national pig prevalence and feed only becomes an important source of infection once contamination of the environment by sows or other slaughter pigs is reduced to low levels.

A more extensive discussion of the role of the sow as a source of infection is given in an accompanying paper (Hill et al., prepa). Briefly, the extent of the role of the sow as a source of infection for slaughter pigs is uncertain, although longitudinal studies do suggest that sows are commonly infected with the same strain of Salmonella as piglets/weaners within the same cohort (Nollet et al., 2005; VLA, prep). The dynamics of infection are complicated by the presence of multiple strains on farms causing intermittent infections, which is inadequately captured by insensitive sampling methods. Evidence also exists for strains persisting in the

weaning/finishing herd environment, which exposes susceptible pigs to challenge long after they have been weaned; this type of persistent infection of farms is not well captured in the current model due to a lack of data on the environmental load. To summarise, the model results suggest that intervening at the breeding herd is a necessity if slaughter pig prevalence is to be reduced substantially. However, further studies on the link between sow infection/environmental contamination and slaughter pig infection is required to firmly establish the links that exist at a farm and MS level. In addition, the same issue of poor quality of intervention study applies to sows/piglets as much as it does to finishing pigs, indeed more so.

The above result also indicates an important factor that is commonly missed by most, if not all, observational studies, and that is the importance of the magnitude of shedding from indivudal pigs. Most studies simply record the presence/absence of Salmonella in various sample types (faeces, lymh nodes, tonsils etc. . .); however, the relative burden of Salmonella in the environment will be strongly correlated with high-shedding sows/pigs, and the experimental results of Jensen et al. (2006) seem to confirm this. Using data from this study as an example, then most pigs will shed up to 100 CFU/g faeces. If there is one pig shedding 10,000 CFU/g faeces, then that pig contributes as much Salmonella to the environment as 100 low-shedding pigs. It is therefore clear that recording prevalence alone is insufficient to capture the dynamics of Salmonella infection.

The model described in this chapter is farm more complex than even the stochastic cross-contamination model of the last chapter. It includes sources of infection, all stages of the rearing process, 56 different farm types, and a detailed environmental contamination model. These additions, while requiring significant development time, have added much to the realism of Salmonella in pig models, both in this thesis and in the wider scientific literature. Capturing the wide variation in the

shedding rates of sows and pigs is probably the biggest crucial step forward, as it allows the model to replicate the wide distribution of within-batch prevalence observed in the literature. Indeed, the level of sow shedding is the key parameter of the model, being the major determinant of final slaughter pig prevalence.

The steady state level of infection in pens observed in previous models is almost non-existent in this model; the variation in the magnitude of contaminated faecal shedding interrupts the progression to the steady state. However, the simple dynamics of the previous models captured the main dynamics of this model: that once infection is introduced, it is likely to sustain itself among pigs (albeit at a much lower incidence than was observed in the standard SIRS model), and that the introduction of a new infected batch of pigs is much more likely to lead to infection than between-pen transmission, because of the speed of the travelling wave.

Chapter 7

Analysis of intervention mechanisms in reducing Salmonella in slaughter-age pigs

7.1 Introduction

In this chapter we discuss the use of the final farm transmission model, described in Chapter 6, to assess potential intervention mechanisms for reducing the prevalence of lymh-node infection in slaughter-age pigs. The assessment of interventions is one of the primary aims for the development of this model and thesis. The majority of intervention results presented in this chapter are similar to those originally presented in the EFSA QMRA report (Hill et al., prepb), where the effect of on-farm interventions was investigated to predict the effect on the risk of human illness as well as the prevalence of infection in slaughter pigs. The results presented in this chapter are a mixture of those results relevant from the original QMRA,

as well as further investigations to assess the effect of on-farm interventions in more detail. While in this chapter we only explicitly describe the effect of on-farm interventions on the prevalence of infection in slaughter-age pigs, the results are indicative of reductions in human cases as well, as for GB there was a high correlation between national slaughter pig prevalence and the predicted number of human cases attributable to domestic pig meat consumption (Hill et al., prepb).

7.2 Modification of farm transmission model to investigate interventions

7.2.1 Interventions investigated

In concord with the EU and the EFSA Working Group on Salmonella in Pigs the EFSA QMRA consortium priortisied the following specific on-farm interventions: reduction of feed contamination, reducing the number of suppliers to contract finishing farms, improved hygiene/biosecurity and finally interventions for decreasing the pig's susceptibility to infection (e.g. vaccination, use of wet/fermented feed, organic acids). As highlighted by reviews of Salmonella interventions in pigs (O'Connor et al., 2008; Denagamage et al., 2007; Wales et al., 2010) there is a distinct lack of reliable quantiative data to assess the effect of at least three of the main on-farm interventions, i.e. vaccination, feed modifications and feed additives. A literature search carried out as part of the EFSA QMRA intervention analysis (Hill et al., prepb) identified few studies relevant for the quantiative assessment of biosecurity/hygiene control measures, and those which were identified tended to contradict each other. It was therefore concluded that while the EFSA farm

model is capable of assessing specific interventions such as vaccination, organic acids etc..., currently there are not enough quantitative data to assess specific interventions with any confidence.

Hence, in the EFSA QMRA report and this thesis it is has been decided to use the farm model described in Chapter 6 to assess the broad *mechanisms* of intervention. These broad mechanisms of intervention include the reduction of Salmonella infection in the sows (which the analysis of the farm model in Chapter 6 suggested was a major driver in the eventual national slaughter pig prevalence of infection), the reduction/removal of Salmonella from the pen environment, and finally the decrease in susceptibility of pigs to Salmonella infection. These broad mechanisms of intervention can be modelled by re-parameterising key parameters of the model (for example modifying the dose-response relationship parameters to signify an increase in the protective effect of the immune response to Salmonella infection). The interventions investigated and the modifications to the baseline model described in Chapter 6 are described in Table 7.1.

In addition, in order to implement any of the interventions, two critical factors were assumed: that uptake of each intervention is 100% across all farms across a MS; and that all farmers rigorously implement interventions in such a way as to consistently produce the effect desired.

The results of the farm model in Chapter 6 suggest that national breeding herd prevalence is a dominant factor in determining national slaughter pig prevalence (i.e. low breeding herd prevalence leads to low slaughter pig prevalence, and vice versa). Hence, breeding herd interventions would seem to provide potential for reductions in slaughter pig prevalence. However, as for all pig herds, quantitative data are severely lacking to assess interventions at the breeding herd. We therefore

Table 7.1: Interventions investigated within the analysis.

Intervention	**Baseline parameter estimate(s)**	**Intervention analysis parameter estimates**
Reduce breeding herd prevalence, p_{herd}	0.44	p_{herd} = {0,0.01,0.05,0.1,0.2,0.3,0.4,0.5}
Reduce probability of feed batch contamination	0.10	Set p_{feed} = {0.01,0.03,0.07,0.1}.
Increased resistance of pigs to Salmonella infection by using e.g. wet feed, vaccination or organic acids	α_{DR} = 0.1766; β_{DR} = 50235 (wet feed) or 20235 (dry feed)	β_{DR} modified to 200,235 for 1-log increase in dose response and 2,000,235 for 2-log increase for both dry and wet feed farm types.
Increased effectiveness of cleaning and disinfection (C&D)	Cleaning at depopulation removes a fraction p_{clean} of contamination in pen j: p_{clean} = Beta(3,2) or Beta(1,2) for solid or slatted flooring respectively.	p_{clean} modified to Beta(3,50) for 1-log decontamination and Beta(3,500) for 2-log reduction.
Reduce magnitude of shedding by 1 or 2 logs by infected sows	Lognormal (2.36, 4.39)	1 log: Lognormal(1.36,3.39); 2 log: Lognormal(0.36,2.39).
Cap magnitude of pig faecal shedding	c_p varies between 0-10^8 CFU/g faeces	Excess probabilities associated with shedding greater than 4 log CFU/g faeces transferred to probability of shedding 4 log CFU (such that the probability of shedding between 0 and 4 log CFU/g is 1).

assessed a hypothetical range of percentage reductions in the breeding herd prevalence, p_{herd}. The range of values modelled (0-50%) was chosen to reflect the range of breeding herd prevalence recorded across the EU in the breeding pig holding survey by EFSA (EFSA, 2009a).

There are no national data to suggest how prevalence of feedlot contamination (i.e. the percentage of feed batches that are contaminated with Salmonella) might be reduced. Hypothetical changes in the prevalence of feedlot contamination, p_{feed}, rather than hypothetical changes in the numbers of Salmonella present in contaminated feed, were investigated, as the concentration in contaminated feed has been shown to be relatively low when investigated (O'Connor et al., 2008; Sauli et al., 2005). The range of values chosen reflect data that suggests prevalence commonly varies between 1% and 10% (EFSA, 2009b), but also modelling (Cannon and Nicholls, 2002) that suggests prevalence is highly likely to be markedly underestimated using current sampling schemes.

There are three ways to incorporate an improvement in biosecurity or hygiene. First, the efficiency of cleaning and disinfection (C&D) (between batches) in removing Salmonella can be increased. Second, the inclusion of downtime between batches of weaning, growing and finishing pigs (in the same way as for farrowing groups described in Chapter 6) may reduce contamination of the pig pen environment before the repopulation of the pen. Finally, external contamination (e.g. infected rodents, birds) can be prevented from entering the farm. As external contamination (via rodent/bird faeces contamination) was both predicted to be of little importance in the analysis of the farm model (6) and expensive to implement (Monterio Souza et al., prep) no further investigation of biosecurity barriers was carried out in the intervention analysis.

There are qualitative data that do suggest that cleaning can have a positive effect in reducing Salmonella levels within a pen (VLA, 2009). However, there are little data to quantitatively estimate the differences in Salmonella levels before and after C&D. A British experimental study that investigated improvements to standard C&D routines for red meat lairage pens suggested that an extra reduction of 1-2 logs could be achieved over and above typical C&D routines (Small et al., 2007). We therefore increased the baseline model reductions achieved by cleaning by an extra 1 or 2 logs (see Table 7.1). It was assumed that the main mechanism by which downtime achieves a reduction in Salmonella contamination is by the drying out of the pen, which reduces the number of Salmonella in the pen environment that are available for carry-over of infection. Assuming that any reduction achieved by drying is independent of any C&D routines applied then a 4 and 7 day downtime between restocking of pens would achieve an additional 0.16 or 0.28 log reduction in contamination of a pen before restocking (see Table 7.1).

Systematic reviews of vaccination (Denagamage et al., 2007) and pH/moisture content of feed (O'Connor et al., 2008) concluded that there are few studies that are of the relevant quality for assessing the effect of either in reducing Salmonella levels in market age pigs. The overall conclusion from the former systematic review was that there does appear to be a positive effect of vaccination in reducing Salmonella prevalence in pigs, and O'Connor et al. (2008) made a low-confidence assessment that wet feed and acidified feed were effective in reducing Salmonella prevalence relative to dry and non-acidified feed respectively. Recent studies on organic acids, not included in the systematic review, are also inconclusive on the effect of organic acids in reducing Salmonella in pigs at slaughter (VLA, 2009; Wales et al., 2010). Similar conclusions can also be drawn for non-pelleted feed (O'Connor et al., 2008), where evidence does exist for a positive effect, but little data are available to

conclusively prove and enumerate such an effect.

From the above evidence, it was not possible to quantitatively assess the effect these interventions might have on prevalence/shedding magnitude in slaughter pigs. However, vaccination, feed and organic acids can all be considered interventions that increase the resistance of the pig to infection. Vaccination boosts the immune response to infection, while introduction of organic acids and wet feed can be considered to alter the gut ecology/microbiology such that Salmonella do not survive and multiply as easily within the digestive system (hence reducing the potential for infection). Given that the quantitative effects of each mechanism are not known, it was assumed that the qualitative effect is the same - it takes more Salmonella to reach the equivalent baseline probability of pig infection. The dose response model parameters are adjusted until there is roughly a 1 or 2 log increase in the average dose needed to cause the same probability of infection (see Table 7.1). See Figure 7.1 for the effect on the dose-response model.

An important point missing from the vast majority of studies in the literature is the effect of these interventions on microbial numbers in the faeces. Given the current dynamics of infection for both pigs and humans modelled in the QMRA model (Snary et al., prep), which suggest that a consistent 2-log reduction in contamination levels of carcasses would decrease human illness by over 90%, then this mode of reduction (if successful in reducing the magnitude of shedding across all pigs) may provide better results than trying to reduce the prevalence of Salmonella infection in pigs. Analysis of the EFSA QMRA model shows that it is infected faeces leaking onto the exterior of a carcass during processing that contributes most of the risk to human infection (Snary et al., prep). At least one study has shown that there is a reduction in the contamination levels of faecal material from vaccinated sows of around 1-2 logs (Hur et al., 2010). Another study suggested

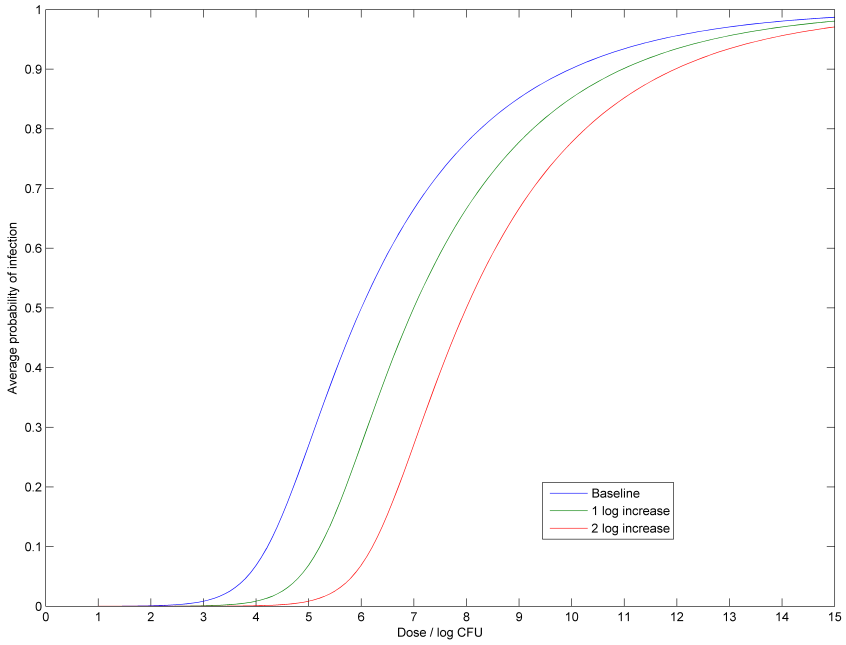

Figure 7.1: Modification of the dose-response model. The dose-response parameter β_{DR} was adjusted until it would take a dose of approximately 1 or 2 logs extra to elicit the same average probability of infection in a pig.

that organic acids capped the magnitude of faecal shedding (Hur and Lee, 2011). Hence, we investigated a) a hypothetical reduction of 1 and 2 logs in the magnitude of shedding of infected sows to replicate this type of intervention mechanism and b) a cap of 10^4 CFU/g faeces produced in pigs beyond the age of weaning due to feeding of organic acids (see Table 7.1).

7.3 Results

The effect of reducing breeding herd prevalence on the slaughter pig prevalence is shown in Figure 7.2. For the UK, which has a high baseline slaughter pig prevalence, there is a strong proportional relationship between reduction in slaughter pig prevalence and reduction in the number of cases. The relationship for MS1 is

not as strongly proportional, but there is a definite downward trend in cases as slaughter pig prevalence is reduced. Breeding herd prevalence has already been established as a significant factor within the farm model, via sensitivity analysis (Hill et al., prepa). Broadly speaking, low breeding herd prevalence (low number of positive sows $\sim$ low number of positive piglets) equates to low slaughter pig prevalence and vice versa. This intervention analysis produces a similar result.

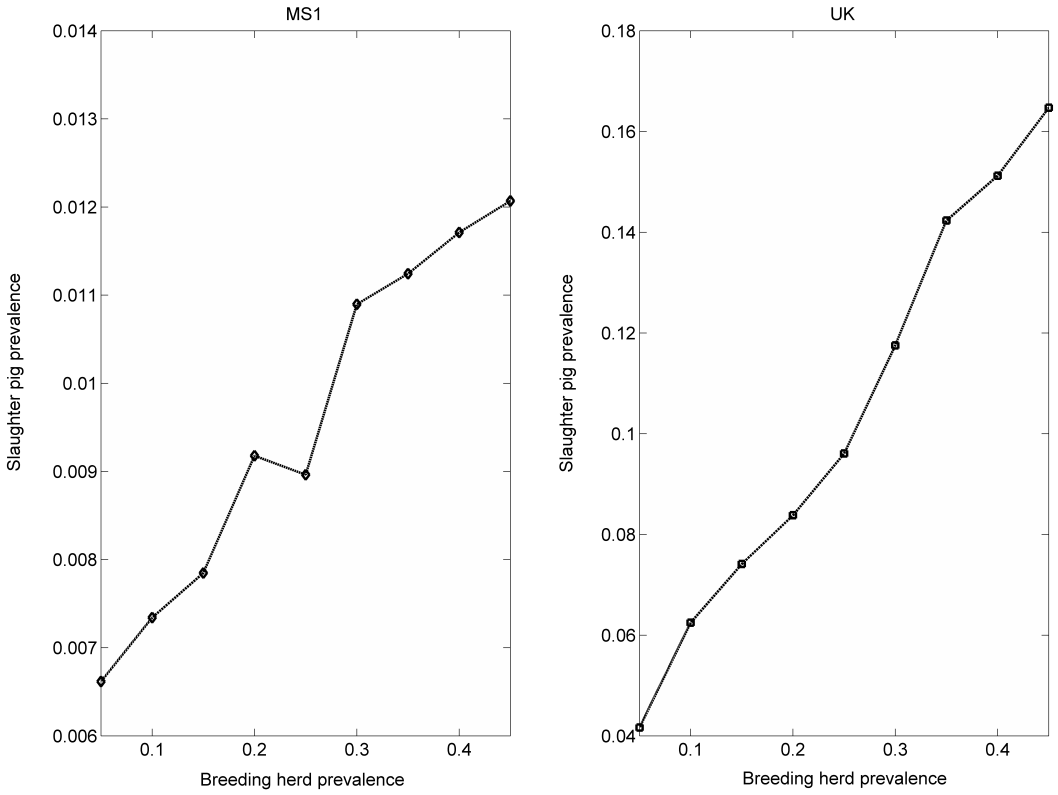

Figure 7.2: Relationship between breeding herd prevalence and slaughter pig prevalence for low-prevalence MS1 and high-prevalence MS UK.

The effect of varying feed contamination within MS1 and the UK is shown in Figure 7.3. The result supports the farm model analysis in Chapter 6, where feed contamination made little impact as a source of infection in the UK (shown here by the minimal rise in slaughter pig prevalence over a 10% point range in

feed contamination prevalence), but showed it to be a major source of infection for a low-prevalence country such as MS1 (shown here having a marked effect in increasing slaughter pig prevalence).

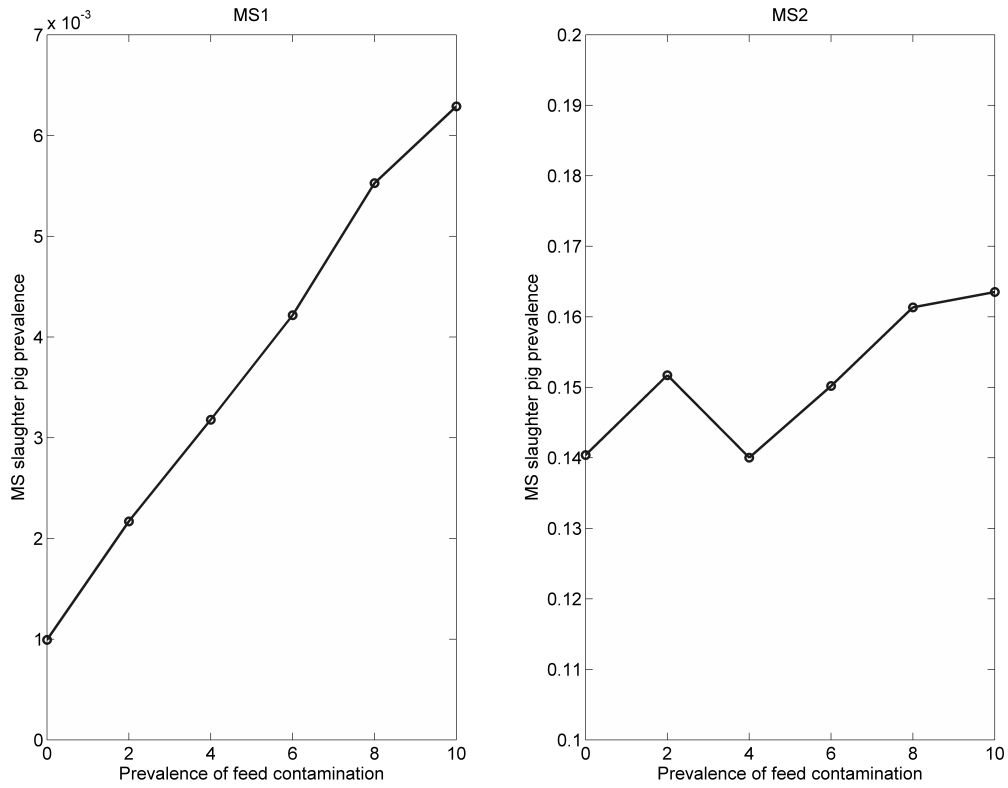

Figure 7.3: The effect on MS slaughter pig prevalence by varying the prevalence of feed contamination.

While the mechanisms for removing Salmonella are different for downtime and cleaning, the effect is similar a reduction in the Salmonella levels present in a pen at the point where a new batch of pigs enters the pen. However, on average, neither the implementation of improved C&D routines or downtime across all farms within a MS significantly reduced the slaughter pig prevalence relative to the baseline model. Within the model, the resistance of the pig to infection is governed by the probability of infection given ingestion of a particular dose. Modifying the

dose-response relationship for ALL pigs at ALL stages of production across a MS produces over a 90% reduction in slaughter pig prevalence given a 1-log increase in dose to produce the same average probability of infection as the baseline model produces.

The effect of reducing the magnitude of contaminated faecal shedding in sows and pigs is substantial, reducing UK slaughter pig prevalence by 33% and 70% given a 1 or 2 log reduction in the magnitude of sow shedding of Salmonella respectively (see Figure 7.4). A cap on the magnitude of faecal shedding, to 4 log CFU/g faeces in pigs in the weaning, growing and finishing stages produced a 70% reduction in slaughter pig prevalence, similar to a 2 log reduction in sow shedding rates.

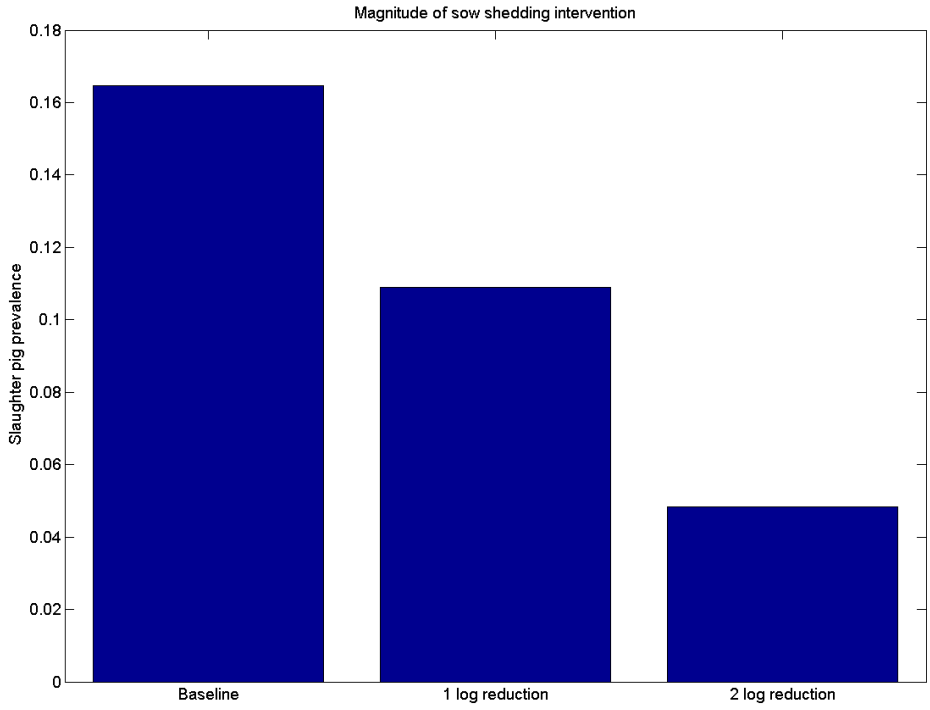

Figure 7.4: Effect of reducing the magnitude of Salmonella shedding by sows by an average of 1 or 2 logs, using UK model.

7.4 Discussion

The baseline model described in Chapter 6 has been modified in order to investigate the relative effect of interventions in reducing slaughter pig prevalence and the distribution of the magnitude of shedding for infected pigs at slaughter-age. There are limited data to quantitatively assess the impact of relevant interventions such as vaccination, organic acids or feed measures, hence we investigated hypothetical changes in the mechanisms of interventions (e.g. reducing the amount of environmental Salmonella contamination that would remain in the pig pen environment after improved C&D procedures).

Given the results of Chapter 6 we should expect that UK slaughter pig prevalence to be strongly correlated with breeding herd prevalence, but for there to be only a small correlation with feed contamination. The results of the hypothetical reductions in breeding herd prevalence and feed contamination prevalence show precisely this effect, again confirming that the model dynamics suggest targeting the breeding herd first and foremost.

Neither of the biosecurity measures investigated, C&D and downtime, produced any visible reduction in slaughter pig prevalence. This is a logical result from the model, given that in Chapter 6 we showed that the majority of infected pigs originated from batches with "super-shedding" pigs, hence the role of environmental contamination in the infection of susceptible pigs was negligible compared to the role of direct contaminated faecal shedding by pigs in the same pen.

Only two of the the on-farm intervention mechanisms investigated produced a visible reduction in slaughter pig prevalence. The first was by reducing the susceptibility of the pig to infection, where modification of the dose-response curve

(such that it takes 1-2 logs extra to produce a similar probability of infection as for the baseline curve) produces a significant effect in reducing slaughter pig prevalence. The effect modelled is by a constant modification of the dose-response relationship, and hence current intervention trials, where the application of organic acids or vaccination is applied only over limited time frames, are unlikely to achieve similar reductions in slaughter pig prevalence.

The second effective on-farm intervention was reducing/capping the level of faecal shedding, which produced a marked reduction in slaughter pig prevalence. Therefore, more promising interventions may be changing feed type (as this can be applied over weaning-finishing) and/or applying organic acids over the whole course of production. However, several systematic reviews have noted that there is not enough evidence to state with any confidence the likely effect of these interventions if universally adopted by pig industries across a MS (Denagamage et al., 2007; O'Connor et al., 2008; Friendship et al., 2009). Reducing feed contamination is only likely to have a measurable effect on slaughter pig prevalence when the transmission of Salmonella from pig to pig has been brought to a low level. As for all interventions modelled here, the magnitude of effect that can be achieved in reality is very uncertain, given that it is not known what the prevalence or contamination levels of feed are across the EU.

Of interest is the results of reducing the magnitude of faecal shedding. An intervention needn't directly be targeted at completely preventing infection, as all of the ones above are. Indeed, interventions such as vaccination and organic acids may be more effective in the mechanism of simply reducing the level of Salmonella shedding that occurs, rather than the rather limited effects of preventing infection completely seen in some studies. The results presented in this thesis are highly speculative, as there are literally a few studies that investigate the effect of in-

terventions on the magnitude of faecal shedding (Hur et al., 2010; Hur and Lee, 2011). However, as has been shown by Loynachan and Harris (2005) Salmonella infection in pigs is dose-dependent, and so reducing the level of contamination in the environment below that necessary to infect pigs would appear to be a suitable intervention. Previous results in Chapter 6 suggest that the environmental contamination level of Salmonella on the farm through feed or rodent/bird contamination is unlikely to result in pig infection very often, and most of the contamination of the farm comes from pigs themselves.

The assessment of contamination level in such detail as described in Chapter 6 was undertaken as by the rationale of dose-dependency it is logical that understanding the doses to which pigs are exposed is important for accurate modelling of transmission dynamics. However, it may have been unnnecessary if it had been that pigs were susceptible to a wide range of doses at a similar probability. The results shown here in the last chapter and this chapter show that modelling the environment, and having a confident assessment of the level of Salmonella pigs are exposed to is important, for understanding transmission and for identifying effective interventions. There is no way to reliably validate these findings at the present time, as we have yet to identify a sufficiently large study that has tracked contamination levels or the doses to which pigs are exposed.

Chapter 8

Discussion & Conclusions

8.1 Introduction

The main aim of research into Salmonella in pigs is to prevent human infection via consumption of pig meat. Several country-level programmes have been put in place to reduce Salmonella in pigs, although the results have been less favourable than expected (Nielsen et al., 2001; BPEx, 2009; Blaha, 2004). The EU is also required to take action on the most important foodborne pathogens, and Salmonella in pig meat is seen as one of the main food/pathogen pairs to address. As such, EU MSs will be expected to implement National Control Plans to reduce the prevalence of Salmonella infection in pigs at slaughter. This course of action has been controversial, as the pig industry would prefer to take action in the abattoir where (perceived) more reliable interventions can be brought to bear to reach a MS target [1].

[1]Certainly in the short term there appear to be much more consistent interventions available at the abattoir; as a review of intervention studies in this thesis highlighted, much more research is needed to produce consistent effects for on-farm interventions such as organic acids or the modification of feeding regimes.

It is difficult for researchers to conduct a large enough study, and control all possible variables, to assess meaningfully the introduction/transmission of Salmonella between pigs, or to assess the effect of on-farm interventions in reducing slaughter pig prevalence. Indeed, at the current time, it is still not known with any certainty the contribution to slaughter pig prevalence originating from sources of infection such as feed and new stock, and there are no consistently proven interventions available for pig farmers to use. Hence, mathematical modelling of transmission and intervention can play a vital role in elucidating key factors for the introduction and transmission of Salmonella between pigs, and the eventual infection status of pigs when they are slaughtered.

With this in mind, this thesis aimed to build upon previous models used to assist the development of Salmonella in pig control policies in several countries (including the UK), in order to assess the major driving factors behind introduction/transmission in British pigs, and to indicate intervention measures that may be useful as part of a future UK NCP.

8.2 Main results

Chapters 2, 3 and 4 deal with deterministic forms of a typical grower-finisher herd model. The 1 and 2 pen models served as a foundation on which to build the more complicated multi-pen and cross-contamination models. However, the dynamics of infection in all of these models was similar. With current parameter estimation, infection was self-sustaining in pen populations across the models, whether there were 1 or 300 pens. Stability analysis of each of the models suggested that the homogeneous infected steady state would be the result of at least one infected pig entering the herd. Travelling wave analysis of the multi-pen models suggested that

the speed of transmission between pens, via faecal-oral transmission, was relatively slow, such that infection would probably be limited to a few pens by the time pigs were sent to slaughter.

The deterministic multi-pen models were converted into stochastic simulations in Chapter 5. Similar dynamics were observed in the standard stochastic model as for the deterministic model, however the stochastic cross-contamination model showed a very different dynamic of infection to the deterministic model. In the stochastic cross-contamination model the greater variation in faecal shedding led to stochastic fade-out of infection more often than not, and only in relatively few cases, where high shedding of Salmonella occurred, did transmission take place. However, if transmission did take place, it produced a similar epidemic curve as to the deterministic model. Overall, the average prevalence of infection was significantly reduced. Hence, the inclusion of faecal contamination and dose-response were seen as two important characteristics of the model, as they had the effect of markedly changing the transmission dynamics.

The final model developed in Chapter 6 is significantly more complex than the previous models. However, it builds on the developments made throughout the thesis, as well as drawing on the development of other models in the field (Lurette et al., 2008a,b; Soumpasis and Butler, 2009), in order to model farm management systems and sources of infection. This is the first model to explicitly deal with both farm management systems and sources of infection. The inclusion of farm management systems and sources of infection were thought to be vital in accurately representing transmission dynamics and hence the effect of interventions. As the results of the farm model show, including sources of infection and farm management practices led to two of the most important conclusions of the modelling conducted in this thesis: that the sow is a major risk factor for slaughter pig

infection, and that AIAO production was the most important farm management factor that would reduce transmission between pigs.

Also of crucial importance to the model developed in Chapter 6 is the explicit inclusion of environmental contamination via faecal shedding of Salmonella, and the corresponding dose-response function implemented. These two factors have been modelled and parameterised in detail, over and above what has been carried out elsewhere in previous models. The inclusion of all of these new (and complicated) factors (environmental contamination, dose-response, source of infection, farm management) produce markedly different dynamics of infection than those seen in previous models, in this thesis and in the literature, but which tend to agree with the observational data regarding the intermittent form of infection on pig farms and between pens (VLA, 2009; Nollet et al., 2005; Jensen et al., 2006).

The prevalence of infection in slaughter-age pigs is highly variable, but is likely to be low by the time of slaughter. This was observed in both case study MSs, despite differing sources of infection and transmission. Within the UK, the major result of the farm transmission model was that the sow appeared to be the major source of infection, such that other sources, such as feed and wildlife, were almost negligible in comparison. Feed and wildlife became important when the breeding herd prevalence was very low ($< 5\%$), as for MS1. Only one farm management practice, All-In-All-Out production, was significantly associated with a reduction in the prevalence of infection at slaughter.

There are still not enough quantitative data in the literature to confidently parameterise on-farm interventions. Instead, we investigated a number of hypothetical scenarios to elucidate the effect of broad intervention mechansims (e.g. changing the susceptibility of the pig to infection, reducing the level of environmental

contamination through C&D). The results of the intervention analysis (Chapter 7) highlighted the major dynamics largely captured in the previous chapter when interrogating the final farm model. C&D practices had little effect on slaughter pig prevalence, as the majority of contamination that causes infection is produced by the infected pigs in the pens during occupation. Breeding herd prevalence was highly correlated with slaughter pig prevalence, confirming the role of the sow as a major source of infection. On-farm interventions such as vaccination and organic acids could work in reducing slaughter pig prevalence, either through significantly modifying the susceptibility of the pig, or perhaps more promisingly, through reducing the magnitude of shedding should a pig become infected.

8.3 Discussion

The models summarised in the previous section allow an insight into the complex dynamics of transmission and intervention on pig farms, which is currently not possible through observational study due to the large number of variables that must be controlled. The final model incorporates several advancements in the field of Salmonella in pig transmission modelling that have not been considered before (e.g. the explicit inclusion of the magnitude of (intermittent and variable) shedding, farm management systems and sources of infection). These advancements highlight new and interesting dynamics, suggesting that the sow is by far the most important source of infection of pigs. In particular, the level of Salmonella shedding of individual pigs/sows appears to be crucial to the dynamics of infection, but this has not been captured before. This seems a fairly intuitive conclusion, given that Salmonella is mainly transmitted via the faecal-oral route and is dose-dependent. However, it is not normally captured in models because of the complexity of doing

so, and the lack of data to parameterise such a model. In the case of Salmonella in pigs, when dealing with various sources, complex management systems and highly variable shedding rates, then the inclusion of shedding dynamics at a more detailed level appears warranted, as the dynamics change markedly according to whether it is included or not.

Linear stability analysis of the deterministic models is something that has not been done in Salmonella in pig modelling before, and provided a useful first analytical capability to assess the dynamics of infection in relatively simple systems. While the relevance of the conclusions drawn from the analyses were limited as in reality there is so much movement and heterogeneity in the pig production system, the conclusions were useful in shaping the direction of the stochastic models, and also indicated, through relatively simple analysis, the importance of the pig as a self-sustaining source of infection to other pigs. Similar linear stability analyses could be useful for other livestock transmission models, especially where simpler production systems exist, such as for broiler chickens. The stochastic models are more appropriate for pig production, where groups of pigs are small and hence random effects will be important. The standard stochastic model did not result in enough heterogeneity in the dynamics of infection to replicate the results of observational and longitudinal studies. However, the cross-contamination and final birth-to-slaughter models replicate the heterogeneity of pig infection well. The final birth-to-slaughter model also includes a much more detailed description of the source of infection and shedding dynamics, based on observation published in the scientific literature: this is necessary if detailed intervention analysis at the farm level is to be sufficiently accurate.

It must be recognised that while great efforts have been made to ensure the correct parameterisation of the final model, there are still large uncertainties about much

of the data used in the model, and the assumptions made about the model itself. Key examples include the dose-response of pigs to Salmonella exposure (the dose-response model was fitted to a very small study of a specific breed of pig, with a specific serotype of Salmonella) and the assumption that pigs are not mixed during rearing (e.g. it is known that pigs are commonly held back from the slaughterhouse and mixed with another cohort if they have not yet reached slaughter weight). The impacts of such assumptions and uncertainties have been discussed in detail in Chapter 6, but one key impact of data scarcity is the lack of any data to validate the model in any significant detail. The dynamics of infection qualitatively match those observed in several studies (Kranker et al., 2003; Nollet et al., 2005; Jensen et al., 2006), but this is as much as we can say at the moment. However, the most important conclusion, that the sow is the driving force of infection in slaughter pigs, is validated to some extent by analysis of the EFSA breeding survey data, which shows a clear relationship between breeding herd prevalence and slaughter pig infection between MSs. There are some clear outliers, e.g. Denmark, and it would be interesting to use the current final model (or extend/modify it) to investigate the factors which cause these individual anomalies.

8.4 Conclusions

In conclusion, this thesis has established a set of models for the investigation of the introduction, transmission and intervention of Salmonella in pigs. The final model suggests that the sow is a major source of infection, and hence intervention should first and foremost be introduced to the breeding herd. However, increasing the susceptibility of the pig to infection, and conducting All-In-All-Out production, would lessen the transmission of infection between pigs during later stages of pro-

duction. The final model has already been used to inform the development of the UK NCP (to investigate the accuracy of several sampling schemes and as an input for Cost-Benefit Analysis), and research will continue to improve the assumptions and parameter estimation of the model.

Bibliography

Anderson, R. M. and May, R. M. (1979). Population biology of infectious diseases 1. *Nature*, 280(5721):361–367. Times Cited: 952.

Arnold, M. E. and Cook, A. J. C. (2009). Estimation of sample sizes for pooled faecal sampling for detection of salmonella in pigs. *Epidemiology and Infection*, 137(12):1734–41.

Arthur, T. M., Keen, J. E., Bosilevac, J. M., Brichta-Harhay, D. M., Kalchayanand, N., Shackelford, S. D., Wheeler, T. L., Nou, X. W., and Koohmaraie, M. (2009). Longitudinal study of escherichia coli o157:h7 in a beef cattle feedlot and role of high-level shedders in hide contamination. *Applied and Environmental Microbiology*, 75(20):6515–6523.

Bailey, N. (1975). *The Mathematical Theory of Infectious Diseases*.

Berends, B. R., Urlings, H. A. P., Snijders, J. M. A., and VanKnapen, F. (1996). Identification and quantification of risk factors in animal management and transport regarding salmonella spp in pigs. *International Journal of Food Microbiology*, 30(1-2):37–53.

Blaha, T. (2004). The present state of the german qs salmonella monitoring and reduction programme. *Deutsche Tierarztliche Wochenschrift*, 111(8):324–326. Times Cited: 8.

Boughton, C., Egan, J., Kelly, G., Markey, B., and Leonard, N. (2007). Quantitative examination of salmonella spp. in the lairage environment of a pig abattoir. *Foodborne Pathogens and Disease*, 4(1):26–32.

BPEx (2009). Annual report of the zoonoses action plan salmonella programme july 2007-march 2008. Technical report.

Brent, G. (1986). *Housing the pig*. Farming Press Ltd, Trowbridge. VLA Library.

Cannon, R. M. and Nicholls, T. J. (2002). Relationship between sample weight, homogeneity, and sensitivity of fecal culture for salmonella enterica. *Journal of Veterinary Diagnostic Investigation*, 14(1):60–62. Times Cited: 12.

Carlucci, A., Napolitano, F., Girolami, A., and Monteleone, E. (1999). Methodological approach to evaluate the effects of age at slaughter and storage temperature and time on sensory profile of lamb meat. *Meat Science*, 52(4):391–395.

Carr, J. (1998). *Garth Pig Stockmanship Standards*. 5m Enterprises, Sheffield.

Cinquin, O. and Demongeot, J. (2002). Positive and negative feedback: Striking a balance between necessary antagonists. *Journal of Theoretical Biology*, 216:229–241.

Commission, M. . L. (2010). *Pig Yearbook 2009*. BPEx Ltd, Milton Keynes.

Davies, R. H. and Wray, C. (1995). Mice as carriers of salmonella-enteritidis on persistently infected poultry units. *Veterinary Record*, 137(14):337–341.

Defra (2010). Zoonoses report 2010. Technical report.

Denagamage, T., O'Connor, A., Sargeant, J., Rajić, A., and McKean, J. (2007). Efficacy of vaccination to reduce salmonella prevalence in live and slaughtered

swine: a systematic review of literature from 1979 to 2007. *Foodborne Pathogens and Disease*, 4(4):539–549.

Dent, J., OReilly, K., Arnold, M., and Cook, A. (2009). Estimating transmission rates of salmonella within and between pens, report to defra, part of project oz0323. Technical report.

Edelstein-Keshet, L. (1988). *Mathematical Models in Biology*.

EFSA (2006). Opinion of the scientific panel on biological hazards (biohaz) related to 'risk assessment and mitigation options of salmonella in pig production'. Technical report.

EFSA (2008a). Microbiological risk assessment in feedingstuffs for food-producing animals - scientific opinion of the panel on biological hazards. Technical report.

EFSA (2008b). Report of the task force on zoonoses data collection on the analysis of the baseline survey on the prevalence of salmonella in slaughter pigs, in the eu, 2006-2007 [1] - part a: Salmonella prevalence estimates. Technical report.

EFSA (2009a). Analysis of the baseline survey on the prevalence of salmonella in holdings with breeding pigs in the eu, 2008 - part a: Salmonella prevalence estimates. Technical report.

EFSA (2009b). The community summary report on trends and sources of zoonoses and zoonotic agents in the european union in 2007. Technical report.

EFSA (2010a). Analysis of the baseline survey on the prevalence of campylobacter in broiler batches and of campylobacter and salmonella on broiler carcasses in the eu, 2008 - part a: Campylobacter and salmonella prevalence estimates. Technical report.

EFSA (2010b). The community summary report on trends and sources of zoonoses and zoonotic agents in the european union in 2008. Technical report.

EFSA (2010c). Scientific opinion on a quantitative microbiological risk assessment of salmonella in slaughter and breeder pigs. Technical report.

Farzan, A. and Friendship, R. M. (2005). A clinical field trial to evaluate the efficacy of vaccination in controlling salmonella infection and the association of salmonella-shedding and weight gain in pigs. *Canadian Journal of Veterinary Research-Revue Canadienne De Recherche Veterinaire*, 74(4):258–263. Times Cited: 0.

FCC (2011). Analysis of the costs and benefits of setting a target for the reduction of salmonella in breeding pigs. report for european commission health and consumers directorate general. Technical report.

Fedorka-Cray, P. J., Whipp, S. C., Isaacson, R. E., Nord, N., and Lager, K. (1994). Transmission of salmonella typhimurium to swine. *Veterinary Microbiology*, 41(4):333–44.

Fine, P. E. M. (1977). Commentary on mechanical analog to reed-frost epidemic model. *American Journal of Epidemiology*, 106(2):87–100. Times Cited: 11.

Frey, H., Mokhtari, A., and Zheng, J. (2004). Recommended practice regarding selection, application and interpretation of sensitivity analysis methods applied to food safety process risk models, prepared for office of risk assessment and cost-benefit analysis, u.s. department of agriculture, washington, dc. Technical report.

Friendship, R., Mounchili, A., McEwen, S., and Rajić, A. (2009). Critical review

of on farm intervention strategies against salmonella. report for the british pig executive. Technical report.

Gleed, P. T. and Sansom, B. F. (1982). Ingestion of iron in sows feces by piglets in farrowing crates with slotted floors. *British Journal of Nutrition*, 47(1):113–117.

Gray, J., Fedorka-Cray, P., Stabel, T., and Kramer, T. (1996). Natural transmission of salmonella choleraesuis in swine. *Applied and Environmental Microbiology*, 62(1):141–146.

Gray, J. T. and Fedorka-Cray, P. J. (2001). Survival and infectivity of salmonella choleraesuis in swine feces. *Journal of Food Protection*, 64(7):945–949.

Gray, J. T., Fedorkacray, P. J., Stabel, T. J., and Ackerman, M. R. (1995). influence of inoculation route on the carrier state of salmonella-choleraesius in swine. *Veterinary Microbiology*, 47(1-2):43–59. Times Cited: 59.

Heard, T. W. and Linton, A. H. (1966). An epidemiological study of salmonella in a closed pig herd. *Journal of Hygiene-Cambridge*, 64(4):411–419.

Hill, A. (In prep.). A cost-benefit analysis for salmonella in pigs in the uk. *Risk Analysis*.

Hill, A., Simons, R., Kelly, L., and Snary, E. (in prepa). A farm transmission model for salmonella in pigs, applicable to eu member states. *Risk Analysis*.

Hill, A., Snary, E., Arnold, M., Alban, L., and Cook, A. (2008). Dynamics of salmonella transmission on a british pig grower-finisher farm: a stochastic model. *Epidemiology & Infection*, 136:320–333.

Hill, A., Swart, A., Simons, R., and Snary, E. (In prep.b). An analysis of on-

farm and abattoir interventions for the reduction of foodborne salmonellosis attributable to pig meat consumption. *Risk Analysis*.

HPA (2009). Salmonella by serotype. `http://www.hpa.org.uk/Topics/InfectiousDiseases/InfectionsAZ/Salmonella/EpidemiologicalData/`.

Hur, J. and Lee, J. H. (2011). Immunization of pregnant sows with a novel virulence gene deleted live salmonella vaccine and protection of their suckling piglets against salmonellosis. *Veterinary Microbiology*, 143(2-4):270–276. Times Cited: 0.

Hur, J., Song, S. O., Lim, J. S., Chung, I. K., and Lee, J. H. (2010). Efficacy of a novel virulence gene-deleted salmonella typhimurium vaccine for protection against salmonella infections in growing piglets. *Veterinary Immunology and Immunopathology*, 139(2-4):250–256. Times Cited: 0.

Ivanek, R., Snary, E. L., Cook, A. J. C., and Grohn, Y. T. (2004). A mathematical model for the transmission of salmonella typhimurium within a grower-finisher pig herd in great britain. *Journal of Food Protection*, 67(11):2403–2409. Times Cited: 12.

Jensen, A. N., Dalsgaard, A., Stockmarr, A., Nielsen, E. M., and Baggesen, D. L. (2006). Survival and transmission of salmonella enterica serovar typhimurium in an outdoor organic pig farming environment. *Applied and Environmental Microbiology*, 72(3):1833–1842.

Kolmogorov, A., Petrovskii, I., and Piscounov, N. (1937). A study of the diffusion equation with increase in the amount of substance, and its application to a biological problem. translated in 1991 by v. m. volosov from bull. moscow univ., math. mech. 1, 125, 1937. In *Selected Works of A. N. Kolmogorov I*, pages

248–270. Kluwer.

Kranker, S., Alban, L., Boes, J., and Dahl, J. (2003). Longitudinal study of salmonella enterica serotype typhimurium infection in three danish farrowto-finish swine herds. *Journal of Clinical Microbiology*, 41(6):2282–2288.

Law, A. and Kelton, W. (2000). *Simulation Modelling and Analysis*.

Leek, A., Callan, J., Henry, R., and O'Doherty, J. (2005). The application of low crude protein wheat-soyabean diets to growing and finishing pigs. *Irish Journal of Agricultural and Food Research*, 44:247–260.

lo fo Wong, D., Dahl, J., Stege, H., van der Wolf, P. J., Leontides, L., von Altrock, A., and Thorberg, B. (2004). Herd-level risk factors for subclinical salmonella infection in european finishing-pig herds. *Preventive Veterinary Medicine*, 62(4):253–266.

Lo Fo Wong, D. and Hald, T. (2000). Salinpork: pre-harvest and harvest control options based on epidemiologic, diagnostic and economic research. Technical report.

Loynachan, A. T. and Harris, D. L. (2005). Dose determination for acute salmonella infection in pigs. *Applied and Environmental Microbiology*, 71(5):2753–2755.

Lurette, A., Belloc, C., Touzeau, S., Hoch, T., Ezanno, P., Seegers, H., and Fourichon, C. (2008a). Modelling salmonella spread within a farrow-to-finish pig herd. *Veterinary Research*, 39(5):49.

Lurette, A., Belloc, C., Touzeau, S., Hoch, T., Seegers, H., and Fourichon, C. (2008b). Modelling batch farrowing management within a farrow-to-finish pig

herd: influence of management on contact structure and pig delivery to the slaughterhouse. *Animal*, 2(1):105–116. Times Cited: 5.

Lurette, A., Touzeau, S., Lamboni, M., and Monod, H. (2009). Sensitivity analysis to identify key parameters influencing salmonella infection dynamics in a pig batch. *Journal of Theoretical Biology*, 258(1):43–52. Times Cited: 2.

Maplesoft (2010). Maple 13 (software). copyright maplesoft, waterloo, on, canada.

May, R. M. and Anderson, R. M. (1979). Population biology of infectious diseases 2. *Nature*, 280(5722):455–461. Times Cited: 489.

MLC (2009). *Pig Yearbook 2008*. BPEx Ltd, Milton Keynes.

Mokhtari, A. and Frey, H. C. (2005). Sensitivity analysis of a two-dimensional probabilistic risk assessment model using analysis of variance. *Risk Analysis*, 25(6):1511–1529.

Monterio Souza, D., Simons, R., and Cook, A. (In prep). A cost-effectiveness analysis for salmonella in pigs.

Murray, J. (2008). *Mathematical Biology: I. An Introduction: Pt. 1 (Interdisciplinary Applied Mathematics)*.

Nielsen, B., Alban, L., Stege, H., Sorensen, L. L., Mogelmose, V., Bagger, J., Dahl, J., and Baggesen, D. L. (2001). A new salmonella surveillance and control programme in danish pig herds and slaughterhouses. *Berliner Und Munchener Tierarztliche Wochenschrift*, 114(9-10):323–326. Times Cited: 35 4th International Symposium on Epidemiology and Control of Salmonella and Other Food Borne Pathogens in Pork SEP 02-05, 2001 LEIPZIG, GERMANY.

Nollet, N., Houf, K., Dewulf, J., Duchateau, L., De Zutter, L., De Kruif, A., and

Maes, D. (2005). Distribution of salmonella strains in farrowtofinish pig herds: a longitudinal study. *Journal of Food Protection*, 68(10):2012–21.

Nollet, N., Maes, D., De Zutter, L., Duchateau, L., Houf, K., Huysmans, K., Imberechts, H., Geers, R., de Kruif, A., and Van Hoof, J. (2004). Risk factors for the herd-level bacteriologic prevalence of salmonella in belgian slaughter pigs. *Preventive Veterinary Medicine*, 65(1-2):63–75.

O'Connor, A. M., Denagamage, T., Sargeant, J. M., Rajić, A., and McKean, J. (2008). Feeding management practices and feed characteristics associated with salmonella prevalence in live and slaughtered market-weight finisher swine: A systematic review and summation of evidence from 1950 to 2005. *Preventive Veterinary Medicine*, 87(3-4):213–228. Times Cited: 1.

Osterberg, J., Lewerin, S. S., and Wallgren, P. (2009). Patterns of excretion and antibody responses of pigs inoculated with salmonella derby and salmonella cubana. *Veterinary Record*, 165(14):404–408. Times Cited: 1.

Osterberg, J. and Wallgren, P. (2008). Effects of a challenge dose of salmonella typhimurium or salmonella yoruba on the patterns of excretion and antibody responses of pigs. *Veterinary Record*, 162(18):580–586. Times Cited: 5.

Pearce, R. A., Bolton, D. J., Sheridan, J. J., McDowell, D. A., Blair, I. S., and Harrington, D. (2004). Studies to determine the critical control points in pork slaughter hazard analysis and critical control point systems. *International Journal of Food Microbiology*, 90(3):331–339. Times Cited: 25.

Proux, K., Cariolet, R., Fravalo, P., Houdayer, C., Keranflech, A., and Madec, F. (2001). Contamination of pigs by nose-to-nose contact or airborne transmission of salmonella typhimurium. *Veterinary Research*, 32(6):591–600.

Renshaw, E. (1991). *Modelling biological populations in space and time*. Cambridge University Press, Cambridge.

Roussel, M. (2005). Stability analysis for odes [pdf document]. Technical report.

Sansom, B. F. and Gleed, P. T. (1981). The ingestion of sows feces by suckling piglets. *British Journal of Nutrition*, 46(3):451–456.

Sauli, I., Danuser, J., Geeraerd, A. H., Van Impe, J. F., Rufenacht, J., Bissig-Choisat, B., Wenk, C., and Stark, K. D. C. (2005). Estimating the probability and level of contamination with salmonella of feed for finishing pigs produced in switzerland - the impact of the production pathway. *International Journal of Food Microbiology*, 100(1-3):289–310.

Simons, R., Hill, A., Swart, A., and Snary, E. (In prep). A transport & lairage model for salmonella in pigs. *Risk Analysis*.

Skov, M. N., Madsen, J. J., Rahbek, C., Lodal, J., Jespersen, J. B., Jorgensen, J. C., Dietz, H. H., Chriel, M., and Baggesen, D. L. (2008). Transmission of salmonella between wildlife and meat-production animals in denmark. *Journal of Applied Microbiology*, 105(5):1558–1568.

Small, A., James, C., Purnell, G., Losito, P., James, S., and Buncic, S. (2007). An evaluation of simple cleaning methods that may be used in red meat abattoir lairages. *Meat Science*, 75(2):220–228.

Snary, E., Simons, R., Swart, A., Vigre, H., Coutinho Calado Domingues, A. R., and Hill, A. (in prep). A quantitative microbiological risk assessment for salmonella in pigs applicable for eu member states. *Risk Analysis*.

Soumpasis, I. and Butler, F. (2009). Development and application of a stochastic

epidemic model for the transmission of salmonella typhimurium at the farm level of the pork production chain. *Risk Analysis*, 29(11):1521–1533.

Soumpasis, I. and Butler, F. (2011). Development of a self-regulated dynamic model for the propagation of salmonella typhimurium in pig farms. *Risk Analysis*, 31(1):63–77.

Straw, B., D'Allaire, S., Mengeling, W., and Taylor, D. (1999). *Diseases of Swine*. Wiley-Blackwell, Iowa, 8th edition edition.

Tannock, G. W. and Smith, J. M. B. (1972). Studies on survival of salmonella typhimurium and salmonella-bovis-morbificans on soil and sheep feces. *Research in Veterinary Science*, 13(2):150.

Tenhagen, B., Wegeler, C., Schroeter, A., Dorn, C., Helmuth, R., and Kasbohrer, A. (2009). Association of salmonella spp. in slaughter pigs with farm management factors.

Turing, A. (1952). The chemical basis of morphogenesis. *The philosophical transactions of the Royal Society of London Series B - Biological Sciences*, 237(641):37–72.

van der Gaag, M. A., Saatkamp, H. W., Backus, G. B. C., van Beek, P., and Huirne, R. B. M. (2004). Costeffectiveness of controlling salmonella in the pork chain. *Food Control*, 15(3):173–180. Times Cited: 21.

VLA (2005). Use of routine data to investigate risk factors for salmonella spp. infection in pigs. Technical report.

VLA (2008). Salmonella in livestock production 2007. Technical report.

VLA (2009). An integrated risk based approach to the control of salmonella in uk pig farms. Technical report.

VLA (In prep). Longitudinal study of salmonella in sows and progeny. Technical report.

Wales, A., Allen, V., and Davies, R. (2010). Chemical treatment of animal feed and water for the control of salmonella. *Foodborne Pathogens and Disease*, 7(1):3–15.

Wheeler, J. G., Sethi, D., Cowden, J. M., Wall, P. G., Rodrigues, L. C., Tompkins, D. S., Hudson, M. J., Roderick, P. J., and Executive, I. I. D. S. (1999). Study of infectious intestinal disease in england rates in the community, presenting to general practice, and reported to national surveillance. *British Medical Journal*, 318(7190):1046–1050. Times Cited: 395.

Willhelm, T. (2009). The smallest chemical reaction system with bistability. *BMC Systems Biology*, 3:90–99.